The Synthesis of the Quinones Dehydroherbarin, Anhydrofusarubin and the Acetal Core of Marticin

Adushan Pillay

A thesis submitted to the Faculty of Science,

University of the Witwatersrand,
Johannesburg

In fulfillment of the requirements for the Degree of Doctor of Philosophy

10th May 2013

Declaration

I declare that the work presented in this thesis was carried out exclusively by myself under the supervision of Prof. C.B. de Koning and Dr A.L. Rousseau. It is being submitted for the degree of Doctor of Philosophy at the University of the Witwatersrand, Johannesburg. It has not been submitted before for any degree or examination at any other university.

10th May 2013

Signed: Adushan Pillay

Abstract

The syntheses of the naturally occurring naphthoquinone fungal metabolites dehydroherbarin and anhydrofusarubin as well as the acetal core of marticin are described in this thesis.

Starting from 2,4-dimethoxybenzaldehyde, dehydroherbarin was prepared in 11 steps in an overall yield of 4.5 %. The naphthalene segment of dehydroherbarin was constructed and functionalized utilizing reactions including a Stobbe condensation, O-allylation, and a Claisen rearrangement with the key step being a regioselective phenyliodine bis(trifluoroacetate) mediated methanol addition to the naphthalene. The pyran ring was assembled by a lithium aluminium reduction followed by Wacker-type oxidation reaction.

Two unnatural synthetic naphthoquinones, (3R,4R) 3-hydroxy-7,9-dimethoxy-3-methly-5,10-dioxo-3,4,5,10-tetrahydro-1*H*-benzo[*g*]isochromen-4-yl nitrate and 3,4-dihydroxy-7,9-dimethoxy-3-methyl-3,4-dihydro-1H-benzo[*g*]isochromene-5,10-dione, were also produced on route to accessing dehydroherbarin.

Anhydrofusarubin was synthesized from 2,4,5-trimethoxybenzaldehyde in 12 steps in an overall yield of 5.3 % by employing the same synthetic methodology developed towards the assembly of dehydroherbarin. To our knowledge, this represents the first formal synthesis of anhydrofusarubin.

The assembly of model system of the 6,6-bicyclic pyran ring arrangement found in the naturally occurring naphthoquinone marticin is also described. 11-(hydroxymethyl)-9-methyl-10,13-dioxatricyclo[7.3.1.$0^{2,7}$]trideca-2(7),4-diene-3,6-dione was produced racemically in 9 steps, starting from 2,5-dihydroxyacetophenone in a 3.3 % overall yield, with the key reaction again being a Wacker-type oxidation reaction

The related 6,7-bicyclic acetal compound, 3,6-dimethoxy-9-methyl-10,13-dioxatricyclo[7.3.1.$0^{2,7}$]trideca-2,4,6-triene, was also made inadvertently in 7 steps, from 2,5-dihydroxyacetophenone in a 6.5 % overall yield.

Acknowledgements

I wish to firstly thank my supervisor Professor C.B de Koning for his continuous support, guidance and motivation throughout the duration of my PhD.

I wish also to thank my co-supervisor Doctor A.L. Rousseau for her invaluable input and assistance.

Professor J.P Michael, Doctor A. Dinsmore and Doctor M.L. Bode are also to be thanked for their insightful discussions.

I am also highly grateful of the unbelievable support from Doctor R. Mampa and Professor L. Carlton whom provided me with NMR spectra and astute knowledge of the NMR machines.

Thanks also go Doctor M.A. Fernandes for undertaking the x-ray crystallographic studies.

It was my good fortune to have the following remarkable colleagues and friends with me in the organic chemistry group: Siyanda Mthembu, Tlabo Leboho, Hanna Klein, Caitlin Zipp, Myron Johnson, Stefania Scalzullo, Priya Pradeep, Winston Khumalo, Jean Dam, Cathy Hadje Georgiou, Gail Branklin, Doctor Dharmendra Yadav and Doctor Santanu Charkrovorty.

Financial support received from the National Research Foundation and the Southern African Biochemistry Informatics and Natural Products Association.

I would lastly like to thank my parents and sister for their neverending love and support.

Chapter 1: Introduction to Quinones

1.1. Quinones Occurrence and Functionality

The simplest, most apt description of a quinone is a compound containing an aromatic diketone chromatophoric group [(O=C-(C=C)$_n$-C=O)] within its structure[1]. Quinones occur widely throughout Nature and are found in bacteria[2], fungi[3], echinoderms[2], higher plants[4], insects[2] and mammals[5]. Arguably, their most important ubiquitous function is linking electron transport chains in metabolic pathways to the oxidative processes[6]. The quinone family differs in size and complexity with additional rings and functional groups, examples of which are illustrated in **Figure 1**[2].

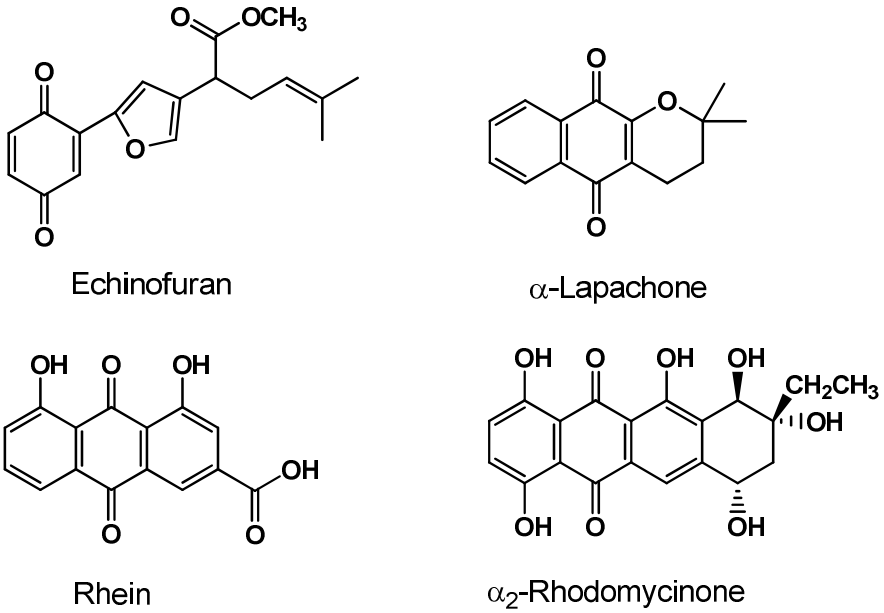

***Figure 1**: Benzoquinone, naphthoquinone, anthraquinone and anthracycline quinone examples*

A great amount of invaluable knowledge on these quinones has been collated, especially with regards to their structure-activity-relationships[5,7-9].

The fundamental principle of quinone reactivity is their ability to act as electrophiles and oxidants, where nucleophilic addition to a quinone occurs *via* a reversible formal two-electron reduction (see section 1.2). This redox trait is compelled by the formation of the lower energy stabilization-benefits of a fully aromatic system[10].

Quinone biological activity is modulated by the presence of ring substituents that effectively control their ensuing electrophilic and oxidative properties[11]. For example, the presence of an electron-withdrawing group bestows increased oxidant properties on the quinoid moiety, with the resultant hydroquinone being less readily oxidised. Conversely with an electron-donating substituent, the oxidative ability is less pronounced but the subsequent hydroquinone is more readily oxidised.

This insight into understanding the vital role of quinones in the intrinsic functioning of cellular systems, and thus diseases, has led to the creation of many prototypes to develop new drugs. Some of the most important medicinal quinones, their origins, structures and biological effects will be discussed in the following section.

1.1.1. Chemotherapeutic quinones

Atovaquone® **1** (**Figure 2**) is a synthetic hydroxynaphthoquinone with antimalarial properties that was synthesized from the lead compound lapachol **2** [12]. This drug is also the only clinical anti-malarial in the class of naphthoquinones[13]. It is metabolically stable and very effective against several other eukaryotic parasites including *Pneumocystis* and *Toxoplasma*[14]. Atovaquone® **1** is an analogue of ubiquinone **3** [an essential co-factor of membrane bound enzymes involved in adenosine 5'-triphosphate (ATP) formation] and is thus highly lipophilic in nature[6]. This drug acts selectively in sensitive parasites by inhibting their mitochondrial electron transport, specifically the enzyme dihydro-orotate dehydrogenase (involved in the biosynthesis of pyrimidines). A combination of atovaquone® **1** and proguanil is administered for prophylaxis and treatment of uncomplicated malaria[15]. Structurally atovaquone® **1** is identical to lapachol **2** with regards to the naphthoquinone system and position of the hydroxy group. The difference between the two compounds is where lapachol **2** possesses a prenyl group at C-2, atovaquone® **1** has a chlorinated benzene moiety linked via a cyclohexane ring to the naphthoquinone unit.

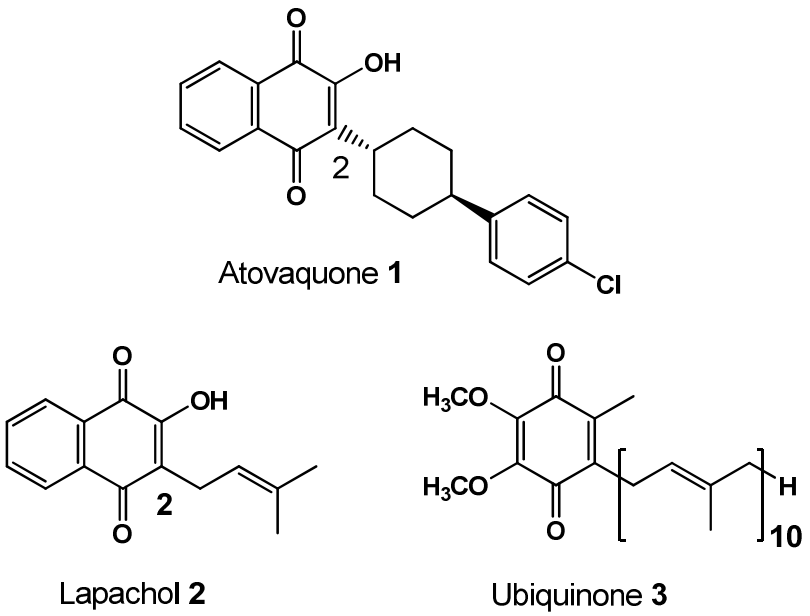

Atovaquone **1**

Lapachol **2**

Ubiquinone **3**

Figure 2

Anthracycline aminoglycosides are important antineoplastic agents that display broad-spectrum anti-tumour activity against both leukemias and solid tumours[16]. These molecules are naturally produced by strains of *Streptomyces*[2] (both natural and mutant variations), often with further chemical modifications being carried out *via* enzymatic or synthetic means. Daunomycin (or daunorubicin, daunosamine) **4** and doxorubicin (or adriamycin) **5** are two anthracycline antibiotics that have outstanding clinical utility as anti-cancer agents (**Figure 3**). Doxorubicin **5**, however displays serious dose-related toxic side effects, such as cardiac toxicity and myeloma suppression[17]. This led to the synthesis of idarubicin **6**, an analogue of doxorubicin **5** that displays improved pharmacological properties. The core skeleton of these three compounds consists of a tetracyclic ring system, of which three of the rings are aromatic, thus resulting in a planar portion of the compound. The fourth non-aromatic ring is called the aglycone intercalator ring[10] and has an aminoglycoside attached to it *via* an oxygen-ether linkage. The anti-tumour activities of anthracyclines are still not fully understood, but there are three modes of action that are proposed: (i) deoxyribonucleic acid (DNA) intercalation and resulting DNA damage *via* the inhibition of topoisomerase II[18], (ii) DNA binding and alkylation and (iii) damage of cellular molecules *via* the production of reactive oxygen species (ROS). These mechanisms are discussed further in section 1.2.

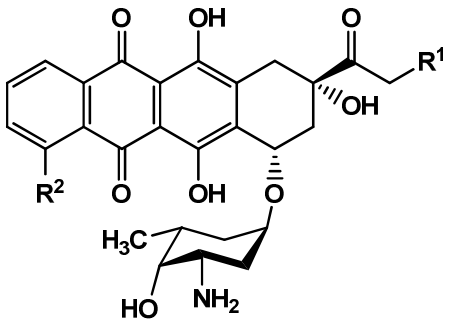

4 Daunomycin $R^1 = H$, $R^2 = OCH_3$

5 Doxorubicin $R^1 = OH$, $R^2 = OCH_3$

6 Idarubicin $R^1 = R^2 = H$

Figure 3

The mitomycins (mitomycin A **7**, mitomycin B **8** and mitomycin C **9**) (**Figure 4**) are a class of anti-tumour quinones that were isolated from *Streptomyces caespitosus* in 1956[19]. Mitomycin C **9** is used clinically for the treatment of solid tumours, owing to its high activity against this cancer type and its reduced toxicity compared to its counterparts, mitomycin A **7** and mitomycin B **8**. These molecules contain quinone, carbamate and aziridine moieties that are ordered as a pyrrolo[1,2-*a*]indole. This unique structural arrangement facilitates the mitomycin's mode of cytotoxic action, which is the cross-linkage of DNA (potentially *via* the bioreductive alkylation process) with great efficiency for the specific sequence CpG[19].

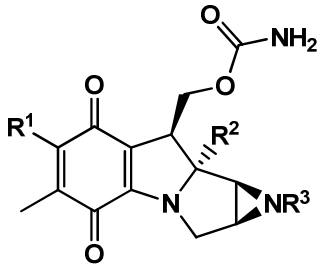

7 Mitomycin A $R^1 = NH_2$, $R^2 = OCH_3$, $R^3 = H$

8 Mitomycin B $R^1 = OCH_3$, $R^2 = OCH_3$, $R^3 = H$

9 Mitomycin C $R^1 = OCH_3$, $R^2 = OH$, $R^3 = CH_3$

Figure 4

Mitoxantrone **10** (**Figure 5**) is a synthetic anti-tumour drug designed in the 1970's[20] to (i) possess structural features predicated to favour DNA intercalation and (ii) have significantly reduced cardiac toxicity, which is a crucial problem of antineoplastic agents[17]. This quinone is utilized in the treatment of leukaemia, lymphoma and breast cancer[10]. Mitoxantrone **10**, a dihydroxyanthracenedione, contains (i) a *para*-quinone moiety with adjacent phenolic substituents in an aromatic system that allow for tautomerism and (ii) an ethylene spacer between two nitrogens with hydroxyethyl

substituents on the aliphatic amines. The anti-cancer activity of mitoxantrone **10** is attributed to its ability to inhibit topoisomerase II[20].

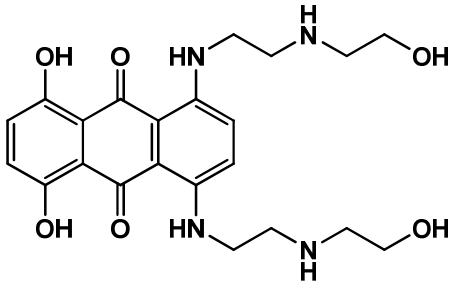

Mitoxantrone **10**

Figure 5

1.2. Mechanism of Biological Activities

There are three main accepted modes of biological action of quinones: (i) their involvement in the production of ROS, (ii) their role as bioreductive alkylating agents and (iii) their participation in DNA intercalation.

1.2.1. Production of reactive oxygen species (ROS)

The reductive potential of quinone compounds is a well understood process[11]. The one electron or two electron reduction of a quinone leads to the formation of a semiquinone radical or hydroquinone respectively (**Scheme 1**). Within cellular systems, there are many natural ubiquitous non-selective reducing enzymes that can specifically transfer one electron [nicotinamide adenine dinucleotide phosphate (NADPH)-cytochrome P 450, NADPH-cytochrome b_5 reductase and NADPH-ubiquinone oxidoreductase] or two electrons (DT-diaphorase) to quinone compounds[10]. Under aerobic conditions (found in healthy cells or tumours with sufficient blood supply) the quinone one-electron bioreduction predominates, resulting in the formation of the semiquinone radical that is readily autooxidised back to the original quinone by molecular oxygen. This process yields superoxide anion radicals ($O_2^{\cdot-}$) and is known as quinone redox cycling. Superoxide anion radicals are converted to hydrogen peroxide by superoxide dismutase (SOD). Hydrogen peroxide

is then broken down to the labile compounds H_2O and O_2 by catalase. However, the hydrogen peroxide can also rapidly react with intracellular iron[21] ions (Fenton reaction) to generate highly reactive hydroxyl radicals ($HO^{\cdot}$) that primarily contribute to the cytotoxic effects of ROS.

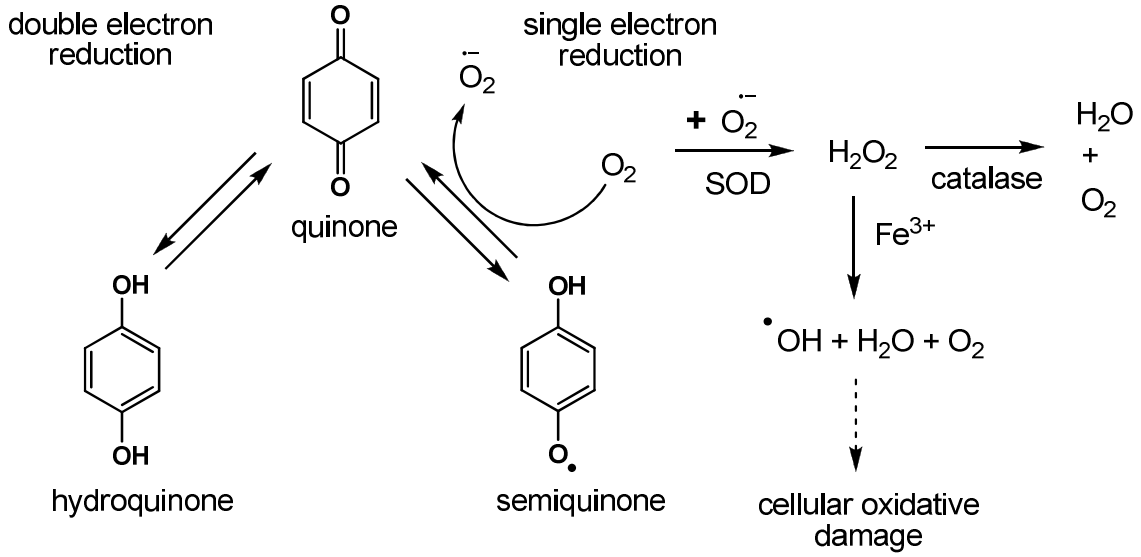

Scheme 1

The production of ROS is a normal process during cellular aerobic metabolism and cells are equipped with sufficient anti-oxidative defence systems including radical scavengers such as ascorbic acid or tocopherol and antioxidant enzymes such as catalase, SOD and glutathione peroxidase. However, when unnatural quinoid compounds are present in aerobic cells, there is an excessive release of ROS that results in an oxidant-anti-oxidant imbalance. This accounts for the pathological effects produced by these species. In principle, ROS can potentially react with all the components of the cell including nucleic acids, carbohydrates, lipids or proteins[10].

In theory, ROS creation is possible for all compounds containing a quinone moiety that possesses a reductive potential sufficient to accept an electron from the mentioned enzymatic reductants. Significant toxicity of anthracyclines[17] is attributed to ROS production.

1.2.2. Bioreductive alkylating agents

Bioreductive alkylation is another important process by which many quinone containing compounds may act. In this process *in vivo* reduction of the quinone substructure results in the formation of a highly reactive quinone methide[22]. Bioreductive alkylation has been shown to be preferential in anaerobic cellular environments[10] and requires the two electron reduction of the quinone moiety to the hydroquinone, conditions contrary to those favouring the production of ROS. In particular, solid tumours often have hypoxic cellular regions as the rate of tumour growth tends to isolate the central cancer cells away from the vicinity of oxygen (and nutrient) rich blood vessels[22]. The ubiquitous two-electron reducing enzyme DT-diaphorase is evidently overexpressed in a wide range of tumours and its involvement in the reduction of quinones is well established[10]. Thus, the combination of these two factors creates an environment which favours *in vivo* bioactivation and the bioalkylation process, possibly explaining why quinones display superior toxicity to oxygen-deficient cells in comparison to their oxygenated counterparts.

The basic mechanism of bioreductive alkylation is illustrated in **Scheme 2** and can be viewed as taking place over four successive steps[22].

i. Quinone **11** behaves as an intracellular two-electron acceptor and undergoes *in vivo* bioreduction to hydroquinone **12**.
ii. The substituent at the benzylic position of **12** is lost (as HX) through mesomeric assisted cleavage, forming quinone methide **13**.
iii. Quinone methide **13**, a Michael acceptor, is now primed to readily undergo addition to biological nucleophiles, including DNA, proteins, lipids and carbohydrates.
iv. The resulting hydroquinone-biological nucleophile adduct **14** is then autooxidized to its biologically inactive form **15**. The biological molecule is now covalently bonded to the quinone, and is rendered unable to carry out its normal cellular function, therefore potentially resulting in apoptosis.

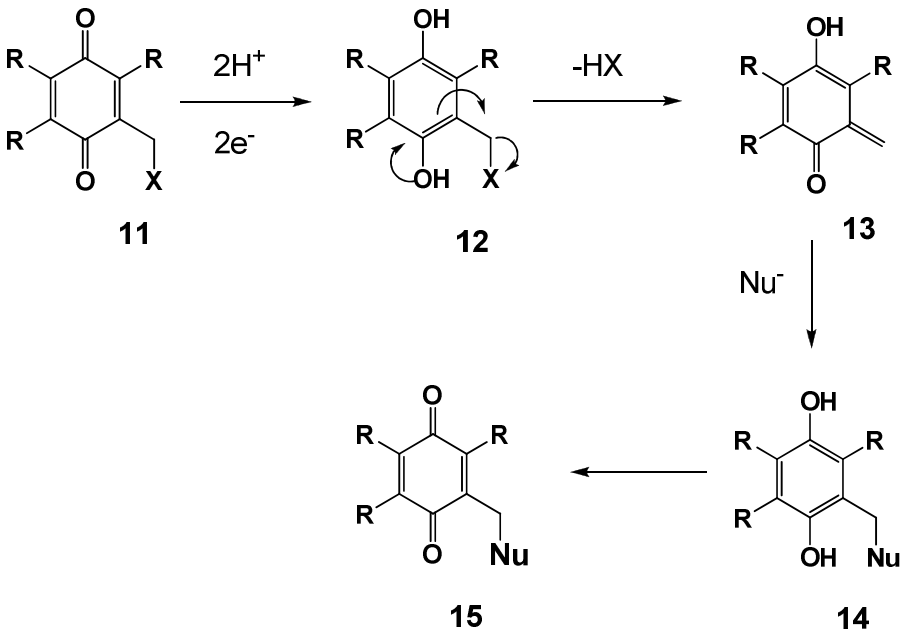

11 **12** **13** **15** **14**

Scheme 2

Mitomycin C **9** carries out its anti-tumour activity by this mode of action[11]. Additionally, the anthracycline antibiotics have also been postulated to be bioreductive alkylating agents[22].

1.2.3. DNA intercalation and Topoisomerase II inhibition

Early investigations towards understanding the mechanism of action of anthracyclines showed that their main target is DNA and that they interact with this macromolecule by intercalation between adjacent base pairs[23]. This DNA binding property was shown to possibly contribute to their anti-tumour properties, but does not account for the potent activity of these compounds on its own[10]. The recent consensus is that the main mode of anthracycline anti-cancer activity is by the inhibition of the enzyme topoisomerase II. In fact, about half of the drugs used currently for anti-tumour chemotherapy target this protein[7]. Topoisomerases are mammalian enzymes that regulate DNA topology through transient single-strand (topoisomerase I) or double-strand (topoisomerase II) breaks and are therefore extensively involved in transcription, replication and chromosome segregation[10,24]. These enzymes make excellent anti-cancer targets, firstly because they are highly active in proliferating cells, and secondly, they are potentially cytotoxic molecular

scissors (as a result of their ephemeral strand breaking ability). Anthracyclines stabilise the topoisomerase II-bridged DNA complex and consequently convert topoisomerase II into an endogenous toxin. Topoisomerase II persistently continues to produce these bridged DNA complexes whilst the presence of the anthracylines causes a major increase in DNA strand breaks. This event causes numerous cellular responses that result in cell death[25].

1.3. Fusarium solani: Importance and Biosynthesis of Napthoquinone Metabolites

The fungus genus *Fusaria*, and primarily *Fusarium solani* (Mart.) Appel & Wr. Emend. Snyd. & Hans. is an important plant parasite that contributes to the pathological condition blight[26,27]. Blight targets the most rapidly dividing areas of the plant such as roots and shoots, thus being significantly more destructive in younger seedlings compared to older plants[28]. The symptoms of blight are diverse and include: leaf necrosis[29], cortical rot[30], veinal chlorosis[31] and xylem dysfunction (reducing water intake and increased vessel plunging). *F. solani* infects many economic crop species, namely: citrus[32], tomatoes, maize, radishes, beans, lettuces, lentils, rice and peas[33].

Due to the damage *Fusaria* species cause on valuable food plants, there is an immense amount of plant pathology research directed at investigating all aspects of this fungus. This is an ongoing process and has led to the isolation and structural elucidation of a broad range of fungal metabolites, including sugars, organic acids, alcohols, hormones, toxins and antibiotics[34]. These metabolites cover a vast number of compound classes and not all will be mentioned.

With regards to this project, we are interested in the phytotoxins created by the fungus that contain the naphthoquinone structural framework shown in **Figure 6**.

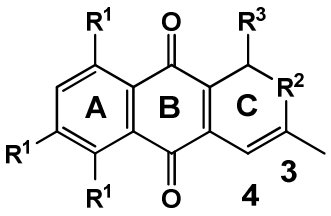

R^1 = H or OH or OCH_3
R^2 = O or N
R^3 = H or H_2

Figure 6

There are many structural similarities found amongst many of these naphthoquinones. To generalise, one could depict these compounds possessing three distinct regions: A, B and C. The A region is mostly an aromatic ring containing methoxy/hydroxyl groups in varying numbers and substitution patterns. The B region is also a ring structure, and usually is present as a quinone moiety. In some cases the A region can possess a quinone functionality and the B region may be a hydroquinone group. Lastly, the C region is often a ring system consisting of a basic pyran/furan/pyridine system, with many possible structural modifications existing.

It is quite common in these naphthoquinones for hydration to occur across positions C-3 and C-4 to form a hemiacetal functionality, or dehydration across these positions if already hydrated, resulting in an isochromene moiety. A number of these phytotoxins contain an acetal linkage at position C-3.

In the C region the R_2 group may either be an oxygen or a nitrogen atom. The natural occurrence of the pyran ring system is considerably greater than that of the furan ring system.

Thus, these selected oxygen containing naphthoquinones can be classified into 3 main categories: hemiacetals (**Table 1**), isochromenes (**Table 2**) and acetals (**Table 3**). Structurally similar compounds found in other species are also shown.

Fusarubin **16** and dihydrofusarubin **17** are tautomers, but fusarubin is more commonly encountered as this structure is favoured by electronic factors[35]. Fusarubin **16** has many more listed biological activities compared to the other tabulated compounds. This can be attributed to the greater natural occurrence of fusarubin **16** amongst many fungal species which consequently allows for the

compound to be more easily available for bioactivity screening. The structural similarities between fusarubin **16** and other hemiacetals such as delitzchianone A **22**, delitzchianone B **23** and 8-hydroxyherbarin **25** are evident. This suggests that these molecules most likely also possess similar biological activities and thus require biological testing.

Table 1: *Naphthoquinone hemiacetal compounds found in fungal and plant sources, with listed biological activities.*

Hemiacetal	Source (s)	Bioactivities
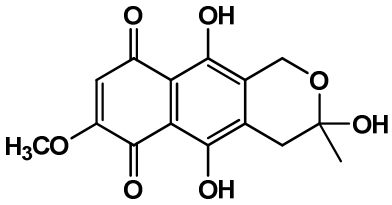 Fusarubin **16**	*F.solani*[34], *Neocosmospora vasinfectum*, *Neocosmospora africana*, *Nectria haematococca*, *Fusarium decemcellulare*, *Fusarium moniliforme*	Phytotoxic[34], antimicrobial[35] (*Saccharomyces cerevisiae, Streptomyces albus, Mycobacterium phlei, Bacillus subtilis, Staphylocccus aureus*), cytotoxic
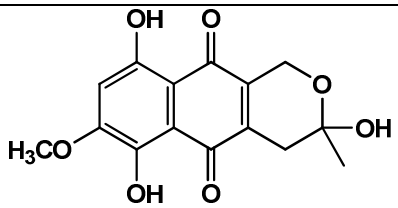 Dihydrofusarubin **17**	*F.solani*	
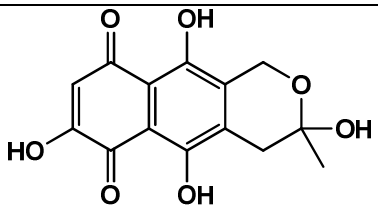 *O*-Demethylfusarubin **18**	*F.solani*	

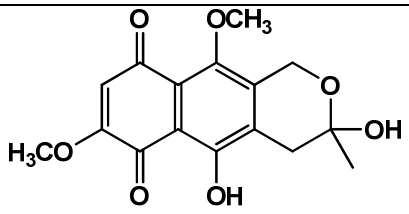 9-*O*-Methylfusarubin **19**	*F.solani*, *Fusarium martii*	
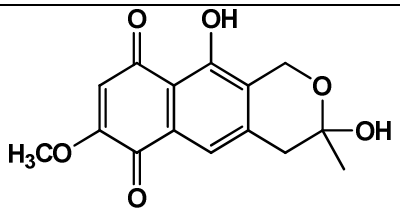 Deoxyfusarubin **20**	*N. haematococca*	
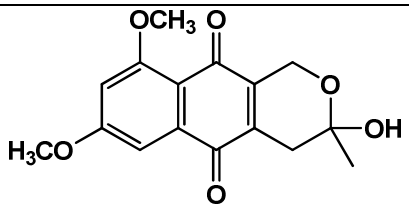 Herbarin 2**1**	*Torula herbarum*, *Amorosia littoralis*[36], *Usnea cavernosa*[37], *Corynespora* sp. BA-10763[38]	Antibacterial[35] (*B. subtilis*), antifungal (*Bacillus mycoides, Pythium debaryanum*)
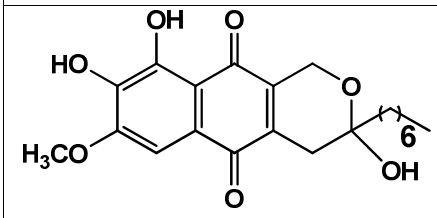 Delitzchianone A **22**	*Delitzchia winteri*[39]	
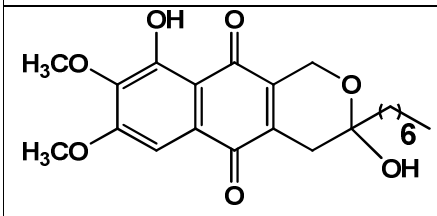 Delitzchianone B **23**	*Delitzchia winteri*	
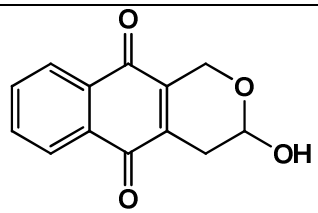 Psychorubin **24**	*Psychotria rubra*[35]	cytotoxic (KB tumour cells)

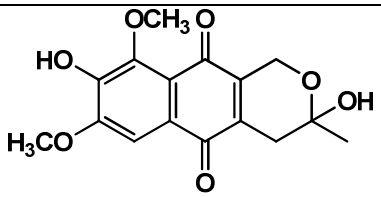 8-Hydroxyherbarin **25**	*Corynespora* sp. BA-10763[38]	

Anhydrofusarubin **26** is the dehydrated form of fusarubin **16** and thus shares similar biological activities. Many of the other compounds in this table need to be tested for their biological activity as it is highly probable that they will possess useful therapeutic properties. Anhydrofusarubin-lactone **29** and anhydrofusarubin-lactol **30** are structurally identical to anhydrofusarubin **26** save for the difference in the C-ring, which is the lactone functionality in **29** and the lactol functionality in **30** respectively. Another structurally similar molecule is the isoquinoline bostrycoidin **34,** which contains a nitrogen atom in the C-ring section where anhydrofusarubin **26** has an oxygen atom. Obionin B **39** is an unusual isochromene that contains an *ortho*-quinone moiety.

Table 2: *Naphthoquinone isochromene and isoquinoline compounds found in fungal and plant sources, with listed biological activities.*

Isochromene	Source (s)	Bioactivities
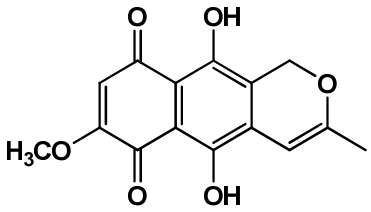 Anhydrofusarubin **26**	*F.solani*[34], *N.vasinfectum*, *N. africana*, *F.decemcellulare*, *Fusarium* spp. PSU-F15/F15[41], *Fusarium* sp. BCC14842[42]	phytotoxic, insecticidal[40], anti-tumour (KB and MCF-7)[41]
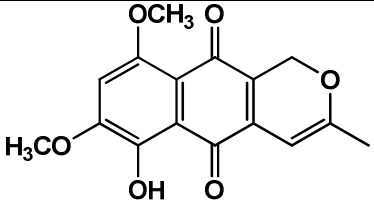 9-*O*-Methylanhydrofusarubin **27**	*Fusarium oxysporum*	

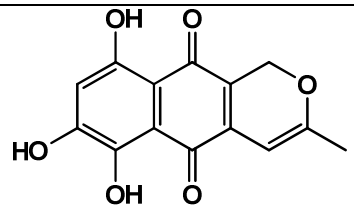 *O*-Demethylanhydrofusarubin **28**	*Gibberella fujikuroi*	
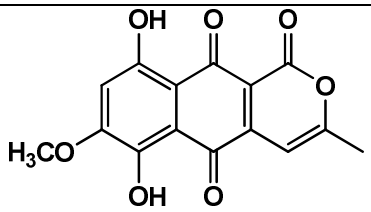 Anhydrofusarubin-lactone **29**	*F.solani*, *N.haematococca*	
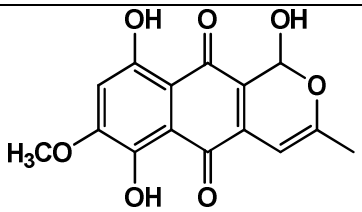 Anhydrofusarubin-lactol **30**	*F.solani*, *N.haematococca*	
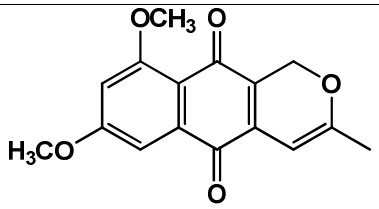 Dehydroherbarin **31**	*Torula herbarum*	Antibacterial[35] (*B. subtilis*), antifungal (*B. mycoides, P. debaryanum*)
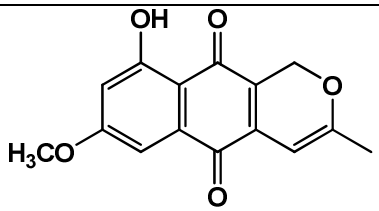 Deoxyanhydrofusarubin **32**	*N.haematococca*, *Trichopezizella nidulus*[43]	antimicrobial
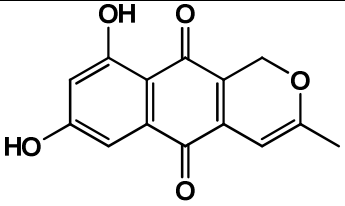 6-*O*-Demethyl-5-deoxyfusarubin **33**	*N.haematococca*, *Trichopezizella nidulus*[43]	antimicrobial

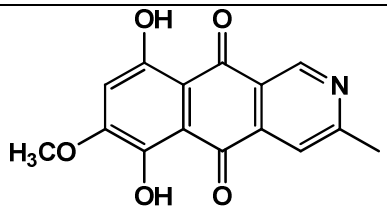 Bostrycoidin **34**	*Fusarium bostrycoides, F.solani, F.decemcellulare F.*sp. BCC14842[42]	
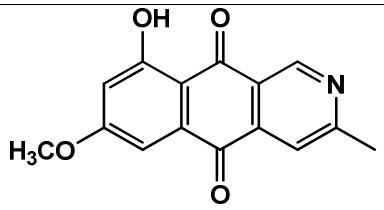 5-Deoxybostrycoidin **35**	*N.haematococca*	
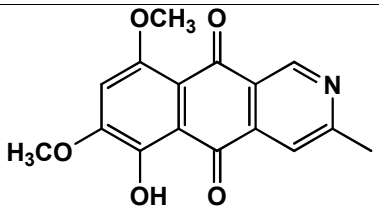 *O*-Methylbostrycoidin **36**	*F.decemcellulare*	
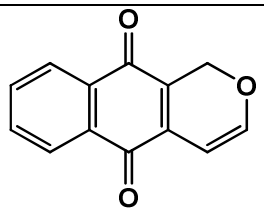 Pentalongin **37**	*Pentas longiflora*[44]	antifungal
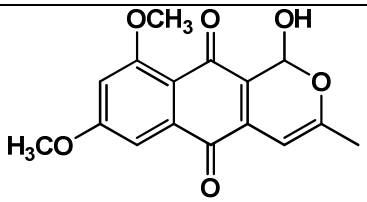 1-Hydroxydehydroherbarin **38**	*Usnea cavernosa*[37], *Corynespora* sp. BA-10763[38]	
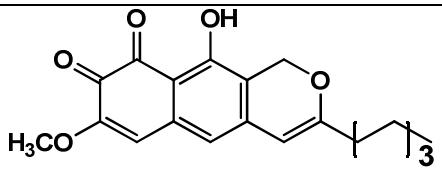 Obionin B **39**	Fungal extract (MSX 63619)[45]	cytotoxic

The naphthoquinone compounds in **Table 3** all contain an acetal linkage at C-3. *O*-methyldihydrofusarubin **40** has been shown to display anti-cancer and antibacterial

properties. *O*-Ethylfusarubin **43** and *O*-methylhebarin **44** possess antifungal activity, which is quite an uncommon occurrence considering their fungal origins.

Table 3: *Naphthoquinone acetal compounds found in fungal and plant sources, with listed biological activities.*

Acetal	Source (s)	Bioactivities
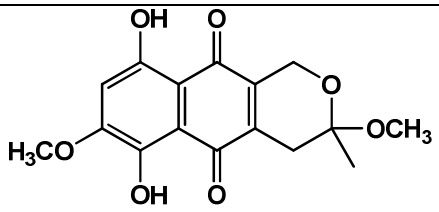 *O*-Methyldihydrofusarubin **40**	*F.solani*,	Cytotoxic[35] (mouse leukemia L1210), antibiotic (gram positive bacteria)
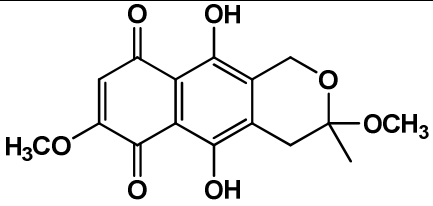 *O*-Methylfusarubin **41**	*F.solani*, *F.martii*	Antibacterial[35], antifungal
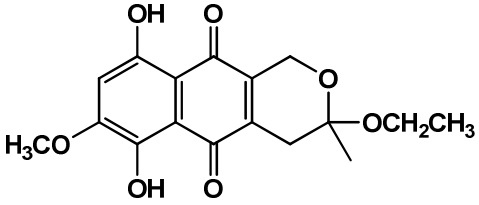 *O*-Ethyldihydrofusarubin **42**	*F.solani*, *N.haematococca*	
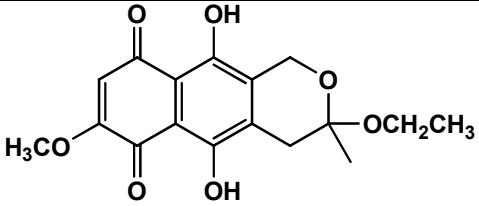 *O*-Ethylfusarubin **43**	*F.solani*, *F.martii*	Antibacterial[35], antifungal
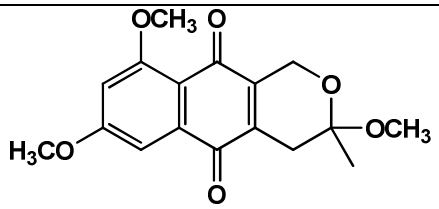 *O*-Methylherbarin **44**	*Torula herbarum*	Antibacterial[35] (*B. subtilis*), antifungal (*B. mycoides, P. debaryanum*)

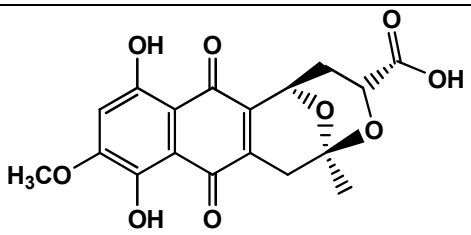 Marticin **45**	*F.solani*, *F.martii*	phytotoxic, anti-bacterial, antimicrobial[35] (*S. aureus, S. pyogenes*)
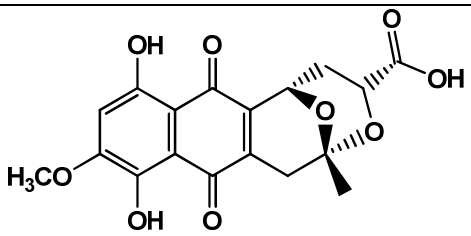 Isomarticin **46**	*F.solani*, *F.martii*	phytotoxic, antimicrobial[35] (*S. aureus, S. pyogenes*)

The diastereomers marticin **45** and isomarticin **46** are structurally fascinating molecules that possess 6,6-bicyclic pyran ring systems. These acetals display the highest phytotoxic activity of the naphthoquinone pigments[46,47]. Studies have demonstrated that they are highly toxic to tomatoes and peas with extensive damage to plant tissue at 8-30 $mg.kg^{-1}$, with toxicity being increased at low pH[48]. Marticin **45** and isomarticin **46** have been shown to promote electrolyte loss of host cells which subsequently allows amino acids, proteins and ions to be leached from the roots. These nutrients are then utilized by the parasitic rhizosphere *F.solani* for its own metabolic needs. The main mechanism of action of the marticins in tissues of higher plants still remains to be fully elucidated. However, inhibition of malate or citrate dehydration in the citric acid cycle is possible[49].

Naturally occurring compounds that contain fused pyran ring systems are rare and a few examples of this class of molecule are discussed.

Averufin **47** (**Figure 7**) is a decaketide quinone intermediate in the biosynthesis of the mycotoxins aflatoxins B_1 and G_1[50]. This molecule possesses a 6-membered bicylic fused-pyran ring system that is structurally similar to the system found in marticin **45**. Isagarin **48** is a medicinal naphthoquinone isolated from the roots of *Pentas longiflora*, and contains a 6,5-bicyclic pyran ring system[51]. The cytotoxic

antibiotic nogalamycin **49** is produced by the bacteria *Streptomyces nogalater*[52]. This complex compound has a 6,6-bicyclic pyran ring system in the amino sugar region[53].

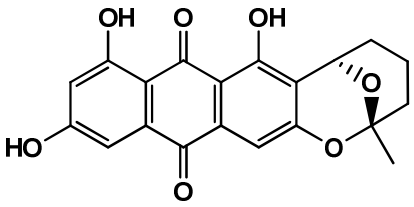

Averufin 47

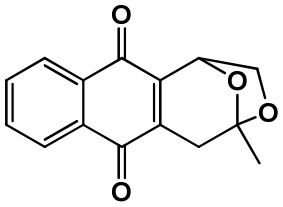

Isagarin 48

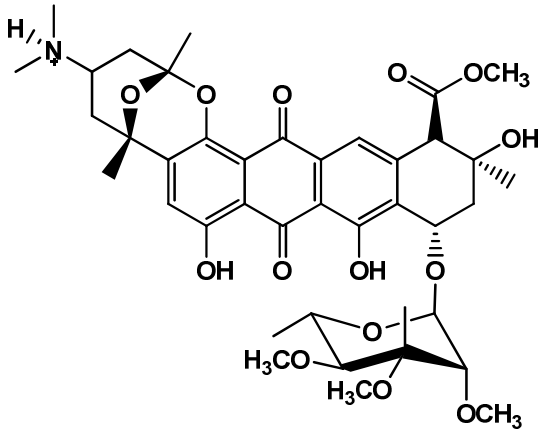

Nogalamycin 49

Figure 7

1.3.1. Biosynthesis of pyranonaphthoquinones and derivatives

The overall structural similarities between the naphthoquinones displayed in **Tables 1**, **2** and **3** can be attributed to their common biosynthetic origin, which is the polyketide synthetase (PKS) pathway[54,55]. This class of quinone is believed to be formed from the variation of the number of coenzyme A esters (an adenine nucleotide linked by a 5'-pyrophosphate to pantothenic acid) which results in a hypothetical polyketide chain that can further fold and aromatize. The PKS pathyway exists primarily in micro-organisms such as fungi, and a few plant species.

Naphthoquinones are heptaketide quinones and thus contain seven keto groups on the hypothetical polyketide chain (**Scheme 3**).

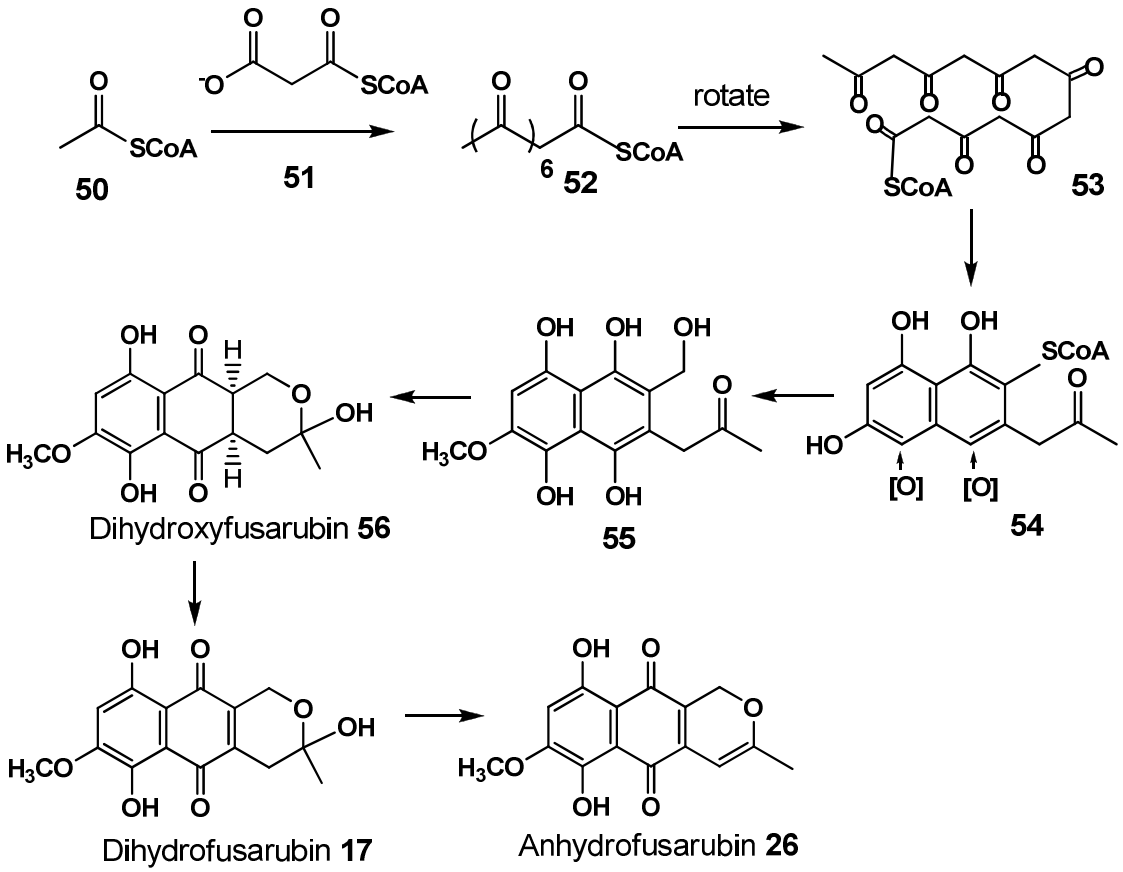

Scheme 3

One acetyl coenzyme A unit **50** is combined to six malonyl coenzyme A moieties **51** in a linear fashion to afford a heptaketide **52** which can "rotate" to afford **53**. The aromatization of **53** followed by the introduction of oxygen at the two depicted positions of **54** yields a hydroquinone. Next, the non-hydrogen bonded hydroxyl group is methylated and the coenzyme A protein detaches to give the primary alcohol in compound **55**. The nucleophilic attack of the primary alcohol on the ketone group, followed by autooxidation of the hydroquinone unit produces dihydroxyfusarubin **56**. Under alkaline conditions (found in the *F.solani* cultures) **56** oxidizes spontaneously in air to dihydrofusarubin **17**. The hemiacetal functionality in dihydrofusarubin **17** readily dehydrates in the presence of mildly acidic conditions to produce anhydrofusarubin **26**.

Marticin **45** has been deduced to be formed by addition of a C_3 unit (shown in red) originating from an intermediate of the Krebs cycle such as succinate or oxalacetate

to the heptaketide skeleton of dihydrofusarubin **17** or one of its precursors (**Scheme 4**) [54].

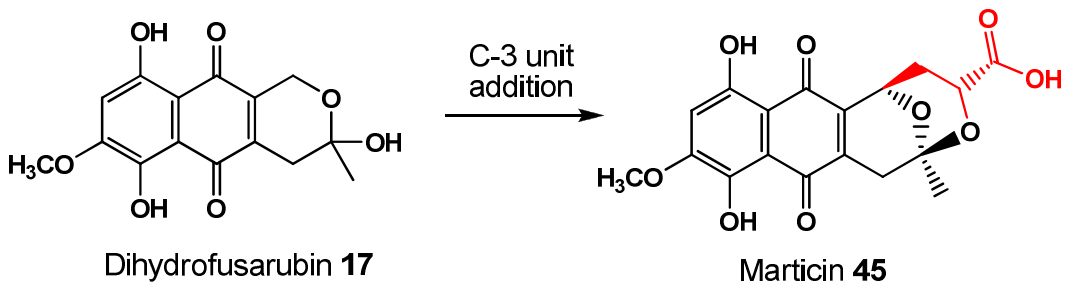

Dihydrofusarubin **17** Marticin **45**

Scheme 4

1.4. Summary of Chapter One

By comparing the various naphthoquinone structures (section 1.3) and quinone structural requirements for biological activity (section 1.2) it is not surprising that many of these naphthoquinones display a diverse spectrum of bioactivities based on *in vivo* and *in vitro* tests. An even more intriguing comparison can be made between the structural similarities of the fungal naphthoquinones to the chemotherapeutic quinones (section 1.1.1), illustrating the potential medicinal importance of the fungal naphthoquinones discussed.

1.5. References

1. Fotie, J., *Anti-Infective Agents in Medicinal Chemistry*, 2006, **5**, 357-366.
2. Thomson, R.H., *Naturally Occurring Quinones III: Recent Advances*, 1987, University Press, Cambridge.
3. Medsentsev, A.G., Arinbasarova, A.Y., Akimenko, V.K., *Applied Biochemistry and Microbiology*, 2005, **41**, 503-507.
4. Jacobs, J., Claessens, S., De Kimpe, N., *Tetrahedron*, 2008, **64**, 412-418.
5. Verma, R.P., *Anti-Cancer Agents in Medicinal Chemistry*, 2006, **6**, 489-499.
6. Kawamukai, M., *Journal of Bioscience and Bioengineering*, 2002, **94**, 511-517.

7. Sperry. J., Lorenzo-Castrillejo, I., Brimble, M.A., Machin, F., *Bioorganic and Medicinal Chemistry*, 2009, **17**, 7131-7137.
8. Morton, R.A., *Biochemsitry of Quinones*, 1965, Academic Press INC. (London) LTD.
9. Li, L.H., Krueger, W.C., *Pharmacology and Therapetics*, 1991, **51**, 239-255.
10. Asche, C., *Mini-Reviews in Medincal Chemistry*, 2005, **5**, 449-467.
11. Hillard, E.A., Abreu, F.C., Ferreira, D.C., Jaouen, G., Goulart, M.O., Amatore, C., *Chemical Communications*, 2008, **23**, 2612-2628.
12. Ferreira, V.T., Ferreira, S.B, de Carvalho da Silva, F., *Organic and Biomolecular Chemistry,* 2010, **8**, 4793-4802.
13. Muregi, F.W., *Current Drug Discovery Technologies*, 2010, **7**, 280-316.
14. Hudson, A.T., *Parasitology Today*, 1993, **9**, 66-68.
15. Srivastava, I.K., Vaidya, A.B., *Antimicrobial Agents Chemotherapy*, 1999, **43**, 1334-1339.
16. Jung, K., Reszka, R., *Advanced Drug Delivery Reviews*, 2001, **49**, 87-105.
17. Achmatowicz, O., Szechner, *Topics in Current Chemistry*, 2008, **282**, 143-186.
18. Gewirtz, D.A., *Biochemical Pharmacology*, 1999, **57**, 727-741.
19. Galm, U., Hager, M.H., Van Lanen, S.G., Ju, J., Thorson, J.S., Shen, B., *Chemical Reviews*, 2005, **105**, 739-758.
20. Bast, R.C., Kufe, D.W., Pollock, R.E., Weichselbaum, R.R., Holland, J.F., Frei, E., Holland-Frei Cancer Medicinem 5th Edition, © 2000, BC Decker Inc, Ontario.
21. Powis, P., *Free Radical Biology and Medicine*, 1989, **6**, 63-101.
22. Moore, H. W., *Science*, 1997, **197**, 527-532.
23. Quadrifoglio, F., Ciana, A., Manzini, G., Zaccara, A., Zunino, F., *International Journal of Biological Macromolecules*, 1982, **4**, 413-418.
24. McClendon, A.K., Osheroff, N., *Mutation Research*, 2007, **623**, 83-97.
25. Burden, D.A., Osheroff, N., *Biochimica et Biophysica Acta 1400*, 1998, 139-154.
26. Baker, R.A., Tatum, J.H., Nemec, S.Jr., *Mycopathologia*, 1990, 111, 9-15.
27. Baker, R.A., Tatum, J.H., *Proceedings of the Florida State Horticultural Society*, 1983, **96**, 53-55.

28. Oliveira, J., *The Synthesis of Isochromanols. Potential Bioreductive Alkylating Agents*, 2000, PhD Thesis, University of the Witwatersrand.
29. 4. Baker, R.A., Tatum, J.H., Nemec, S.Jr., *Physiology and Biochemistry*, 1981, **71**, 951-954.
30. Nemec, S.Jr., Phelps, D., Baker, R.A., *Physiology and Biochemistry*, 1989, **79**, 700-705.
31. Phelps, D.C., Nemec, S.Jr., Baker, R.A., Mansell, R., *Physiology and Biochemistry*, 1990, **80**, 298-302.
32. Medentsev, A.G., Akimenko, V.K., *Phytochemistry*, 1992, **31**, 77-79 and references cited therein.
33. Gopalakrishnan, S., Beale, M.H., Ward, J.L., Strange, R.N., *Phytochemistry*, 2005, **66**, 1536-1539.
34. Medentsev, A.G., Akimenko, V.K., *Phytochemistry*, 1998, **47**, 935-959.
35. Brimble, M.A., Duncalf, L.J., Nairn, M.R., *Natural Product Reports*, 1999, **16**, 267-281.
36. Van Wagoner, R.M., Mantle, P.G., Wright, J.L.C., *Journal of Natural Products*, 2008, **71**, 426-430.
37. Paranagama, P.A., Wijeratne, E.M.K., Burns, A.M., Marron, M.T., Gunatilaka, M.K., Arnold, A.E., Gunatilaka, A.A.L., *Journal of Natural Products*, 2007, **70**, 1700-1705
38. Wijeratne, E.M.K., Bashyal, B.P., Gunatilaka, M.K., Arnold, A.E., Gunatilaka, A.A.L., *Journal of Natural Products*., 2010, **73**, 1156-1159.
39. Cao, S., Clardy, J., *Tetrahedron Letters*, 2011, **52**, 2206-2208.
40. Claydon, N., Grove, J.F., Pople, M., *Journal of Invertebrate Pathology*, 1977, **30**, 216-223
41. Trisuwan, K., Khamthong, N., Rukachaisirikul, V., Phongpaichit, S., Preedanon, S., Sakayaroj, J., *Journal of Natural Products,* 2010, **73**, 1507-1511
42. Kornsakulkarn, J., Dolsophon, K., Boonyuen, N., Boonruangprapa, T., Rachtawee, P., Prabpai, S., Kongaeree, P., Thongpanchang, C., *Tetrahedron*, 2011, **67**, 7540-7547
43. Thines, E., Anke, H., Sterner, O., *Journal of Natural Products*, 1998, **61**, 306-308.

44. Jacobs, J., Claessens, S., De Kimpe, N., *Tetrahedron*, 2008, **64**, 412-418.
45. Ayers, S., Graf, T.N., Adcock, A.F., Kroll, D.J., Shen, Q., Swanson, S.M., Wani, M.C., Darveax, B.A., Pearce, C.J., Oberlies, N.H., *Tetrahedron Letters*, 2011, **52**, 5128-5130.
46. Holenstein, J. E., Stoessl, A., *Canadian Journal of Chemistry*, 1984, **62**, 1971-1976
47. Kern, H., Naef-Roth, S., *Phytopathol Z*, 1965, **53**, 45-64.
48. Kern, H., *Phytopathology*, 1978, **10**, 327-345.
49. Naef-Roth, S., *Production and bioassay of phytotoxins*, In Wood, R. K. S., Ballio, A., Graniti, A., (eds), *Phytotoxins in Plant Diseases*, 1972, Academic Press, New York.
50. Brase, S., Encinas, A., Keck, J., Nising, C. F., *Chemical Reviews*., 2009, **109**, 3903-3990
51. Kestelyn, B., van Puyvelde, L., De Kimpe, N., *Journal of Organic Chemistry*, 1999, **64**, 438-440.
52. Li, L.H., Krueger, W.C., *Pharmacology and Therapetics*, 1991, **51**, 239-255.
53. Banerjee, T., Mukhopadhyay, *Biochemical and Biophysical Research Communications*, 2008, **374**, 264-268.
54. Inouye, H., Leistner, E., *The Chemistry of Quinoid Compounds. Vol II*, 1998, © John Wiley & Sons Ltd., New York.
55. Clayden, J., Greeves, N., Warren, S., Wothers, P., *Organic Chemistry*, 2005, Oxford Univeristy Press Inc., New York.

Chapter 2: Synthetic Methods for the Assembly of Polyhydroxylated Naphthalenes and Cyclic Acetals

The plethora of potential lead compounds that fungal metabolites present is a continuously expanding field and the syntheses directed towards some of these naphthoquinones is reviewed in this chapter. The main emphasis is on synthetic methods towards creating a polyhydroxylated naphthalene core that is the dominant structural characteristic found in many of the naphthoquinones, such as fusarubin **16**, anhydrofusarubin **26**, dehydrohebarin **31** and marticin **45**. Fused pyran ring systems, such as the one found in marticin **45,** are also examined and synthetic routes accessing these bicyclic acetals are discussed.

2.1. Strategies towards Synthesizing Polyhydroxylated Naphthalene Systems

There are four main synthetic routes that are used to create polyhydroxylated naphthalene systems, namely: (i) the Diels-Alder reaction, (ii) Hauser and Staunton-Weinreb annulations, (iii) formylation-peroxidation reactions and (iv) phenol or naphthol *para*-oxidations using oxidants/catalysts.

2.1.1. Diels-Alder reaction

The Diels-Alder cycloaddition reaction has been shown to be one of the most effective means to obtain simple or complex multi-ring systems[1] (**Scheme 5**). Many naphthalene systems have been assembled[1,2] using this ring forming reaction, as a potentially unlimited number of dienes and dienophiles can be reacted to form the naphthalene motif.

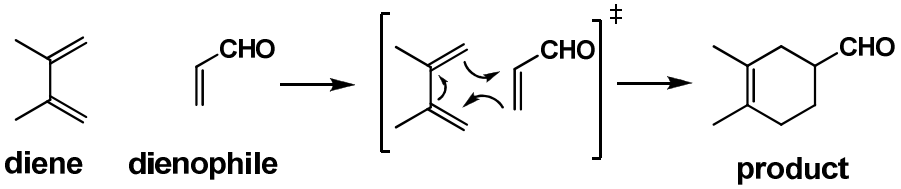

Scheme 5: *Basic Diels-Alder reaction*[3]

Within the scope of polyhydroxylated naphthalene species, there are two main classes of dienes that are employed. These are the cyclic dienes and vinyl ketene acetal dienes. The cyclic dienes are usually more stable in nature than their open-chain vinyl ketene acetal counterparts, and initially form adducts[4-7] when reacted with a dienophile. When dealing with unsymmetrical dienophiles or dienes, there is always the possibility of obtaining more than one regioisomeric product. It has been shown that the regioselective introduction of a halogen atom (usually a bromine) into the dienophile often allows for a single regioisomer to form when the Diels-Alder reaction is carried out[7-9].

2.1.1.1. Cyclic dienes

In his PhD dissertation, de Koning demonstrated how a pentamethoxy naphthalene system can be synthesized from vanillin in six steps[10] (**Scheme 6**). 2,3-Dibromo-1,4,5-trimethoxybenzene **57** was obtained from the cheap, commercially available vanillin in four steps[11,12]. 2,3-Dibromo-1,4,5-trimethoxybenzene **57** was treated with *n*-butyllithium (0.9 molar equivalents) at low temperature to generate a highly reactive benzyne intermediate *in situ*, which was reacted with 2-methoxyfuran **58** to generate two adduct regioisomers **59**. When subjected to mild acidic conditions (silica gel), the adducts **59** ring open to form their mono-naphthol equivalents **60**. Methylation of these regioisomers **60** yielded the single pentamethoxynaphthalene **61**.

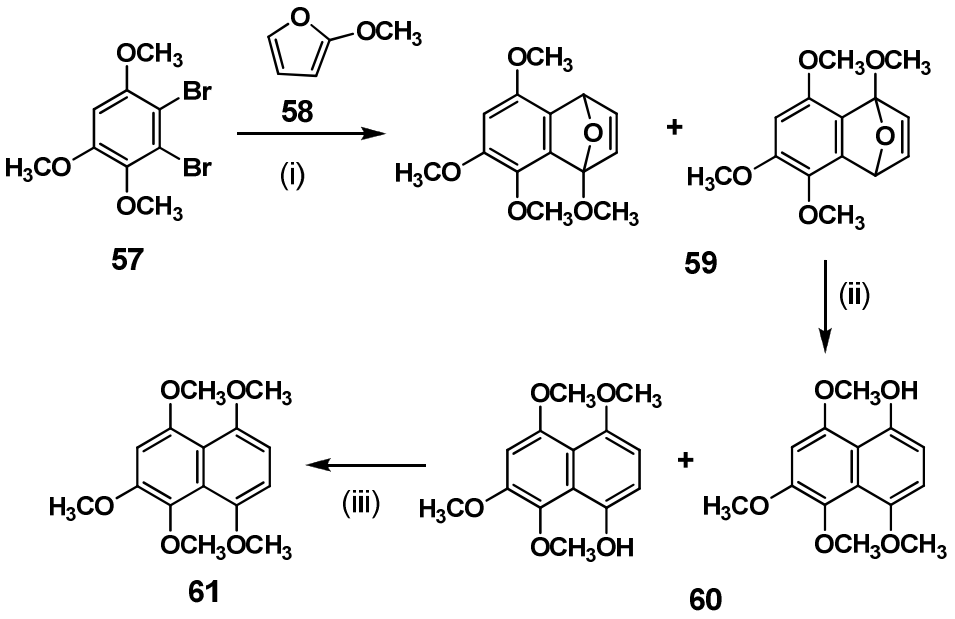

Scheme 6: *Reagents and conditions: (i)* ^{n}*BuLi, THF, -78 °C, then* ***58****, rt; (ii)* H^{+} *(silica gel); (iii)* K_2CO_3, Me_2SO_4, Me_2CO, *reflux, 68 % over 3 steps.*

In another study directed at the synthesis of the building blocks of rubromycins[13], 1,2,4-trimethoxybenzene **62** was brominated with bromine in chloroform (**Scheme 7**). This mono-brominated species **63** was treated with the sterically bulky base lithium diisopropylamine and then furan **64**, forming adduct **65**. Exposure of the adduct **65** to catalytic amounts of perchloric acid facilitated regioselective ring-opening. The resulting phenol **66** was *ortho*-brominated with pyridinium perbromide to afford 2-bromo-5,7,8-trimethoxynaphthalen-1-ol **67**. This compound **67** was oxidized with ceric ammonium nitrate, reduced with sodium dithionite and methylated to provide 2-bromo-1,4,5,7,8-pentamethoxynaphthalene **68**.

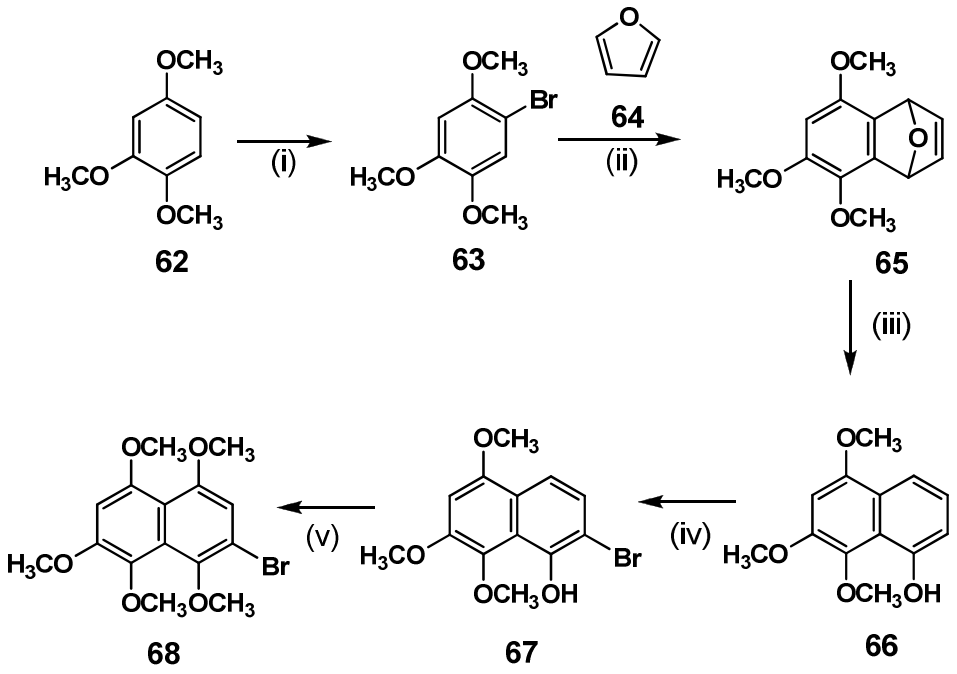

Scheme 7: *Reagents and conditions: (i) Br_2, $CHCl_3$, 0 °C, 100 %; (ii) LDA, then* ***64****, -78 °C to rt, 100 %; (iii) $HClO_4$ (cat.), THF, rt, 100 %; (iv) PHBP, THF, rt, 60 %; (v) CAN (20 % in H_2O), CH_3CN, rt, then $Na_2S_2O_4$, TBABr (cat.), CH_2Cl_2, rt, then Me_2SO_4, NaOH, TBABr (cat.), CH_2Cl_2, rt, 46 % over 3 steps.*

2.1.1.2 Open chain dienes

The majority of these 'open-chain' dienes have a skeleton that is based on the molecule ethyl acetoacetate **69**. Some of the more commonly used dienes have been named after their respective creators. The most generally known are Brassard's diene **70**[14], Chan's diene **71**[15], Dane's diene **72**[16], Danishefsky's diene **73**[17] and Rawals diene **74**[17] (**Figure 8**).

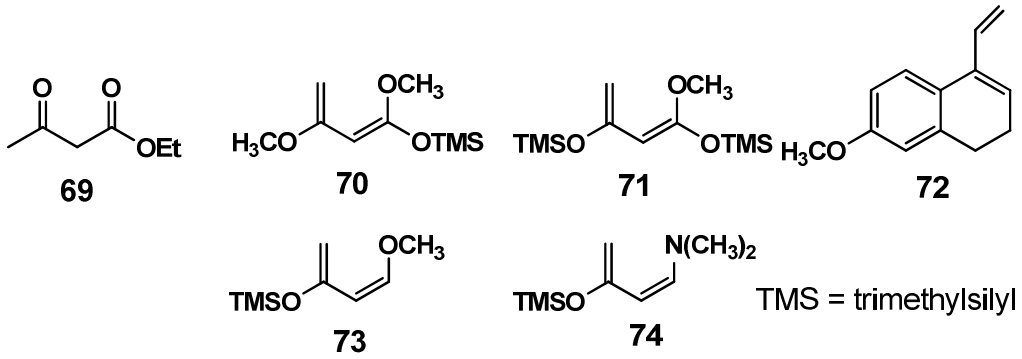

Figure 8: *Structures of common dienes.*

With regards to the synthesis of polyhydroxylated naphthalenes, a few of these dienes allow for the introduction of a new ring system containing one (Danishefsky's diene **73**) or two (Brassard's diene **70**, Chan's diene **71**) hydroxy groups. **Scheme 8** is an example of the implementation of Diels-Alder methodology in the synthesis of pyranonaphthoquinone antibiotics. The brominated 1,4-benzoquinone **75** is obtained from (*S*)-2-methyloxirane in 10 steps[18]. The reaction of **75** with Chan's diene **71** generates naphthoquinone **76** in a low yield of 24 %. The position of the bromine atom in **75** regiochemically controls the Diels-Alder reaction as only one regioisomer (out of a possible two) forms. Reaction of brominated 1,4-benzoquinone **75** with complex diene **77** gives rise to three products **78**, **79** and **80** in trace amounts.

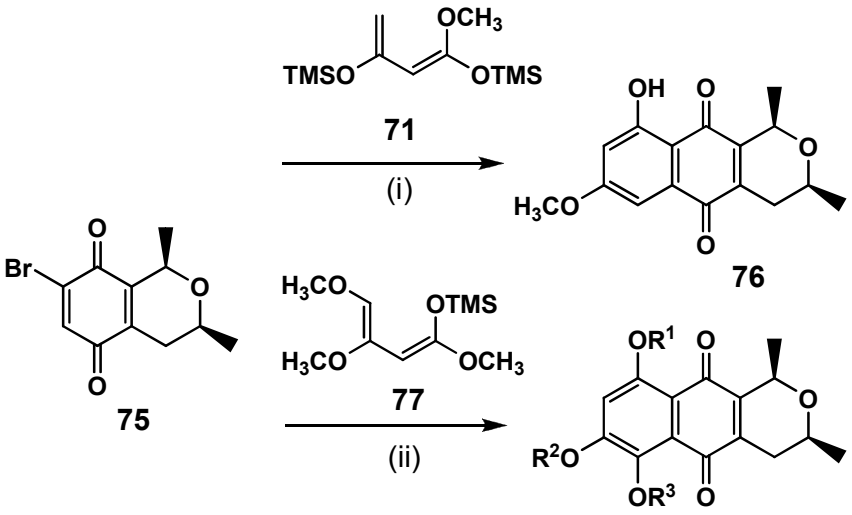

78 $R^1 = R^2 = R^3 = CH_3$

79 $R^1 = R^3 = CH_3$, $R^2 = H$

80 $R^1 = H$, $R^2 = R^3 = CH_3$

Scheme 8: *Reagents and conditions: (i)* ***71****, C_6H_6, rt, 24 %; (ii)* ***77****, C_6H_6, rt, 0.8 % for* ***78****, 0.2 % for* ***79****, 0.4 % for* ***80****.*

The first reported synthesis of dehydrohebarin **31** in 2000 by De Kimpe and co-workers (**Scheme 9**) employed the Diels-Alder reaction[19]. Benzoquinone **81** was treated with vinyl ketene acetal diene **82** to undergo a regioselective cycloaddition reaction to afford the 1,4-naphthoquinone **83**. The phenol substituents in **83** were methylated using a combination of silver(I) oxide and methyl iodide to yield 6,8-dimethoxy-2-methyl-1,4-naphthoquinone **84**. Reaction of **84** with acetonylpyridinium chloride **85** and triethylamine resulted in the formation of 3-acetonylnaphthoquinone **86** in a 79 % yield. Naphthoquinone **86** was selectively monobrominated using *N*-bromosuccinimide with a catalytic amount benzoyl peroxide to provide 3-acetonyl-2-bromomethyl-1,4-naphthoquinone **87**. Treatment of **87** with triethylamine in refluxing toluene facilitated the selective cyclization to the natural product dehydrohebarin **31** in an 84 % yield.

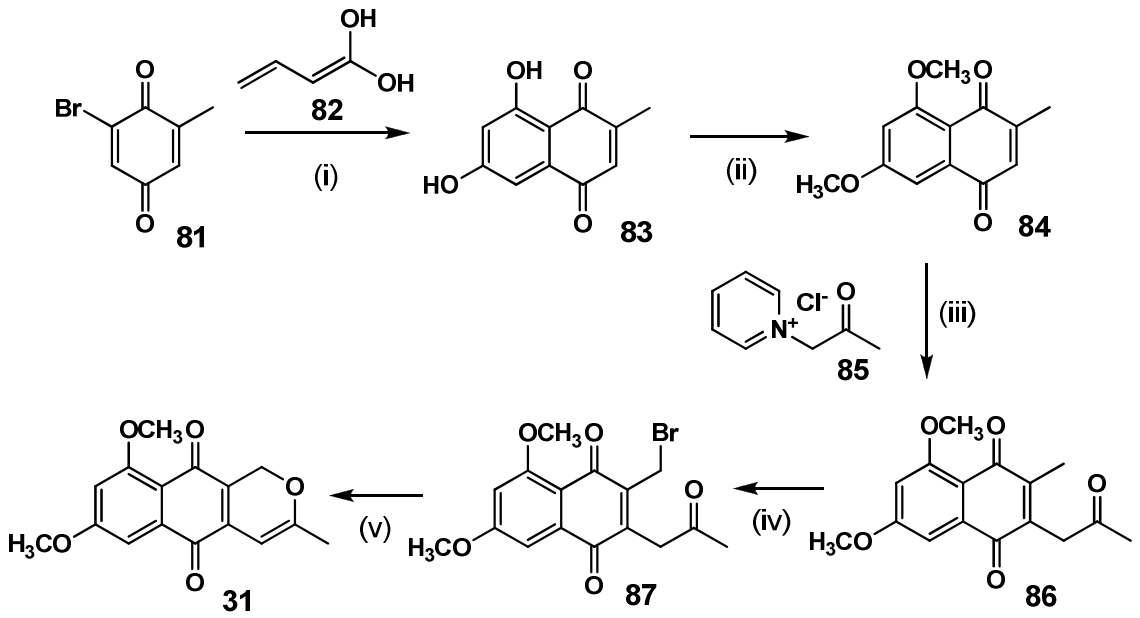

Scheme 9: *Reagents and conditions: (i)* ***82****, THF, -78 °C, 76 %; (ii) Ag_2O, CH_3I, $CHCl_3$, rt, 95 %; (iii)* ***85****, Et_3N, CH_3CN, rt, 79 %; (iv) NBS, benzoyl peroxide, CCl_4, reflux, 80 %; (v) Et_3N, toluene, reflux, 84 %.*

2.1.1.3 Evaluation of Diels-Alder reaction in the synthesis of hydroxylated naphthoquinones

There is no doubt of the versatility, applicability and synthetic prowess of the Diels-Alder reaction with regards to formation of aromatic rings in natural product synthesis. Theoretically one could create almost any desired ring system and substituent arrangement pattern. However, there are a few problems that the Diels-Alder reaction poses, especially when employed towards creating polyhydroxylated naphthoquinones. These are: (i) regioselectivity is an issue when a halogen is not present in the dienophile and thus formation of multiple regioisomers is possible; (ii) some of the desired dienes (such as in **Figure 8** and **Scheme 8**) are tricky to make and/or expensive (2-methoxyfuran **58**) or difficult (furan **64**) to obtain; (iii) reactions can be very low yielding (see **Scheme 8**) and thus can potentially be carried out only at the end of the synthesis. These limitations must be taken into account when designing routes to access substituted naphthalenes or naphthoquinones.

2.1.2. Annulation reactions

An annulation reaction can be defined as a transformation resulting in the addition of a new ring to a compound via two novel bonds[20].

2.1.2.1. Hauser annulation

The Hauser annulation reaction involves the annulation of an acceptor possessing a polarised/activated multiple bond **88** with a 3-(nucleofugal) benzo[*c*]furanone, for example **89** to form a naphthol/naphthoquinone annulated product **90**[20]. The proposed mechanism of the Hauser annulation is depicted in **Scheme 10**. The first step is the deprotonation of a phthalide such as **89** at C-3 with the ensuing anion **91** undergoing Michael addition with the acceptor **88**, forming carbanion **92**. The lactone functional group on carbanion **92** then undergoes an intramolecular Dieckmann cyclization to yield intermediate **93**. Electronic movement within **93** results in the expulsion of benzenesulfinate ion, giving quinone **94**. Base-promoted tautomerization and subsequent protonation of **94** results in formation of annulated ring system **90**, which can for example, be protected as the *para*-aromatic dimethyl ether.

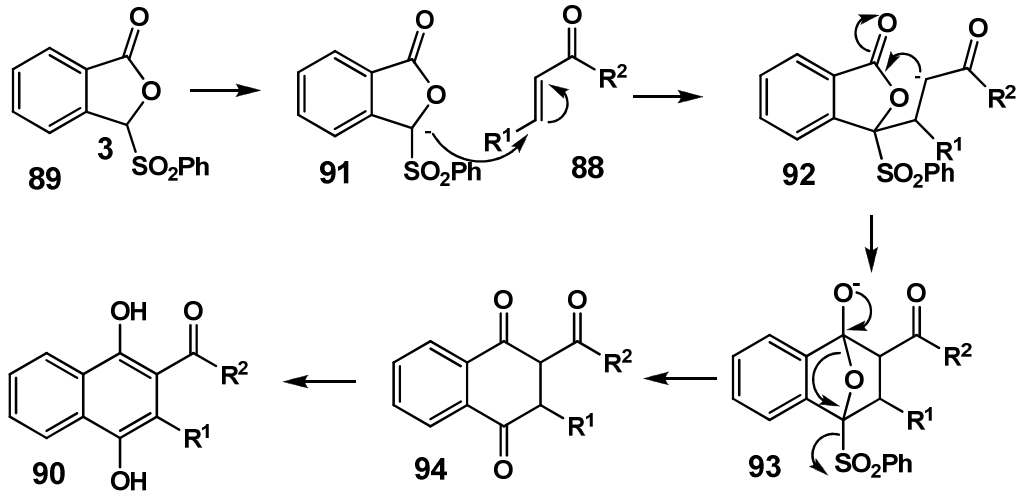

R^1 = alkyl group
R^2 = alkyl or *O*-alkyl group

Scheme 10

In a reported synthesis of thysanone, a human rhinovirus (HRV) 3C-protease inhibitor, a Hauser annulation was employed to create the required tetra-hydroxylated naphthalene framework[21] (**Scheme 11**). Diethyl 2,4-dimethoxybenzamide **95** was regioselectively formylated using *ortho*-lithiation with subsequent dimethylformamide quenching to provide formylbenzamide **96**. Treatment of **96** with hydrochloric acid and acetic acid facilitated the intramolecular cyclization to give 3-hydroxy-5,7-dimethoxyphthalide **97**. Phthalide **97** was converted to cyanophthalide **98** with potassium cyanide. With the required cyanophthalide **98** in hand, the Hauser annulation was now possible. The cyanophthalide **98** was reacted with *sec*-butyllithium (to generate a carbanion) and ethyl acrylate (a Michael acceptor) to deliver the desired tetra-oxygenated naphthalene **99**.

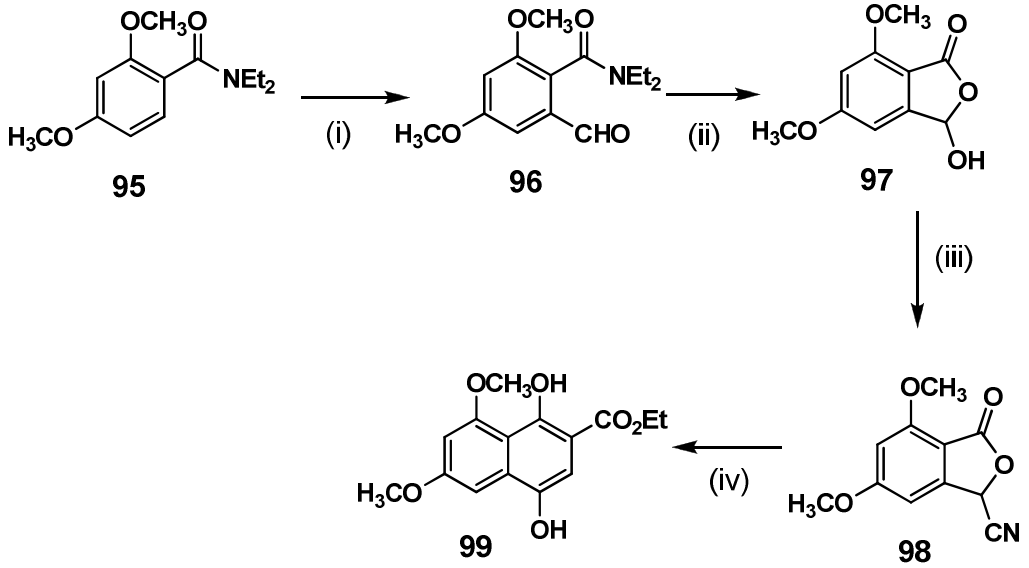

Scheme 11: *Reagents and conditions: (i) ^{t}BuLi, THF, -78 °C, then DMF, 99 %; (ii) CH_3CO_2H, 10 % HCl, reflux, 85 %; (iii) KCN, conc. HCl, 0 °C then rt, 85 %; (iv) ^{s}BuLi, THF, -78 °C, ethyl acrylate, -78 °C, 54 %.*

2.1.2.2. Staunton-Weinreb annulation

The Staunton-Weinreb annulation process (**Scheme 12**) is fashioned around a reaction discovered independently by Weinreb and Staunton during their investigations on the synthesis of polyketide natural products[22]. A substrate structural requirement for the Staunton-Weinreb annulation is the presence of an

alkoxy substituent *ortho* to the ester of for example **100** to allow formation of the intermediate chelate **101**. The chelated species **101** reacts with enone **102** to give enolate **103** which leads to annulation product **104**. The exact sequence of steps for the transformation of **103** to **104** is still uncertain.

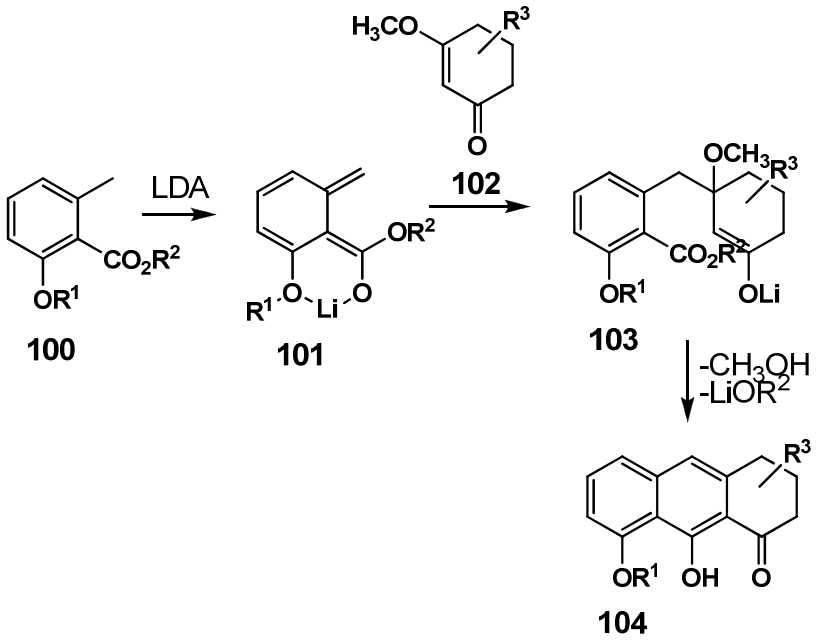

Scheme 12

A recent study towards the synthesis of naphthoquinones by Brimble and co-workers produced an efficient route to dehydroherbarin **31**[23] (**Scheme 13**). The starting materials lactone **105** and aromatic coupling partner **106** were synthesized from 4-hydroxy-6-methyl-2*H*-pyran-2-one and 2,4-dihydoxy-6-methylbenzoate respectively. Staunton-Weinreb annulation of **105** and **106** afforded naphthol **107** in a low yield of 27 %. Naphthol **107** was treated with diisobutylaluminium hydride to facilitate reduction and hydrogenation of the lactone functionality to form isochromene **108**. Oxidation of **108** with salcomine **109** under an oxygen atmosphere produced dehydroherbarin **31**.

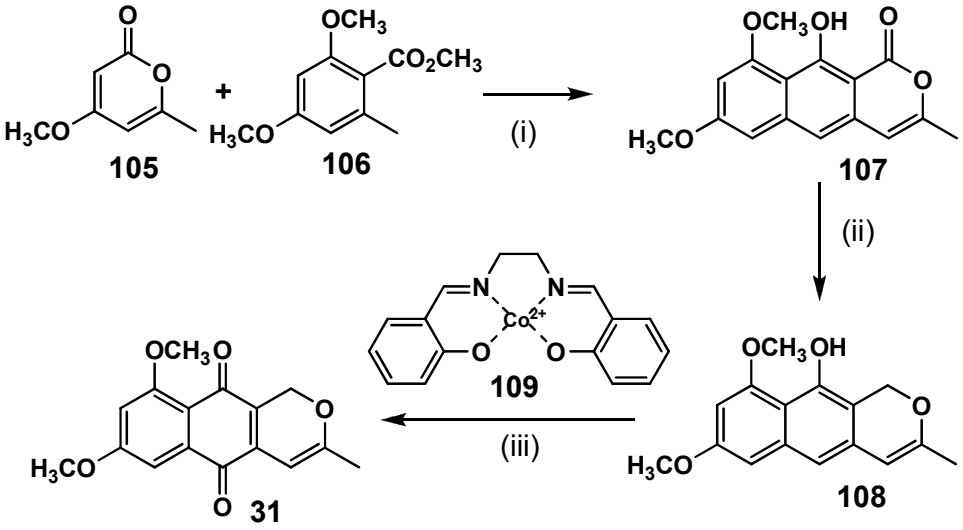

Scheme 13: *Reagents and conditions: (i) LDA, THF, -78 °C to rt, 27 %; (ii) DIBAL-H, THF, rt, 67 %; (iii)* ***109****, O_2(g), CH_3CN, rt, 72 %.*

2.1.2.3. Evaluation of annulation reactions towards hydroxylated naphthoquinones

The Hauser and Staunton-Weinreb annulation reactions both have considerable strengths when applied to the synthesis of hydroxylated naphthoquinones. They both allow for the regioselective introduction of a varied number of oxygenated substituents to the naphthoquinone framework. However, both these reactions also have their pitfalls. In the Hauser annulation, the formation of the phthalide (such as **98**) may not be a trivial process and includes multiple steps, some of which are carried out a low temperature and may require the use of the highly toxic compound potassium cyanide. The Staunton-Weinreb annulation is limited only to systems that have alkoxy groups adjacent to an ester and can be problematic when stereogenic centres are present in the enone (such as **105**) fragment[22]. Thus the use of these reactions comes with caution (Hauser annulation) and structural limitations (Staunton-Weinreb annulation).

2.1.3. Formylation/peroxide oxidation

Another creative approach to polyhydroxylated naphthalene systems is the introduction of a formyl group through the use of the Vilsmeier–Haack reaction that

can be sequentially transformed into a phenol or naphthol substituent under Baeyer-Villiger conditions[24]. An example of this was employed in an investigation towards the synthesis of hybocarpone (**Scheme 14**). The starting naphthalene **110** in this pathway already possesses a pentamethoxynaphthalene core that was derived by means of a Diels-Alder reaction, and thus its synthesis will not be covered. The Vilsmeier-Haack formylation of naphthalene **110** afforded the 1,2,4,6,8-pentamethoxynaphthalene-5-aldehyde **111**. Exposure of the aromatic aldehyde **111** to acidic hydrogen peroxide produced the 2,3,5,7-tetramethoxy-1,4-naphthoquinone **112** in a 72 % yield. The reductive methylation of the naphthoquinone **112** gave the hexamethoxynaphthalene **113**.

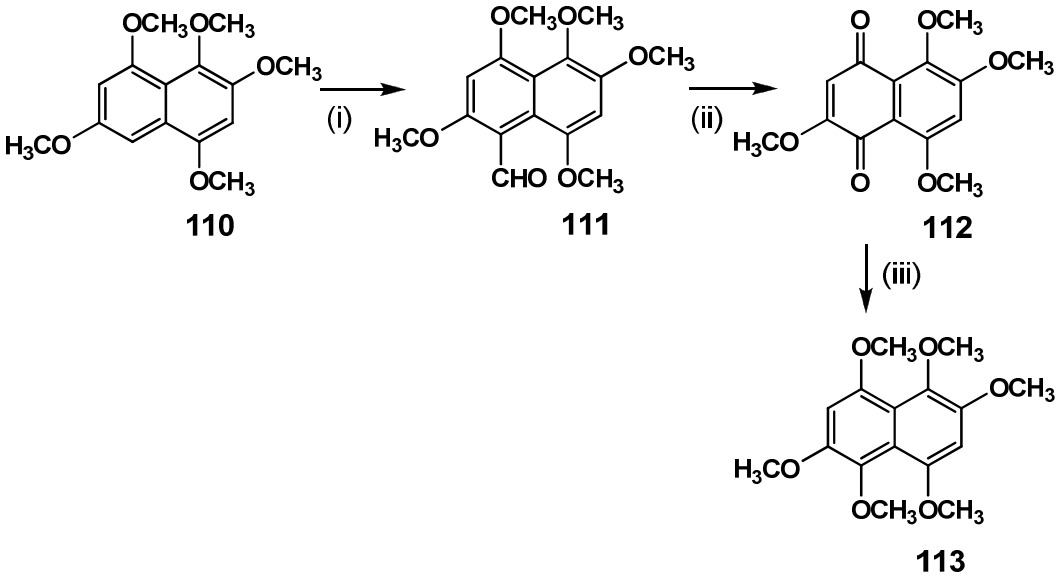

Scheme 14: *Reagents and conditions: (i) $POCl_3$, DMF, CH_2Cl_2, then NaOAc, H_2O, 83 %; (ii) H_2O_2, H_2SO_4, CH_3OH, 72 %; (iii) Na_2SO_4, Me_2SO_4, KOH, NBu_4Br, THF, H_2O, rt, 74 %.*

2.1.4. Phenolic para-oxidation via oxidants/catalysts

Another route to polyoxygenated naphthoquinones is the oxidation of the *para*-position relative to a phenolic (or naphtholic) substituent (**Scheme 15**). This strategy is commonly used in the synthesis of natural products[25-28] and is usually carried out late in the synthesis. This oxidation can be achieved via a vast array of reagents, including: salcomine[29], Fremy's salt[24], $Ph_2Se_2O_3$[30], ceric ammonium nitrate[9],

hypervalent iodide compounds[31] [PIFA, $PhI(OAc)_2$, $PhI(CF_3CO_2)_2$], thallium nitrate[4] and by a Jones oxidation. It often occurs that more than one of the oxidants must be tested to achieve the desired oxidation reaction, if at all. These kinds of oxidations are notoriously difficult and often give *ortho*-oxidized products[31,32].

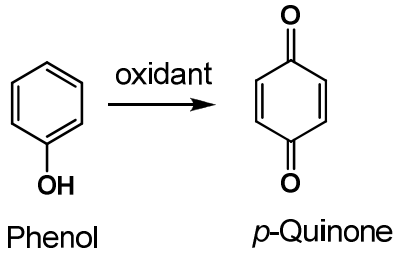

Scheme 15

2.1.4.1. Phenyliodine bis(trifluoroacetate) para-methyl-ether insertion

The hypervalent iodine reagent phenyliodine bis(trifluoroacetate) (PIFA) was mentioned in the previous section (**2.1.4**) as an oxidant that can be used for the regioselective *para*-oxidation of phenols. The typical PIFA oxidation procedure requires a source of oxygen, and thus water is used as a co-solvent for this purpose[31,32]. An example of this is shown in **Scheme 16** where the naphthol **114** is oxidised to the pseudohydroxyquinone equivalent **115** with PIFA.

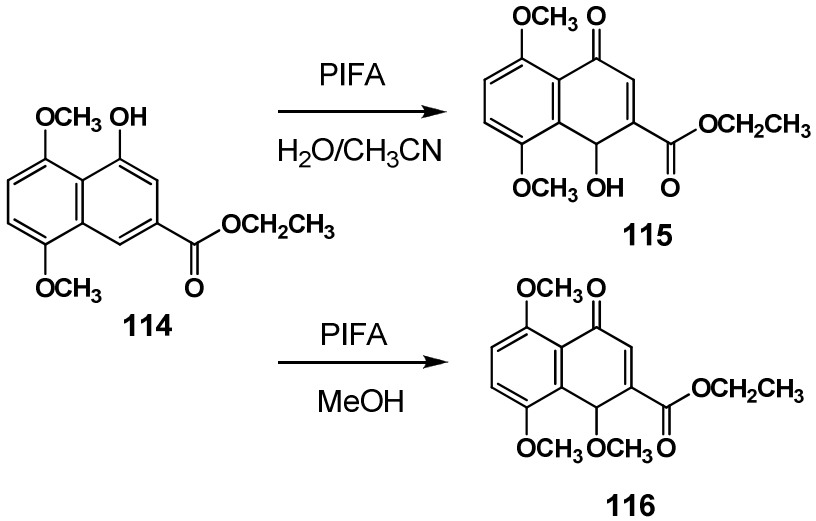

Scheme 16

A major flaw of this oxidation is that yields are very low (often less then 50 %) and an acidic iron(III) solution (for oxidation of pseudohydroxyquinone) is often necessarily added to facilitate the formation of the desired quinone moiety. A discovery was recently made by Kozlowski and co-workers[32] that showed that methanol could be utilized instead of water as an oxygen source (**Scheme 16**). This finding allowed for the regioselective insertion of an aromatic methyl-ether group onto the naphthalene ring **114** forming pseudomethoxyquinone **116**. This process directly resulted in significantly higher yields of the desired product (more than 80 %). Effectively this is the addition of a nucleophile (methanol) to an electron rich oxygenated aromatic system.

2.2. Selected Syntheses of Naturally Occurring Fused-Cyclic Acetals

Fused cyclic acetals constitute the structural framework of few natural products (see section 1.3), but these complex ring systems have induced considerable interest in synthetic chemists. The principle of cyclic acetal formation is actually a simple process and the most common example of this is illustrated in **Scheme 17**[33].

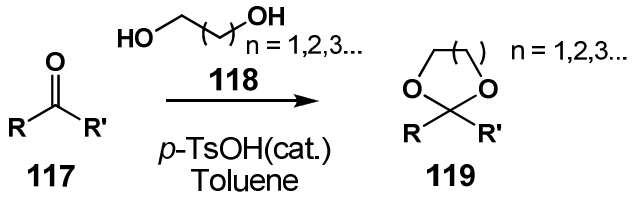

Scheme 17

Acetals are often utilized as carbonyl protecting groups for aldehydes and ketones in synthetic organic chemistry. The reaction of a carbonyl compound such as **117** with a diol **118** in the presence of a Brönsted or Lewis acid catalyst results in the formation of an acetal/dioxane **119**. A typical procedure employs *para*-toluenesulfonic acid as a catalyst in refluxing toluene, which allows for the continuous removal of water from the reaction mixture using a Dean-Stark apparatus. A mixture of *o*-esters or molecular sieves can also provide effective water removal through chemical reaction or physical sequestration respectively. Cyclic acetals offer stability against many types of nucelophiles and bases. Deprotection is

carried out by (i) acid catalyzed transacetalization in acetone or (ii) hydrolysis in wet solvents or aqueous acid.

2.2.1. Synthesis of cyclic acetals via Wacker-oxidations

As mentioned in the previous paragraph, acetal formation requires a diol and a carbonyl compound. This is easily achieved for carbonyl protection purposes when this reaction process is intermolecular. However, with regards to natural product cyclic pyran systems, the acetal synthesis is intramolecular in nature and creating three reactive functionalities in close proximity is synthetically difficult. Ideally, one would envisage the timely introduction of an intramolecular carbonyl group, such as a ketone, into a system with two alcoholic groups primed for nucleophilic attack, and hence acetal formation.

The Wacker oxidation was discovered in 1958 and involves the oxidation of ethylene **120** to acetaldehyde **121** using palladium(II) chloride as a catalyst and copper(II) chloride as the sacrificial oxidant under an oxygen atmosphere[34] (**Scheme 18**). This reaction was extended to more complex olefins and it was found that in general, terminal alkenes **122** were transformed into methyl ketones **123**, as opposed to aldehydes.

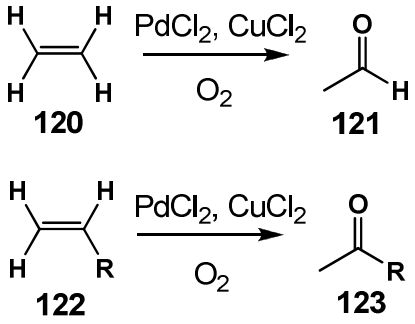

Scheme 18

Thus, the Wacker oxidation is a reaction that allows for planned introduction of a ketone functional group and has consequently been used extensively in the creation of cyclic acetals.

Isagarin **48** was synthesized by Ploysuk et al. in 2007 in five steps[35] (**Scheme 19**) using the Wacker oxidation as a key step in their synthesis. 2-Bromonaphthoquinone **124** was allylated at C-3 by a radical allylation process using vinyl acetic acid and ammonium persulfate in aqueous acetonitrile forming the allylated naphthoquinone **125**. Reductive methylation of naphthoquinone **125** with tin(II) chloride and dimethyl sulfate afforded methyl-ether protected naphthoquinone **126**. Treatment of **126** with *n*-butyllithium (allowing for a bromine-lithium exchange) and the O-silyl protected aldehyde **127** at low temperature provided naphthoquinone **128**. Desilylation of naphthoquinone **128** with tetra-*n*-butylammonium fluoride, followed by a Wacker oxidation gave the cyclic acetal compound **129** in good yield (71 %). Ceric(IV) ammonium nitrate oxidative demethylation of cyclic acetal naphthoquinone **129** afforded isagarin **48** as a racemic mixture. This is the only example of this type of Wacker oxidation on an aromatic substrate.

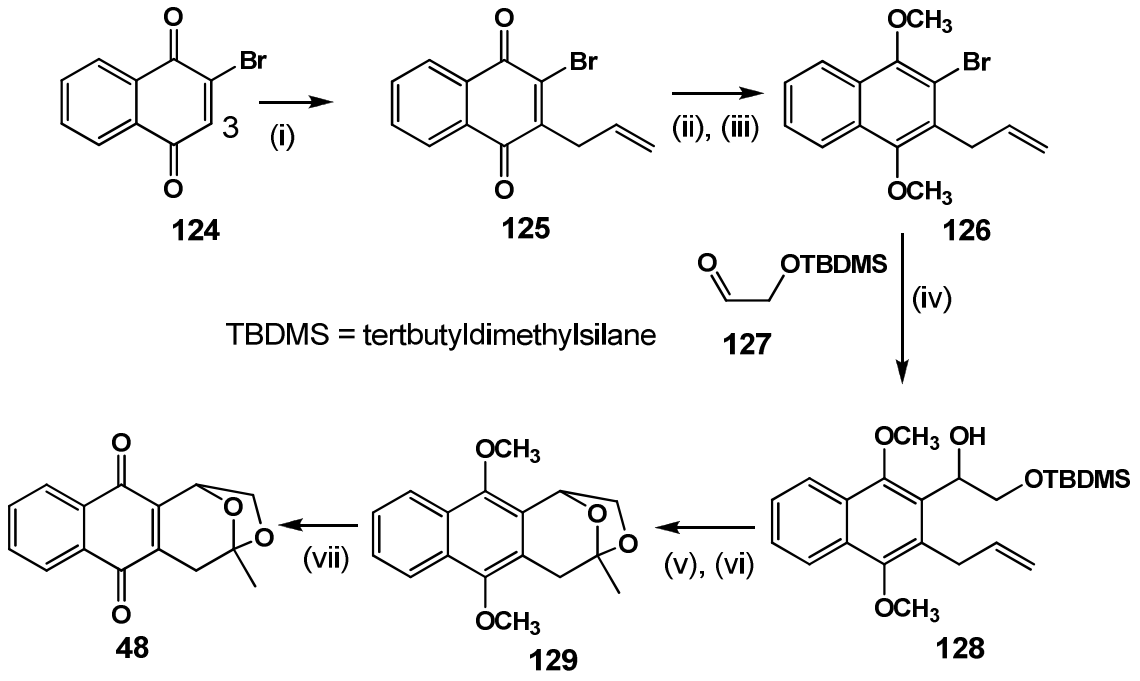

Scheme 19: *Reagents and conditions: (i) vinyl acetic acid, $(NH_4)_2S_2O_4$, $AgNO_3$, CH_3CN/H_2O, 60-70 °C, 72 %; (ii) $SnCl_2$, HCl, EtOH, 50 °C; (iii) Me_2SO_4, KOH, 65 °C, 75 %; (iv) ^nBuLi, THF, -78 °C, then* ***127****, 70 %; (v) TBAF, THF, rt, 87 %; (vi) $PdCl_2$, $CuCl_2$, O_2, DME, 65 °C, 71 %; (vii) CAN, MeCN, H_2O, rt, 95 %.*

The synthesis of the degradation products of daphniphyllum alkaloids (which are aliphatic bicyclic acetals) was conducted by Kongkathip and co-workers in 1999[36] (**Scheme 20**). Reduction of synthesized ester **130** produced triol **131,** which underwent intramolecular ketalization under Wacker oxidation conditions to yield acetal **132** in a 63 % yield over two steps. The bicyclic acetal **132** consists of a 6,5-fused bicyclic ring system.

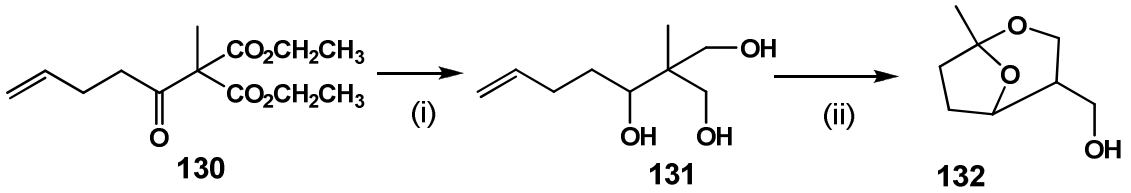

130 131 132

Scheme 20: *Reagents and conditions: (i) LAH, rt; (ii) $PdCl_2$, $CuCl_2$, O_2, DME, 65 °C, 63 % (over 2 steps).*

In the synthesis of amberketal and a homologue[37], Kongkathip and colleagues subjected diol **133** to a Wacker oxidation affording the 5,6-fused bicyclic ring system **134** (**Scheme 21**).

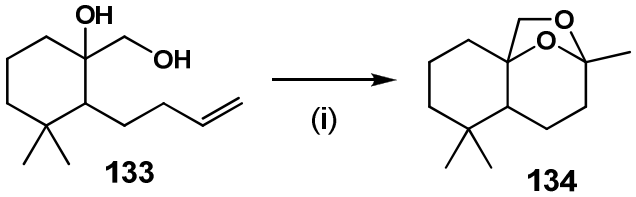

133 134

Scheme 21: *Reagents and conditions: (i) $PdCl_2$, $CuCl_2$, O_2, DME, 65 °C, 55 %.*

In a short synthesis of a bark beetle pheromone, the aliphatic 1,2-diol **135** was oxidised under Wacker oxidative conditions to yield the desired cyclic acetal brevicomin **136** in a 45% yield[38] (**Scheme 22**). Brevicomin **136** also possesses a 5,6-fused bicyclic ring system.

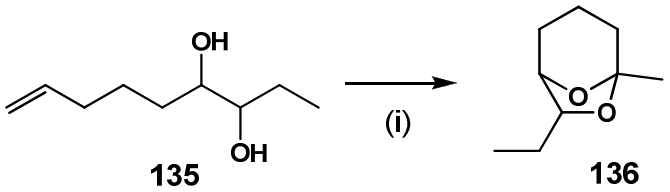

Scheme 22: *Reagents and conditions: (i) $PdCl_2$, $CuCl_2$, O_2, DME, 65 °C, 45 %.*

In yet another synthesis the target compound was a potent attractant of the striped ambrosia beetle, *Trypodendron lineatum* OLIV[39]. The final step of the synthetic pathway was the oxidation of the diastereomeric alkene system **137** with palladium(II) chloride and copper(II) chloride in anhydrous tetrahydrofuran (**Scheme 23**). A mixture of the desired cyclic acetals; endo-**138** and exo-1,3-dimethyl-2,9-dioxabicyclo [3.3.1] nonane **139** was formed in a 50 % yield.

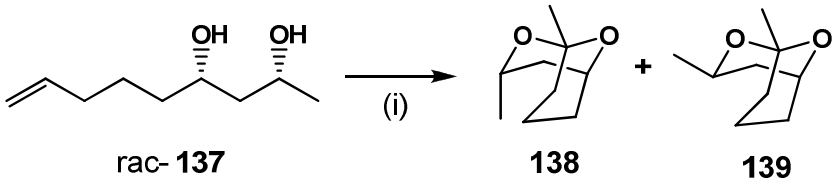

Scheme 23: *Reagents and conditions: (i) $PdCl_2$, $CuCl_2$, O_2, THF, rt, 50 %.*

The formal total synthesis of (-)-saliniketals was investigated by Yadav *et al*. in 2009[40]. One of the salient features of their synthesis was an intramolecular Wacker-type oxidation. Advanced intermediate 1,3-diol **140** was treated with $PdCl_2$ and $CuCl_2$ in tetrahydrofuran under an oxygen atmosphere to form [3.2.1]-dioxabicycle **141** (**Scheme 24**).

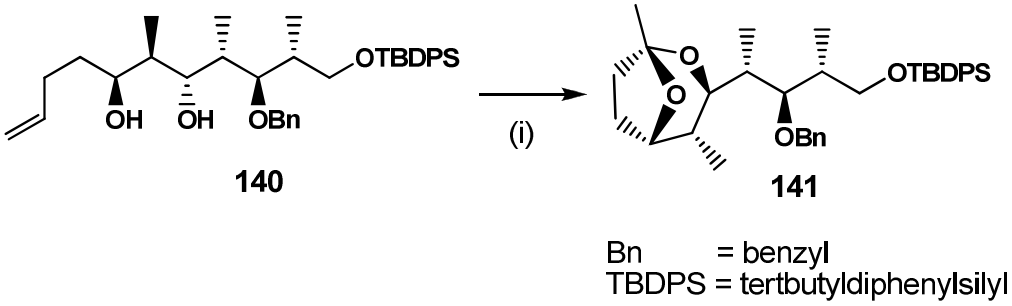

Scheme 24: *Reagents and conditions: (i) $PdCl_2$, $CuCl_2$, O_2, THF, 0 °C, 90 %.*

2.2.2. Novel methods to access cyclic acetals

Other than the Wacker oxidation reaction, there are a few other synthetic strategies that allow for cyclic acetal creation on aromatic targets that are of interest to us in this thesis. Four of these methods are reported.

The anthraquinone averufin **47** is an important intermediate in the biosynthesis of aflatoxin B_1, and Townsend *et al*. have reported its synthesis in 1988[41]. It was earlier noted (see section 1.3) that averufin **47** contains a fused 6,6-bicyclic pyran ring system. The synthetic manner by which this fragment of the compound was assembled is shown in **Scheme 25**. The benzylic aldehyde **142** was reacted with protected ketone **143**, which was pre-exposed to *n*-butyllithium (thus underwent a bromine lithium exchange), providing substrate **144**. Treatment of the protected acetal compound **144** with concentrated sulfuric acid for 24 hours facilitated selective deprotection to furnish the desired cyclic acetal **145**.

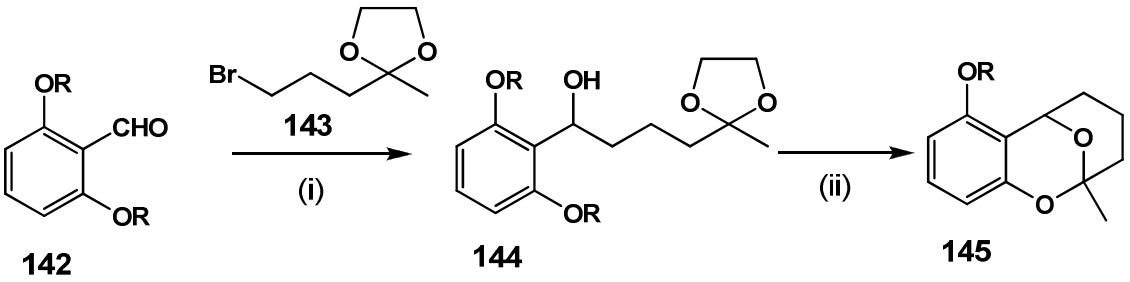

R = $-CH_2OCH_3$

Scheme 25: *Reagents and conditions: (i)* ***143,*** *^{n}BuLi, THF, -10 °C, 4 h, 89 %; (ii) H_2SO_4 conc., CH_3COOH (50 %), rt, 26 h, 67 %.*

The gold-catalyzed reactions of 2-(ynol)aryl aldehydes were investigated by Le-Ping and co-workers in 2010[42]. Benzobicyclo[*n*.3.1]acetals were produced when triazole-gold catalysts were used. 2-(6-Hydroxyhex-1-ynyl)benzaldehyde **146** was smoothly transformed into the benzobicyclo[4.3.1]acetal **147** using their gold-triazole catalyst (**Scheme 26**). The acetal **147** consists of a 6,8-fused bicyclic ring system.

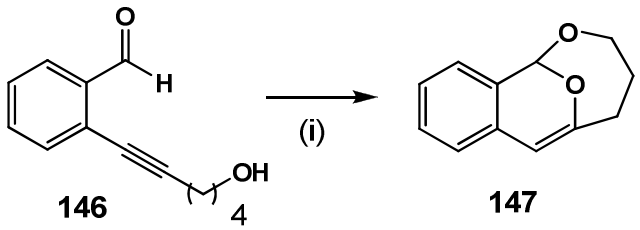

Scheme 26: *Reagents and conditions: (i)Triazole-Au (5 mol %), CH_2Cl_2, rt, 1 h, 82 %.*

The use of a 2,3-dichloro-5,6-dicyanobenzoquinone (DDQ) induced oxidative coupling of a variety of isochromans and alcohols was studied by Xu and co-workers in 1993[43]. Of particular interest in this study was the isochromane substrate **148** which was treated with DDQ to yield the aromatic fused-pyran **149** (**Scheme 27**).

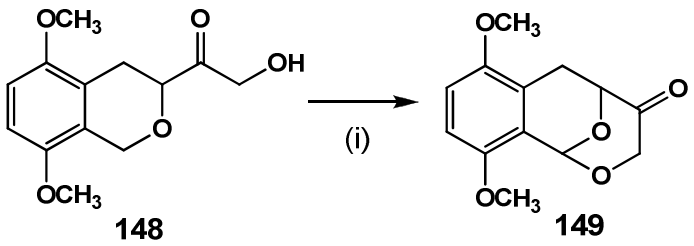

Scheme 27: *Reagents and conditions: (i) DDQ, CH_2Cl_2, rt, 70 %.*

An interesting manner to access cyclic acetals was discovered as a test reaction by Wünsch[44]. The reaction of 2-(2-bromophenyl)-acetaldehyde acetal **150** with *n*-butyllithium and aldehyde **151** produced intermediate **152**. This, in turn, was treated with hydrochloric acid to afford the 6-membered bicylic acetal compound **153** in a 42 % yield (**Scheme 28**).

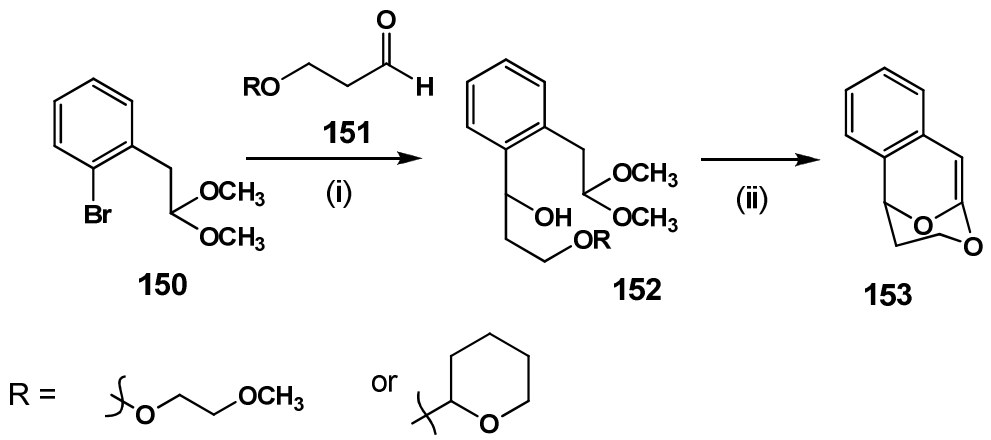

Scheme 28: *Reagents and conditions: (i) ^{n}BuLi, THF, -80 °C, 55 %; (ii) HCl, CH_2Cl_2, rt, 42 %.*

2.3. Project Goals

Based on the literature presented in the preceeding chapters, the importance of quinones and naphthoquinones both biologically and structurally is well illustrated. In addition, there is a need for further research with regards to uncovering potentially useful biological activities of the fungal naphthoquinones, many of which have not been adequately studied (see section 1.3). The isolation of the naphthoquinones from natural sources for this purpose is a possibility, but unpredictable structural variance and quantity of material greatly limit this option. Thus a promising probable route to access these desired metabolites is through synthetic means. However, there are also many problems associated with this approach (such as expensive reagents, low yields) and there is a general need for simpler, more robust synthetic pathways to access in particular the oxygenated core of some of these naphthoquinones.

Ongoing synthetic research in our laboratories has resulted in some valuable input towards the synthesis of fungal naphthoquinones. J. Oliveira had successfully completed synthetic routes to benzylic hemiacetal **154** and benzylic isochromene **155**[45] (**Scheme 29**). A comparison of these two substrates with the B and C-ring sections (see **Figure 6**) of the hemiacetals (**Table 1**) and isochromenes (**Table 2**) can render them as suitable model systems/intermediates. In Oliveira's synthesis, 2,5-dihydroxybenzoic acid **156** was allylated/methallylated to afford **157**. A Claisen

rearrangement facilitated the rearrangement of the allyl/methyallyl group to the desired C-2 position to yield **158**, which was then methylated to afford the aromatic methyl ether **159**. This protected species **159** was then reduced with lithium aluminium hydride to furnish the primary alcohol **160.** The allyl/methallyl group was then oxidized (Wacker oxidation for the allyl group/ozonolysis for the methallyl group) to afford hemiacetal **154** and isochromene **155**.

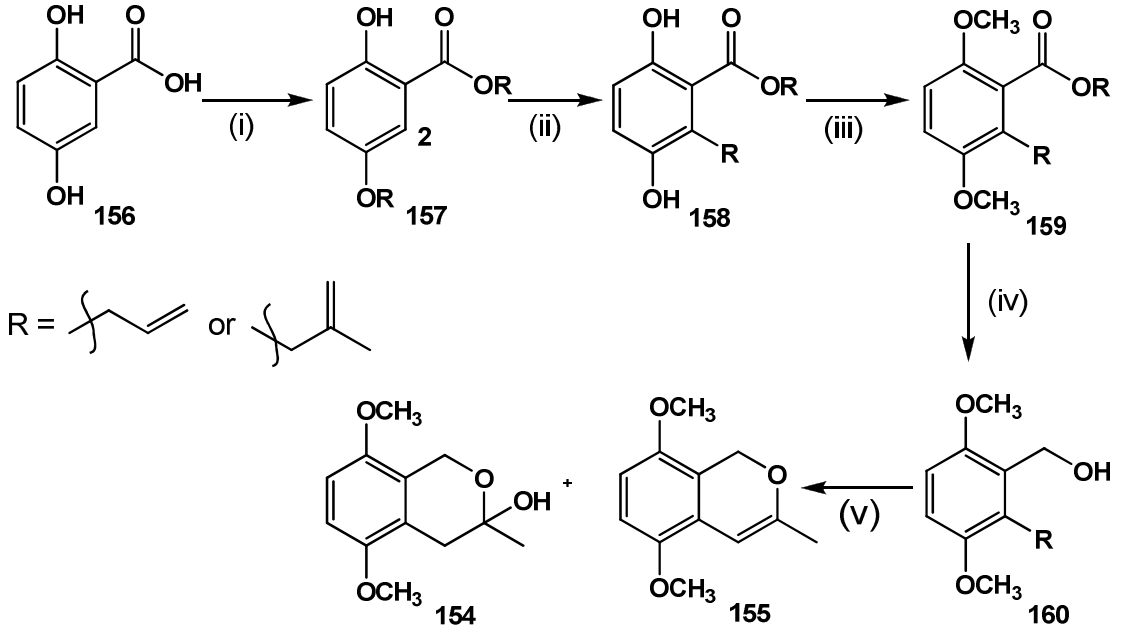

Scheme 29: *Reagents and conditions: (i) K_2CO_3, allyl bromide/methallyl chloride, Me_2CO, reflux, 84 %/50 %; (ii) neat, 170 °C/180 °C; (iii) Me_2SO_4, K_2CO_3, Me_2CO, reflux, 87 %/33 % over 2 steps; (iv) LAH (2 equivalents), Et_2O, rt, 98 %/90 %; (v) $PdCl_2$, $CuCl_2$, O_2, DMF/H_2O, rt, 50 % for **155**, 20% for **154**, or O_3, CH_3OH, -40 °C, 18 % for **155**, 81% for **154**.*

The next step forward for Oliveira was to incorporate the synthetic knowledge derived from **Scheme 29** into a more complex naphthalene system that would enable the complete synthesis of two naturally occurring naphthoquinones. This vision was nearly realised, by employing a Stobbe condensation strategy to smoothly create the desired naphthoquinone system **166** (**Scheme 30**). The Stobbe condensation of aldehyde **161** with diethyl succinate followed by cyclization with sodium acetate in acetic anhydride produced acetate **162**. The acetate of **162** was deprotected with sodium hydroxide to yield **163**, which was methallylated to form **164**

and subjected to Claisen rearrangement conditions at high temperature to furnish phenol **165**. The salcomine oxidation of this phenol produced quinone **166**, but due to low yields of the reaction no further progress was made. There was an attempt to complete the construction of ring-system C by bypassing the oxidation, and instead carrying out the protection of naphthol **165**. The naphthol **165** was protected as a methyl ether producing **167**, which was reduced with lithium aluminium hydride to yield alcohol **168**. The alcohol **168** was subjected to ozonolysis with **169** as the desired target, but unfortunately none of the desired product was isolated.

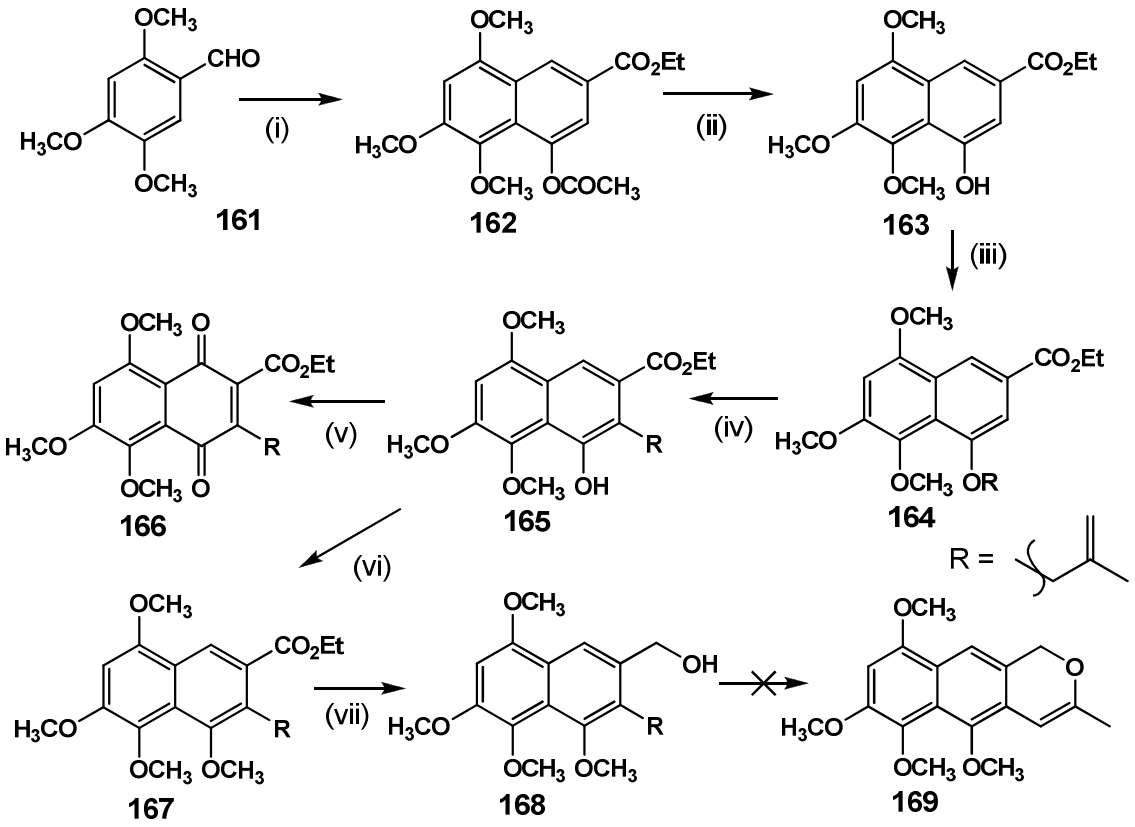

Scheme 30: *Reagents and conditions: (i) Diethyl succinate,* $KOBu^t$, ^tBuOH, reflux; NaOAc, Ac_2O, reflux, 77% over two steps; (ii) NaOH, $EtOH/H_2O$, HCl conc., 92%; (iii) *K_2CO_3, methallyl chloride, Me_2CO, reflux, 97 %; (iv) neat, 180 °C, 83 %; (v) salcomine, $O_2(g)$, DMF, 18%, (vi) Me_2SO_4, K_2CO_3, Me_2CO, reflux, 82 %; (vii) LAH (2 equivalents), Et_2O, rt, 81 %.*

Schemes 29 and **30** provided us with a foundation in the synthetic pursuit of these naphthoquinone systems for this PhD. The general aims of this project are to build on the previous research done and to complete a robust, feasible synthetic route to the fungal metabolites such as dehydroherbarin **31** and anhydrofusarubin **26**.

We also have an interest in expanding this work in creating the 6,6-bicyclic fused pyran naphthoquinone marticin **48.** There are no reported syntheses of this naphthoquinone and therefore the synthesis poses a challenging task.

2.3.1. Direct project objectives

The first objective was to create quinone equivalents of hemiacetal **154** and isochromene **155** (prepared by Oliveira), such as **170** and **171** respectively by oxidation. We then planned to carry out Diels-Alder reactions on these benzoquinones in an attempt to convert them to naphthoquinone systems (**Scheme 31**). This could be done by using a commercial diene such as 2-methoxyfuran **58** and if the reaction is successful, we could employ Brassards diene **70** in the reaction. This will allow for the addition of the "A-ring" (see **Figure 6**) with the substitution pattern found in naphthoquinones such dehydroherbarin **31** and herbarin **21**, if the regiochemistry was correct.

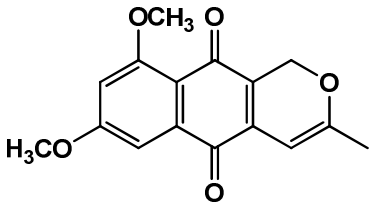

Dehydroherbarin **31**

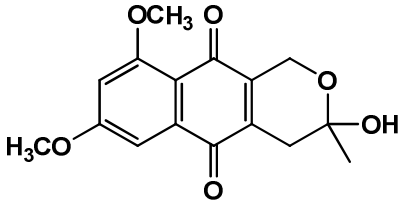

Herbarin 2**1**

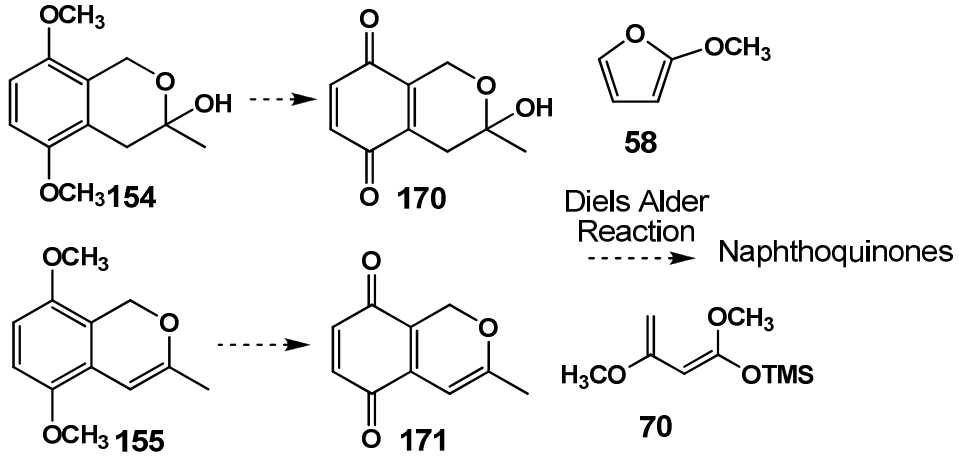

Scheme 31

The second aim of the PhD was to complete and extend the work started by Oliveira on the use of the Stobbe condensation for the synthesis of the desired naphthoquinones, starting with for example 2,4-dimethoxybenzaldehyde **172**. Dehydroherbarin **31** seemed to be a suitable naphthoquinone target for this methodology, as shown in a partial retrosynthesis outlined in **Scheme 32**. Dehydroherbarin **31** potentially could be obtained by the salcomine[23] oxidation of phenol **173**, which in turn can be formed from the deprotection of **174**. The isochromene **174** we hoped could be derived from the Wacker oxidation of alcohol **175**, which is the reduction product of ester **176**. Ester **176** could be formed from protection of phenol **177** that is made from 2,4-dimethoxybenzaldehyde **172** in four steps using Stobbe condensation methodology[27].

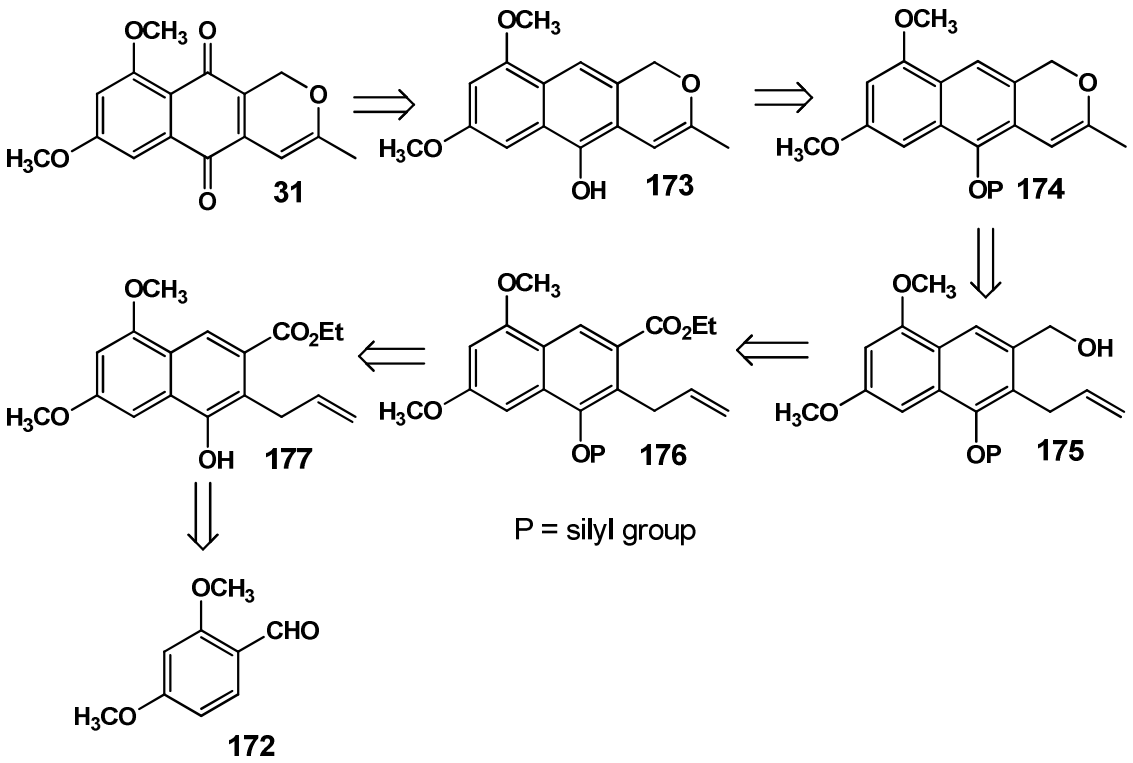

Scheme 32

The third aim of this PhD was to apply the methodology developed from the synthesis of dehydroherbarin **31** to a more highly oxygenated and related naphthoquinone target, anhydrofusarubin starting with 1,2,4-trimethoxybenzaldehyde **178** (**Scheme 33**). The synthesis of anhydrofusarubin **26** will be our objective for the following reasons: (i) the synthesis of anhydrofusarubin **26** has never been accomplished; (ii) it possesses potent anti-tumour activity and the preparation of larger amounts of material will allow for further biological studies.

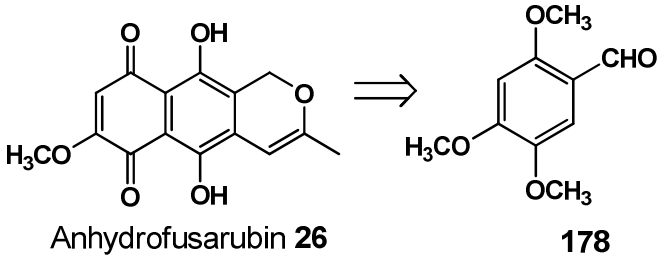

Scheme 33

The fourth aspect of this PhD to be researched would be to assemble a model system of the 6-membered bicyclic acetal skeleton found in marticin **45**. A racemic mixture of compound **179** is our initial model target (**Scheme 34**). The first retrosynthetic step led us to the 1,3-diol compound **180**, which should form **179** if subjected to a Wacker oxidation. This 1,3-diol **180** can be made from the selective reduction of the 1,3-diketone **181**. This step could be problematic as it requires the reduction of two ketone functionalities in the presence of an ester. However, in theory this should be possible by using for example a selective enzymatic procedure. The diketone could be obtained from the Claisen condensation reaction of ketone **182** with diethyl oxalate. Ketone **182** we hoped could be made from the commercially available 2,5-dihydroxyacetophenone **183** in three steps[27].

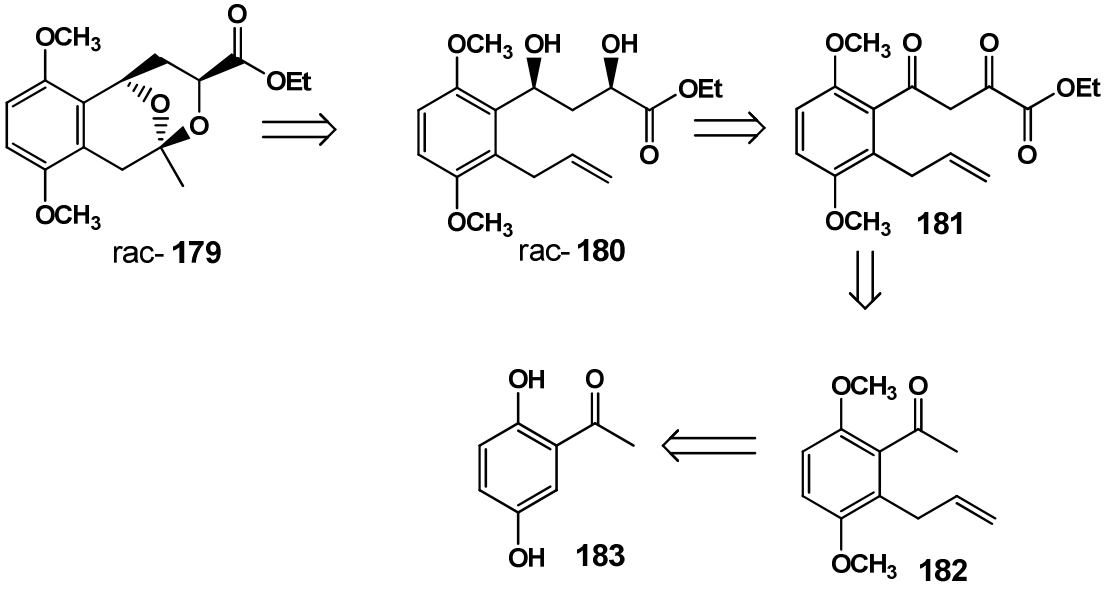

Scheme 34

Finally, and if time permitted, once the synthetic methodology to create acetal model compound **179** is established, as well a viable method for the synthesis of the pentaoxygenated naphthalene, these methods could be combined and applied to the synthesis of marticin **45** (**Scheme 35**) from **184**[10].

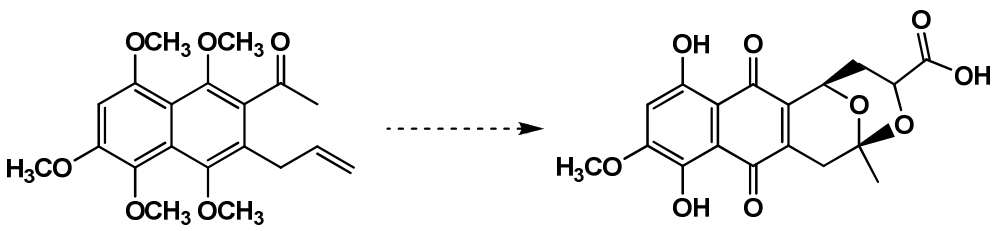

184 rac- Marticin **45**

Scheme 35

We also wish to investigate the anti-tumour activity of all target quinones where initially the potential for bioactivity will be assessed in an *in vitro* MTT assay on two colon cancer cell lines: CaCo-2 and HT-29 as well as the breast cancer cell line MCF 7 at the Medical School of our University.

2.4. References

1. Nicolaou, K.C., Snyder, S.A., Montagnon, T., Vassilikogiannakis, G., *Angewandte Chemie International Edition*, 2002, **41**, 1668-1698.
2. de Koning, C.B., Rousseau, A. L., van Otterlo, W. A. L., *Tetrahedron*, 2003, **59**, 7-36.
3. Clayden, J., Greeves, N., Warren, S., Wothers, P., *Organic Chemistry*, 2005, Oxford Univeristy Press Inc., New York.
4. Clive, D.L., Khodabocus, A., Vernon, P.G., Angoh, A.G., Bordeleau, L., Middleton, D. S., Lowe, C., Kellner, D., *Journal of the Chemical Society Perkin Transactions 1*, 1991, 1433-1444.
5. Giles, R.G.F., Green, I.R., van Eeden, N., *Synthetic Communications*, 2011, **36**, 1695-1706.
6. Baker, R.W., Baker, T.M., Birkbeck, A.A., Giles, R.G.F., Sargent, M.V., Skelton, B.W., White, A.H., *Journal of the Chemical Society Perkin Transactions 1*, 1991, 1589-1600.
7. Karichiappan, K., Wege, D., *Australian Journal of Chemistry*, 2000, **53**, 743-747.
8. Pena-Lopez, M., Martinez, M.M., Sarandeses, L. A., Sestelo, J.P., *Journal of Organic Chemistry*, 2010, **75**, 5337-5339.
9. Bergeron, D., Caron, B., Brassard, P., *Journal of Organic Chemistry*, 1993, **58**, 509-511.

10. de Koning, C.B., *The Syntheses of Some Naturally Derived Naphthoquinones*, 1987, PhD Thesis, University of Cape Town.
11. Dorn, H.W., Warren. W.H., Bullock, J.L., *Journal of American Chemical Society*, 1939, **61**, 144-147
12. Lam, T.B.T., Iiyama, K., Stone, B.A., *Phytochemistry*, 1996, **41**, 1507-1510.
13. Brasholz, M., Sörgel, S., Azap, C., Reißig, H.U, *European Journal of Organic Chemistry*, 2007, 3801-3814.
14. Bergeron, D., Caron, B, Brassard, P., *Journal of Organic Chemistry*, 1993, **58**, 509-511.
15. Heckrodt, T., Mulzer, J., *Topics in Current Chemistry:Natural Product Syntheses II*, 2005, ©Springer, Verlag Berlin Heidelberg.
16. Weimar, M., Durner, G., Bats, J.W., Gobel, M.W., *Journal of Organic Chemistry*, 2010, **75**, 2718-2721.
17. Danishefsky, S.J., *Journal of American Chemical Society*, 1974, **96**, 7807-7808.
18. Tewierik, L.M., Dimitriadis, C., Donner, C.D., Gill, M., Willems, B., *Organic and Biomolecular Chemistry*, 2006, **4**, 3311-3318.
19. Kesteleyn, B., De Kimpe, N., *Journal of Organic Chemistry*, 2000, **65**, 640-644.
20. Mal, D., Pahari, P., *Chemical Reviews*, 2007, **107**, 1892-1918.
21. Brimble, M.A., Houghton, S.I., Woodgate, P.D., *Tetrahedron*, 2007, **63**, 880-887.
22. White, J.D., Demnitz, F.W.J., Xu, Q., Martin, W.H.C., *Organic Letters*, **2008**, 10, 2833-2836.
23. Wadsworth, A.D., Sperry, J., Brimble, M.A., *Synthesis*, 2010, **15**, 2604-2608.
24. Chai, C.L.L., Elix, J.A., Moore, F.K.E., *Journal of Organic Chemistry*, 2005, **71**, 992-1001.
25. Kraus, G.A., Ogutu, H., *Tetrahedron*, 2002, **58**, 7391-7395.
26. Sperry, J., Brimble, M.A., *Synlett,* 2008, **12**, 1910-1912.
27. Mmutlane, E.M., Michael, J.P., Green, I.R., de Koning, C.B., *Organic and Biomolecular Chemistry*, 2004, **2**, 2461-2470.

28. Govender, S., Mmutlane, E.M., van Otterlo, W.A.L., de Koning, C.B., *Organic and Biomolecular Chemistry*, 2007, **5**, 2433-2440.
29. Bloomer, J.L., Stagliano, K.W., *Tetrahedron Letters*, 1993, **34**, 757-760.
30. Brząszcz. M., Kloc, K., Maposah, M., Młochowski, J., *Synthetic Communications*, 2000, **30**, 4425-4434.
31. Couladouros, E.A., Strongilos, A.T., *European Journal of Organic Chemistry*, 2002, 3341-3350.
32. Lowell, A.N., Fennie, M.W., Kozlowski, *Journal of Organic Chemistry*, 2008, **73**, 1911-1918.
33. Green, T.W., Wuts, P.G.M, *Protective Groups in Organic Chemistry*, 1999, Wiley-Interscience, New York.
34. Tsuji, J., *Synthesis*, 1984, 369-384.
35. Ploysuk, C., Kongkathip, B., Kongkathip, N., *Synthetic Communications*, 2007, **37**, 1463-1471.
36. Kongkathip, B., Sookkho, R., Kongkathip, N., Taylor, W.C., *Chemistry Letters*, 1999, 1095-1096.
37. Kongkathip, B., Kongkathip, N., Janthorn, S., Virarangsiyakorn, D., *Chemistry Letters*, 1999, 51-52.
38. Byrom, N.T., Grigg, R., Kongkathip, B., J.C.S. *Chemical Communications*, 1976, 216-217.
39. Kongkathip, B., Kongkathip, N., *Tetrahedron Letters*, 1984, **25**, 2175-2176.
40. Yadav, J.S., Hossain, S.S., Madhu, M., Mohapatra, D.K., *Journal of Organic Chemistry*, 2009, **74**, 8822-8825.
41. Townsend, C.A., Christensen, S.A., Davis, S.G., *Journal of the Chemical Society Perkin Transactions 1*, 1988, 839-861.
42. Le-Ping, L., Hammond, G. B., *Organic Letters*, 2010, **12**, 4640-4643.
43. Xu, Yao-Chang, Lebeau, E., Gillard, J.W., Attardo, G., *Tetrahedron Letters*, 1993, **34**, 3841-3844.
44. Wünsch, *B., Arch Pharm (Weinheim)*, 1990, **323**, 933-936.
45. Oliveira, J., *The Synthesis of Isochromanols. Potential Bioreductive Alkylating Agents*, 2000, PhD Thesis, University of the Witwatersrand.

Chapter 3: The Synthesis of Dehydroherbarin and Anhydrofusarubin

3.1. A Diels-Alder Approach to Naphthoquinones

Our initial approach for the assembly of the oxygenated naphthoquinone system was to build onto the work started by Oliveira[1]. We envisaged carrying out Diels-Alder reactions on the quinone equivalents of the aromatic compounds hemiacetal **154** and isochromene **155**, in other words the benzoquinones **170** and **171** respectively (**Scheme 31**).

3.1.1. Deprotection of dimethyl ethers

The desired aromatic dimethyl ether hemiacetal **154** and isochromene **155** were both synthesized based on the reported methodology[1]. The ceric ammonium nitrate deprotection of the aromatic dimethyl ethers presented itself as the simplest first approach for the preparation of benzoquinones[2]. The ceric ammonium nitrate (CAN) -mediated oxidation process proved successful, and benzoquinones **170** and **171** were furnished as dark red amorphous solids in yields of 55 % and 63 % respectively (**Scheme 36**).

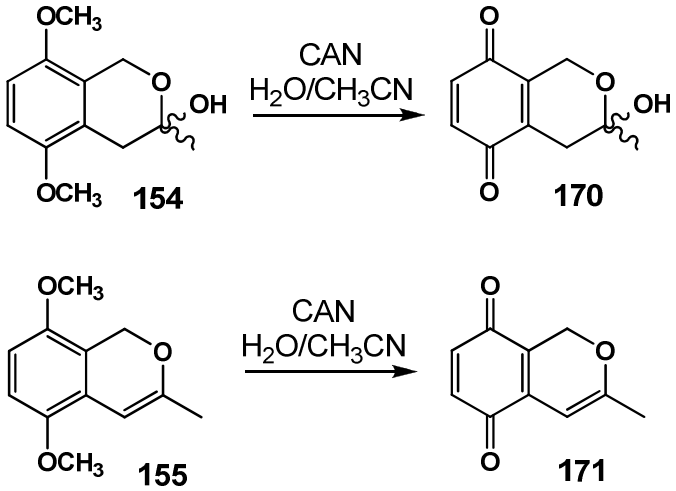

Scheme 36

The reaction conditions for the oxidation were the same for both substrates. An aqueous solution of CAN was added dropwise to the aromatic dimethyl ethers **154** and **155** which were dissolved in acetonitrile. The reaction progress was visible as the lightly coloured solution intensified to an orange solution, signalling the formation of a quinone chromophore *in situ*.

The formation of the benzoquinones **170** and **171** was confirmed spectroscopically, using ^{1}H NMR, ^{13}C NMR and IR spectroscopy. The ^{1}H NMR spectra of **170** and **171** displayed no aromatic methoxy-ether peaks, which was the first clear sign that the oxidation reaction had been successful. The ^{1}H NMR spectrum of **170** showed the quinone protons, each as a doublet at 6.71 ppm and 6.80 ppm, and the methyl group as a singlet at 1.47 ppm, as expected. The ^{13}C NMR and IR spectra for both compounds confirmed the presence of the newly formed quinone nuclei. The two carbonyl signals for the hemiacetal quinone **170** (187.4 ppm and 186.7 ppm) and isochromene quinone **171** (184.8 ppm and 184.2 ppm) were present in the ^{13}C NMR spectra. There was also an absence of signals arising from aromatic methyl ethers in both cases in the ^{13}C NMR spectra. The IR spectral data clearly depicted carbonyl stretching frequencies at 1738 cm^{-1} and 1654 cm^{-1} for the hemiacetal quinone **170** and 1652 cm^{-1} and 1600 cm^{-1} for the isochromene quinone **171**.

3.1.2. Attempted Diels-Alder reaction of benzoquinones

With the desired benzoquinones in hand, the next step was to utilize the Diels-Alder reaction to form the required naphthoquinone derivative. Use of these quinone compounds as dienophiles represents a classical approach to the Diels-Alder reaction for two reasons: (i) the quinone contains no halogen atom which controls regioselectivity[3] when an unsymmetrical diene is employed and (ii) there is no possibility of the formation of a highly reactive benzyne[4] intermediate which greatly improves the reaction time. These 'classical' Diels-Alder reactions are notoriously slow and chlorinated or benzene-like solvents are normally used[5,6]. The first reaction tested was the reaction using equal molar equivalents of isochromene quinone **171** and symmetrical diene, furan **64,** in dichloromethane stirred at room temperature. We anticipated the potential formation of the naphthoquinone adduct **185** as shown

in **Scheme 37**. After 72 h, with no visible change in the reaction, the mixture was refluxed with continuous monitoring by TLC. There was still no visible product formation by TLC and as the boiling point of the diene furan **64** is only 32 ºC, there was no point changing to a higher boiling solvent, unless it was a sealed tube reaction.

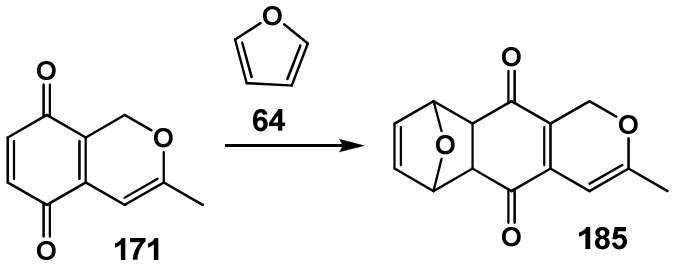

Scheme 37

Repeating the reaction with dienophile **170** and furan **64** was also not successful. The diene was therefore changed to 2-methoxyfuran **58** with a higher boiling point. If successful, the combination of hemiacetal quinone **170** and 2-methoxy furan **58** would form regioisomeric adducts **186** (**Scheme 38**).

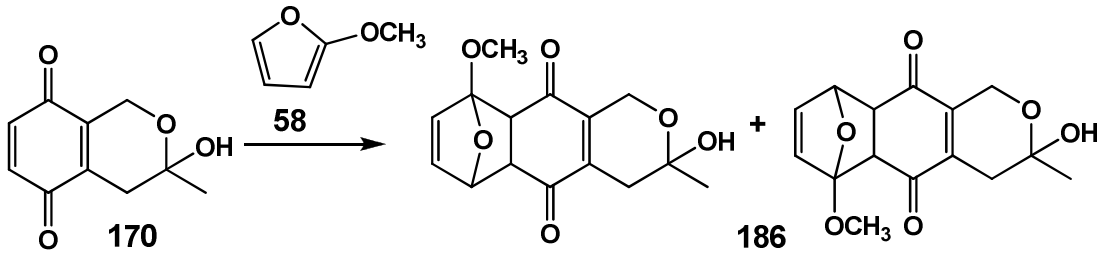

Scheme 38

This reaction appeared more promising as the reaction mixture rapidly changed colour upon addition of the diene **58** in dichloromethane. However, work-up and purification of the mixture showed that all that had occurred was decomposition and all the starting material was consumed. Carrying out the reaction at lower temperatures (0 ℃ to -40 ℃) made no impact on minimising the observed decomposition. Once again a similar fate was observed when using isochromene quinone **171**. Using chloroform as a solvent, either at ambient temperature or at reflux, did not result in reaction for either dienophile, however no decomposition was

observed in these cases. The next solvent that was used was dichlorobenzene. When dienophile **170** and 2-methoxyfuran **58** were refluxed in dichlorobenzene an orange compound formed. Unfortunately attempts to purify this product by column chromatography were disappointing as the orange material decomposed when exposed to silica.

At this point it was deemed acceptable to abandon this Diels-Alder route and move towards the next planned approach to the synthesis of the required oxygenated naphthoquinones.

3.2. Synthesis of Dehydroherbarin and Unusual Analogues

The second synthetic route we planned to employ towards building the naphthalene skeleton of dehydroherbarin **31** was based on Stobbe condensation methodology, followed by a Friedel-Crafts acylative cyclisation reaction to generate the naphthalene nucleus. This approach for the assembly of naphthalene systems has been implemented with high success as described in the literature[7,8].

3.2.1. Naphthalene core construction

The Stobbe condensation reaction (**Scheme 39**) commences with a base-promoted (usually potassium *tert*-butoxide) enolization of a succinate ester, that subsequently acts as a nucleophile by attacking a ketone or aldehyde producing an alkylidenesuccinic acid[9]. For our purposes, we used diethyl succinate **187** and sodium ethoxide as the base, and 2,4-dimethoxybenzaldehyde (**172**) as the electrophile. The reaction was carried out in refluxing tetrahydrofuran for 2 h, followed by treatment with hydrochloric acid that is required to first neutralize the unreacted sodium ethoxide and protonate the *cis*-alkylidene acid **188**.

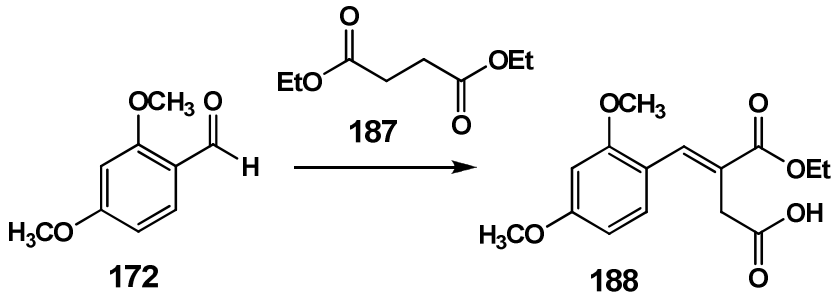

Scheme 39

The acid **188** was isolated by solvent extraction and immediately subjected to conditions for the naphthalene ring-forming process (**Scheme 40**), which was achieved by subjecting **188** to refluxing acetic anhydride in the presence of sodium acetate for 3 h.

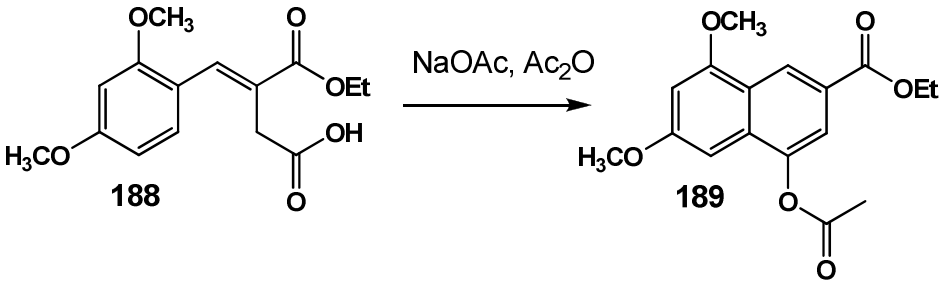

Scheme 40

This Friedel-Crafts acylative procedure resulted in the formation of the desired naphthalene skeleton **189** in a good yield of 83 % over two steps. The ^{1}H NMR spectrum clearly displayed four *meta*-coupled (J = 1.1 to 1.9 Hz) aromatic protons between 6.5 and 8.8 ppm, confirming the presence of the correctly substituted naphthalene core. The ester side chain was also shown to be present by a characteristic quartet at 4.42 ppm and accompanying triplet at 1.42 ppm that integrated for two and three protons respectively. The singlet integrating for three protons at 2.47 ppm indicated the presence of the acetate group. The ^{13}C NMR spectrum contained two carbonyl peaks at 169.3 and 166.3 ppm corresponding to both ester carbonyls. The two aromatic methyl ether moieties gave rise to signals at 55.4 and 55.8 ppm. These findings were in accordance with the literature spectroscopic data for this compound[7].

3.2.2. Pyran ring system assembly

With the required basic naphthalene core (compound **189**) in place, the next stage was the construction of the unsaturated pyran ring system. By retrosynthesis the isochromene **174** can be disconnected to give the primary alcohol **175** (**Scheme 41**). We believed that **174** could be synthesized from **175** by means of a Wacker oxidation reaction. Compound **175** could be obtained from naphthalene **189** by the introduction of an allyl group at position C-2 of **189** followed by the reduction of the ester group of **189** into a primary alcohol.

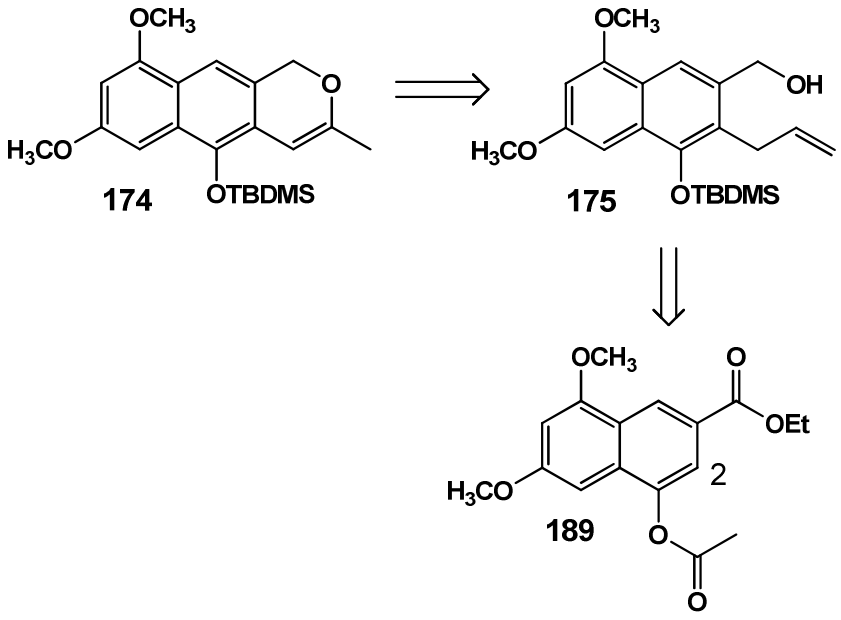

Scheme 41

3.2.2.1. Allyl chain introduction

We planned to introduce an allyl moiety at position C-2 of naphthalene **189** *via* a Claisen rearrangement from an adjacent naphthol, but we first needed to remove the acetate group and replace it with an allyl chain. Thus, the next step in our synthesis was the hydrolysis of the acetoxy functionality in naphthalene **189** under basic conditions (**Scheme 42**). Substrate **189** was dissolved in methanol, treated with an aqueous solution of potassium hydroxide and stirred for 6 h at room temperature. We also expected the saponification of the ethyl ester group under these conditions. On completion of the reaction, organic solvent was removed and the residue was

acidified with hydrochloric acid to form the intermediate **190**. Naphthalene **190** was not purified but was immediately dissolved in dry acetone and heated under reflux in the presence of potassium carbonate and excess allyl bromide to produce diallylated naphthalene **191** as a yellow solid in an 83 % yield over two steps (**Scheme 42**).

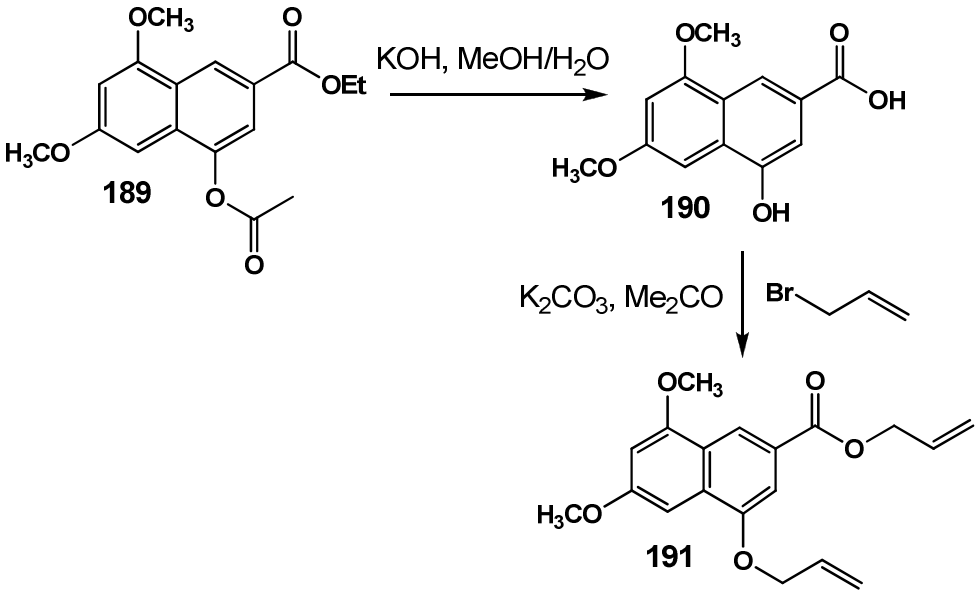

Scheme 42

The ^{1}H NMR spectrum of **191** lacked the ester and acetate signals observed in the spectrum of the precursor, but included six new signals that indicated the introduction of two allyl groups. A multiplet at 6.14 ppm could be assigned to two overlapping vinylic CH groups. The signals for the ester and aryl ether chain vinylic CH_2 protons were observed at 5.25 ppm and 5.39 ppm respectively. The methylene protons of the ether allyl chain were found at 4.74 ppm as a doublet (J = 5.2 Hz), which was upfield from the ester allyl chain methylene protons that were assigned as a doublet of triplets (J = 5.6 and 1.3 Hz) at 4.86 ppm. Six new signals were visible in the ^{13}C NMR spectrum also corresponded to the presence of two allyl groups. Vinylic CH signals were observed at 133.2 ppm ($OCH_2\mathbf{C}H=CH_2$) and 132.6 ppm ($COOCH_2\mathbf{C}H=CH_2$), with the two vinylic CH_2 signals upfield at 118.0 ppm ($O\mathbf{C}H_2CH=CH_2$) and 117.6 ppm ($COO\mathbf{C}H_2CH=CH_2$). Lastly the methylene carbon signals were both found in the expected region (50-70 ppm[10]), at 69.2 ppm ($OCH_2CH=\mathbf{C}H_2$) and 65.5 ppm ($COOCH_2CH=\mathbf{C}H_2$).

With the required aromatic *O*-allyl substituent in place we could now carry out the sigmatropic Claisen rearrangement by heating the aromatic diallyl compound **191** neat at 180 °C for 18 h (**Scheme 43**). The reaction proceeded smoothly, affording a product (**192**) with increased polarity, implying the presence of a free naphthol.

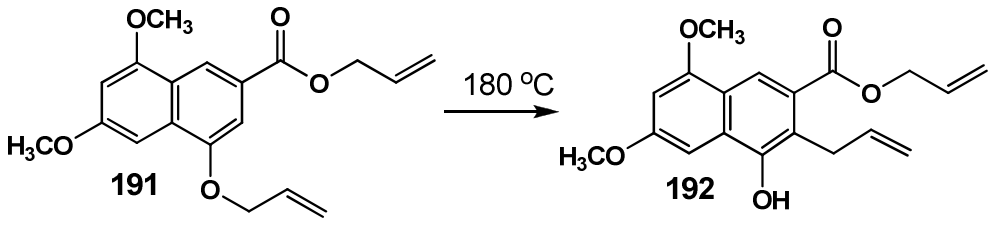

Scheme 43

The ^{1}H NMR spectrum of the product displayed only three aromatic signals as expected, (i.e. one less than the precursor) and the appearance of a D_2O exchangeable naphthol proton signal at 5.84 ppm. The allyl chain methylene protons shifted significantly upfield to 3.94 ppm as the allyl chain had shifted from oxygen to carbon which also marked the reaction's success. The ^{13}C NMR spectrum also contained clear evidence of the naphthol allyl group migration, as the C-allyl CH_2 group appeared at 31.7 ppm compared to at 69.2 ppm in the starting material. This substantial upfield shift correlates to the allyl moiety being attached to the naphthalene ring *via* a carbon-linkage and no longer *via* an oxygen-linkage. The presence of the naphthol hydroxyl group was observed in the IR spectrum as a broad peak at 3539 cm^{-1}. The mass spectrum of **192** confirmed the same molecular ion as the parent compound **191** as expected.

The next step towards the synthesis of the isochromene precursor **174** required the reduction of the allyl ester functionality. However, we needed to first protect the free naphthol moiety. Based on our planned subsequent synthetic conditions, we decided that a *tert*-butyldimethylsilyl (TBDMS) protecting group would suffice for the naphthol protection. Furthermore this protecting group is introduced under very mild conditions and generally in high yields[8]. Thus, the treatment of naphthol **192** with TBDMSCl, imidazole and catalytic amounts of dimethylaminopyridine (DMAP) in dry acetonitrile afforded the protected naphthol **193** in a 93 % yield (**Scheme 44**).

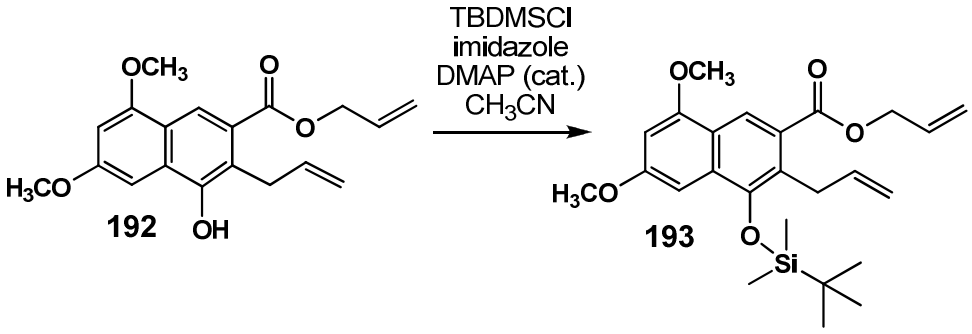

Scheme 44

The ^{1}H NMR spectrum of **193** was very indicative of the reaction's success. The appearance of methyl protons at 0.23 ppm and 1.13 ppm that integrated for six and nine protons respectively, together with the disappearance of the naphthol proton at 5.84 ppm from the starting material, all indicated that the desired product had formed. Three new signals were present in the ^{13}C NMR spectrum, which could all be assigned to the presence of a *tert*-butyldimethethylsilyl protecting group. These were at 26.1 ppm and -2.9 ppm for the methyl carbon atoms, whereas the tertiary carbon atom directly attached to the silicon atom appared at 18.8 ppm. The IR spectrum of the product lacked the free hydroxyl stretching frequency present in the IR spectrum of starting material **192**, whilst the HRMS data confirmed the mass of the desired product.

3.2.2.2. Allyl ester reduction and Wacker oxidation

With the naphthol protected, the reduction of the allyl ester of **193** to a primary alcohol could now be carried out. Excess lithium aluminium hydride was used for this conversion (**Scheme 45**), which was smoothly carried out in dry tetrahydrofuran at 0℃ to yield the desired primary alcohol **175** as a clear oil.

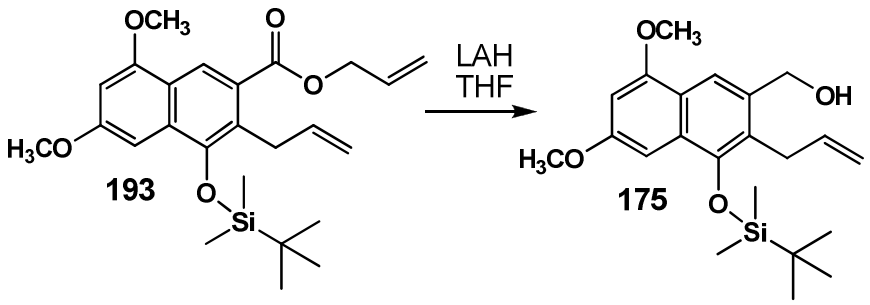

Scheme 45

The ^{1}H NMR spectrum of **175** was devoid of the three signals that corresponded to the allyl ester chain protons, but still contained the three signals of the allyl group at C-2 of the naphthalene nucleus. The emergence of a singlet at 4.79 ppm was suggestive of a benzylic CH_2 which confirmed that the allyl ester group reduction was successful. The ^{13}C NMR spectrum also showed the disappearance of three allyl ester carbon signals but a new signal at 64.4 ppm was once again indicative of a CH_2 group adjacent to an aromatic ring system. The ester carbonyl carbon atom was also absent in the ^{13}C NMR spectrum. The spectral data of the primary alcohol correlate with those reported for this compound[8].

With the aromatic primary alcohol **175** in hand, possessing an allyl chain at position C-2 of the naphthalene nucleus, the scene was now perfectly set to carry out a Wacker oxidation to create a dihydropyran ring. This ring forming process is facilitated by a palladium catalyst that enables nucleophilic attack on the proximal alkene system[11]. The exact mechanistic details of this reaction are still under investigation, but its major features are generally accepted[11] as shown in **Scheme 46**. The alkene π orbitals in naphthalene **175** coordinate to the palladium catalyst to form palladium-alkene π-complex **194**. Next, one of the chloride atoms is possibly replaced by a water molecule to give complex **195**. The *syn* addition of water to the alkene forms a (β-hydroxyalkyl)palladium complex such as **196**. The β-hydride elimination process gives enol **197** that tautomerizes to ketone compound **198**. The primary alcohol group of **175** is poised for the formation of a six-membered pyran ring, prompting the ketalisation of ketone **198**. This event is immediately followed by a dehydration reaction to afford pyran ring-containing naphthalene compound **174**. This reductive elimination of **196** forms Pd(0) and hydrochloric acid. The sacrificial

oxidant $CuCl_2$ reoxidizes Pd(0) to Pd(II) *in situ* whilst Cu(II) is reduced to Cu(I). Molecular oxygen serves as the terminal oxidizing agent for the reaction and it maintains the active catalytic system by reoxidizing Cu(I) to Cu(II).

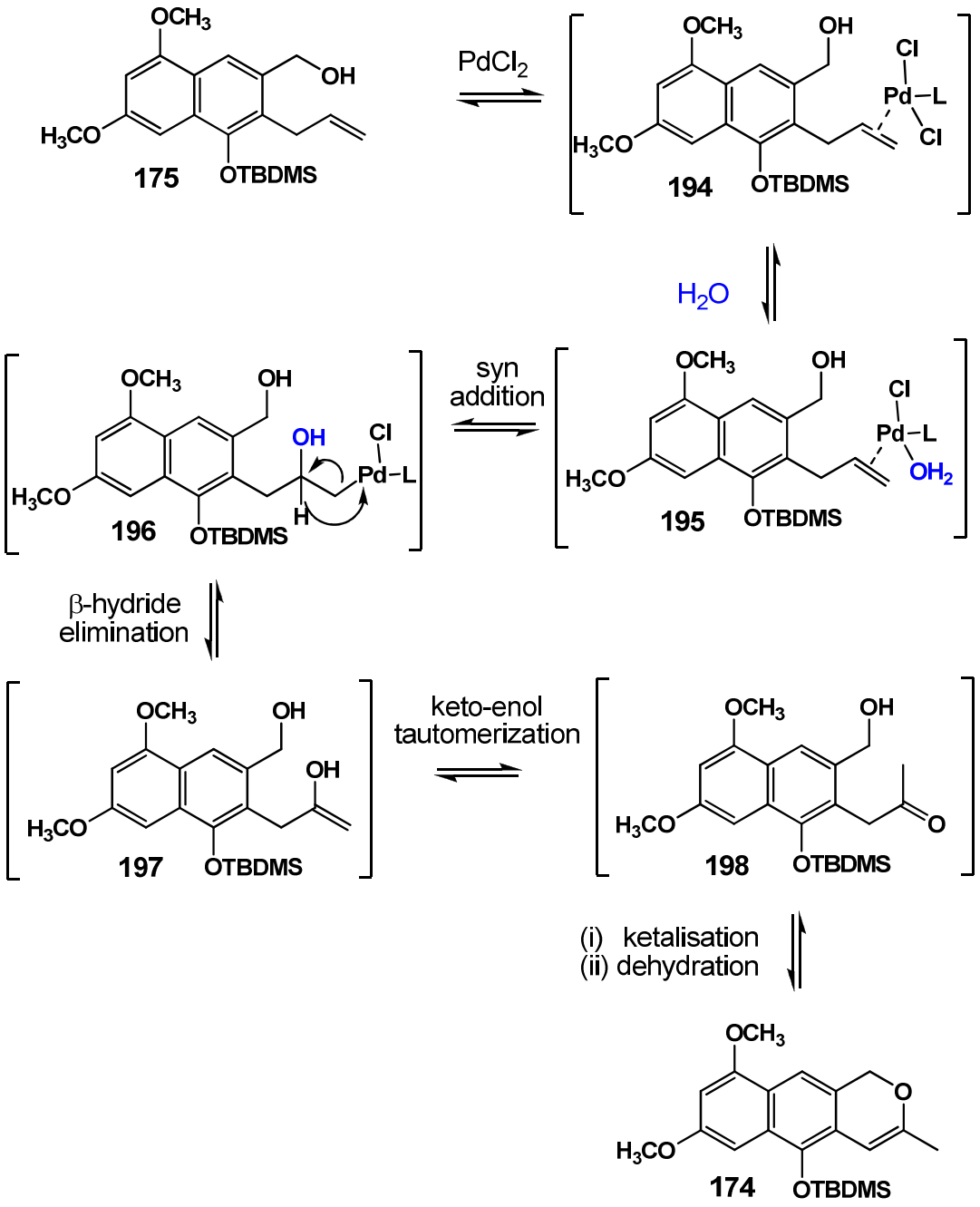

Scheme 46

The Wacker oxidation on our substrate **175** was performed in a combined dimethylformamide and water solvent system with $PdCl_2$ (0.1 equivalent) catalyst

and $CuCl_2$ (1.0 equivalent) under an oxygen atmosphere. The mixture was stirred vigorously for a much longer duration (24 h) compared to normal reaction times[12] (2 h) due to the low solubility of the strongly non-polar species **175**. The isochromene product **174** was afforded in a moderate yield of 52 %, with the remainder of the material being unreacted starting material.

Given that isochromene compound **174** was the only isolated product, and with no expected ketone intermediate species **198** present, we propose that the Wacker oxidation reaction of our substrate proceeds *via* a different path compared to the one presented in **Scheme 46**. The strongly nucleophilic primary benzylic alcohol oxygen atom undergoes an intramolecular attack (**Scheme 47**) of the electrophilic palladium-alkene π-complex **194** to yield intermediate **199** which undergoes β-hydride elimination to give **200**. The alkene group of compound **200** rearranges to a lower energy isomer, which is the isochromene **174**. It should be noted that a similar reaction was reported by S. Pelly in her PhD thesis[9].

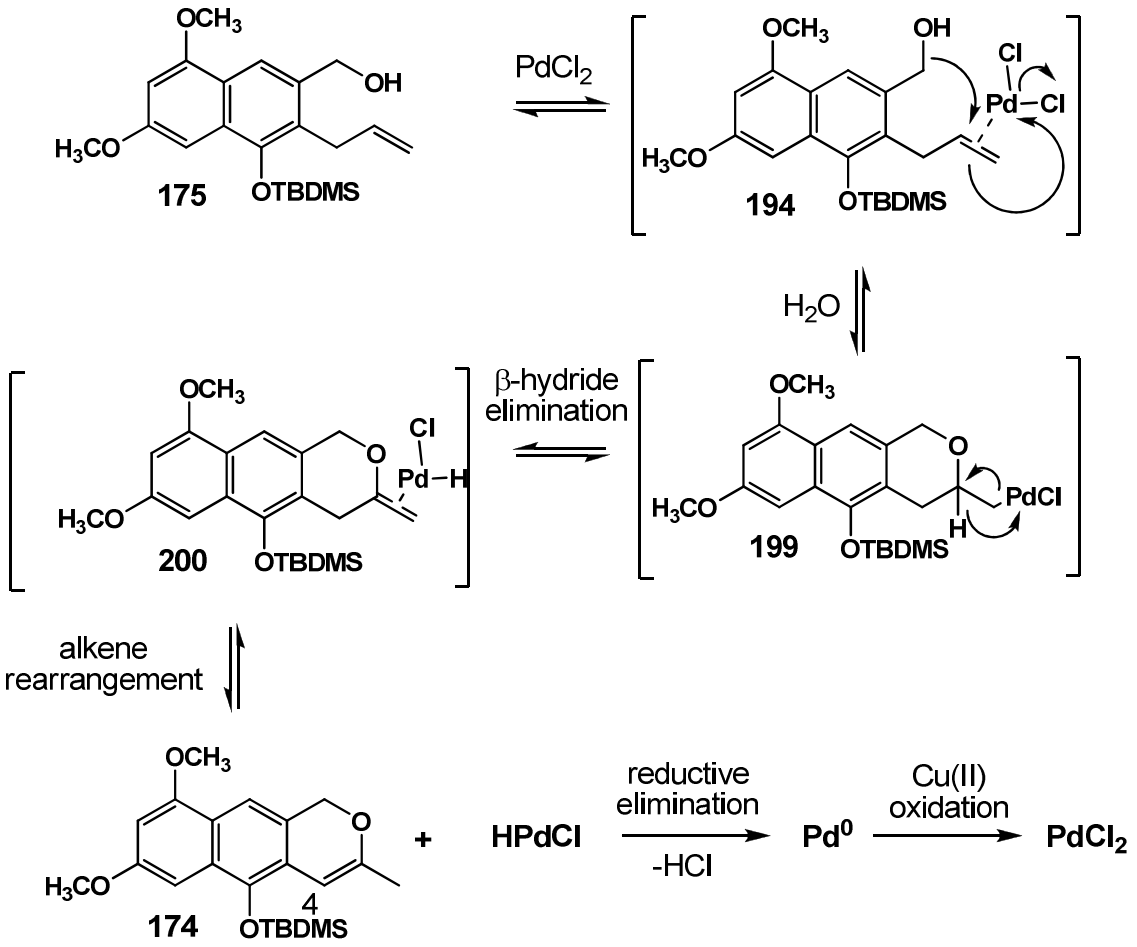

Scheme 47

The structure of the pyran ring containing compound **174** was confirmed by the spectral data. The ^{1}H NMR spectrum of **174** lacked the three C-2 allyl chain proton signals but instead displayed the isochromene proton (at C-4) and isochromene methyl protons (at C-3) at 6.02 ppm and 2.05 ppm respectively. The rest of the ^{1}H NMR spectrum was concordant with that of the parent molecule, affirming that the protected naphthalene system remained intact. In the ^{13}C NMR spectrum the presence of a methyl carbon atom at 19.2 ppm, methine carbon at 97.8 ppm and C-3 considerably upfield at 156.5 ppm confirmed the existence of the isochromene system. There was also a visible downfield shift of the benzylic CH_2 group from 64.4 ppm in the parent compound to 69.3 ppm in the product. The HRMS data for the product was found to be 387.1984 amu which was in accordance with the calculated value of 387.1992 amu for a molecular formula of $C_{22}H_{31}O_4Si$.

3.2.3. Naphthoquinone formation

Now that the naphthalene core and pyran ring system of dehydroherbarin **31** were constructed, the last phase was to oxidize the naphthalene system to a naphthoquinone. This first required the removal of the TBDMS protecting group, followed by the implementation of a selective *para*-oxidation reagent.

3.2.3.1. *tert*-Butyldimethylsilyl deprotection

The selective removal of a TBDMS alcohol protecting group is a fairly trivial procedure[13] which simply entails treating the TBDMS protected compound **174** with *tetra*-n-butylammonium fluoride in dry tetrahydrofuran at ambient temperature (**Scheme 48**). The expected deprotected phenol **173** was isolated as a white crystalline solid that displayed increased polarity on silica gel TLC compared to the starting material.

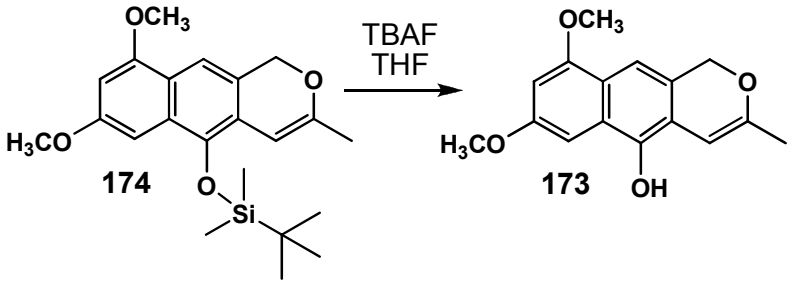

Scheme 48

The ^{1}H NMR spectrum of **173** closely resembled that of the parent compound **174** as expected, but lacked the two signals corresponding to the TBDMS group. A new naphthol proton signal emerged at 7.94 ppm. The existence of this moiety was also supported by the hydroxyl stretching frequency at 3348 cm^{-1} visible in the IR spectrum. The ^{13}C NMR spectrum of **173** also confirmed that the TBDMS removal was successful as the three signals responsible for this group were absent.

3.2.3.2. Salcomine naphthoquinone oxidation

With compound **173** available, the last step was the oxidation of the naphthol to a *para*-naphthoquinone as found in the target compound dehydroherbarin **31** (**Scheme 49**).

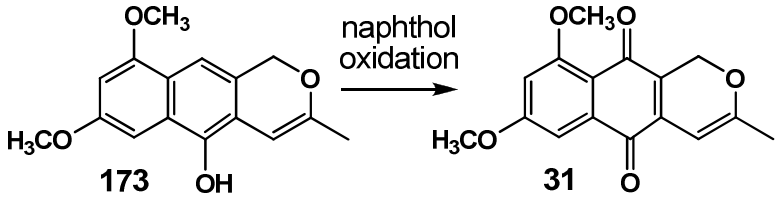

Scheme 49

We envisaged that this oxidation reaction could be achieved by employing the salcomine catalyst **109**, *N,N'*-bis-(salicylidene)ethylenediaminocobalt(II). This commercially available oxidation reagent has been shown in the literature to successfully carry out this process on a variety of naphthol systems[7,14-16]. However, the desired oxidation reaction did not occur with our substrate **173.** Instead, the salcomine catalyst **109** facilitated the oxidation of the enol ether of the pyran ring to produce dicarbonyl **201** (**Scheme 50**). This was an unexpected result as the catalyst **109** has never before been shown to perform an oxidation reaction of this type. The reaction was then carried out in dimethylformamide, which is another solvent used for salcomine oxidations, but unfortunately this led to the same undesired product **201** being formed.

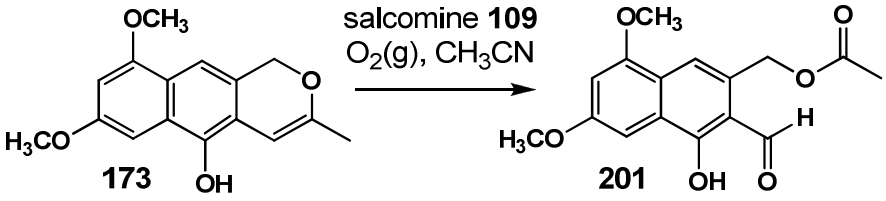

Scheme 50

We postulated that the isochromene ring, which is a "disguised" enol-ether system, is electron rich and thus more susceptible to oxidation. The acetate and aldehyde functional groups in the product support this idea, implying that an "ozonolysis-like" reaction had occurred at the alkene enol ether moiety.

The spectroscopic data of **201** was markedly different to that of the expected product dehydroherbarin **31** and starting material **173**. The ^{1}H NMR spectrum of **201** contained three naphthalene protons as found in the precursor compound, depicting that the *para*-oxidation did not occur as this would involve the disappearance of one of these aromatic signals. An acetate methyl signal appeared at 2.09 ppm, as well as an aldehyde peak at 10.26 ppm. The naphthol hydrogen displayed a significant downfield shift to 13.49 ppm (also with improved signal intensity) owing to hydrogen bonding to the adjacent aldehyde group. In the ^{13}C NMR spectrum, the absence of the pyran ring was confirmed by the lack of the three peaks contributing to the dehydrated isochromene system. The appearance of the acetate methyl carbon atom shift at 21.0 ppm and two carbonyl signals as 170.4 ppm and 195.2 ppm reinforced our proposed structure of product **201**. The IR spectrum contained a broad hydroxyl stretching band and two sharp carbonyl bands at 1737 cm^{-1} and 1620 cm^{-1}, which correlate with compound **201**. Fortunately, we were able to crystallize the salcomine oxidation product, and hence X-ray crystallography confirmed the structure of the compound (**Figure 9**).

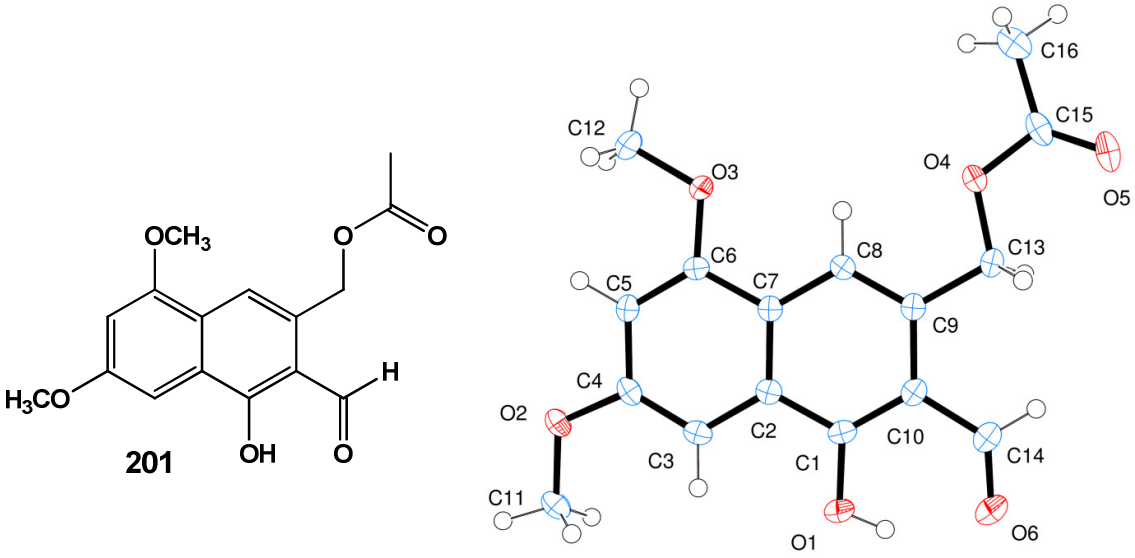

Figure 9

3.2.3.3. Ceric ammonium nitrate naphthoquinone oxidation

Since the salcomine oxidation reaction was unsuccessful we opted to test other selective *para*-oxidizing agents. Ceric ammonium nitrate (CAN) is commonly used

for the demethylation of aromatic *para*-dimethyl ether systems[2]. This reagent has also been demonstrated to oxidize electron-rich naphthols to their respective naphthoquinone equivalents[17]. Thus, we attempted the desired oxidation reaction shown in **Scheme 49** by employing CAN as the oxidant. The reaction was carried out in an acetonitrile/water solvent system, to afford a product that we initially believed to be dehydroherbarin **31**, but was later spectroscopically determined to be naphthoquinone **202** (**Scheme 51**).

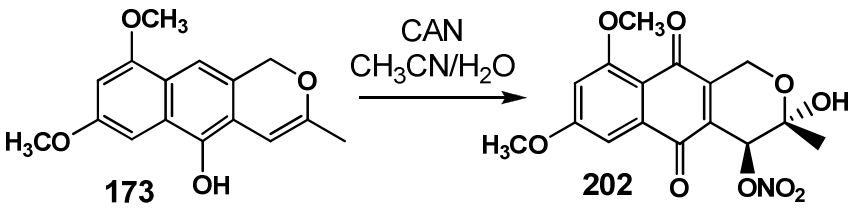

Scheme 51

Our initial confusion regarding the reaction was that both the ^{1}H NMR and ^{13}C NMR spectral data of compound **202** were very similar to those of dehydroherbarin **31**[18]. The ^{1}H NMR spectrum of **202** contained only two major differences to that of parent compound **173**: (i) there are two aromatic protons present that display *meta*-coupling (J = 2.4 Hz) which implies that oxidation to the naphthoquinone had worked and (ii) the isochromene methyl group shifted upfield by 0.4 ppm to 1.57 ppm. These findings were in close accordance with dehydroherbarin **31**. The hydrogen atom at C-4 appeared at 6.00 ppm. The quinone functionality was clearly observed in the ^{13}C NMR spectrum of **202** as carbonyl signals appeared at 183.3 ppm and 180.6 ppm, likewise in dehydroherbarin **31**. The only two considerable irregularities between the ^{13}C NMR spectra of naphthoquinone **202** and dehyrohebarin **31** were the shifts of C-3 (95.9 ppm in **202** and 161.5 ppm in **31**) and C-4 (73.3 ppm in **202** and 93.8ppm in **31**). Overall this data suggested that the structure of the product was similar to that of the target compound, but contained substantial structural differences across the alkene functionality.

An X-ray crystal structure of our product **202** (**Figure 10**) gave the conclusive evidence we required.

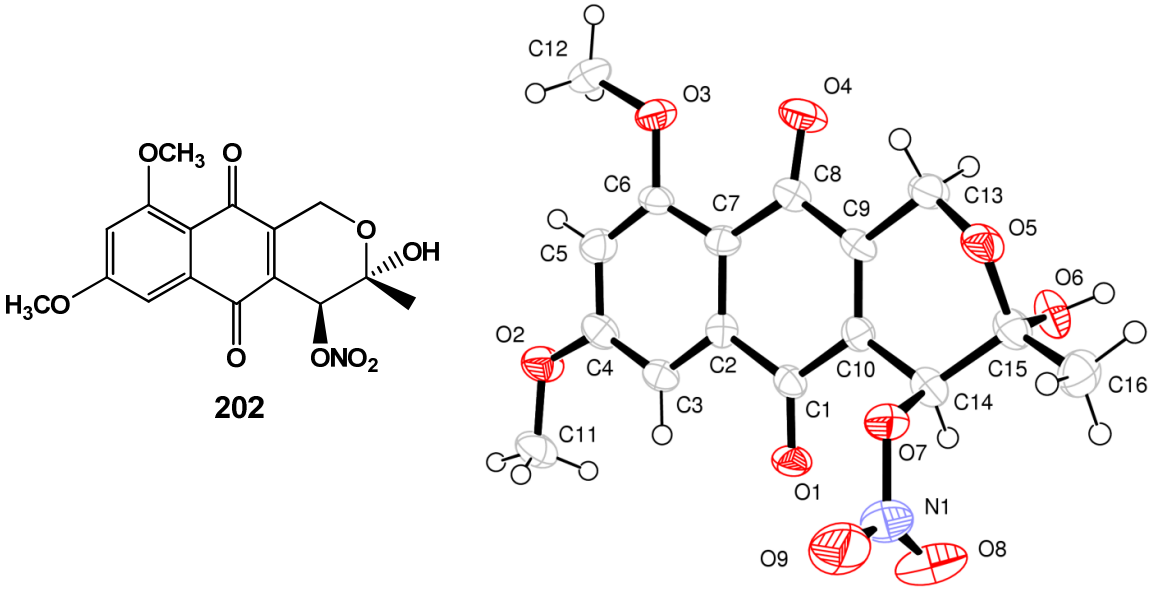

Figure 10

The crystal structure confirmed that the oxidation of the phenolic moiety to a quinone was successful, but there was also evidence that the enol ether ring system had once again undergone a reaction. The isochromene functionality was now absent and a nitrate moiety and a hydroxyl functionality had added across the alkene.

This bizarre reaction was undesired but fascinating none-the-less. There was some literature precedence[19] for this “nitration” reaction and the mechanistic postulate is outlined in **Scheme 52**. We propose that the nitration/hydration process occurs before oxidation to the quinone. The first step is the single electron oxidation of the alkene of **173** by CAN which furnished radical cation species **203**. It is reasonable to assume that the radical centre becomes hydrated to form the hemiacetal **204**. The cationic site of **204** could be quenched by a nitrate anion from CAN to yield intermediate **205**, which then undergoes a formal oxidation by CAN of the naphthol to form the isolated product **202**.

Compound **202** was found to be stable to mildly acidic solutions and could be stored at room temperature without any traces of decomposition.

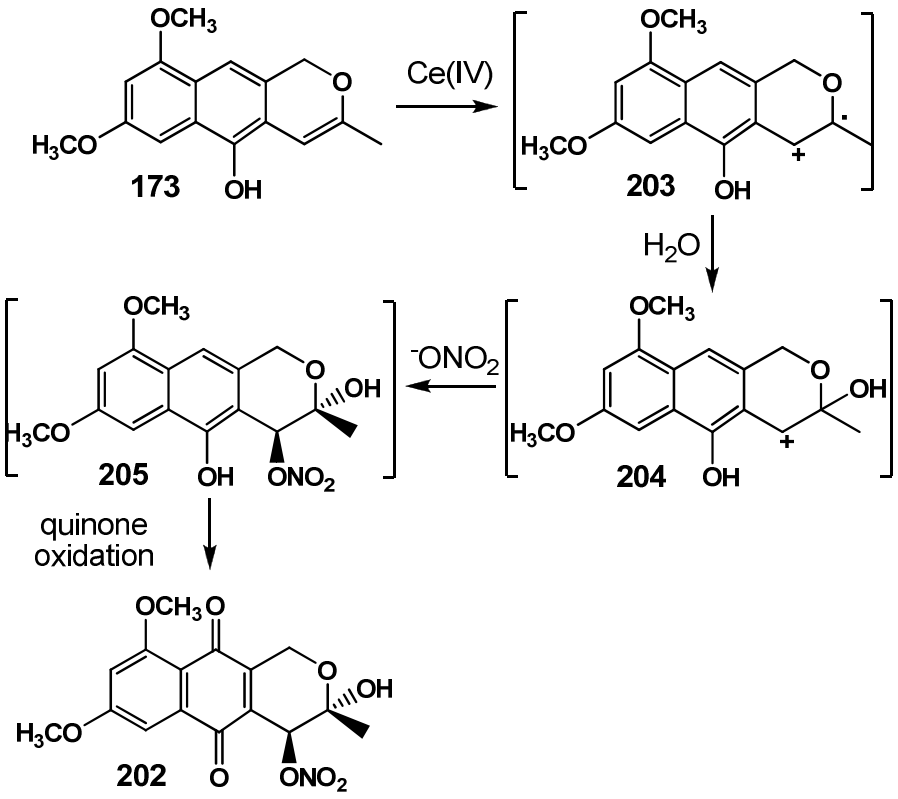

Scheme 52

3.2.4. Tetraoxygenated naphthalene system formation

Given our inability to oxidize naphthol **173** to our target naphthoquinone, dehydroherbarin **31**, we decided to test an alternative synthetic approach. The oxidation pattern in dehydroherbarin **31** is a 1,4,6,8-tetraoxygenated naphthalene core. Thus a logical synthetic plan would be to introduce the required oxygen substitution pattern of the naphthalene nucleus earlier in the synthesis, since this had proven to be a challenging final step.

Hence the tetraoxygenated isochromene **206** could be disconnected to aromatic allyl ester **207** (**Scheme 52**). Compound **207** we hoped could be synthesized from naphthalene **192** where extra oxygenation *para* to the naphthol would be required.

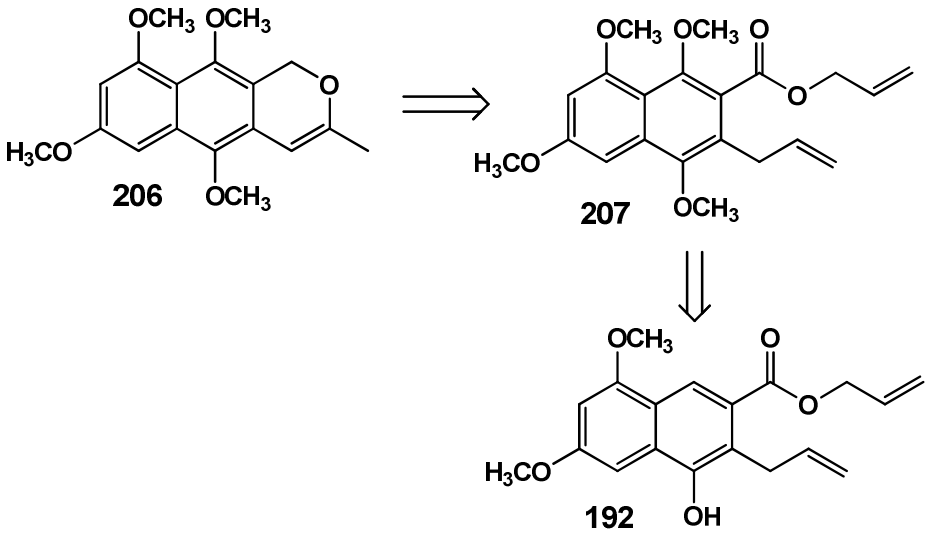

Scheme 52

3.2.4.1. Phenyliodine bis(trifluoroacetate) *para*-methyl-ether insertion

It was previously mentioned (see section **2.1.4.1**) that PIFA **208** (**Figure 11**) in methanol solvent enabled the regioselective addition of a methoxy group into a naphthol system[20]. Thus we subjected our naphthol **192** to these reagents and effectively presumably formed the pseudohydroxyquinone **209** (**Scheme 53**). This unstable compound was not isolated and was immediately exposed to sodium ethoxide base for 20 min at ambient temperature to afford the desired aromatized tetraoxygenated naphthalene system **210** in a 60 % yield over two steps.

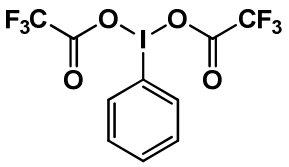

208

Figure 11

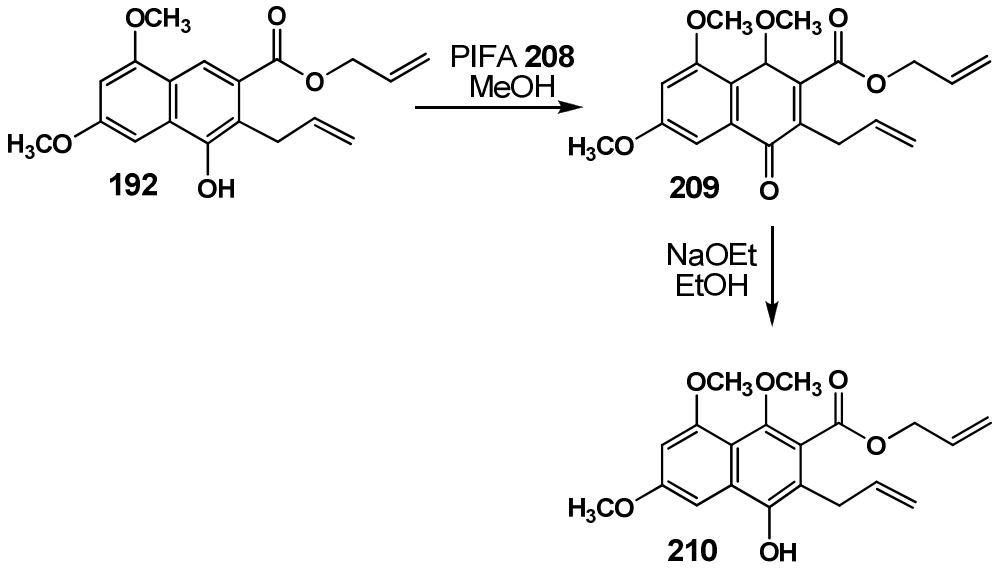

Scheme 53

The ^{1}H NMR spectrum of naphthalene **210** showed the emergence of a new aromatic methyl ether signal at 3.82 ppm and naphthol proton signal at 5.58 ppm. These observations combined with the disappearance of the C-8 aromatic hydrogen signal strongly supported the notion of the *para*-methyl-ether insertion being successful. The ^{13}C NMR spectrum also confirmed the presence of another methoxy group on **210** as the data revealed three aromatic methoxy substituents in the 55-65 ppm range and similarly there were now four aromatic carbon-oxygen bonded atoms in the 145-158 ppm region. The IR spectrum showed the presence of a hydroxyl functional group at 3257 cm^{-1}. The HRMS data for compound **210** was in agreement with its calculated mass.

The accepted mechanism for this process is shown in **Scheme 54**[20,21]. Treatment of **192** with PIFA **208** affords intermediate **211** which then undergoes nucleophilic attack by a molecule of methanol at the *para* position. This nucleophilic attack is followed by the elimination of the hypervalent iodine substituent at the naphthol position to form pseudohydroxyquinone **209**. The tautomerization of **209** to naphthol **210** was achieved with sodium ethoxide base (or potassium *tert*-butoxide).

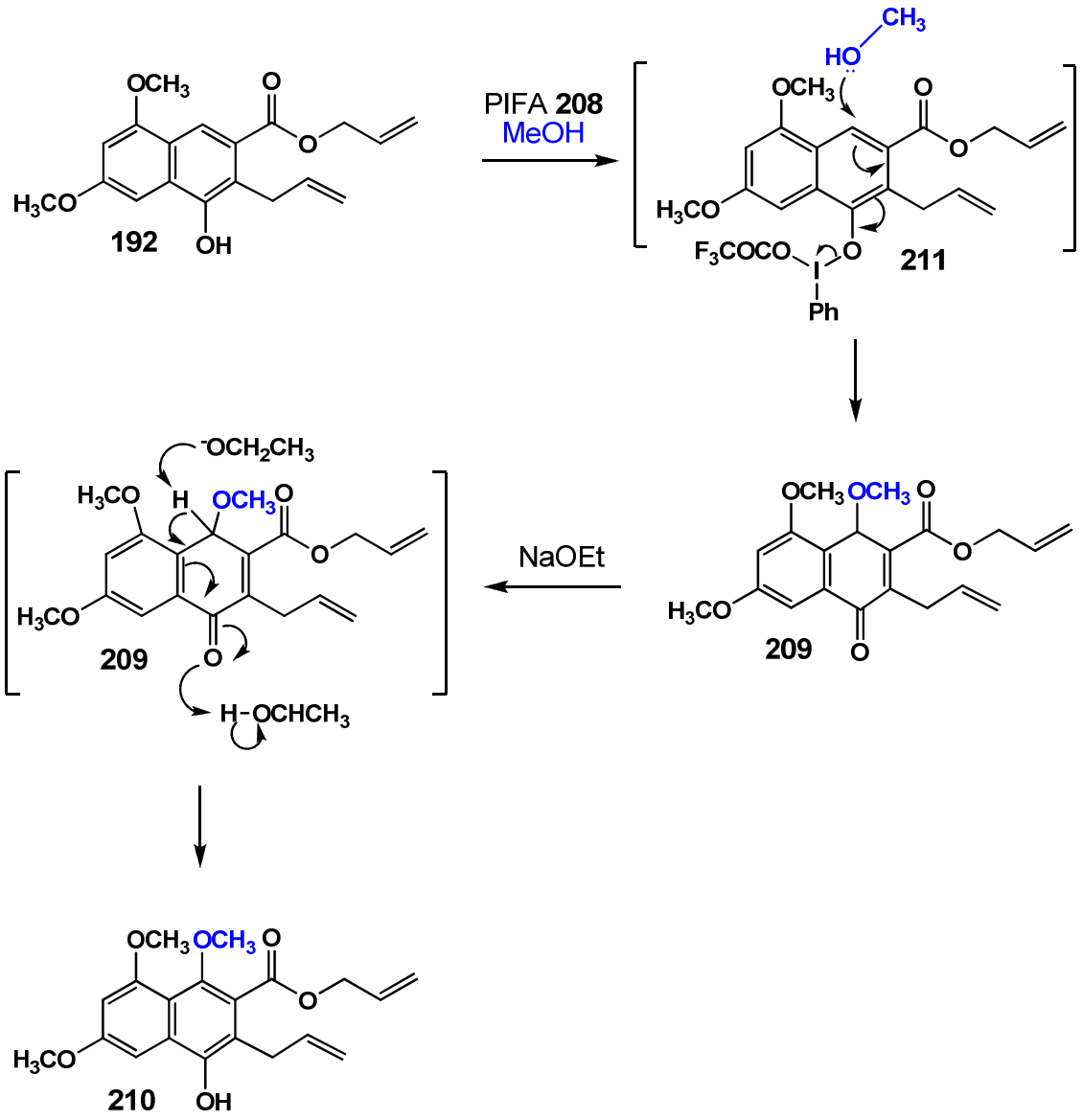

Scheme 54

3.2.4.2. Phenol methylation

Having succeeded in making the desired tetraoxygenated core of dehydroherbarin **31**, the next step was to protect the free naphthol as a methyl ether, as this "reactive" functional group may be problematic with subsequent synthetic steps that use metal ions. The methylation of a naphthol moiety is a simple process and the naphthol **210** was refluxed in dry acetone in the presence of potassium carbonate and dimethylsulfate to afford the aromatic methyl ether **212** in a high yield of 89 % (**Scheme 55**).

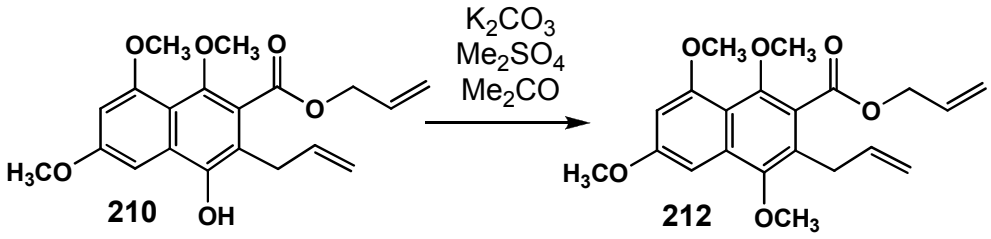

Scheme 55

The ^{1}H and ^{13}C NMR spectra of **212** were very similar to that of compound **210**. The ^{1}H NMR spectrum of **212** contained a total of four methyl ether signals at 3.95 ppm, 3.92 ppm, 3.86 ppm and 3.84 ppm, each accounting for three protons. The absence of the hydroxyl proton signal was also noted in the ^{1}H NMR spectrum, as well as in the IR spectrum. The presence of four aromatic methoxy signals was also evident in the ^{13}C NMR spectrum as four methyl ether carbon atoms were observed in the 55-64 ppm range. The HRMS data for compound **212** confirmed the existence of the newly installed aromatic methyl ether.

3.2.5. Pyran ring development

With our new improved synthetic plan being successful thus far, we could now progress towards assembling the isochromene ring. The methodology we planned to use for the construction of the pyran ring would be the same as before. Therefore, we needed to simply reduce the allyl ester to a primary alcohol followed by a Wacker oxidation to allow for ring closure.

3.2.5.1. Allyl ester group reduction and Wacker oxidation

The lithium aluminium hydride reduction of the allyl ester naphthalene **212** was initially performed in dry tetrahydrofuran (as previously done) but no reaction occurred. Changing the solvent to diethyl ether proved fruitful as primary alcohol naphthalene **213** was isolated as a white crystalline solid in a yield of 84 % (**Scheme 56**).

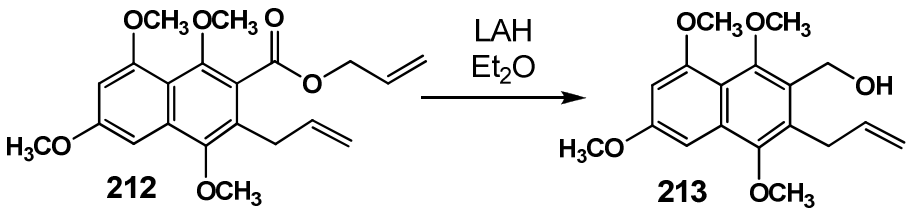

Scheme 56

The NMR spectroscopic data of naphthalene **213** contained many similar traits to those seen in the first reduction reaction which formed the related compound **175**. The ^{1}H NMR spectrum of **213** lacked the three signals originating from allyl ester chain hydrogens, but contained a benzylic CH_2 which strongly implied that the reduction of the allyl ester group had occurred. The emergence of a hydroxyl stretching band at 3481 cm^{-1} in the IR spectrum reinforced this credence. In the ^{13}C NMR spectrum the disappearance of three allyl ester carbon atoms was evident, as was the appearance of a CH_2 at 57.4 ppm was seen. The identity of the benzylic CH_2 functionality was further confirmed by a DEPT 90 NMR experiment. The HRMS data for naphthalene **213** was in agreement with the calculated value for this compound.

The next step towards the pyran ring assembly was the Wacker oxidation (see **Scheme 47**). Much to our delight, this reaction worked exactly the same as carried out before, but with shorter reaction times (2 h) as the primary alcohol **213** displayed high solubility in the solvent system (**Scheme 57**). The isochromene **214** had a lower polarity on TLC compared to the starting material **213** as expected.

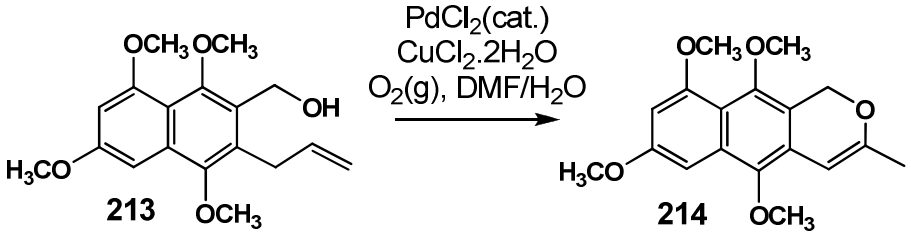

Scheme 57

The ^{1}H NMR spectrum of **214** was remarkably simpler than that of the precursor **213** and the C-2 allyl chain proton signals were clearly absent. The unsaturated pyran ring protons were observed at 1.99 ppm (CH_3), 5.27 ppm (C-1 CH_2 protons) and 5.94

ppm (C-4 CH proton). Four aromatic methyl ether signals and two aromatic naphthalene protons were also present which implied that the naphthalene core was intact. The ^{13}C NMR spectrum of **214** contained three new peaks which corresponded to the existence of the isochromene ring system. These were (i) C-3 atom shift at 156.1 ppm, (ii) the C-4 methine carbon at 95.8 ppm and (iii) methyl atom signal at 21.0 ppm. The HRMS data for the product was found to be 339.1209 amu which was in accordance with the calculated value of 339.1208 amu for **214**.

3.2.6. Dehydroherbarin formation via *para*-methyl ether oxidation

The naphthalene compound **214** possessed both the tetraoxygenated pattern and pyran ring system found in dehydroherbarin **31**. The last step that remained was to convert **214** into dehydroherbarin **31** by the selective oxidative demethylation of the aromatic *para*-methyl ethers of the substituted naphthalene (**Scheme 58**).

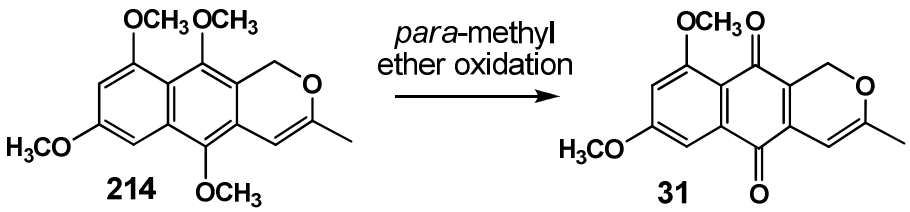

Scheme 58

Based on literature precedence, there were three possible reagents/reactions that could facilitate this step. These were: (i) CAN[22], (ii) silver(II) oxide[23] and (iii) PIFA[24]. The CAN oxidation of naphthalene **214** was executed as before in an acetonitrile/water reaction medium, but unfortunately this led to the formation of an uncharacterisable mixture of products (**Scheme 59**)[22]. No trace of compound **202** was observed in the analysis of the crude reaction mixture.

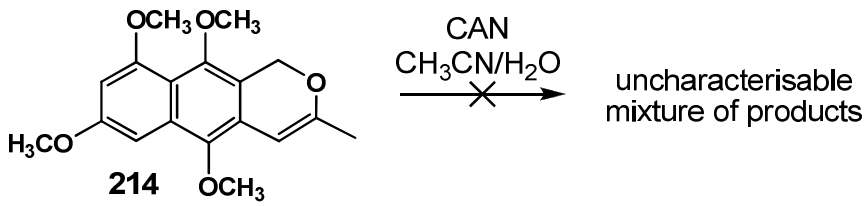

Scheme 59

Treatment of the naphthalene **214** with silver(II) oxide and nitric acid in dioxane solvent[23] also proved futile as the result of this reaction was an array of unidentifiable products (**Scheme 60**).

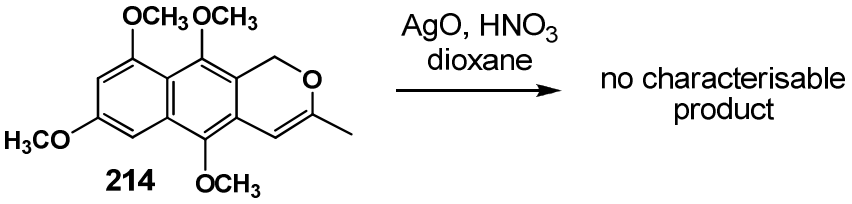

Scheme 60

With the previous two oxidations being unsuccessful, the last procedure to test employed the hypervalent iodine reagent PIFA **208**. In this process, when PIFA **208** is used in an acetonitrile/water solvent system it effectively functions as an oxidizing agent[24]. Naphthalene **214** readily dissolved in the reaction medium and was reacted with 1.5 equivalents of PIFA **208** over a duration of 2 h (**Scheme 61**). The result of this reaction was the successful formation of our target compound dehydroherbarin **31**, albeit in a low yield of 25 %.

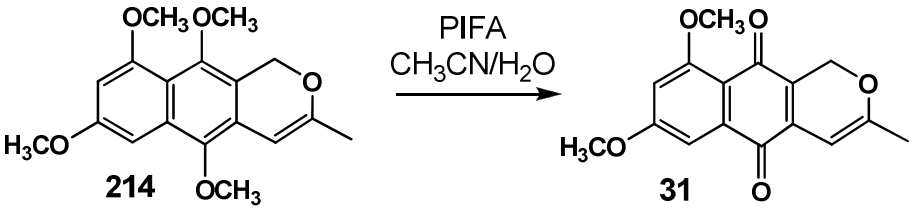

Scheme 61

Since dehydroherbarin **31** is a natural product, we validated the success of its synthesis by comparing our NMR spectroscopic data with the literature spectral information of this naphthoquinone[18]. The ^{1}H NMR spectrum of dehydroherbarin **31** is essentially the same as the precursor **214** except that the ^{1}H NMR spectrum of dehydroherbarin **31** only contains two aromatic methyl ether peaks at 3.92 ppm and 3.95 ppm. In the ^{13}C NMR spectrum of **31** two quinone carbonyl signals are visible downfield at 180.9 ppm and 182.3 ppm, which confirm the presence of the *para*-quinone motif. This spectrum is also marked by the disappearance of two methoxy carbon atom peaks, adding to the notion that the selective oxidative demethylation

reaction had worked. This represents the third reported synthesis of dehydroherbarin **31**.

The proposed mechanism of this PIFA **208** oxidative demethylation process is displayed in **Scheme 62**[2]. Intermediate **215** depicts how PIFA **208** acts as an electron sink for the dimethyl ether aromatic system, with the resultant loss of $OCOCF_3$. The phenyliodonio moiety then functions as a good leaving group as shown in intermediate **216**, which then undergoes a nucleophilic addition reaction with water at the newly formed methyl oxonium functionality. A second water molecule adds to the alternate methyl oxonium group, followed by the loss of methanol overall from intermediate **217** to afford the intermediate shown in **Scheme 62** which led to dehydroherbarin **31**. It can also be assumed that hydrophobic aggregation between the iodine (III) compound and the substrate encourages the reaction progression in an aqueous medium.

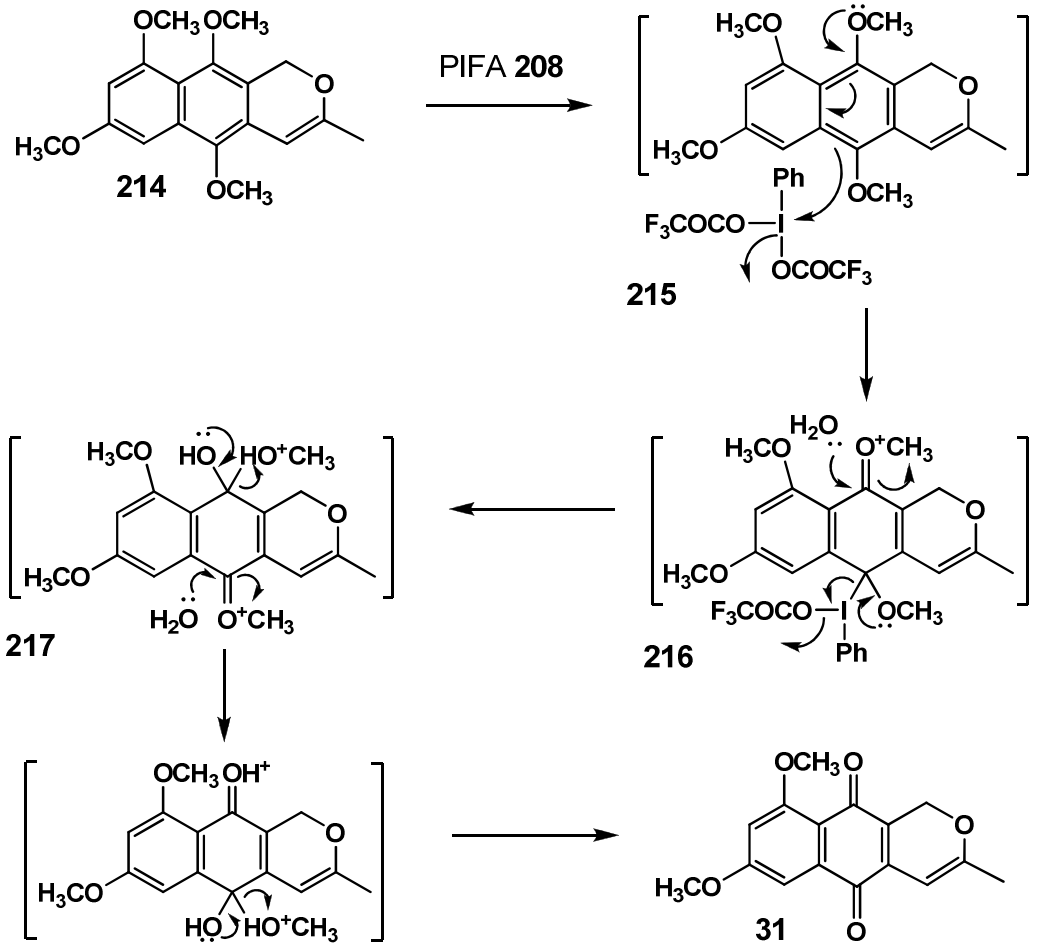

Scheme 62

The PIFA oxidation of naphthalene **214** was repeated in order to obtain more dehydroherbarin **31**. This process was carried out on a larger scale and more dilute compared to the previous reaction conditions. This "dilute" oxidative demethylation reaction led to the formation of the unusual naphthoquinone diol **218** (**Scheme 63**) which was isolated as a brown amorphous solid in a low yield of 24 %. This result was unexpected, as the initial reaction (done under more concentrated conditions **Scheme 61**), afforded only the desired product **3**. The effect of scaling this reaction up has not been further evaluated, and is a case for future work.

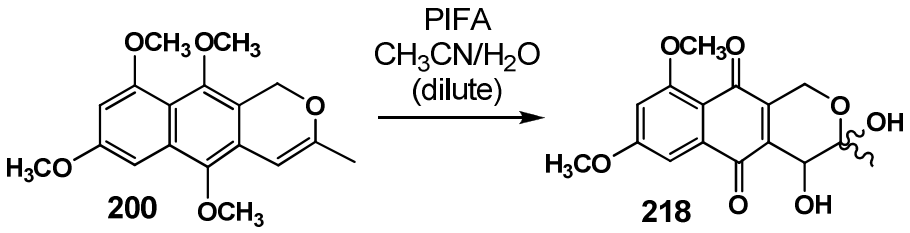

Scheme 63

It was quite interesting that the NMR spectra of diol compound **218** very closely resembled the data for the unusual compound **202**. This was not surprising given the single structural difference between these two naphthoquinones. The ^{1}H NMR spectrum of **218** varied from the proton spectrum of **202** in only a single aspect: that is, that the hydrogen atom shift at C-4 in **218** was significantly more upfield at 4.35 ppm. The remainder of the ^{1}H NMR suggested that the same naphthoquinone skeleton found in **202** was also present in naphthoquinone **218**. The ^{13}C NMR spectrum of **218** contained the quinone carbonyl signals at 181.1 ppm and 182.8 ppm. In the IR spectrum, these ketone carbonyls were also observed at 1725 cm^{-1} and 1649 cm^{-1}. The distinctive hemiacetal carbon peak at 95.9 ppm and adjacent methyl carbon shift at 24.5 ppm were also seen in the ^{13}C NMR spectrum. Confirmation of our proposed structure of **218** was provided by the HRMS analysis.

The stereochemistry of the alcohol-containing carbon atoms in naphthoquinone **218** was not clearly distinguishable using NMR techniques and future work would possibly entail aquiring this information by crystallographic means.

3.3. Synthesis of Anhydrofusarubin

The next stage in this PhD project was to apply the newly developed methodology from the synthesis of dehydroherbarin **31** towards the more complex naphthoquinone, anhydrofusarubin **26**. Comparing dehydroherbarin **31** and anhydrofusarubin **26** on a structural basis, there are two substantial differences (**Figure 12**): (i) anhydrofusarubin **26** has a pentaoxygenated pattern on the naphthalene framework and (ii) the second ring system of **26** contains a *para*-substituted hydroquinone functional group. These structural variations, when considered from a synthetic viewpoint imply the following adaptations: (i) the starting material should possess the required first-ring oxygenated substitution arrangement and (ii) the *para*-quinone oxidation and adjacent hydroquinone formation should be conducted at the end of the synthesis, given their highly reactive and thus sensitive nature.

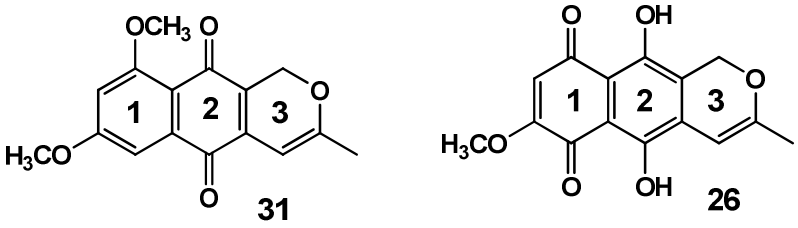

Figure 12

The planned synthesis of the pyran ring of **26** will be the same as used in **31**, whilst the PIFA methyl-ether insertion shall also be attempted to construct the pentaoxygenated naphthalene framework.

3.3.1. Naphthalene nucleus assembly

The construction of the naphthalene segment of anhydrofusarubin **26** should follow the same reactions as previously employed (see **section 3.2.1**) but requires the starting material 2,4,5-trimethoxybenzaldehyde **178**, which inherently contains the desired oxygen substitution pattern of one of the rings in the final product. Therefore 2,4,5-trimethoxybenzaldehyde **178** was subjected to a Stobbe condensation with diethyl succinate **187** and sodium ethoxide base (**Scheme 64**) in boiling

tetrahydrofuran for 2 h. The reaction mixture was then made acidic, and the intermediate was isolated by extraction and immediately reacted with anhydrous sodium acetate in refluxing acetic anhydride to facilitate the required Friedel-Crafts acylative process. This afforded the naphthalene **162** in a yield of 82 % over two steps.

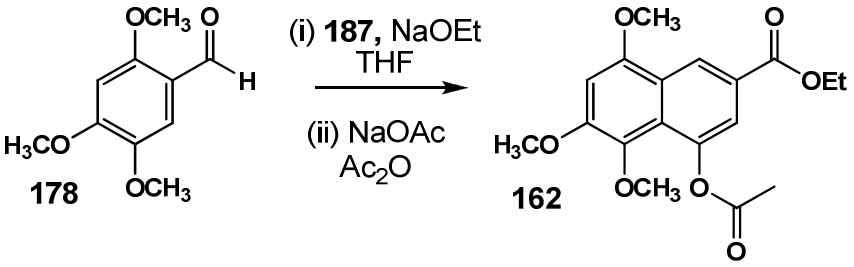

Scheme 64

The ^{1}H NMR signals of **162** compared very well with those of naphthalene **189**, save for two differences. There were two aromatic methyl ether signals at 3.81 ppm and 3.98 ppm that accounted for nine protons, which equated to three methoxy groups residing on the molecule. The aromatic region only displayed three naphthalene proton signals as expected. Naphthalene **162** is not a novel compound and spectroscopic data compared well with the existing literature data,[1, 23] confirming that the reaction had been successful.

3.3.2. Allyl chain introduction and rearrangement

With the naphthalene core in hand, the required functional group manipulations could be performed to allow for the formation of the third ring, the unsaturated pyran.

3.3.3.1. Saponification and deacetylation with subsequent allylation

These steps are the same in principle as those dicussed in **section 3.2.2.1:** base induced saponification and deacetylation of **162** to form intermediate **219**, followed by *O*-allylation of the resulting naphthol. Thus, **162** was dissolved in methanol, and exposed to aqueous potassium hydroxide (**Scheme 65**). Upon complete conversion of starting material, the reaction mixture was acidified and intermediate **219** isolated by filtration. The crude **219** residue was dissolved in acetone and refluxed in the

presence of excess allyl bromide and potassium carbonate. The diallylated naphthalene **220** was isolated in an 84 % yield over two steps.

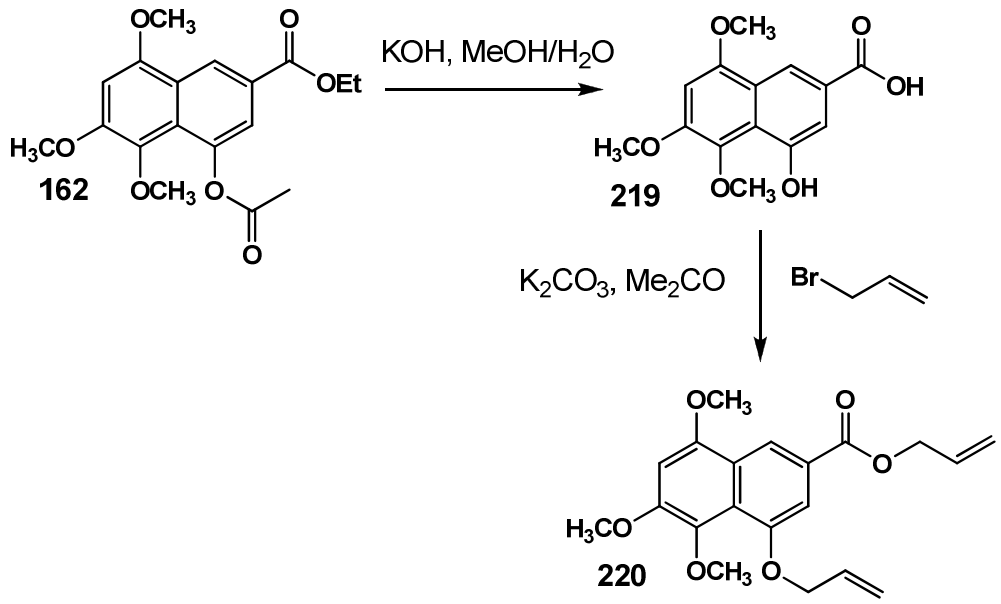

Scheme 65

The NMR spectral data for compound **220** validated that the naphthalene now contained two allyl chains that replaced the former ethyl ester group and acetate substituents. The ether bound allyl chain introduced three new signals in the ^{1}H NMR spectrum at 4.71 ppm (OC**H$_2$**CH=CH$_2$), 5.32-5.35 ppm (OCH$_2$CH=C**H$_2$**) and 6.15-6.27 ppm (OCH$_2$C**H**=CH$_2$). The allyl ester similarly also contributed to the emergence of three peaks at 4.87 ppm (COOC**H$_2$**CH=CH$_2$), 5.41-5.57 ppm (COOCH$_2$CH=C**H$_2$**) and 5.97-6.28 ppm (COOCH$_2$C**H**=CH$_2$, overlapped with OCH$_2$C**H**=CH$_2$). The ^{13}C NMR spectrum of **220** lacked the four peaks found in the precursor **162** that originated from the acetate and ethyl ester functionalities, but six new signals were observed for the newly installed allyl ester and allyl ether groups. The HRMS for naphthalene **220** was in agreement with the calculated mass.

3.3.3.2. Allyl chain rearrangement

The repositioning of the phenolic allyl ester moiety **220** to C-2 could now be tested by heating the substrate at high temperature. It was found that the Claisen rearrangement of **220** required a temperature of 190 °C. The reaction progress was

difficult to monitor as the starting compound **220** and product **221** possessed the same R_f on TLC, but fortunately ^{1}H NMR spectroscopic analysis of the crude mixture proved useful.

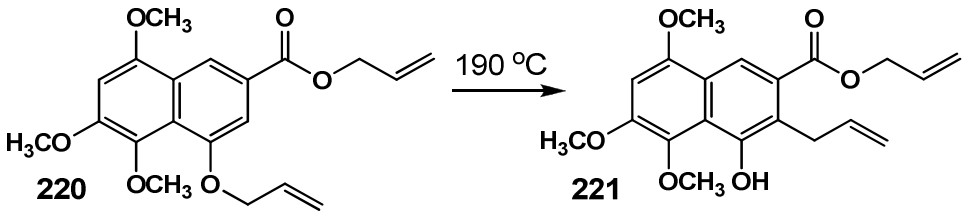

Scheme 66

Since this reaction was performed previously on substrate **191**, we were aware of the two main changes to look for in data: that is the presence of a free naphthol and an allyl ester group situated at C-2. The IR spectrum contained a broad hydroxyl stretching band at 3280 cm^{-1} which was the first sign that the reaction had worked. The ^{1}H NMR spectrum of Claisen product **221** further illustrated this by depicting three informative changes, (i) signals from the C-allyl group methylene protons emerged upfield at 3.89 ppm, (ii) the C-2 aromatic proton peak disspeared and (iii) the naphtholic proton signal appeared at 10.08 ppm. The signal arsing from the allyl CH_2 substituent had moved upfield to 30.1 ppm, confirming the new carbon-carbon bond formation as seen in the ^{13}C NMR spectrum. Once again the HRMS analysis supported the structure of **221**.

3.3.3. Pyran ring construction: test of reactions on intermediate species

The naphthalene **221** is an important intermediate in the synthesis of anhydrofusarubin **26**. At this stage, we planned to form the pyran ring as before (see **Scheme 57**) to test the viability of these steps on the new substrate before introduction of additional oxygenation on the second ring. In order to achieve this, we were required to protect the naphthol, reduce the allyl ester to the benzylic alcohol **223** and then employ a Wacker oxidation on **223** to hopefully yield the target **169** (**Scheme 67**).

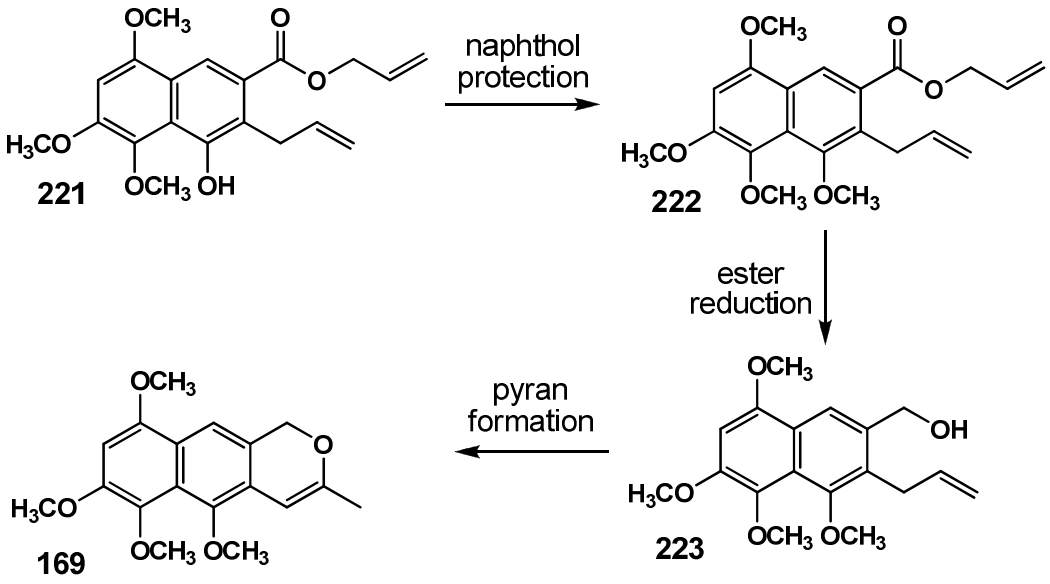

Scheme 67

3.3.3.1. Naphthol methylation

The naphthol **221** was methylated with dimethyl sulfate using potassium carbonate as a base to afford the aromatic tetramethyl ether **222** in a 90 % yield (**Scheme 68**).

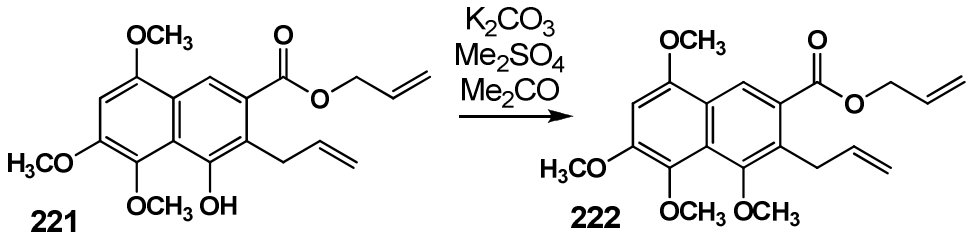

Scheme 68

The IR spectrum of **222** was devoid of a hydroxyl stretching band, while the ^{1}H NMR spectrum contained no naphthol signal. A fourth aromatic methyl ether signal was observed in the ^{1}H NMR spectrum at 4.02 ppm, whilst the ^{13}C NMR spectrum also displayed a total of four aromatic methyl ether carbon atom signals in the 56 ppm to 63 ppm range. The HRMS data supported the presence of the additional methoxy group.

3.3.3.2. Allyl ester reduction and Wacker oxidation

With the naphthol protected, the allyl ester of **222** could now be promptly reduced. The effective reducing agent lithium aluminium hydride smoothly facilitated this step by converting the ester group of **222** to its respective primary alcohol to yield product **223** (**Scheme 69**).

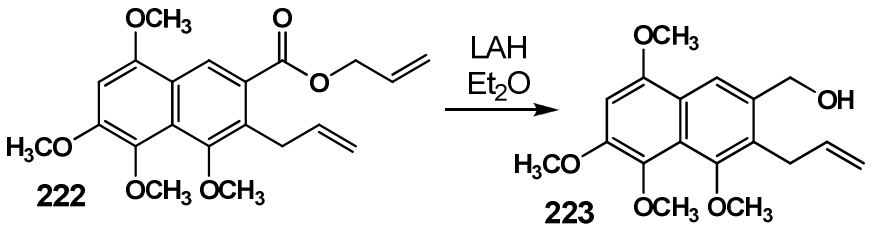

Scheme 69

Naphthalene **223** is a known compound and the NMR spectroscopic data corresponded to the literature values[24]. The ^{1}H NMR of **223** showed the appearance of the benzylic methylene protons at 4.76 ppm, with the expected loss of three allyl ester chain signals and the carbonyl signal. The DEPT 90 NMR experiment verified that the peak at 63.6 ppm in the ^{13}C NMR spectrum was due to a CH_2 moiety.

Now that the benzylic alcohol **223** was available we reacted this starting material under Wacker oxidation conditions (**Scheme 70**) and gratifyingly the isochromene system was formed as a white crystalline product **169**.

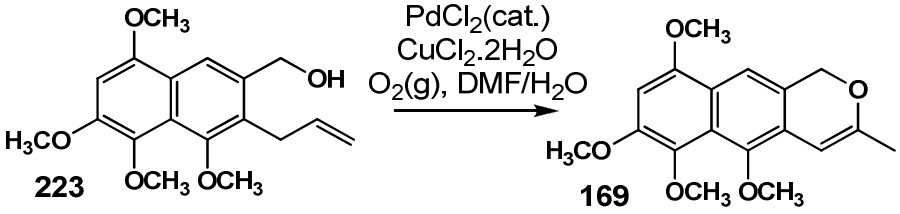

Scheme 70

The ^{1}H and ^{13}C NMR spectroscopic data showed the disappearance of the C-2 allyl chain, but contained evidence of the isochromene portion of **169**. The pyran ring protons in the ^{1}H NMR spectrum were observed at 2.00 ppm (CH_3), 5.12 ppm (C-1 methylene protons) and 6.09 ppm (C-4 methine proton). Similarly in the ^{13}C NMR

spectrum, the isochromene ring carbon atoms emerged in the typical regions, at 20.1 ppm (CH_3), 156.1 ppm (C-3) and 96.0 ppm (C-4). The HRMS data for the product was found to be 339.1207 amu which was in line with the calculated value of 339.1208 amu for **169**.

Now that we had tested methodology on naphthalene **221**, we could proceed to implement this methodology on the pentaoxygenated framework which would lead to anhydrofusarubin **26**. However, this first required the preparation of the pentaoxygenated naphthalene core.

3.3.4. Synthesis of pentaoxygenated naphthalene system by PIFA methyl ether insertion

PIFA **208** in methanol would again be utilized to introduce the methyl ether motif onto a naphtholic system (see **section 3.2.4.1**). The starting material **221** was dissolved in methanol and treated with 1.3 equivalents of PIFA **208** for 10 min to produce pseudohydroxyquinone **224** (**Scheme 71**). This intermediate was immediately exposed to sodium ethoxide to yield the tautomerized product **225** as an orange amorphous solid. The success of this reaction was a considerable step forward towards synthesizing anhydrofusarubin **26**, as the assembly of the desired pentaoxygenated naphthalene **225** was now achieved.

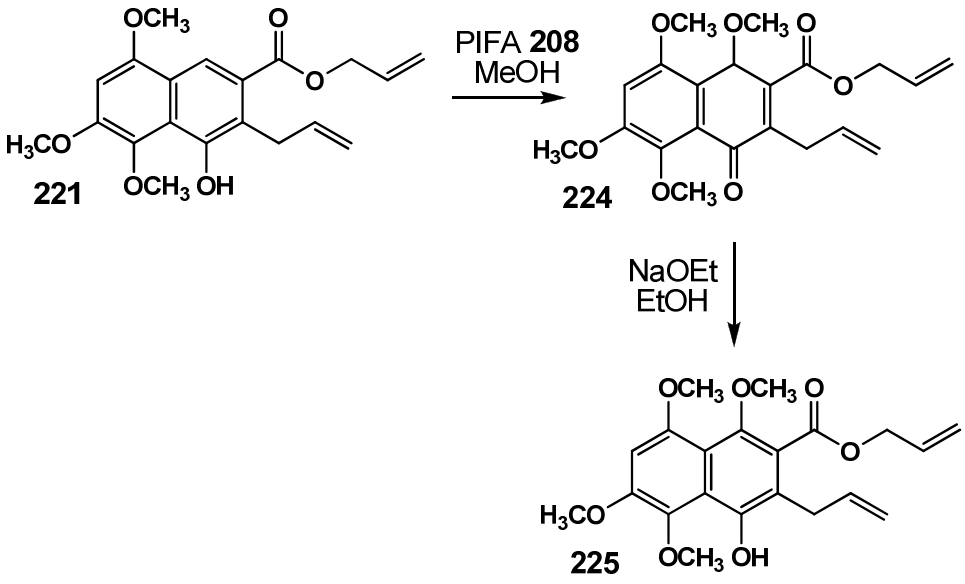

Scheme 71

Analysis of the ^{1}H NMR spectrum of **225** showed the appearance of a total of four aromatic methyl ether signals between 3.78 ppm and 3.98 ppm, and the disappearance of the aromatic proton at C-8. The naphthol signal was still visible at 10.24 ppm and also gave its distinctive stretching band at 3215 cm^{-1} in the IR spectrum. The ^{13}C NMR spectrum showed four aromatic carbon-oxygen bonded atoms in the expected range of 145-154 ppm. Thorough examination of the accompanying two-dimensional spectra (specifically HMBC and HSQC) revealed that a fifth aromatic carbon-oxygen bonded atom was situated unusually upfield at 115.1 ppm, overlapped with the allyl group terminal alkene protons. The increased mass of product **225** compared to its precursor **221** was accurately determined utilizing HRMS.

3.3.5. Synthesis of pyran ring on pentaoxygenated naphthalene core

The next three steps of the anhydrofusarubin synthesis follow the same procedures tested in **section 3.3.3**. Thus we planned to methylate the naphthol, reduce the allyl ester to a benzylic alcohol and then convert the product to the required isochromene.

3.3.5.1. Naphtholic methylation

Naphthol **225** was efficiently methylated to afford **226** in an 81% yield by exposure to dimethyl sulfate and potassium carbonate in refluxing acetone (**Scheme 72**).

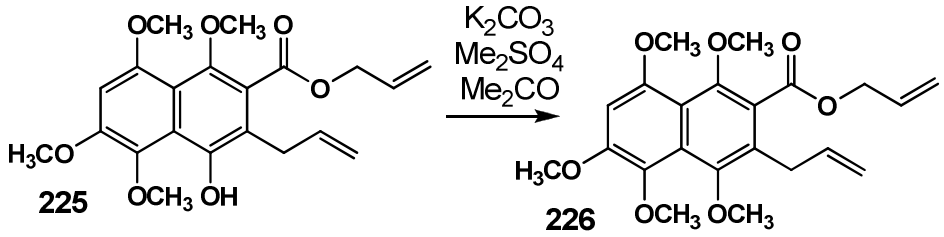

Scheme 72

The ^{1}H NMR spectrum of **226** contained five aromatic methyl ether signals at 3.73 ppm, 3.75 ppm, 3.77 ppm, 3.93 ppm and 3.95 ppm. The ^{13}C NMR spectrum clearly depicted the existence of five aromatic methyl ether moieties in the range of 56.7 ppm to 63.8 ppm. The presence of the pentaoxygenated naphthalene was again confirmed by five aromatic carbon-oxygen bonded atoms, with the unusual positioning of one of these again at 115.8 ppm.

3.3.5.2. Primary alcohol formation and Wacker oxidation

Reduction of the allyl ester group of naphthalene **226** to **227** was achieved through treatment with lithium aluminium hydride in diethyl ether for 2 h (**Scheme 73**). Purification of the resultant primary alcohol **227** proved problematic, and as such it was not purified further and was subsequently subjected to a palladium-catalyzed Wacker oxidation. The reaction time was 2 h with a constant stream of molecular oxygen bubbling through the solution. The result of these two processes was the formation of the isochromene **228** in a somewhat disappointing yield of 49 %.

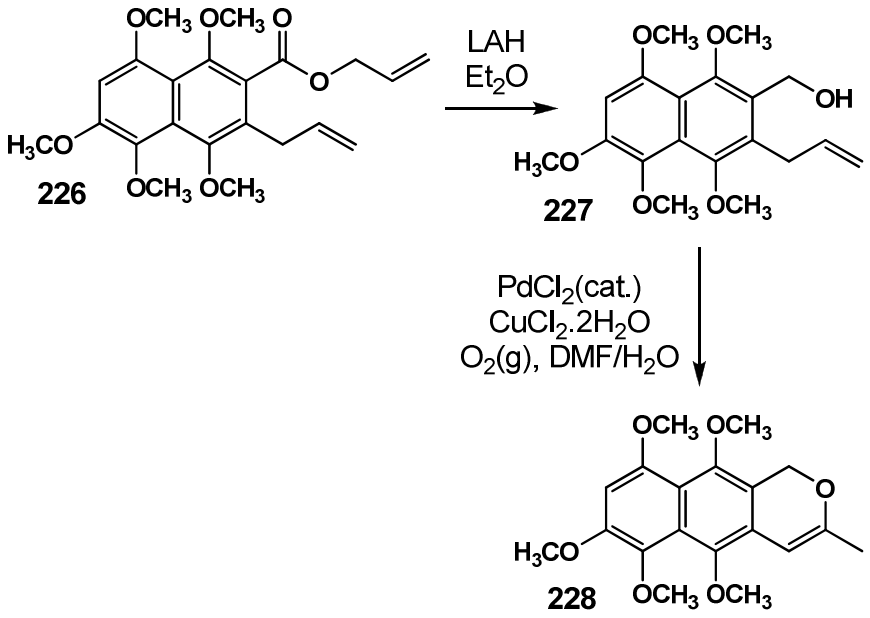

Scheme 73

The ^{1}H NMR spectrum of **228** provided a very clear image of the newly "simplified" naphthalene system. There were nine signals in this spectrum, five accounting for aromatic methyl ether groups (3.74-3.99 ppm), one for the remaining naphthalene proton (6.64 ppm), and three for the pyran ring [2.00 ppm (CH_3), 5.27 ppm (C-1 CH_2) and 6.03 (C-4 CH)]. The ^{13}C NMR spectrum contained the five aromatic carbon-oxygen bonded atom peaks at 136.8 ppm, 142.6 ppm, 147.3 ppm, 150.0 ppm and 153.3 ppm. The allyl chain carbon signals were absent. The isochromene ring signals emerged in close proximity to those found in the previous pyran-ring containing compounds (**sections 3.2.2.2, 3.2.5.1. 3.3.3.2**).

3.3.6. Anhydrofusarubin synthesis *via* regiospecific and regioselective demethylation reactions

The bulk of the synthesis towards anhydrofusarubin **26** had now been completed and all that remained was the *para*-oxidation, to produce naphthoquinone **229,** followed by subsequent demethylation of the remaining aromatic methyl ethers to form the naphthazarin moiety **26** (**Scheme 74**).

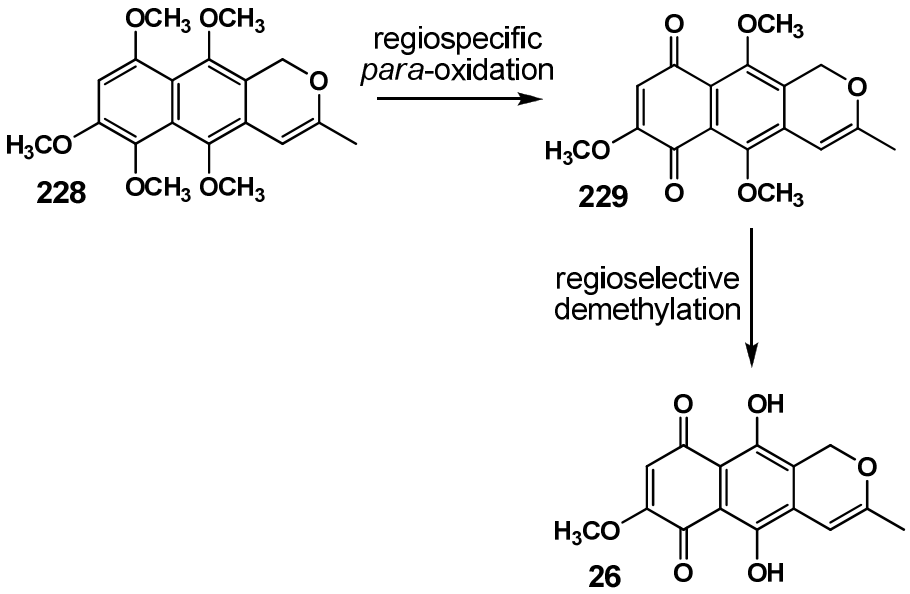

Scheme 74

3.3.6.1. Quinone introduction through silver (II) oxide oxidative demethylation

Silver(II) oxide has been shown to be an effective reagent for the oxidation of aromatic dimethyl ethers and has preferential oxidative selectivity towards the most electron-rich ring in a given system[25]. Thus, we postulated that the most electron-rich ring in naphthalene **228** would be the ring bearing the three methoxy substituents and should provide the desired quinone product if reacted with silver(II) oxide in the presence of nitric acid. Following this hypothesis, we dissolved **228** in 1,4-dioxane with 5.0 equivalents of silver(II) oxide that remained as a colloidal suspension (**Scheme 75**). Concentrated nitric acid (6 M) was added dropwise to the mixture which was reacted for 5 min, resulting in the formation of an intensely coloured solution. Work-up of the reaction and purification by column chromatography led to the isolation of what we assumed were two quinone products, the first as an orange crystalline compound and the second as a dark red amorphous solid.

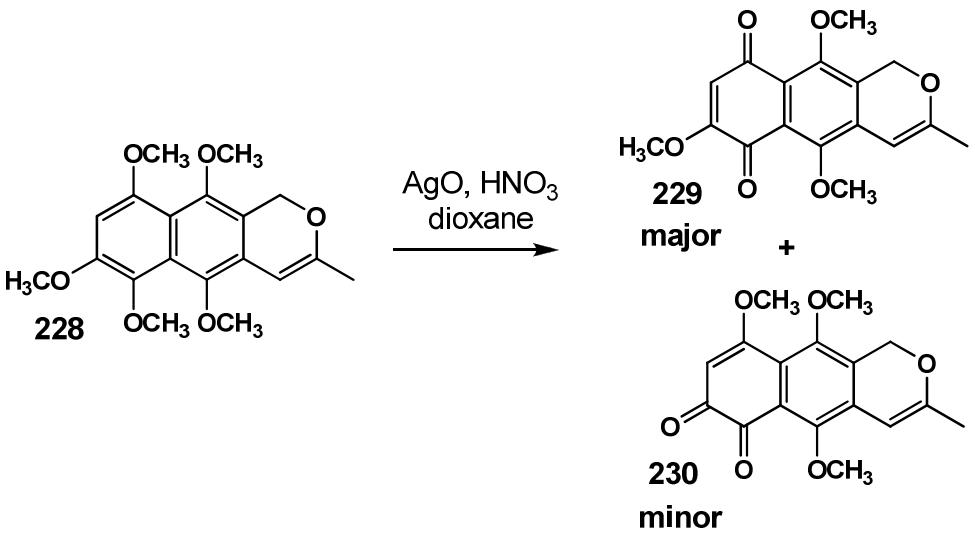

Scheme 75

NMR spectroscopic analysis of both compounds confirmed that two aromatic methyl ethers were now absent in both products. The data also confirmed that the remainder of the naphthalene systems were intact. However, the problem that arose was that these naphthoquinones were isomers (both had the same HRMS values) of each other, with one being the desired *para*-quinone **229** and the other presumably an unwanted *ortho*-quinone **230**, neither of which could be accurately and unambiguously assigned using NMR spectroscopic techniques (including all types of two dimensional experiments). Luckily, given the crystalline nature of the major product, we were able to grow good quality crystals that allowed for the required structural elucidation by X-ray crystallography. **Figure 13** shows that the first product isolated was indeed the target *para*-quinone **229**. Therefore, by process of elimination, the minor red product was labelled as the *ortho*-quinone **230**. **Figure 14** shows the colour of these intensely coloured compounds as a solution in dichloromethane.

Now knowing the exact structures of the two products, the NMR spectra can be analysed in more detail. The only difference in the ^{1}H NMR spectra of the parent compound **228** and naphthoquinone products **229** and **230** is the loss of two aromatic methyl ether peaks, accounting for six protons in the starting material. Interestingly, all three methoxy signals in the *para*-quinone **229** are in close proximity

with two of these overlapping. By comparison, the *ortho*-quinone methyl ethers are all observed more than 0.5 ppm apart.

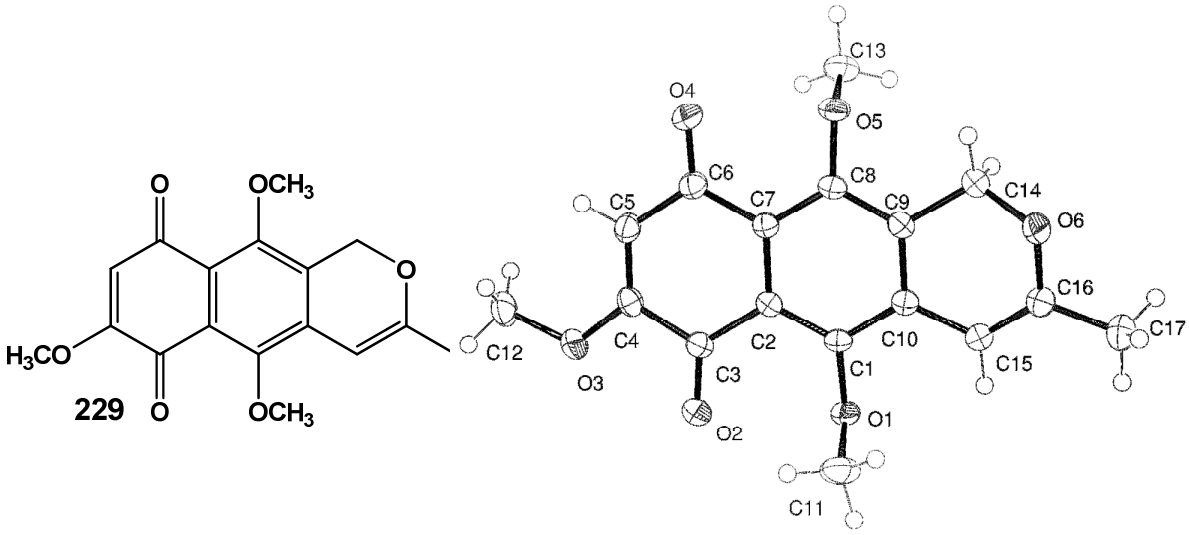

Figure 13

The ^{13}C NMR spectra of structural isomers **229** and **230** are also very similar to each other except for two distinct differences: (i) the three aromatic naphthalene carbon signals bonded to oxygens in **229** appear in the narrow region of 149.8-159.0 ppm whereas in **230** one of these peaks is found at a considerable downfield shift of 171.0 ppm and (ii) the *para*-quinone **229** carbonyl carbon atoms are found at 179.3 ppm and 183.7 ppm whilst in the *ortho*-quinone **230** the carbonyl carbon atoms are very similarly positioned at 179.4 ppm and 179.8 ppm.

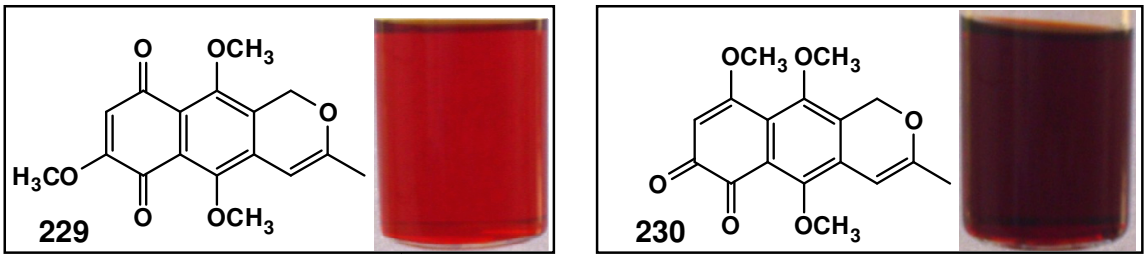

Figure 14

3.3.6.2. Anhydrofusarubin formation by boron trichloride selective demethylation

The last step that remained in our synthetic route was the selective deprotection of two aromatic methyl ethers. This transformation was successfully achieved by employing boron trichloride, a Lewis acid (**Scheme 76**).

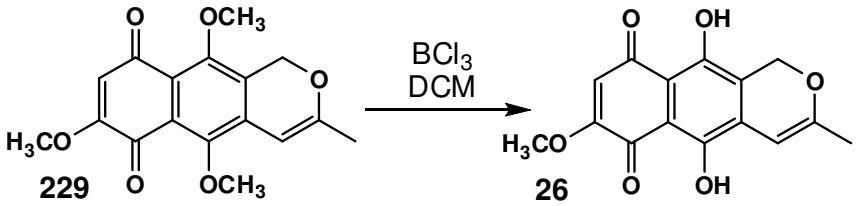

Scheme 76

There is literature precedence[26] to suggest that boron trichloride can selectively demethylate the methyl ethers at C-5 and C-10 of a naphthalene system such as **229**. The boron containing reagent can coordinate to each of the quinone carbonyl groups independently and cleave the adjacent methoxy functionalities, thus ensuring the selectivity of this reagent. Naphthoquinone **229** was dissolved in dry dichloromethane, cooled to -78 ℃ and carefully treated with 3.0 equivalents of boron trichloride. This reaction was eventually warmed to room temperature and quenched with water. Purification of the reaction mixture yielded anhydrofusarubin **26** as a dark purple solid (**Figure 15**).

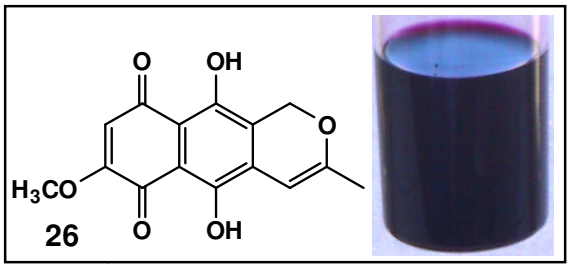

Figure 15

Our acquired ^{1}H NMR and ^{13}C NMR spectra of **26** perfectly matched the literature data reported for this natural product[27,28]. The ^{1}H NMR spectrum of **26** only contained a single signal arising from a methoxy substituent (on C-7) signal at 3.92 ppm and two hydrogen bonded phenolic peaks far downfield at 12.65 ppm and 13.04

ppm. These changes in relation to parent quinone **229** provided evidence for the presence of the dihydroquinone moiety. The ^{13}C NMR spectrum contained two signals resulting from the *para*-quinone motif at 178.0 ppm and 182.8 ppm, and only one peak due to a methyl ether carbon atom. The recorded melting point range was 195-196 °C which was in close accordance with the reported literature value of 199-202 °C[29]. The HRMS data for anhydrofusarubin **26** was found to be 288.0633 amu which was in line with the calculated value of 288.0635 amu for our molecular formula of $C_{15}H_{12}O_6$. This represents the first total synthesis of anhydrofusarubin **26**.

3.4. Concluding Remarks Pertaining to the Synthesis of Dehydroherbarin and Anhydrofusarubin

Using a novel approach to constructing highly oxygenated naphthoquinones, we have successfully synthesized two natural products: dehydroherbarin and anhydrofusarubin. Dehydroherbarin **31** was made from the commercially available 2,4-dimethoxybenzaldehyde **172** in 11 steps in an overall yield of 4.5 % (**Scheme 77**) and anhydrofusarubin **26** was made from the commercially available 2,4,5-trimethoxybenzaldehyde **178** in 12 steps in an overall yield of 5.3 % (**Scheme 78**).

Our synthesis of dehydroherbarin **31** is longer than the other two listed syntheses for this naphthoquinone[16,18], however our process was focused on creating new methodology towards accessing highly oxygenated naphthalene compounds (**Scheme 77**). This plan was successfully accomplished. There are three key stages in our synthesis of dehydroherbarin **31:** (i) the Stobbe condensation approach towards the synthesis of the naphthalene core, (ii) PIFA aromatic methyl ether insertion to efficiently and regioselectively introduce the required oxygenation pattern of the substrate and (iii) isochromene ring assembly using Wacker-type chemistry.

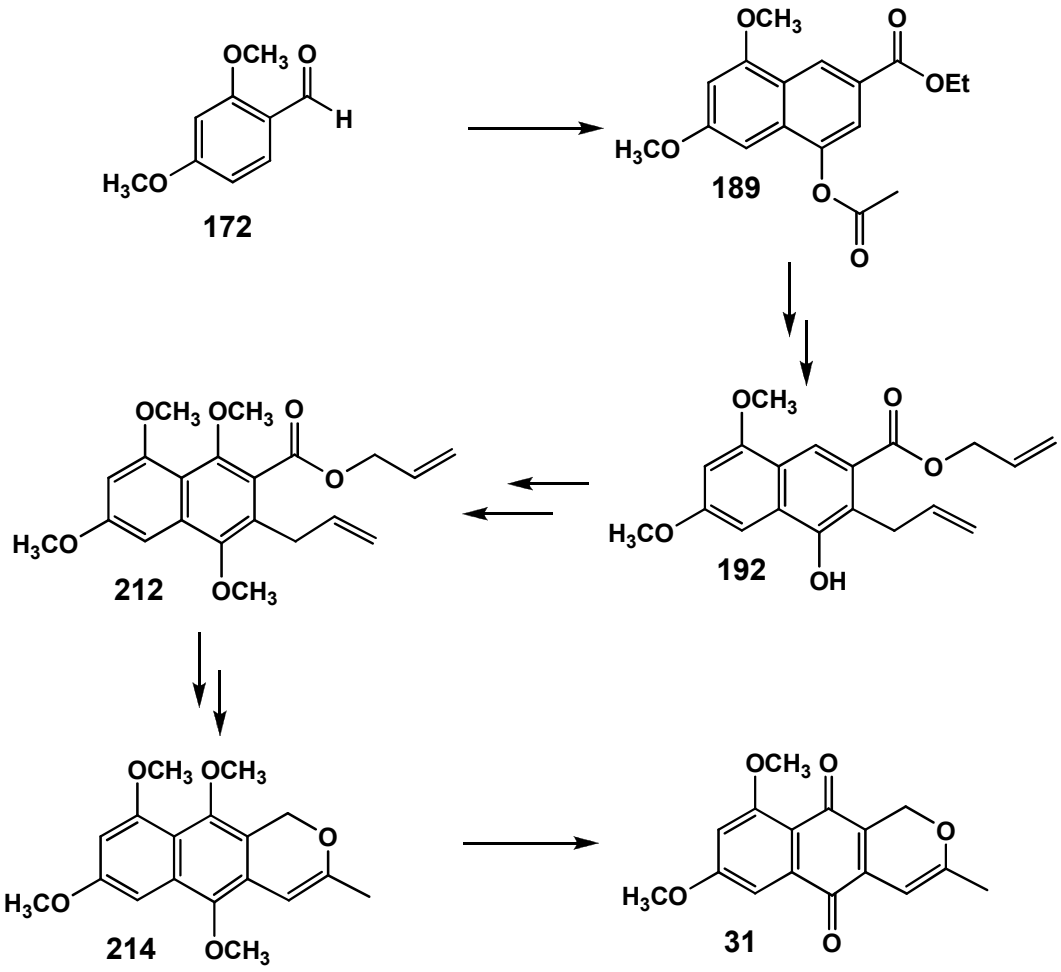

Scheme 77

The synthesis of anhydrofusarubin **26** was efficiently executed based on the synthetic framework developed in the pursuit of **31**. The steps are very similar with the only considerable differences/challenges being the last demethylation reaction.

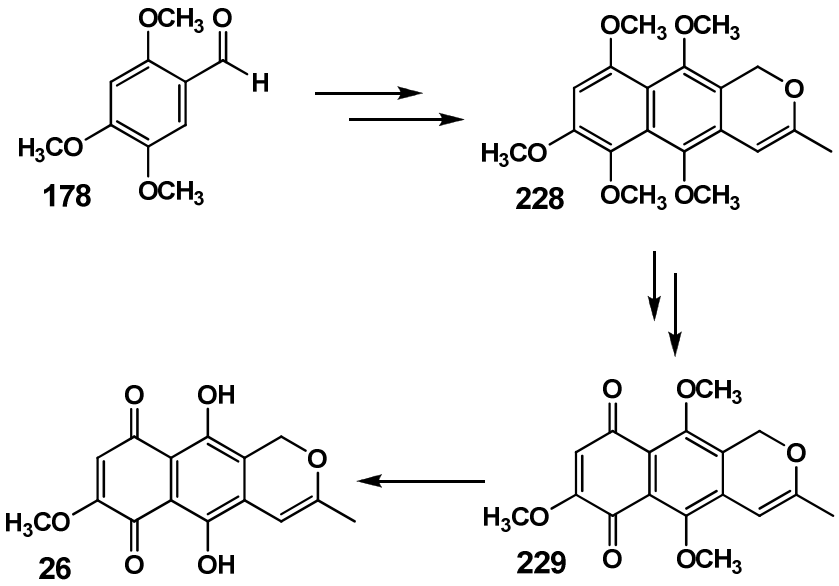

Scheme 78

Two unusual synthetic naphthoquinones **202** and **218** were also inadvertently made (**Figure 16**). Naphthoquinone **202** was produced from a CAN-mediated process whereas diol **218** was isolated when carrying out a PIFA demethylation under dilute conditions.

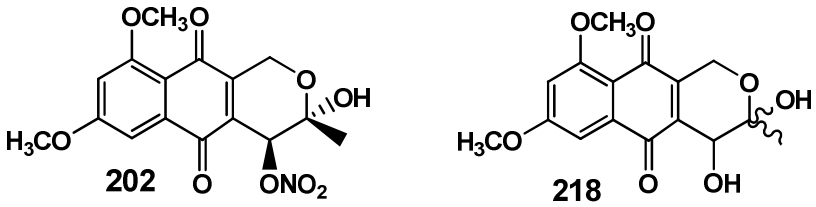

Figure 16

3.5. References

1. Oliveira, J.R, *The Synthesis of Isochromanols. Potential Bioreductive Alkylating Agents,* 2000, PhD Thesis, University of the Witwatersrand.
2. Tohma, H., Morioka, H., Harayama, Y., Hashizume, M., Kita, Y., *Tetrahedron Letters*, 2001, **42**, 6899-6902.
3. Warrener, R.N., Evans, D.A.C., Russel, R.A., *Tetrahedron Letters*, 1984, **25**, 4833-4836.

4. Karichiappan, K., Wege, D., *Australian Journal of Chemistry*, 2000, **53**, 743-747.
5. Cameron, D.W., Feutrill, G.I., McKay, P.G., *Australian Journal of Chemistry*, 1982, **35**, 2095-2109.
6. Nicolaou, K.C., Snyder, S.A., Montagnon, T., Vassilikogiannakis, G., *Angewandte Chemie International Edition*, 2002, **41**, 1668-1698.
7. Mmutlane, E.M., Michael, J.P., Green, I.R., de Koning, C.B., *Organic and Biomolecular Chemistry*, 2004, **2**, 2461-2470.
8. Kraus, G.A., Ogutu, H., *Tetrahedron*, 2002, **58**, 7391-7395.
9. Pelly, S., *Novel Methods for the Synthesis of Naturally Occurring Oxygen and Nitrogen Heterocycles*, 2009, PhD Thesis, University of the Witwatersrand.
10. Clayden, J., Greeves, N., Warren, S., Wothers, P., *Organic Chemistry*, 2005, Oxford Univeristy Press Inc., New York.
11. Takacs, J.M., Jiang, X., *Current Organic Chemistry*, 2003, **7**, 369-396.
12. de Koning, C.B., Green, I.R., Michael, J.P., Oliveira, J.R., *Tetrahedron*, 2001, **57**, 9623-9634.
13. Green, T.W., Wuts, P.G.M, *Protective Groups in Organic Chemistry*, 1999, Wiley-Interscience, New York.
14. Bloomer, J.L., Stagliano, K.W., *Tetrahedron*, 1993, **34**, 757-760.
15. Sperry, J., Brimble, M.A., *Synlett*, 2008, **12**, 1910-1912.
16. Wadsworth, A.D., Sperry, J., Brimble, M.A., *Synthesis*, 2010, **15**, 2604-2608.
17. Bergeron, D., Caron, B., Brassard, P., *Journal of Organic Chemistry*, 1993, **58**, 509-511.
18. Kesteleyn, B., De Kimpe, N., *Journal of Organic Chemistry*, 2000, **65**, 640-644.
19. Nair, V., Suja, T.D., Mohanan, K., *Synthesis*, 2006, **15**, 2531-2534.
20. Lowell, A.N., Fennie, M.W., Kozlowski, *Journal of Organic Chemistry*, 2008, **73**, 1911-1918.
21. Couladouros, E.A., Strongilos, A.T., *European Journal of Organic Chemistry*, 2002, 3341-3350.
22. Jacobs, J., Claessens, S., De Kimpe, N., *Tetrahedron*, 2008, **64**, 412-418.
23. Sperry, J., Sejberg, J.J.P., Stiemke, F.M., Brimble, M., *Organic and Biomolecular Chemistry*, 2009, **7**, 2599-2603.

24. de Koning, C.B., Manzini, S.S., Michael, J.P., Mmutlane, E.M., Tshabidi, T.R., van Otterlo, W.A.L., *Tetrahedron*, 2005, **61**, 555-564.
25. de Koning, C.B., Giles, R.G.F., Green, I.R., *Journal of the Chemical Society Perkin Transactions 1*, 1991, 2743-2748.
26. de Koning, C.B*., The Syntheses of Some Naturally Derived Naphthoquinones*, 1987, PhD Thesis, University of Cape Town.
27. Kurobane, I., Vining, L.C., McInnes, A.G., Walter, J.A., *Canadian Journal of Chemistry*, 1980, **58**, 1380-1385.
28. Chang-Lun, S., Chang-Yun, W., Dong-Sheng, D., Zhi-Gang, S., Yu-Cheng, G., Yong-Cheng, L., *Chinese Journal of Structural Chemistry*, 2008, **27**, 824-828.

Chapter 4: A Model Study Towards the Synthesis of a Marticin Fused Bicyclic Pyran System

4.1. Approach to a Model Bicyclic Acetal Ring System

The naphthoquinone marticin **45**, as mentioned previously (**section 1.3**), possesses a 6,6-bicyclic pyran ring system as well as a pentaoxygenated naphthalene nucleus. This complex ring arrangement is fascinating from a synthetic perspective and to date there has been no reported synthesis of this compound. Thus we decided to investigate a synthetic route to assemble the fused bicyclic pyran system in marticin **45**.

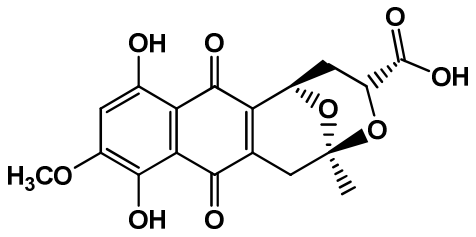

45

Considering that marticin **45** contains four rings within its structural framework, the synthesis of which would initially prove to be a daunting task, we opted to first work on a simpler benzylic model system of the 6-membered bicyclic acetal skeleton. Therefore compound **179** (as a racemic mixture) was chosen as our model target and its retrosynthetic analysis is shown in **Scheme 79**. Target compound **179** could be produced from the Wacker oxidation of 1,3-diol **180** by means of an intramolecular acetal formation. The 1,3-diol **180** can be obtained from the chemoselective reduction of both ketones of **181**. The diketone could be produced as the product of a Claisen condensation reaction of diethyl oxalate **231** and the aromatic ketone **182**. Ketone **182** has been previously prepared in three steps from the commercially available 2,5-dihydroxyacetophenone **183**[1].

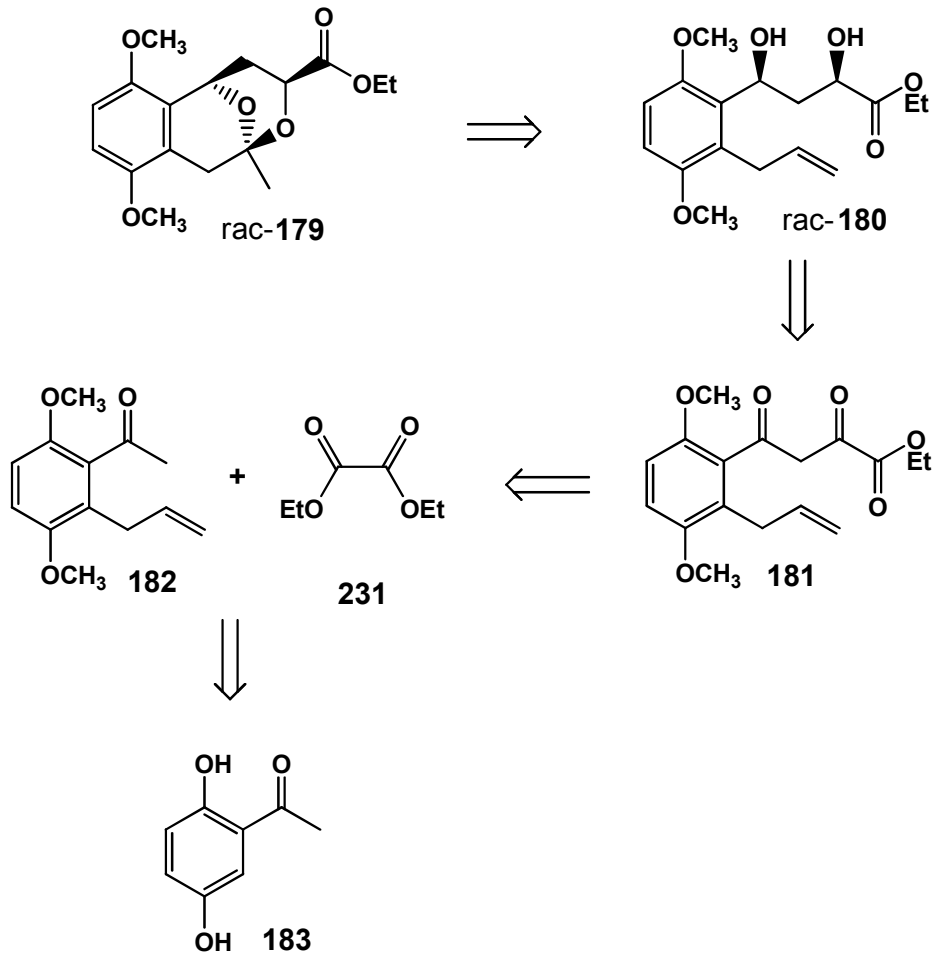

Scheme 79

4.1.1. Selective allylation of 2,5-dihydroxyacetophenone

The first step of our model pathway entailed the selective monoallylation of 2,5-dihydroxyacetophenone **183**. According to literature[2] precedent, reacting 1.3 molar equivalents of both allyl bromide and potassium carbonate base with **183** promotes the formation of only the monoallyl product **243** (**Scheme 80**). This process was effectively repeated in refluxing acetone for 18 h to afford **243** in an 86 % yield. This difference in chemoselectivity between the two phenolic motifs is attributed to the hydrogen bonding between the phenol group at C-6 and adjacent benzylic ketone moiety, which effectively renders this phenol less reactive.

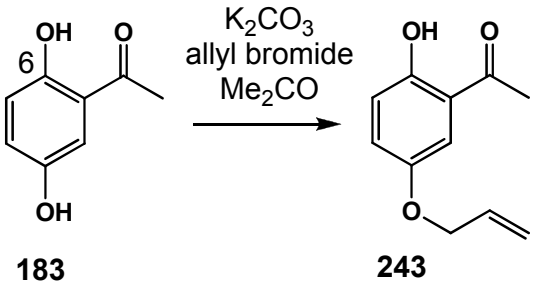

Scheme 80

The ^{1}H NMR spectrum of compound **243** contained eight signals of which the addition of an allyl chain accounts for three. These three were (i) the oxygen-bonded CH_2 protons at 4.47 ppm, appearing as a doublet of doublets (J = 5.3 and 1.3 Hz), (ii) the two vinylic CH protons which had remarkable resolution and the *cis* (doublet of doublets) and *trans* (doublet of triplets) protons could be individually assigned at 5.28 ppm and 5.38 ppm respectively (see **Figure 16**) and (iii) the vinylic CH at 6.02 ppm was observed as a doublet of doublet triplets (J = 17.2, 10.5 and 5.3 Hz).

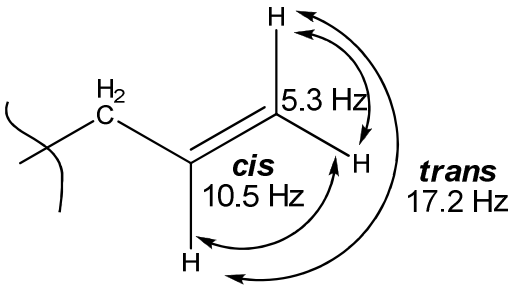

Figure 16

The remainder of the peaks corresponded to those of the parent molecule. The benzylic ketone methyl group appeared as an intense singlet at 2.58 ppm with the phenol appearing at 11.86 ppm. The considerable downfield occurrence of the phenol hydroxyl owing to hydrogen bonding confirmed the success of this chemoselective reaction. Three aromatic hydrogen atoms were observed as signals at 6.86 ppm (doublet, J = 9.0 Hz, H-3), 7.08 ppm (doublet of doublets, J = 9.0 and 3.0 Hz) and 7.17 ppm (doublet, J= 3.0 Hz, H-6). The ^{13}C NMR spectrum corroborated the ^{1}H NMR spectrum, indicating the presence of an allyl group. The methylene carbon peak emerged in the region expected for a carbon bonded to oxygen[3] at 69.8 ppm, with the vinylic CH_2 downfield at 117.8 ppm. Lastly the vinylic

CH signal appeared at 133.1 ppm. As a whole, the NMR spectra for the mono-allylated product **243** were in perfect agreement with those reported in the literature[1,2].

4.1.2. Thermal Claisen rearrangement and subsequent methylation

The next two steps in the synthesis were (i) the regioselective rearrangement of the allyl group of mono-allylated compound **243** to C-2 in **244** and (ii) the methylation of the resulting hydroquinone to form the aromatic dimethoxy containing compound **182** (**Scheme 81**)[2,3]. Thus **243** was heated for 18 h at 140 °C to facilitate the formation of the desired Claisen rearrangement product **244**. The hydroquinone **244** was then methylated with dimethyl sulfate and potassium carbonate in boiling acetone to produce **182** in a 76 % yield.

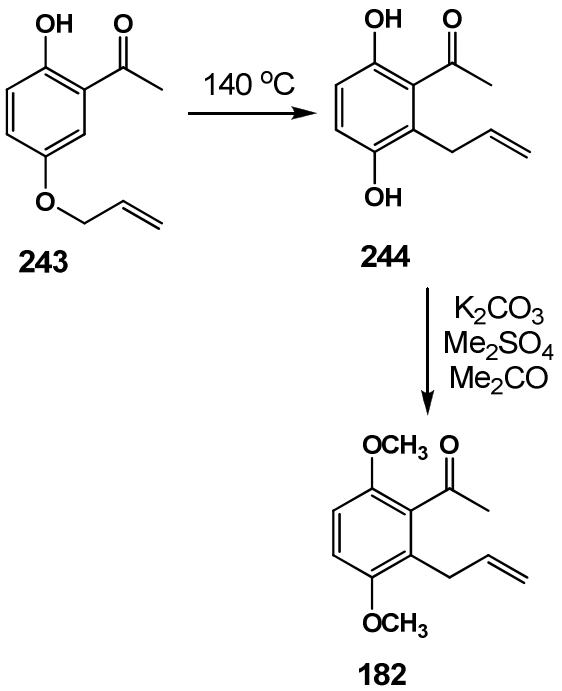

Scheme 81

In the ^{1}H NMR spectrum of **244**, there were three clear observations to confirm that the allyl chain rearrangement was successful: (i) there was the emergence of a second phenolic hydrogen peak at 7.93 ppm, (ii) the allyl chain methylene protons, formerly bonded to oxygen, moved significantly upfield to 3.35 ppm and (iii) only two

aromatic protons were visible. These two aromatic hydrogens exhibited *ortho*-coupling constants (J = 9.0 Hz) from which it was inferred that they were adjacent in proximity, thus confirming that the reaction was indeed regioselective. The ^{13}C NMR spectrum also indicated the migration of the allyl group, as the allyl CH_2 group appeared as a signal at 31.4 ppm compared to at 69.8 ppm in the precursor.

In comparison, the ^{1}H NMR spectrum of compound **182** contained two new singlets from the methoxy groups at 3.73 ppm and 3.75 ppm with the disappearance of hydroquinone signals. In the ^{13}C NMR spectrum two methyl ether shifts were overlapped at 55.9 ppm.

The NMR data for both **244** and **182** were in accordance with the data reported in the literature[3].

4.1.3. Claisen condensation reaction

Now with substrate **182** in hand we could attempt a Claisen condensation reaction. This desired transformation has been carried out successfully in the literature on aromatic ketones and therefore we followed reported procedures[4,5]. Compound **182** was reacted with 2.0 molar equivalents of diethyl oxalate **231** and sodium ethoxide base for 3 h, followed by work-up of the reaction by the addition of hydrochloric acid to yield Claisen condensation product **181a** as a yellow solid in a 90 % yield (**Scheme 82**).

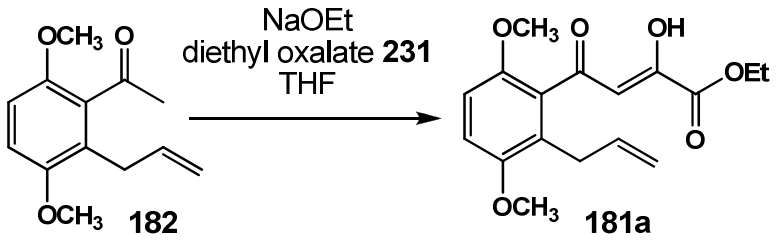

Scheme 82

The proposed mechanism for this Claisen condensation process is shown in **Scheme 83**. Exposure of **182** to ethoxide base forms the enolate **245**, which attacks

the carbonyl carbon of the diethyl oxalate ester to form intermediate **246**. This intermediate species **246** eliminates the alkoxide anion to produce the 1,3-diketone **181b** that loses an acidic *alpha* proton to ethoxide. The resultant enolate species **247** is acidified in the reaction work-up to yield the tautomerized 1,3-diketone **181a**.

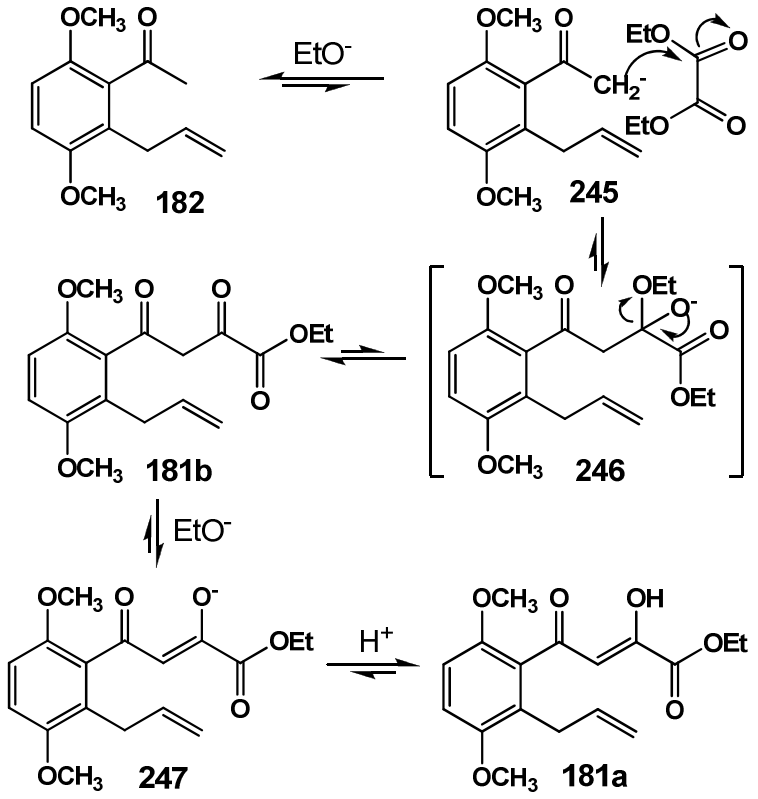

Scheme 83

The spectral data of product **181a** contained conclusive proof of the success of the reaction. The ^{1}H NMR spectrum displayed three new signals: (i) the ethyl ester peaks were observed at 1.34 ppm (CH_3, triplet, J = 7.1 Hz) and 4.31 ppm (CH_2, quartet, J = 7.1 Hz), accounting for a total of five protons and (ii) the enol hydrogen signal appeared at 6.58 ppm as a singlet. The ^{13}C NMR spectrum contained the ethyl ester peaks at 13.9 ppm (CH_3) and 62.4 ppm (CH_2). Two carbonyl signals were also seen at 197.6 ppm (C=O) and 164.5 ppm (CO_2). The carbon atoms of the enol moiety were present at 162.3 ppm [COCH=**C**(OH)] and 105.9 ppm [COC**H**=C(OH)]. The position of the enol was determined by two-dimensional NMR experiments (HMBC and HSQC). The IR spectrum contained a hydroxyl band at 3007 cm^{-1}, with two carbonyl stretching frequencies present at 1738 cm^{-1} and 1730 cm^{-1}. This

confirmed the presence of the enol, ketone and ester moieties. The HRMS data for the product was found to be 321.1338 amu which was in accordance with the calculated value of 321.1342 amu for our molecular formula of $C_{17}H_{21}O_6$.

4.1.4. Sodium borohydride reduction of 1,3-diketone

Our next planned step was the selective reduction of this 1,3-diketone **181a** to its corresponding 1,3-diol counterpart **180** which is depicted in **Scheme 83**.

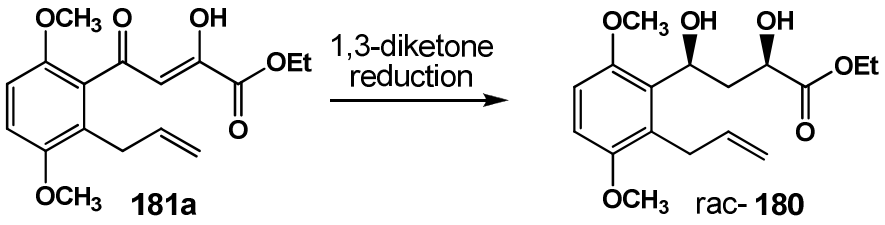

Scheme 83

The mild reducing agent sodium borohydride ($NaBH_4$) was chosen as the reagent for this task and has been shown to efficiently reduce 1,3-diketones to their respective 1,3-diols equivalents, albeit in a racemic fashion[6,7]. Compound **181a** was dissolved in ethanol and treated with 2.0 equivalents of $NaBH_4$ at ambient temperature. Unfortunately the outcome of this reaction was only decomposition (**Scheme 84**). Changing the solvent to methanol yielded the same negative result. This was an unexpected finding as alcoholic solvents are commonly employed for this reaction.

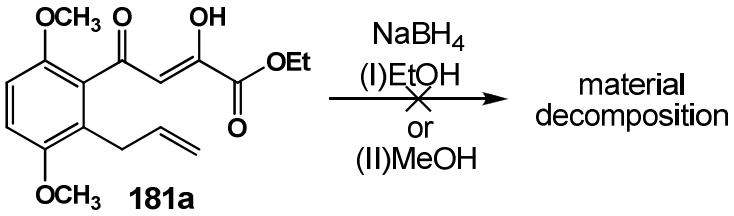

Scheme 84

Thus, we searched for another suitable non-alcoholic solvent medium and found that tetrahydrofuran served this purpose (**Scheme 85**). The reaction in this case afforded a yellow liquid product, compound **248**. This single secondary alcohol-containing

compound **248** was not our desired product as we required the reduction of both ketone groups (**Scheme 83**). The benzylic ketone motif of **248** appeared to be resilient to $NaBH_4$ reduction at ambient temperature so we increased the reaction temperature to reflux for an extended duration, with constant monitoring. This process once again only yielded the starting material **248**.

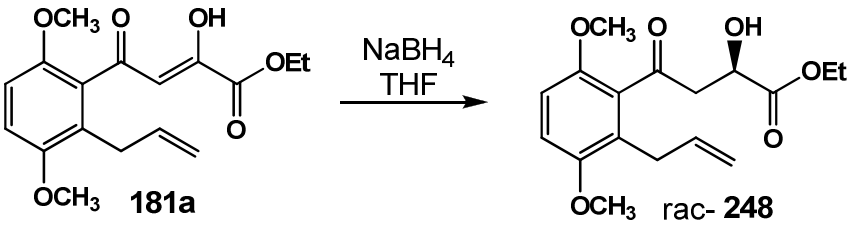

Scheme 85

The NMR spectra of **248** were very similar to those of the parent compound **181a**. The reduction of the enol functionality was apparent in the ^1H NMR spectrum as the newly formed methylene protons were visible as two well resolved couple of doublet of doublets at 3.23 ppm and 3.39 ppm. The hydrogen atom attached to the carbon of the secondary alcohol was observed downfield as a broad singlet at 4.56 ppm. The ^{13}C NMR spectrum, however, clearly showed the existence of the benzylic ketone carbonyl carbon atom at 204.4 ppm. The secondary alcohol carbon emerged considerably upfield at 66.9 ppm with the newly formed CH_2 appearing at 61.6 ppm. The nature of these two carbon atoms was determined using a DEPT 90 NMR experiment. The HRMS of this compound was in accordance with its calculated value.

4.1.5. Wacker Oxidation of secondary alcohol 248

Compound **248** was not our desired substrate but investigating the outcome of a Wacker oxidation on this compound on a theoretical basis suggested that it may indeed form a 6,6-bicyclic pyran ring system (**Scheme 86**). If successful, the Wacker oxidation product **249** could undergo an intramolecular attack of the alcohol moiety on the electrophilic ketone to form intermediate **250**. The newly generated nucleophilic ion of **250** could in turn attack the benzylic ketone group to afford

bicyclic compound **251**, which can be protonated to give cyclic hemiacetal compound **252**, although this may be unstable.

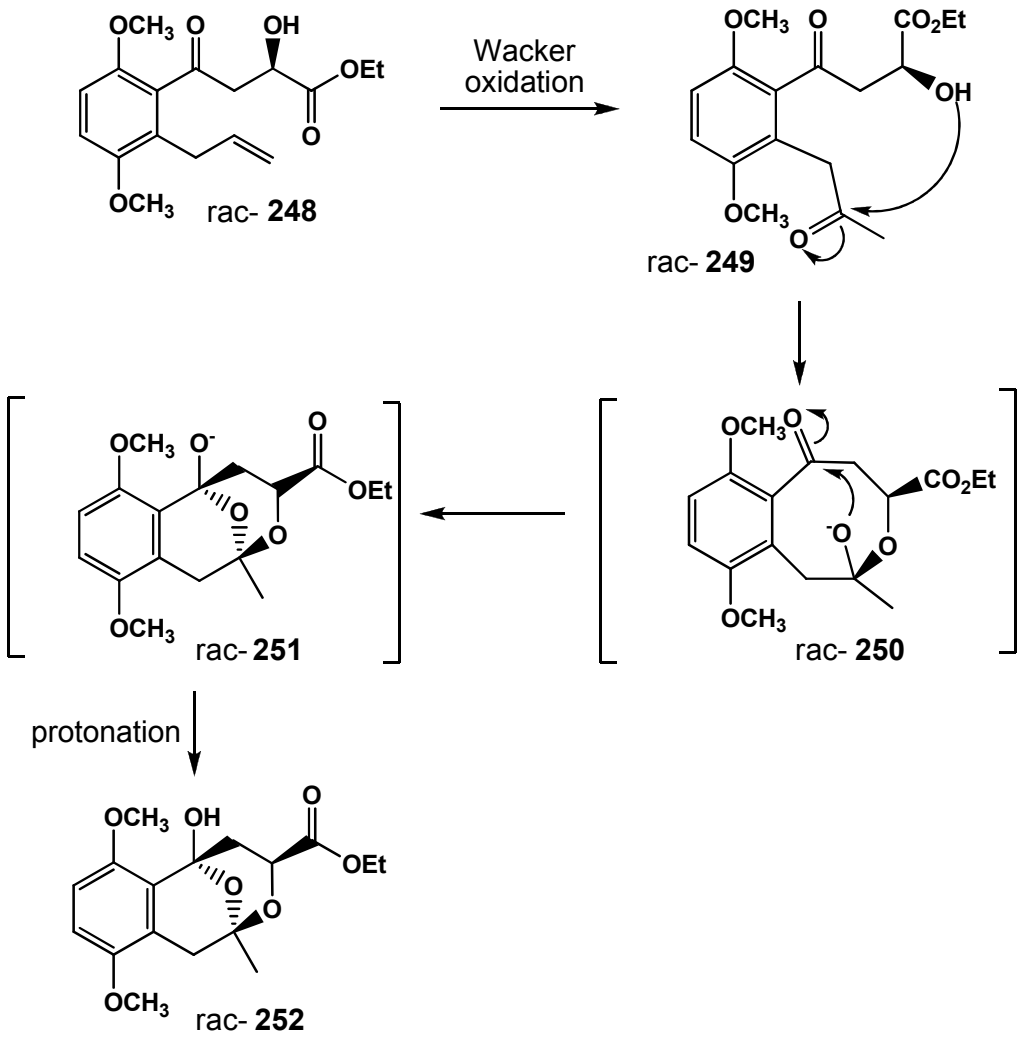

Scheme 86

This reaction was tested experimentally and it was found that the reaction at ambient temperature only led to the recovery of starting material (**Scheme 87**). Extending the duration of the reaction made no impact on the reaction.

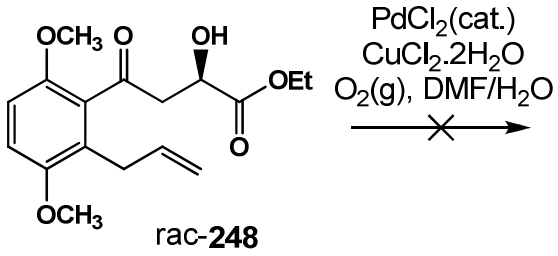

rac-**248**

Scheme 87

We found that increasing the reaction temperature to 70 °C facilitated the reaction (**Scheme 88**). The Wacker oxidation product **249** was isolated as a clear oil in a 67% yield. The isolation of **249** was unexpected because it meant that the reaction did not spontaneously undergo the cyclic ring-forming process as postulated. We then proposed that either the secondary alcohol may not be a sufficiently strong nucleophile to attack the newly formed ketone group, or that the reversibility of the reaction limited the formation of the expected product. It is also possible that the benzylic ketone group allows for limited flexibility and consequently prevents the attack of the secondary alcohol on the ketone.

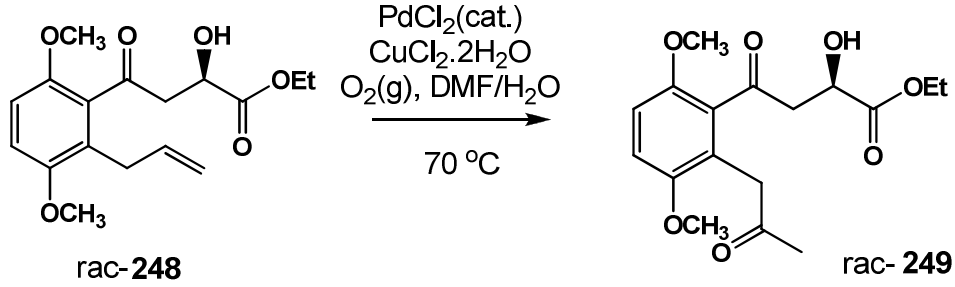

rac-**248** rac-**249**

Scheme 88

The ^{1}H NMR spectrum of Wacker oxidation product **249** contained a few key differences compared to the precursor substrate **248**. The transformation of the alkene portion of the allyl chain was apparent as the benzylic CH_2 was a singlet (compared to a doublet in **248**) that moved downfield to 3.70 ppm. There was also a new methyl peak that appeared at 2.18 ppm, which is adjacent to the newly formed ketone motif. The ^{13}C NMR spectrum now contained two ketone signals as expected, at 204.3 ppm and 206.3 ppm, with the methyl peak emerging at 29.6 ppm. The IR spectrum contained a single broad carbonyl stretch at 1738 cm^{-1}, which could

account for the three carbonyl functionalities if overlaps of the signals are considered. The HRMS data confirmed the calculated mass of compound **249**.

We then attempted to transform the secondary alcohol into a better nucleophile by the selective deprotonation of the secondary alcohol hydrogen atom as this could possibly lead to the reaction in **Scheme 89**. Thus we tested a few suitable bases that could facilitate this process: sodium hydride, sodium ethoxide and potassium *tert*-butoxide. The careful addition (less then one equivalent) of each of these bases unfortunately did not allow for the isolation of any identifiable product(s).

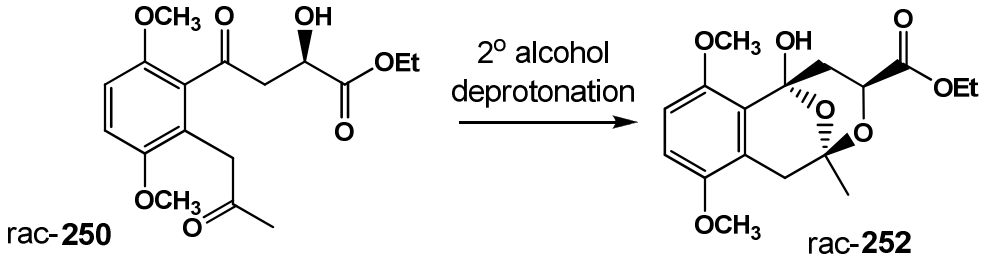

Scheme 89

At this point we decided to change our approach towards accessing the bicyclic acetal ring system.

4.2. Modified Route Towards Construction Of Bicyclic Acetal Rings

As we were unable to reduce the benzylic ketone group to a secondary alcohol using $NaBH_4$, we decided to employ the significantly stronger reducing agent LAH for this task. This reagent should reduce both the carbonyl groups and the ethyl ester motifs to alcohols (**Scheme 90**), converting compound **181a** to the racemic triol **253**. If triol **253** is subjected to a Wacker oxidation, it should preferentially form the 6,6-bicyclic pyran ring system, acetal **254**.

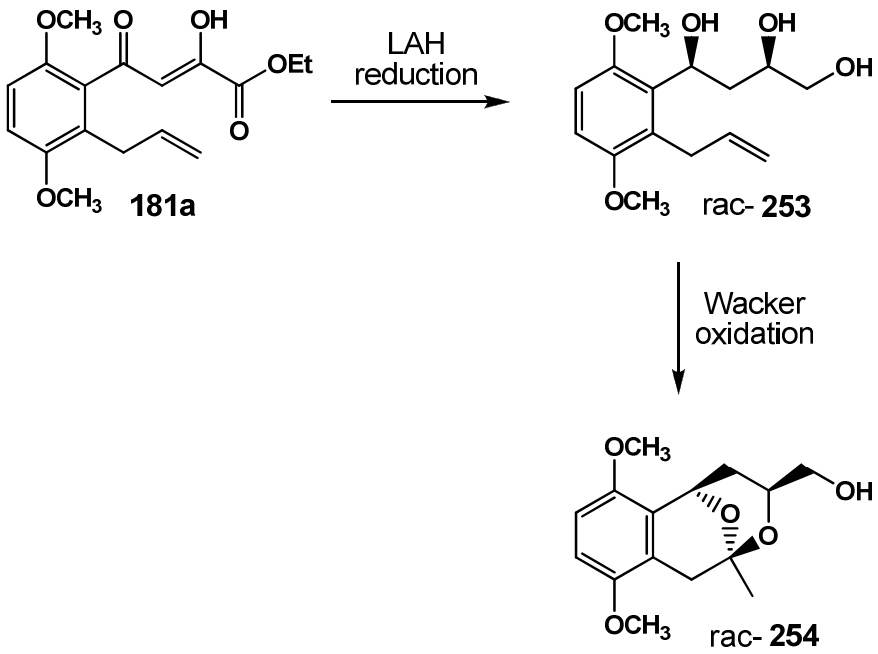

Scheme 90

4.2.1. Lithium aluminium hydride reduction of 1,3-diketone and ethyl ester functionalities

The first part of our new synthetic plan was the LAH reduction of compound **181a** and this was carried out at -10 ℃ in tetrahydrofuran. This process led to the isolation of a single product, 1,2-diol compound **255** in a low yield of 30 % (**Scheme 91**). The enol and ethyl ester groups were reduced to a secondary and primary alcohol respectively, but the benzylic ketone remained intact as was observed in the $NaBH_4$ reduction.

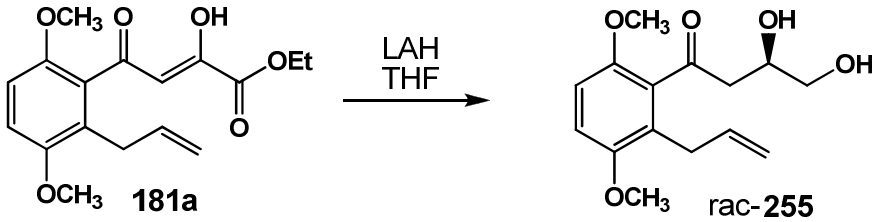

Scheme 91

The NMR spectroscopic data for 1,2-diol **255** closely resembled those of alcohol **248**. The reduction of the ethyl ester motif was evident in the ^1H NMR spectrum as

the disappearance of the characteristic two peaks (triplet and quartet signals) of the ethyl group of the ester, and the emergence of the primary alcohol methylene protons at 3.63 ppm (J = 11.7 and 2.8 Hz) and 3.48 ppm (J = 11.3 and 6.6 Hz), which was observed as two doublet of doublets. In the 1,2-diol **255** the reduction of one of the ketones was also visible as the proton next to the secondary alcohol ($COCH_2C$**H**(OH)) appeared as a multiplet at 4.29 ppm. The adjacent CH_2 protons appeared as a doublet (J = 6.1 Hz) at 2.96 ppm. The ^{13}C NMR spectrum contained the ketone carbon atom at 207.3 ppm, with the two new CH_2 signals seen upfield at 65.8 ppm ($\mathbf{C}H_2OH$) and 47.7 ppm [$CO\mathbf{C}H_2CH(OH)$]. The secondary alcohol carbon appeared as a signal at 68.6 ppm. The ketone carbonyl stretching frequency was observed at 1738 cm^{-1} in the IR spectrum, with the broad alcohol bands occurring at 3015 cm^{-1}. The HRMS data confirmed the mass of the1,2-diol compound **255**.

This was an unusual result as the benzylic ketone moiety was even impervious to reduction by LAH. We therefore decided to increase the temperature of the reaction in an attempt to force this reaction to occur. The 1,2-diol **255** was treated with LAH and heated at reflux for 3 h, frustratingly and surprisingly only to afford the 1,4-diol **256** (**Scheme 92**).

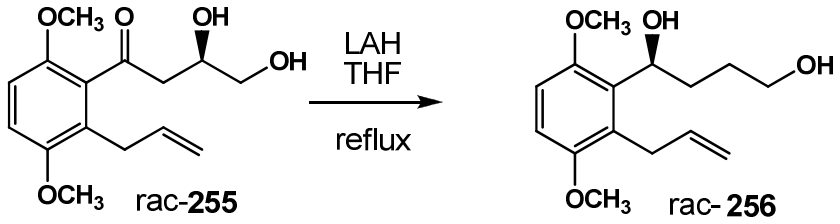

Scheme 92

A proposed mechanism for the transformation of **255** to the 1,4-diol **256** is illustrated in **Scheme 93**. Compound **255** may eliminate water in the refluxing reaction mixture to produce enol **257**, which could tautomerize to aldehyde **258**. The benzylic ketone and resulting aldehyde are then both reduced by LAH to form the 1,4-diol **256**.

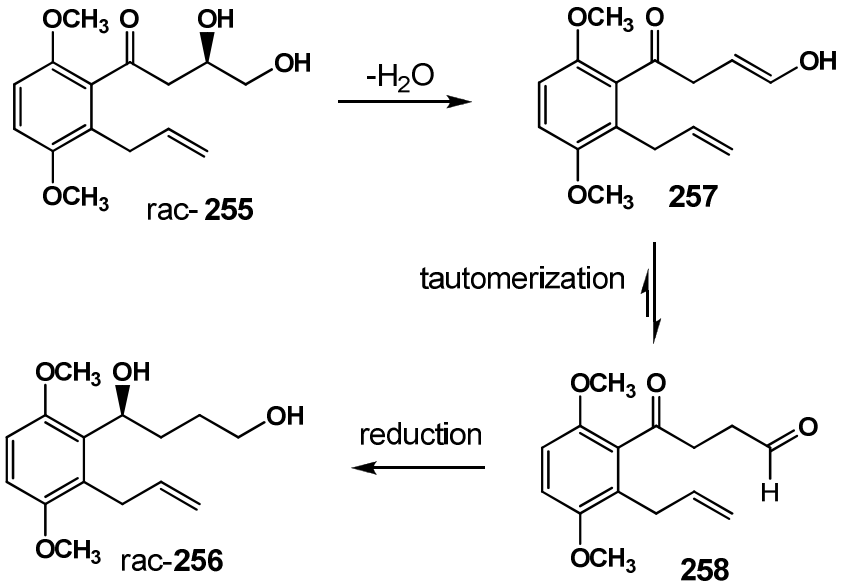

Scheme 93

The ^{1}H NMR spectrum of compound **256** contained a few distinct signs as evidence for the formation of the 1,4-diol. The benzylic CH signal appeared as a doublet of doublets (J = 9.6 and 3.2 Hz) at 4.85 ppm, with the primary alcohol giving rise to a mutiplet at 3.65 ppm. The two central methylene groups were seen upfield between 1.64-2.03 ppm as overlapping signals. Five CH_2 peaks were now observed in the ^{13}C NMR spectrum at 29.9 ppm (Ar**C**H_2CH=CH_2), 30.3 ppm [CH(OH)CH_2**C**H_2], 34.3 ppm [CH(OH)**C**H_2CH_2], 62.7 ppm (**C**H_2OH) and 114.9 ppm (ArCH_2CH=**C**H_2). The reduction of the benzylic ketone was determined by the absence of the former downfield ketone peak and the appearence of a signal at 71.4 ppm arising from the secondary alcohol carbon. The nature of the CH and CH_2 carbon atoms was resolved by a DEPT 90 NMR experiment. The IR spectral data exhibited a broad alcohol stretching band at 3373 cm^{-1} and no carbonyl frequency was observed, which was also indicative of the reduction of the benzylic ketone.

4.2.2. Wacker oxidation of 1,4-diol system

The 1,4-diol **256** was an unwanted side product, but on examining this system from the perspective of cyclic acetal ring formation, we realised that it may be of some benefit to us. Thus we assessed the prospect of subjecting **256** to a Wacker oxidation, which potentially would result in the formation of a 6,7-bicyclic pyran ring

system (**Scheme 94**). This ring arrangement would contain the wrong size acetal system compared to those of our desired model system **254**, but it would give us valuable insight into whether our methodology for constructing these bicyclic compounds was possible. Therefore, we subjected 1,4-diol **256** to Wacker oxidation conditions for 2 h. Once again, we heated the mixture at 70 °C as this temperature was required for the reaction to progress. Much to our delight, the tricylic compound **259** was isolated as a clear oil in a 72 % yield.

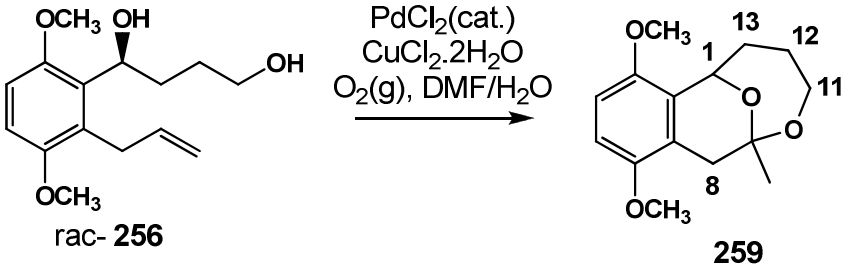

Scheme 94

The ^{1}H NMR spectrum of the bicyclic acetal **259** was quite remarkable as all four of the methylene protons in this molecule were diastereotopic and displayed very unusual chemical shifts. The original benzene skeleton remained intact as the two aromatic methyl ether peaks (overlapped) and two aromatic signals (overlapped) were observed at 3.77 ppm and 6.66 ppm respectively. The benzylic CH proton at C-1 appeared as a multiplet at 5.15 ppm. The benzylic CH_2 hydrogens at C-8 were enantiotopic and the first proton emerged as a doublet (J = 16.8 Hz) at 2.49 ppm and the second proton was found 0.5 ppm downfield at 3.04 ppm also as a doublet (J = 16.8 Hz). The non-equivalent protons at C-13 were observed at 1.76 ppm and 2.60 ppm. Similarly, the enantiotopic protons of C-12 appeared at 1.32 ppm and 1.54. The CH_2 protons at C-11 were observed as a doublet of doublet of doublets at 3.56 ppm (J = 11.8, 3.3 and 2.0 Hz) and a doublet of doublets at 3.80 ppm (J = 11.8 and 1.5 Hz). Lastly, the methyl group at C-3 appeared as a singlet at 1.48 ppm and accounted for three hydrogens as expected. The ^{13}C NMR spectrum of **259** contained four CH_2 signals, compared to five in the precursor **256**, and these emerged at 27.6 ppm (C-12), 32.4 ppm (C-1), 33.6 ppm (C-8) and 60.4 ppm (C-11). The position of C-9 was very distinctive of the presence of the acetal group and it appeared in the expected region at 97.4 ppm. The methyl carbon atom at 25.0 ppm

also supported the structure of **259**. The IR spectrum showed no hydroxyl stretching band which was in accordance with structure **259**. The HRMS of acetal **259** was in agreement with the calculated mass of this compound.

The success of this reaction supported our proposed formation of the 6,6-bicyclic pyran ring system **254** from the triol **253**, provided that the diol **180** could be synthesized.

4.2.3. Chemoselective TBDMSCl protection of 1,2-diol primary alcohol

We have established that the standard LAH reduction of the Claisen condensation product **181a** forms the 1,2-diol **255**. We also discovered that increasing the temperature of this reaction promotes the formation of the 1,4-diol **256**. By examining our postulated mechanism (**Scheme 93**) of the formation of 1,4-diol **256** from 1,2-diol **255**, we realised that it may be possible to prevent the loss of water from the 1,2-diol **255** by protecting the primary alcohol of **255**. This would effectively avert the formation of the 1,4-diol **256** and possibly allow the reduction of the benzylic ketone to occur exclusively. Thus we decided to protect the primary alcohol of the 1,2-diol **255** with a TBDMS group (**Scheme 95**). Our substrate **255** contains two alcohol groups which potentially could both be protected with TBDMSCl, however we know that the primary alcohol should react first. In order to exploit this difference in reactivity, we treated **255** with TBDMSCl and imidazole (base) in a portion-wise manner at 0 °C in acetonitrile solvent. The result was the successful isolation of the TBDMS protected alcohol **260**.

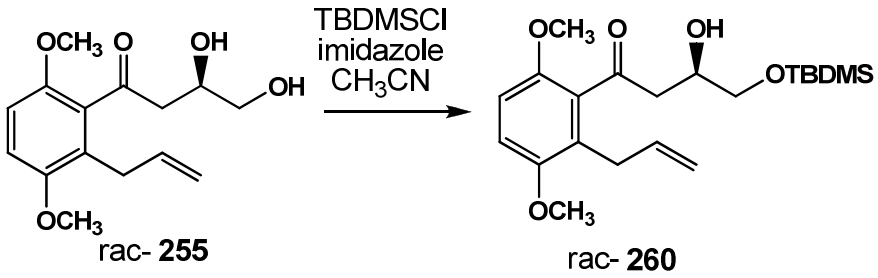

rac- **255** rac- **260**

Scheme 95

The NMR spectra of the TBDMS-protected compound **260** were similar to the spectra of the precursor 1,2-diol **255**. The ^{1}H NMR spectrum of **260** contained two new signals from the TBDMS moiety, i.e. the two sets of methyl group peaks at 0.00 ppm and 0.83 ppm which accounted for a total of fifteen protons. The methylene hydrogens adjacent to the benzylic ketone motif (COC**H$_2$**CH(OH)), appeared as two doublet of doublets at 2.91 ppm (J = 17.9 and 7.8 Hz) and 3.04 ppm (J = 17.9 and 4.4 Hz) whereas the CH_2 next to the TBDMS-protected oxygen atom was seen at 3.56 ppm as a multiplet. The secondary alcohol hydroxyl signal was observed at 2.97 ppm. The ^{13}C NMR spectrum possessed three new signals as expected from the TBDMS group, these were at: -5.4 ppm [OSi(**C**H$_3$)$_2$C(CH$_3$)$_3$]., 18.3 ppm [OSi(CH$_3$)$_2$C(**C**H$_3$)$_3$)], and at 25.9 ppm [OSi(CH$_3$)$_2$**C**(CH$_3$)$_3$]. The HRMS data for the product was found to be 395.2254 amu which was in accurate accordance with the calculated value of 395.2245 amu for the molecular formula of $C_{21}H_{35}O_5Si$.

4.2.4. Lithium aluminium hydride reduction of protected alcohol and subsequent Wacker oxidation

With the TBDMS product **260** in hand, we could attempt the LAH reduction of the benzylic ketone to an alcohol. Compound **260** was refluxed in tetrahydrofuran in the presence of LAH for 2 h (**Scheme 96**). TLC analysis revealed that the starting material was depleted after this duration and we proceeded to work up the reaction and purify potential products. This process proved futile as we realized that the product(s) formed decomposed on the silica gel chromatography column. Thus we opted to skip the purification step and immediately carry out a Wacker oxidation on the crude material from the LAH reduction (**Scheme 96**). This reaction was done at 70 ℃ for 2h and successfully resulted in the formation of our desired target compound **254** as a white solid in a yield of 67 % over two steps.

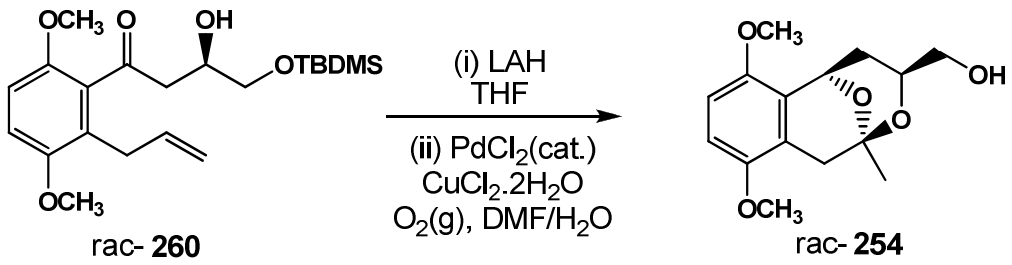

rac- **260** rac- **254**

Scheme 96

Acetal **254** did not contain the TBDMS protecting group that was present in the starting material **260** which meant it was cleaved during the LAH reduction step. Thus the addition of the TBDMS group to 1,2-diol **255** assisted the benzylic ketone reduction and thereafter was removed *in situ*. The triol **253** was the likely unstable intermediate from our initial LAH reduction reaction and its possible transformation to acetal **254** *via* the Wacker oxidation is shown in **Scheme 97**.

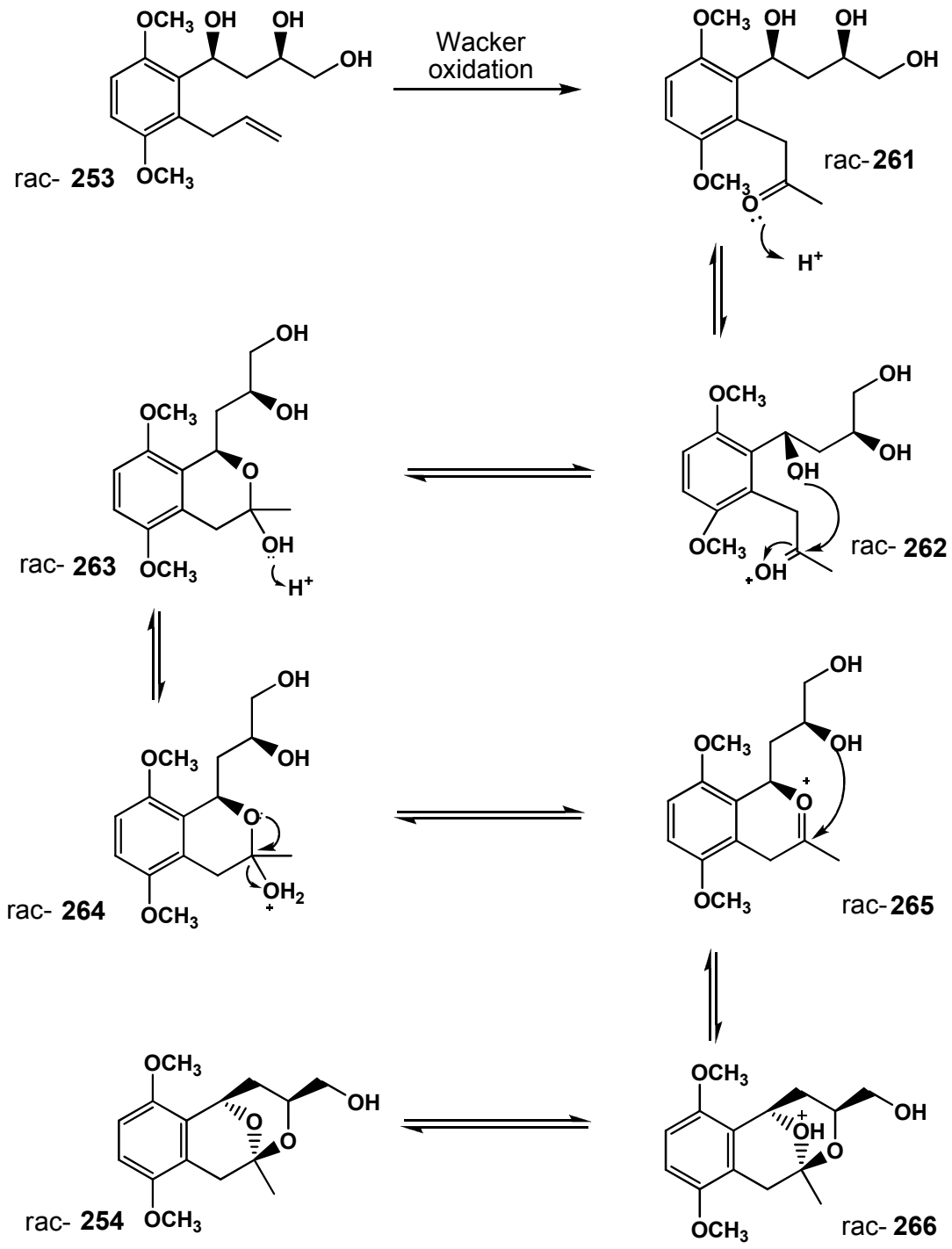

Scheme 97

The alkene motif in the allyl chain of triol **253** is oxidised to a ketone by a Wacker oxidation process to afford intermediate **261**. The newly formed ketone group of **261** is protonated and is consequently attacked by one of the secondary alcohol moieties as shown in **262**, which results in the development of hemiacetal **263**. The

hemiacetal group of **263** is protoated to afford **264** and subsequently dehydrates to produce the intermediate **265**. The benzylic secondary alcohol attacks the strongly electrophilic oxocinium carbonyl motif which generates the bicyclic acetal compound **266**. Unstable acetal **266** undergoes deprotonation to produce the more stable species **254**, which is our isolated product. There are a few contradictions in this proposed mechanism that warrant further explanation: (i) the primary alcohol group in triol **253** is a better nucleophile then either of the secondary alcohol moieties, but we believe that the driving force of the 1,3-diol acetal combination over the 1,4-diol acetal fusion is the lower energy stabilisation benefit of forming a 6,6-bicyclic ring system over a 6,7-bicyclic ring system and (ii) the ability of the secondary alcohol to act as a suitable nucleophile in this scenario compared to compound **249** can be attributed to the increased flexibility found in the triol skeleton of **253**.

The triol precursor **253** was produced by employing the non-stereoselective reducing agent LAH and given the 1,3-diol relationship between the secondary alcohol groups there are therefore four possible stereoisomers of **253**. These are the two *trans*-diol diastereomers **253a** and **253b** and the two *cis*-diol diastereomers **253c** and **253d** (**Figure 18**).

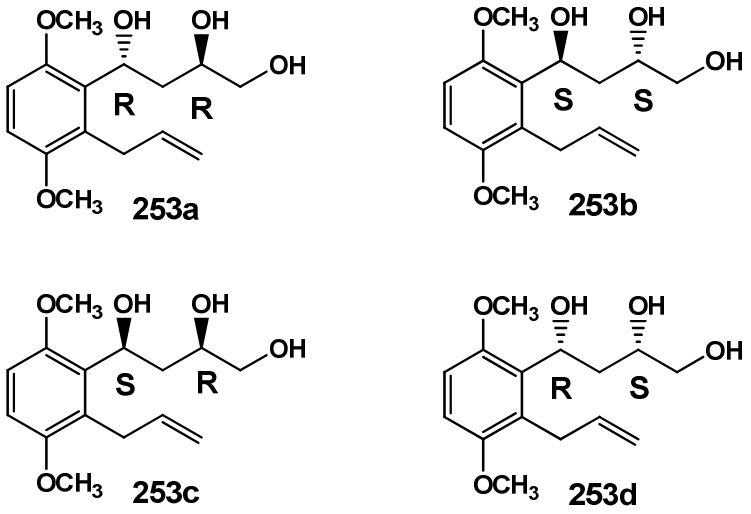

Figure 18

Therefore, based on these possible precursor triol stereoisomers (**Figure 18**), acetal **254** should occur as a mixture of four diastereomers: that is, **254a** and **254b** and their respective mirror images (**Figure 19**).

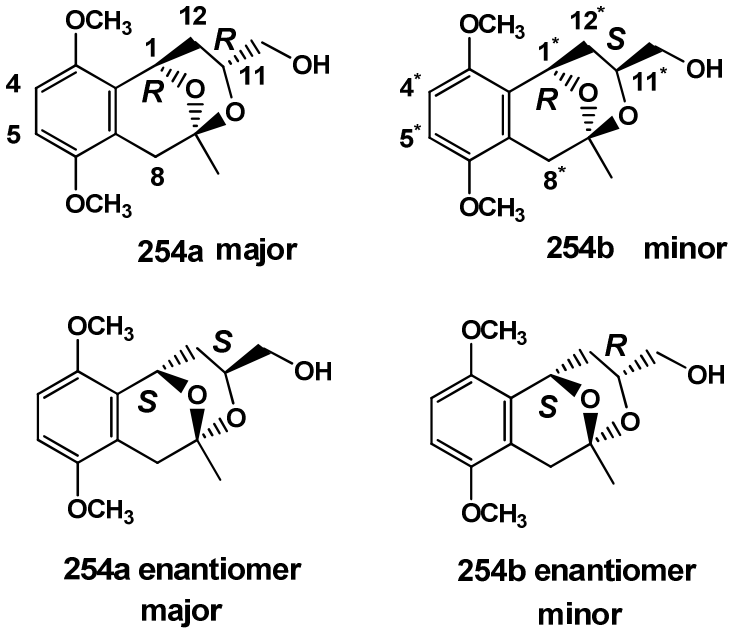

Figure 19

These structural predictions are in accordance with our experimental findings. The ^{1}H NMR spectrum of **254** contained a mixture of two compounds, which were found in a 2.3 :1 ratio (**Table 4**). We were able to grow crystals of **254** and thus obtain vital crystallographic data that confirmed that the major diastereomers [(*R,R*) and (*S,S*)] (~ 65 %) were **254a** and its mirror image (**Figure 20**) and the minor diastereomers [(*R, S*) and (*S,R*)] (~ 35 %) were **254b** and its mirror image (**Figure 21**). This further implied that triols **253a** and **253b** were the major isomers whereas triols **253c** and **253d** were the minor isomers.

*Table 4: ^{1}H NMR signals of diastereomers **254a** and **254b**.*

Proton	**254a** (Shift in ppm)	**254b** (Shift in ppm)
H-5/H-5*	6.64 (d, *J* = 8.8 Hz)	6.64 (d, *J* = 8.8 Hz)
H-4/H-4*	6.67 (d, *J* = 8.8 Hz)	6.67 (d, *J* = 8.8 Hz)
H-1/H-1*	5.40 (brd, *J* = 3.9 Hz)	5.25 (brd, *J* = 9.1 Hz)

OCH_3	3.77 (s), 3.76 (s)	3.77 (s), 3.76 (s)
H-12a/H-12a*	2.09–2.02 (m)	2.30 (ddd, *J* = 13.0, 10.1, 5.3 Hz)
H-12b/H-12b*	1.40 (dt, *J* = 12.9, 2.0 Hz)	1.57 (ddd, *J* = 13.0, 11.1, 1.55 Hz)
H-11/H-11*	3.83 (m)	4.09–4.03 (m)
C**H$_2$**OH	3.48 (br s)	3.60–3.54 (m, C**H$_a$**H$_b$OH), 3.41–3.35 (m, CH$_a$**H$_b$**OH)
H-8a/H-8a*	2.98 (d, *J* = 18.8 Hz)	2.83 (d, *J* = 17.3 Hz)
H-8b/H-8b*	2.85 (d, *J* = 18.8 Hz)	2.59 (d, *J* = 17.3 Hz)
CH_3	1.53 (s)	1.52 (s)

Between these two diastereomers there are a few substantial differences observed in the ^{1}H NMR spectra. The coupling constant of the broad doublet of H-1 is 3.9 Hz in the major product and is 9.1 Hz in the minor diastereomer. The proton H-12a of the major product appeared as a multiplet where H-12b is resolved as a doublet of triplets (*J* = 12.9, 2.0 Hz), whereas both H-12a* and H-12b* for the minor acetal product are seen as a doublet of doublet of doublets (*J* = 13.0, 10.1, 5.3 Hz) and (*J* = 13.0, 11.1, 1.55 Hz).

In the ^{13}C NMR spectra the signals of the diastereomers **254a** and **254b** were found in unequal ratios. However, the signals for these isomers were very close to each other as expected. The important C-9 /C-9* peaks appeared at 96.0 ppm and 97.4 ppm respectively. Each diastereomer contains three CH_2 signals and these were observed at 65.9 ppm (*C*H$_2$OH)/ 64.9 ppm (*C*H$_2$OH*) 32.8 ppm (C-8)/33.2 ppm (C-8*) and 30.4 ppm (C-12)/32.8 ppm (C-12*). The acetal ring CH signals occurred at 65.7 ppm (C-1)/ 65.0 ppm (C-1*) and 68.3 ppm (C-11)/ 66.7 ppm (C-11*). The methyl carbon peaks appeared downfield at 29.5 ppm (CH_3) and 24.6 (CH_3*).

The X-ray crystal structures of **254a** (**Figure 20**) and **254b** (**Figure 21**) provided us with conclusive structural evidence for the existence of the 6,6-bicyclic acetal rings. The important stereochemistry of the diastereomers was unambiguously assigned

with this information. As mentioned previously, the major diastereomers were **254a** and its mirror image and the minor diastereomers were **254b** and its mirror image.

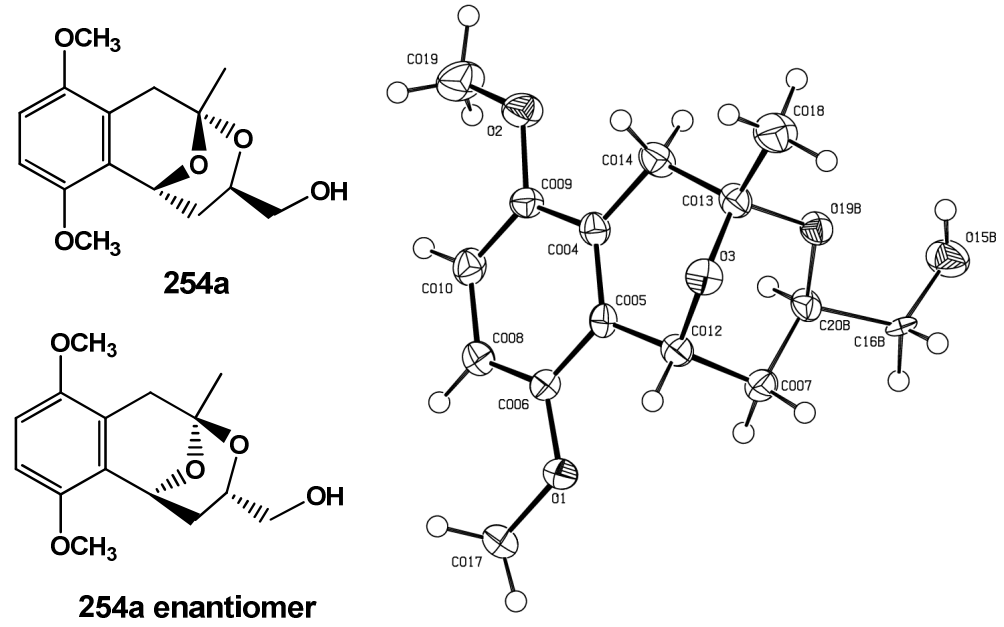

Figure 20

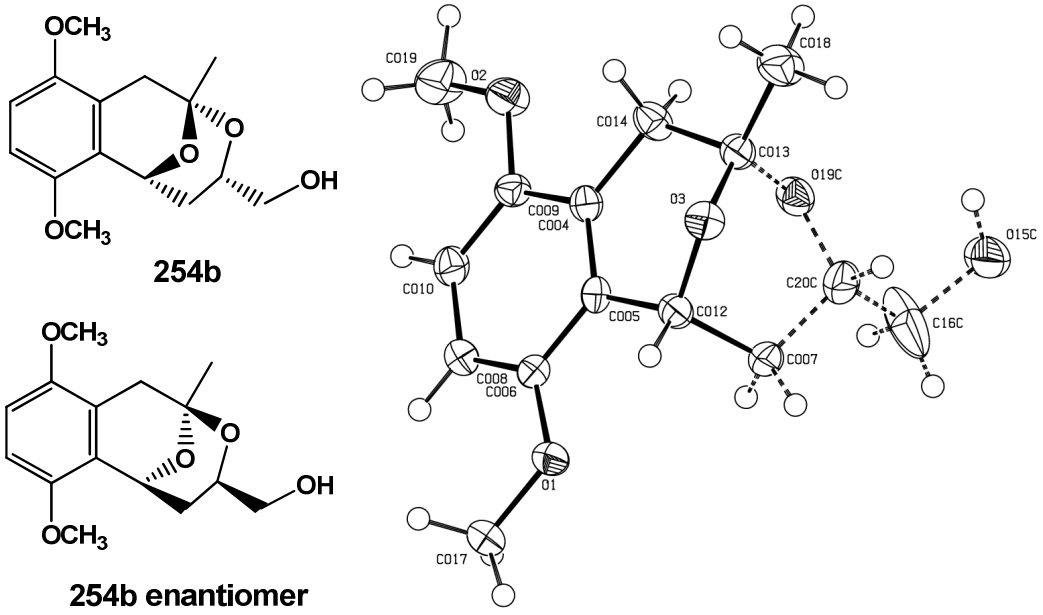

Figure 21

4.3. Structural Adjustments of 6,6-bicyclic pyran ring system

With the tricyclic ring system in place we attempted to transform **254** to a model system that closely resembled marticin **45**. This entailed oxidizing the primary alcohol group of acetal **254** to a carboxylic acid (compound **267**) and oxidizing the aromatic methyl ethers of **267** to a *para*-quinone to afford **268** (**Scheme 98**).

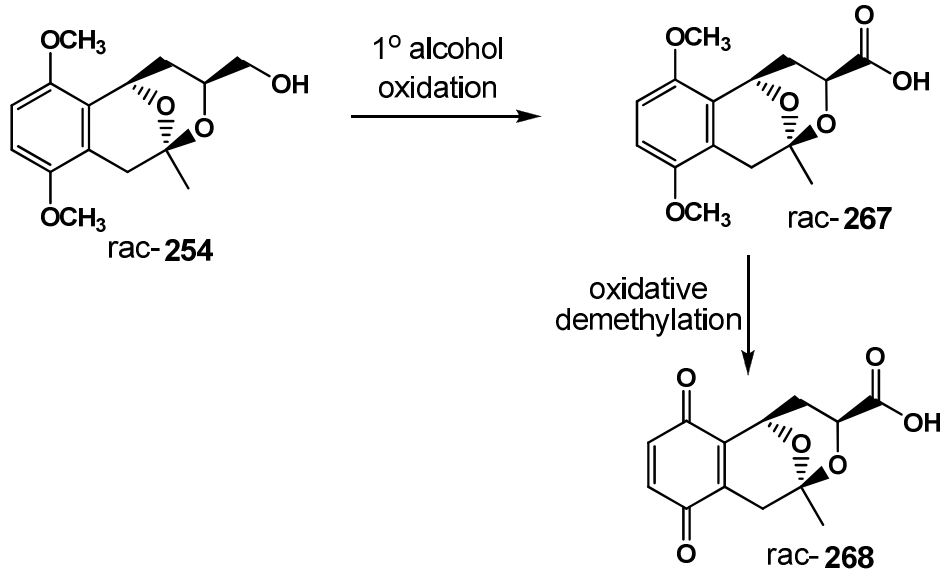

Scheme 98

4.3.1. Aliphatic primary alcohol oxidation

The acetal ring system of **254** is sensitive to acidic and basic media and this limited our choice of aliphatic alcohol oxidizing reagents as many of these procedures require such conditions in their reaction processes[8,9]. Due to these constraints we had to carry out this transformation over two steps, as we found no suitable mild process that was feasible overall. We thus decided to first use the Dess-Martin periodinane catalyst **270** which is a mild reagent that can potentially oxidize the primary alcohol of **254** to the aldehyde **269**[10] (**Scheme 99**). If this was successful we would then employ a sodium chlorite oxidation[11] of aldehyde **269** to the carboxylic acid **267**. The acetal **254** was dissolved in dichloromethane and reacted with **270** at room temperature over a 24 h period. Unfortunately, the work-up and column

chromatography of the reaction afforded no identifiable product(s) or starting material.

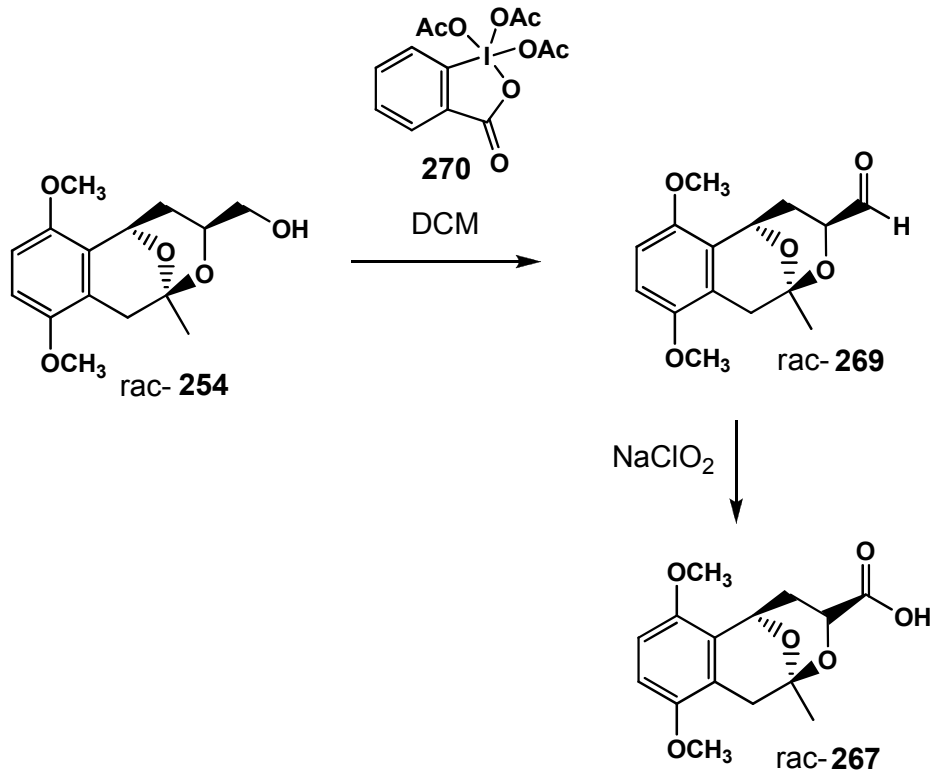

Scheme 99

The acetal fragment of **254** did not appear to tolerate the oxidation process on the aliphatic alcohol. We therefore decided to move onto the next planned step from **Scheme 98** which was the oxidation of the aromatic system in acetal **254** to the quinone.

4.3.2. Ceric ammonium nitrate oxidation of bicylic acetal ring product

Based on our previous success with CAN as an oxidizing agent[12] (see **section 3.1.1**) of aromatic compounds, we decided to employ this reagent for our attempted quinone formation, which is shown in **Scheme 100**. Acetal **254** was dissolved in acetonitrile whilst the CAN was added slowly in an aqueous medium over a 30 min period. The desired compound quinone **271** was isolated as a mixture of diastereomers (**271a** and **271b**, **Figure 22**) in a high yield of 89 %. The quinones, as

expected, possessed a bright red colour, compared to the white starting material, and they were considerably more polar as was observed by silica gel TLC analysis.

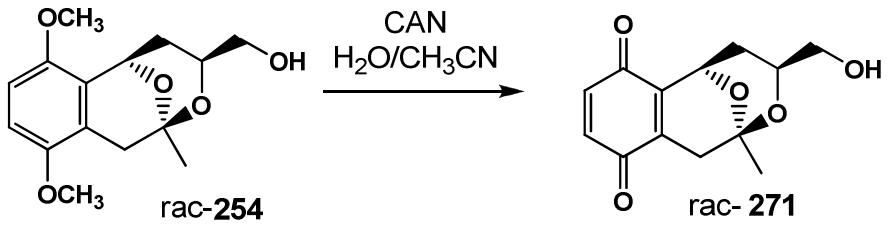

Scheme 100

The proportions of **271a** and **271b** were also found to be in a 2.3: 1 ratio which was determined from the ^{1}H NMR spectrum and this was in accordance with the findings for the precursor compound **254**.

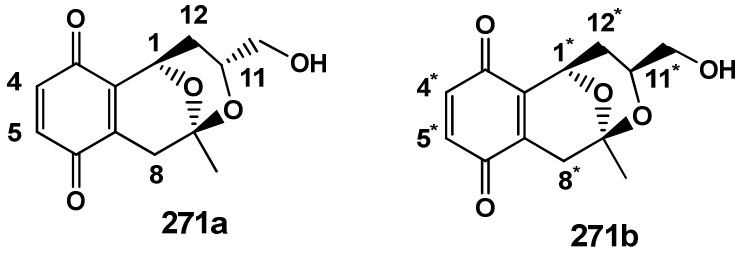

Figure 22

The NMR spectral data of **271** strongly supported that the reaction went as planned. In the ^{1}H NMR spectrum, the existence of the two diastereomers **271a** and **271b** was clearly evident, as was the loss of the aromatic methyl ether signals. The remainder of the proton peaks were the same as those found for the precursor **254** (see **Table 4**) and will therefore not be discussed. The ^{13}C NMR spectrum contained the expected four quinone signals at 185.3 ppm and 184.7 ppm for the major diastereomer **271a** and at 186.4 ppm and 185.3 ppm for the minor diastereomer **271b**. There was also an absence of aromatic methyl ethers peaks in the 50-60 ppm range. The IR spectral data included a quinone stretching band at 1754 cm^{-1}.

4.4. Concluding Remarks Pertaining to the Synthesis of Bicyclic Acetal Ring Systems.

During the course of this PhD we have successfully assembled a model system of the 6,6-bicyclic pyran ring arrangement found in the naturally occurring naphthoquinone marticin **45**. This model compound **271** was produced as a racemic mixture of **271a** and **271b** in 9 synthetic steps in a 3.3 % overall yield (**Scheme 101**). An interesting side product that was synthesized en route to **271** was the 6,7-bicyclic acetal compound **259** that was made in 7 steps in a 6.5 % overall yield (**Scheme 102**). Synthesis of both of these bicyclic acetal compounds employed the commercially available 2,5-dihydroxyacetophenone **183** as starting material.

The key stages in the synthesis of quinone **271** were: (i) the Claisen condensation reaction with diethyl oxalate **231**, (ii) TBDMSCl protection of the primary alcohol group of **255** and (iii) the LAH reduction followed by immediate Wacker oxidation of **260**.

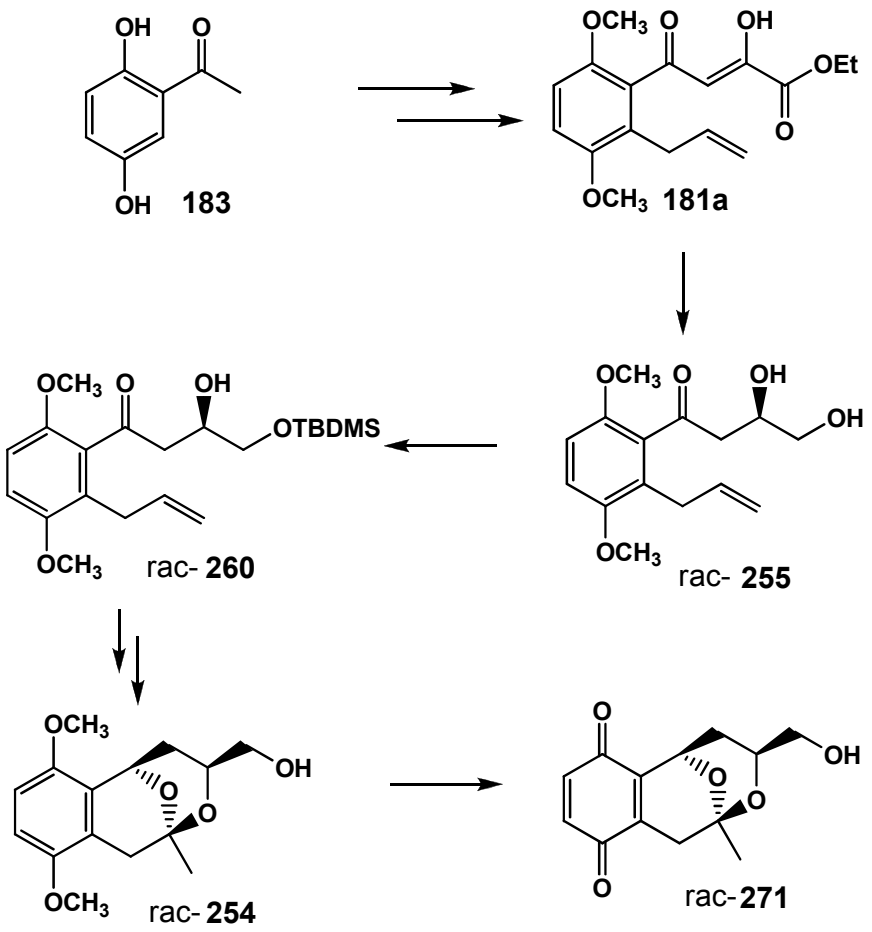

Scheme 101

The reactions pertaining to 6,7-bicyclic acetal compound **259** were similar to those towards quinone **271**, with the only unique step being the LAH reduction of **255** to the 1,4-diol **256**.

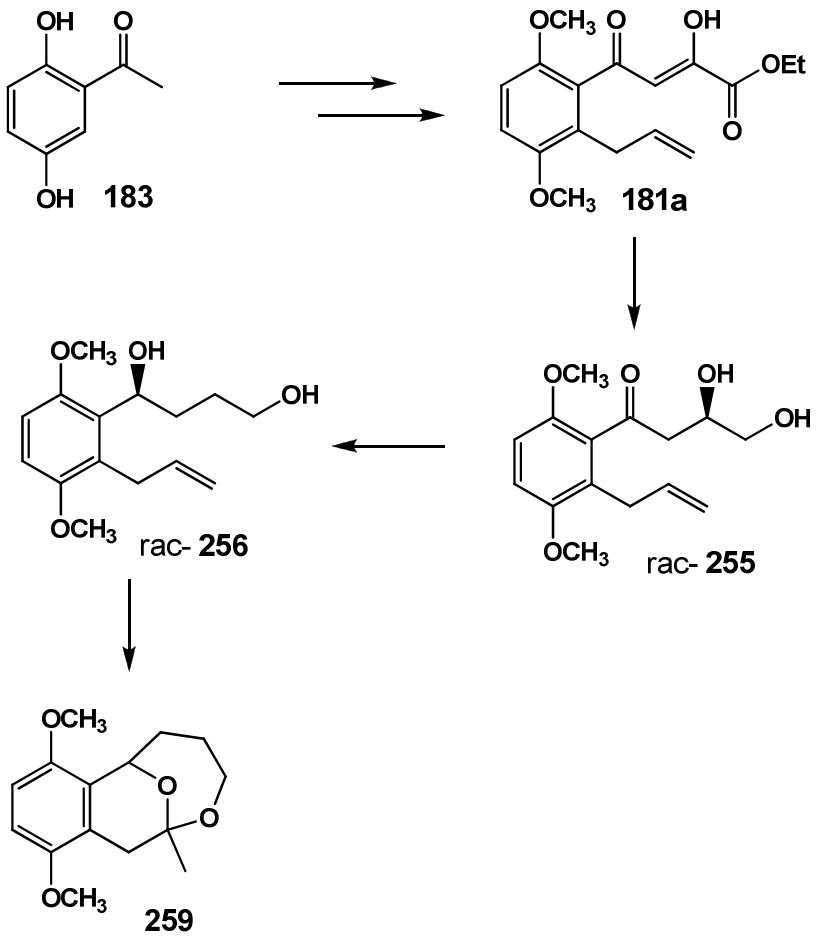

Scheme 102

4.5. References

1. Green, I.R., Hugo, V.I., Oosthuisen, F.J., van Eeden, N., Giles, R.G.F., South *African Journal of Chemistry*, 1995, **48**, 15-22.
2. Mmutlane, E.M., Michael, J.P., Green, I.R., de Koning, C.B., *Organic and Biomolecular Chemistry*, 2004, **2**, 2461-2470.
3. Clayden, J., Greeves, N., Warren, S., Wothers, P., *Organic Chemistry*, 2005, Oxford Univeristy Press Inc., New York.
4. Chang, C., Yang, T., *Tetrahedron Asymmetry*, 2003, **14**, 2239-2245.
5. Zhang, J., Didierlaurent, S., Fortin, M., Lefrançois, D., Uridat, E., Vevert, J.P., *Bioorganic and Medicinal Chemistry Letters*, 2000, **10**, 2575-2578.
6. Chênevert, R., Thiboutot, S., *Canadian Journal of Chemistry*, 1986, **64**, 1599-1601.

7. Kukolja, S., Draheim, S.E., Graves, B.J., Hunden, D.C., Pfeil, J.L., Cooper, R.D.G., Ott, J.L., Counter, F.T., *Journal of Medicinal Chemistry*, 1985, **28**, 1896-1903.
8. Heilbron, I., Jones, E.R.H., *Journal of the Chemical Society*, 1949, 604-607.
9. Ciufoni, M.A., Swaminathan, S., *Tetrahedron Letters*, 1989, **30**, 3027-3028.
10. Meyer, S.D., Schreiber, S.L., *Journal of Organic Chemistry*, 1994, **59**, 7549-7552.
11. Lindgren, B., Nilson, T., *Acta Chemica Scandinavica*, 1973, **27**, 888-890.
12. Tohma, H., Morioka, H., Harayama, Y., Hashizume, M., Kita, Y., *Tetrahedron Letters*, 2001, **42**, 6899-6902.

Chapter 5: Summary and Future Work

5.1. Synthesis of Naphthoquinones

New synthetic methodology pertaining to the synthesis of tetraoxygenated and pentaoxygenated naphthoquinones was successfully developed in this PhD project. The naturally occurring fungal naphthoquinones dehydroherbarin **31** and anhydrofusarubin **26** were synthesized by employing this novel methodology. Dehydroherbarin **31** was made from the commercially available 2,4-dimethoxybenzaldehyde **172** in **11** steps in an overall yield of 4.5 % (**Scheme 103**). This is the third reported synthesis of this secondary metabolite.

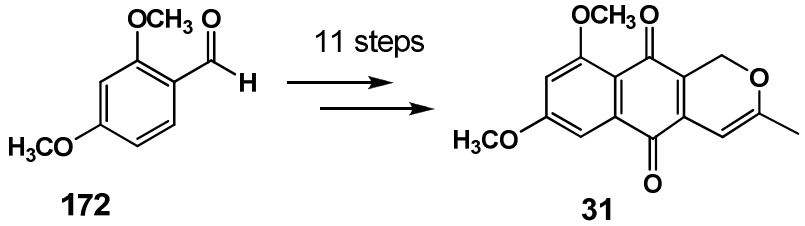

172 **31**

Scheme 103

Two unnatural synthetic naphthoquinones **202** and **218** were also produced on route to accessing dehydroherbarin **31** (**Figure 23**).

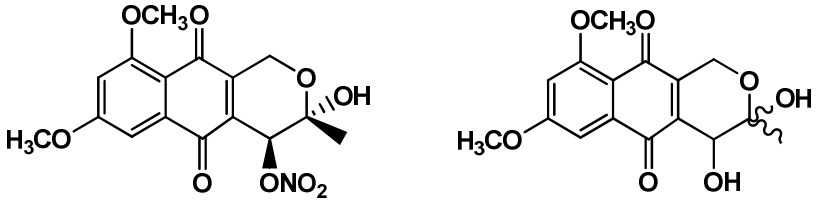

202 **218**

Figure 23

Anhydrofusarubin **26** was made from the commercially available 2,4,5-trimethoxybenzaldehyde **178** in 12 steps in an overall yield of 5.3 % (**Scheme 104**). This is the first total synthesis of anhydrofusarubin.

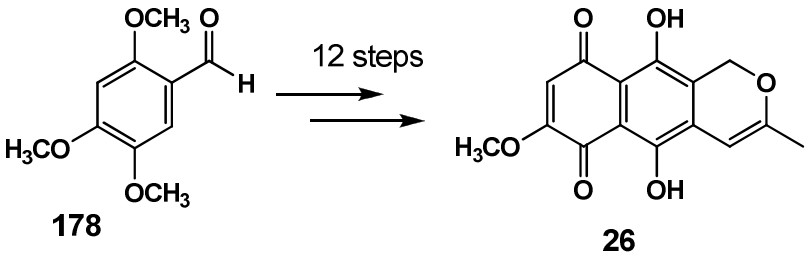

178 26

Scheme 104

5.2. A Model Study towards the Synthesis of a Marticin Fused Bicyclic Pyran System

A model system of the 6,6-bicyclic pyran ring arrangement found in the naturally occurring naphthoquinone marticin **45** was successfully synthesized. The model compound **271** was produced as a racemic mixture of **271a** and **271b** in 9 steps, starting from commercially available 2,5-dihydroxyacetophenone **183** in a 3.3 % overall yield (**Scheme 105**).

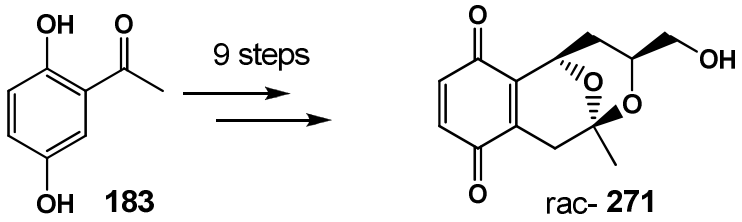

183 rac- **271**

Scheme 105

We also synthesized the 6,7-bicyclic acetal compound **259** in **7** steps, from 2,5-dihydroxyacetophenone **183** in a 6.5 % overall yield (**Scheme 106**).

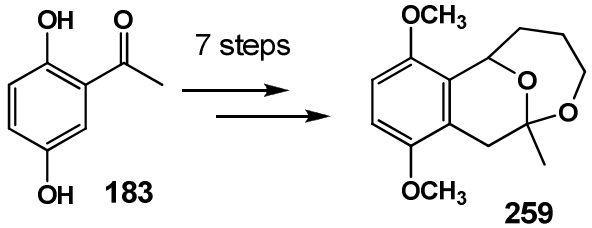

183 **259**

Scheme 106

5.3. Future Work

5.3.1. Cancer screening of synthesized naphthoquinones

The biological testing for anti-tumour activity of all target compounds is still planned and will be carried out in the near future. Very preliminary results have indicated that the poor solubility of the quinones in water could be a problem.

5.3.2. Synthesis of anhydrofusarubin-lactone and anhydrofusarubin-lactol

The naphthoquinones anhydrofusarubin-lactone **29** and anhydrofusarubin-lactol **30** are two other fungal metabolites from the genus *Fusaria* that closely resemble anhydrofusarubin **26**. These compounds contain the same pentaoxygenated core as anhydrofusarubin **26** and only differ by possessing an oxygen substituent at position C-1 (**Figure 24**). The synthesis and biological activities of these two naphthoquinones have never been reported. Thus a synthetic route to these compounds would allow for the investigation of their biological properties and possibly determine their structural importance.

Scheme 103

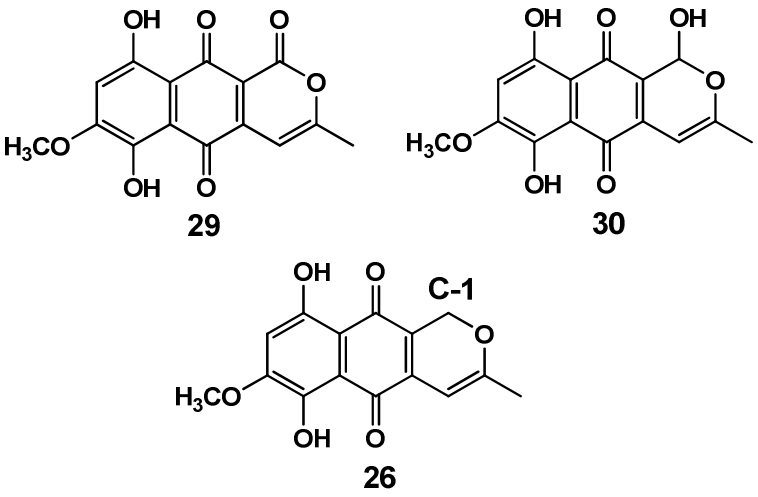

Figure 24

Based on the noted structural similarities we propose that these two naphthoquinones could be synthesized by employing a few minor modifications to the synthetic pathway used to assemble anhydrofusarubin **26** (**Scheme 107**). The

allyl ester of naphthalene **226** (produced in eight steps from 2,4,5-trimethoxybenzaldehyde **178**) can be converted to a carboxylic acid, compound **272**, by a saponification reaction under basic conditions. The Wacker oxidation of acid **272** would result in the formation of lactone **273**. The silver(II) oxidation and boron trichloride demethylation of **273** would yield anhydrofusarubin-lactone **29**. Alternatively, lactone **273** could be selectively reduced to lactol **274** by DIBAL. Oxidative and selective demethylation processes would potentially afford anhydrofusarubin-lactol **30**.

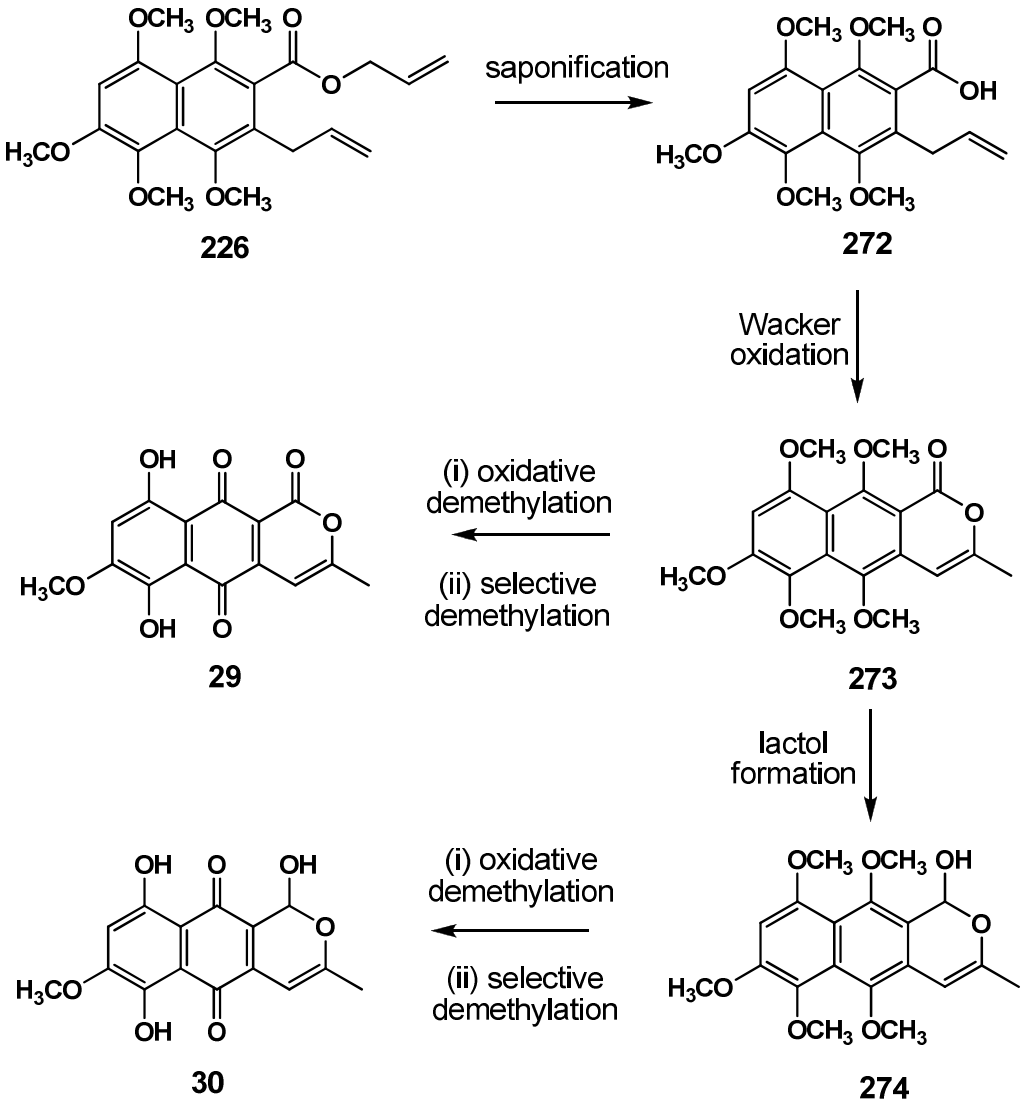

226 **272** **29** **273** **30** **274**

Scheme 107

5.3.3. Synthesis of fusarubin by hydration of anhydrofusarubin

There is literature precedence for the addition of a water molecule across a dehydrated isochromene ring system to form a hemiacetal**.** This process entails refluxing the substrate in toluene in the presence of catalytic amounts of *p*-toluenesulfonic acid, and could be applied to the pentaoxygenated isochromene **228** to potentially form hemiacetal **275** (**Scheme 108**). The oxidation and demethylation of **275** would yield fusarubin **16**, which is the hydrated form of anhydrofusarubin **26**.

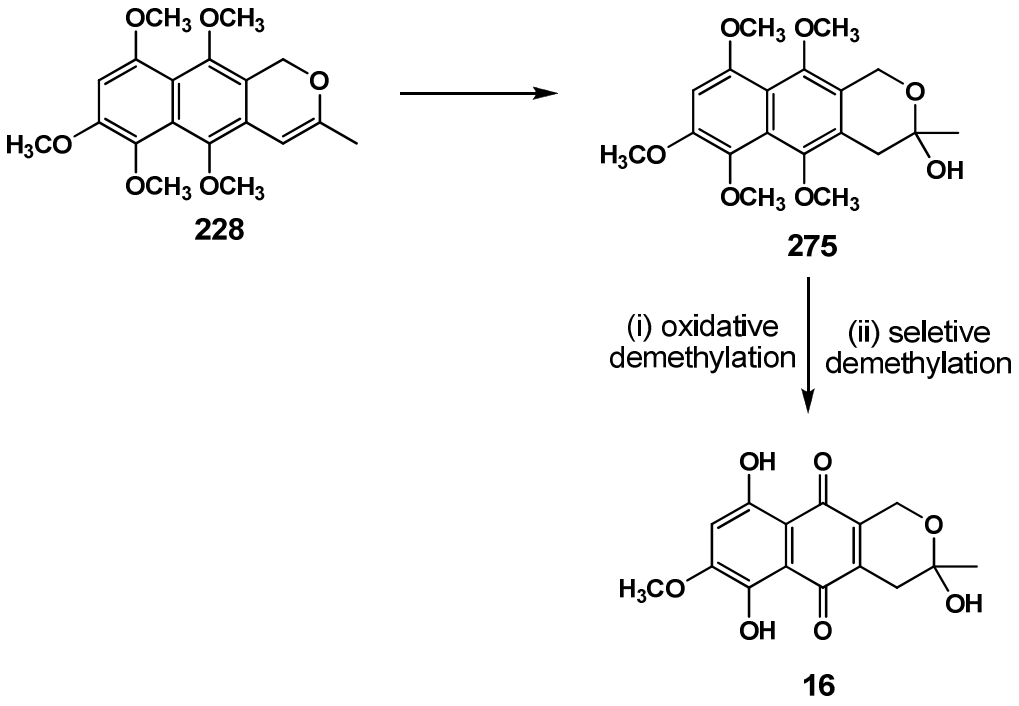

Scheme 108

5.3.4. Synthesis of acetal Naphthoquinones using Wacker methodology

The Wacker oxidation is usually carried out in a water/dimethylformamide solvent system. Water molecules have been proposed to participate in the reaction and could be added to the substrate from the catalyst via *syn* addition (see **Scheme 46**). There is some literature on alternative solvent systems for the Wacker oxidation[2], such as methanol or ethanol. Essentially, these solvents could also play a role in the reaction, as a water molecule has been proposed to, and this would result in the formation of an acetal derivative as opposed to the usual hemiacetal. If this

methodology was applied to our pentaoxygenated naphthalene **227** (**Scheme 109**), we could form acetal **276** which can be oxidized and demethylated to afford the naturally occurring naphthoquinone **277**.

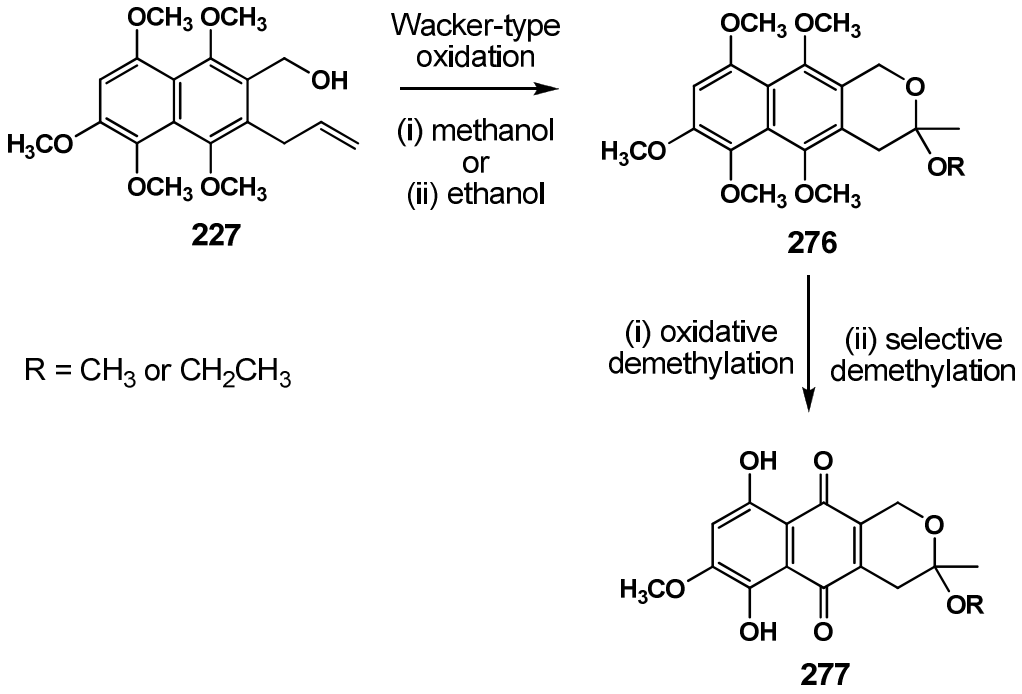

Scheme 109

The natural products, *O*-methylfusarubin **41** and *O*-ethylfusarubin **43** potentially could be synthesized in this manner which would be a novel approach to assembling naphthoquinones containing acetal moieties (**Figure 25**).

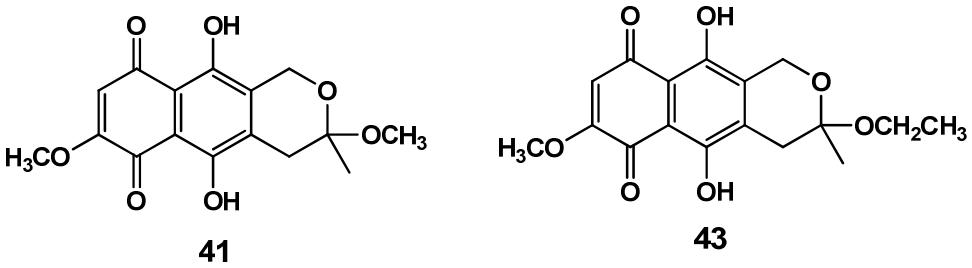

Figure 25

5.3.5. Diastereoselective Synthesis of Marticin

Considering that we have an efficient route to assemble a pentaoxygenated naphthalene core and methodology towards accessing the bicyclic acetal ring system of marticin, it would be possible to combine this synthetic knowledge and apply it to the synthesis of marticin **45**. Naphthalene **227** could be oxidized to an aldehyde and the desired ester/alcohol side chain could be stereoselectively added (**A**) to afford **278** (**Scheme 110**). The Wacker oxidation (**B**) of **278** would potentially form the bicyclic acetal compound **279** which could be oxidized and demethylated (**C**) to yield marticin **45**.

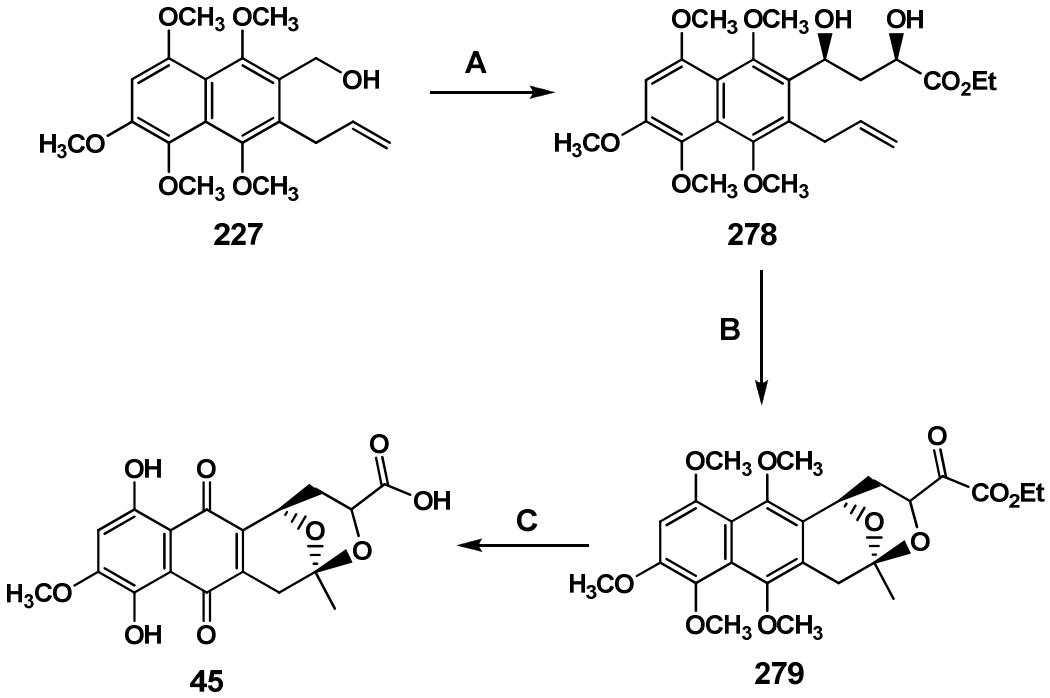

Scheme 110

5.4. References

1. Kesteleyn, B., De Kimpe, N., Van Puyvelde, L., *Synthesis*, 1999, **11**, 1881-1883.
2. Takacs, J.M., Jiang, X., *Current Organic Chemistry*, 2003, **7**, 369-396.

Chapter 6: Experimental Procedures

6.1. General Modus Operandi

6.1.1. Purification of solvents and reagents

Solvents utilized for chromatographic techniques (ethyl acetate and *n*-hexane) were distilled preceding use by means of conventional distillation processes. The solvents employed in reactions were first dried over the suitable drying agent, followed by distillation under an inert atmosphere (argon or nitrogen gas). Acetonitrile and dichloromethane were distilled over calcium hydride, whereas tetrahydrofuran was distilled over sodium with benzophenone as an indicator. All the required chemicals or reagents were obtained from FLUKA, SIGMA-ALDRICH or MERCK and were used without further purification.

6.1.2. Chromatography procedures

Normal chromatography was performed with silica gel 60 (Macherey-Nagel, particle size 0.063-0.200 mm) adsorbent, with both isocratic and gradient eluent systems being employed. Thin layer chromatography (TLC) of the compounds was executed on Macherey-Nagel Alugram Sil G/UV254 plates pre-coated with 0.25 mm silica gel 60. The TLC plates were viewed under UV light (λ 254 nm and 366 nm).

6.1.3. Spectroscopic and physical data

Nuclear magnetic resonance (NMR) spectra were recorded on either a Bruker AVANCE 300 MHz or a Bruker AVANCE III 500 MHz spectrometer. All spectra were recorded in $CDCl_3$, or d_6-acetone. All chemical shift values are reported in parts per million referenced against trimethylsilane which is given an assignment of zero parts per million. Coupling constants (*J*-values) are given in Hertz (Hz).

The infra-red spectra were recorded on a Bruker Tensor 27 standard system spectrometer. Measurements were made by loading the sample directly onto a diamond cell. The measurments are reported on the wavenumber scale (ν/cm^{-1}).

Melting points were determined on a Reichert hot-stage microscope, and remain uncorrected.

High resolution mass spectra were obtained with a Waters-LCT-Premier mass spectrometer. The sample was dissolved in methanol to a concentration of 2 ng/µl and introduced by direct infusion. The ionization mode was electrospray positive with a capillary voltage of 2500 V and a desolvation temperature of 250 °C using nitrogen gas at 250 L/hr.

The intensity data was recorded on a Bruker APEX II CCD area detector diffractometer with graphite monochromated Mo *K*α radiation (50 kV, 30 mA) with temperature of measurement at 173(2) K, using the APEX 2[1] data collection software. The collection method involved ω-scans of width 0.5 and 512×512 bit data frames. The data reduction was achieved by means of the program *SAINT+* and face indexed absorption corrections were made using *XPREP*[2].

Crystal structures were solved employing direct methods using *SHELXTL*[2]. Non-hydrogen atoms were first refined isotropically followed by anisotropic refinement by full matrix least-squares calculations based on *F*2 using SHELXTL. The hydrogen atoms were first located in the difference map then positioned geometrically and allowed to ride on their respective precursor atoms. Diagrams and publication material were generated using SHELXTL, PLATON151 and ORTEP-3[3].

6.1.4. Other general procedures

All the glass reaction vessels were dried in an oven. The term "*in vacuo*" refers to the removal of solvent by use of a rotary evaporator. The residual solvent of purified material was removed by utilizing a high vacuum pump (*ca.*0.1 mm Hg) at ambient temperature until constant mass was achieved.

6.2. Experimental Work Pertaining to the Diels-Alder Approach to Naphthoquinones

6.2.1. Synthesis of 3-Hydroxy-3-methyl-3,4-dihydro-1*H*-isochromene-5,8-dione 170

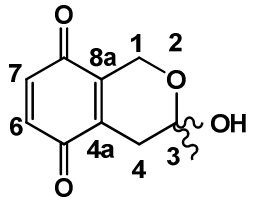

170

5,8-Dimethoxy-3-methylisochroman-3-ol **7** (2.20 g, 9.86 mmol) was dissolved in a mixture of CH_3CN and H_2O (200 ml, 50:50 v/v ratio). CAN (16.2 g, 29.6 mmol, 3.0 equiv.) was added to the reaction mixture which was then stirred vigorously for 30 min at rt. EtOAc (50 ml) and NaCl (aq) (50 ml) were then added and the upper organic layer was separated, dried over anhydrous $MgSO_4$, filtered and concentrated under reduced pressure. Column chromatography (eluant 30 % EtOAc/hexane) of the residue afforded 3-hydroxy-3-methyl-3,4-dihydro-1*H*-isochromene-5,8-dione **8** as an amorphous red solid (1.053 g, 55 %). $\mathbf{R_f}$ = 0.26 (30 % EtOAc/hexane); **IR** ν_{max}(cm^{-1}) = 3353 (OH), 1738 (C=O), 1654 (C=O); **^{1}H NMR** (300 MHz, MeOD) δ_H = 6.80-6.71 (2H, m, H-6 and H-7), 4.56-4.56 (1H, m, Ar$C\mathbf{H_a}H_bO$), 4.30-4.20 (1H, m, $ArCH_a\mathbf{H_b}O$), 2.68-2.58 (1H, m, $\mathbf{H_a}H_b$-4), 2.46-2.36 (1H, ddd, *J* 18.9 and 4.3 and 2.8, $H_a\mathbf{H_b}$-4), 1.47 (3 H, CH_3); **^{13}C NMR** (75 MHz, MeOD) δ_C = 187.4 (C=O), 186.9 (C=O), 139.9 (C-8a), 138.4 (C-4a), 137.6 (C-6), 137.2 (C-7), 98.4 (C-3), 58.6 (C-1), 33.2 (C-4), 23.0 (CH_3).

6.2.2. Synthesis of 3-Methyl-1*H*-isochromene-5,8-dione 171

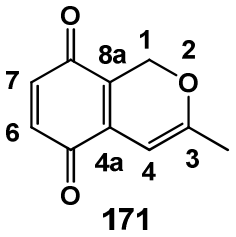

171

5,8-dimethoxy-3-methy-1*H*-isochromene **9** (1.20 g, 5.82 mmol) was dissolved in a mixture of CH_3CN and H_2O (100 ml, 50:50 v/v ratio). CAN (9.47 g, 17.5 mmol, 3.0 equiv.) was added to the reaction mixture which was then stirred vigorously for 30 min at rt. EtOAc (50 ml) and NaCl (aq) (50 ml) were then added and the upper organic layer was separated, dried over anhydrous $MgSO_4$, filtered and concentrated under reduced pressure. Column chromatography (eluant 30 % EtOAc/hexane) of the residue afforded 3-methyl-1*H*-isochromene-5,8-dione **10** as an amorphous orange solid (0.646 g, 63 %). $\mathbf{R_f}$ = 0.41 (30 % EtOAc/hexane); **IR** $\nu_{max}(cm^{-1})$ = 3428 (OH), 1652 (C=O), 1600 (C=O); **^{1}H NMR** (300 MHz, $CDCl_3$) δ_H = 6.70-6.63 (2H, m, H-6 and H-7), 5.75 (1H, s, H-4), 5.02 (2H, s, $ArCH_2O$), 2.01 (3H, s, CH_3); **^{13}C NMR** (75 MHz, $CDCl_3$) δ_C =184.8 (C=O), 184.2 (C=O) 165.3 (C-3), 137.1 (C-7), 135.0 (C-8a) 134.8 (C-6), 119.5 (C-4a), 94.4 (C-4), 62.7 (C-1), 20.3 (CH_3).

6.2.3. Attempted Diels Alder reaction of 3-Methyl-1*H*-isochromene-5,8-dione 171 with furan 64

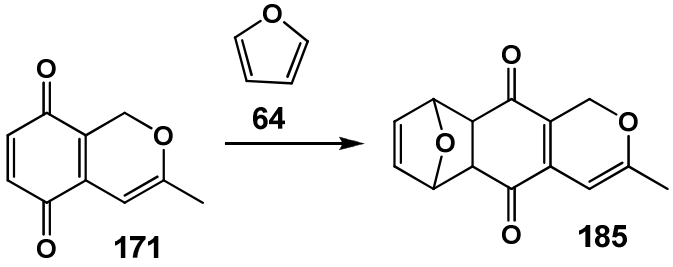

171 **185**

Quinone **171** (0.300 g, 1.70 mmol) and furan **64** (2.31 g, 34.0 mmol, 20.0 equiv.) were refluxed for 6 h. The reaction was cooled to rt and purified by chromatography column which only resulted in the full recovery of starting material.

6.2.4. Attempted Diels Alder reaction of 3-Hydroxy-3-methyl-3,4-dihydro-1*H*-isochromene-5,8-dione 170 with 2-methoxyfuran 58

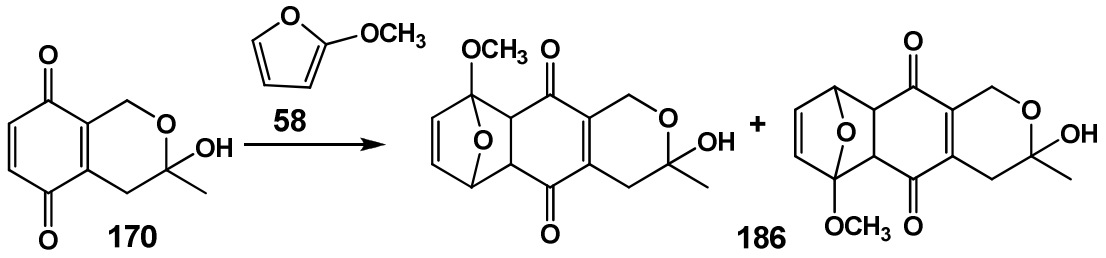

Quinone **170** (0.500 g, 2.57 mmol) and 2-methoxyfuran **58** (0.253 g, 2.57 mmol, 1.0 equiv.) were dissolved in dichlorobenzene (10 ml) and refluxed for 1 h (after this time TLC analysis showed that the starting material was fully consumed). The reaction was cooled to rt and directly loaded onto a silica chromatography column. The material from the reaction decomposed on contact with the purification column.

6.3. Experimental Work Pertaining to the Syntheisis of Dehydroherbarin and Unusual Analogues

6.3.1. Synthesis of Ethyl 4-acetoxy-6,8-dimethoxy-2-naphthoate 189

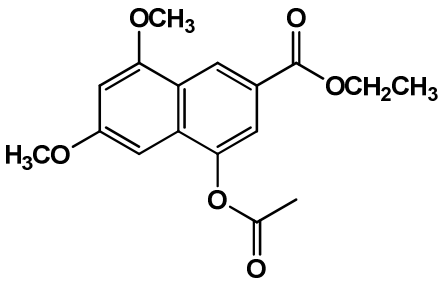

To a solution of 2,4-dimethoxybenzaldehyde (4.00 g, 24.1 mmol) and diethyl succinate (5.45 g, 31.3 mmol) in dry THF (50 ml), at 0 °C, was added NaOEt (3.28 g, 48.1 mmol). The reaction mixture was refluxed for 2 h, cooled to rt and then acidified to pH 3 with aqueous HCl [33% (v/v)]. The product precipitated and was extracted with EtOAc (2 × 50 ml). The combined organic extracts were dried over anhydrous $MgSO_4$, filtered, and the filtrate was concentrated *in vacuo*. The residue and anhydrous NaOAc (2.57 g, 31.3 mmol) were dissolved in acetic anhydride (50 ml) and refluxed for 3 h. The solvent was removed *in vacuo* and the resulting residue was dissolved in EtOAc (60 ml). Aqueous $NaHCO_3$ was slowly added to the EtOAc layer until all the traces of acetic anhydride were removed. The organic layer was then separated, dried over $MgSO_4$, filtered, and the filtrate was concentrated *in vacuo*. The residue was purified by column chromatography (30% EtOAc /hexane) to afford ethyl 4-acetoxy-6,8-dimethoxy-2-naphthoate **189** (8.69 g, 82%) as a yellow solid. $\mathbf{R_f}$ = 0.64 (40 % EtOAc/hexane); **^{1}H NMR** (300 MHz, $CDCl_3$) δ_H = 8.79 (1H, d, *J* 1.1, H-1), 7.81 (1H, d, *J* 1.1, H-3), 6.66 (1H, d, *J* 1.9, H-5), 6.51 (1H, d, *J* 1.9, H-7), 4.42 (2H, q, *J* 7.1, OCH_2CH_3), 3.98 (3H, s, OCH_3), 3.91 (3H, s, OCH_3), 2.46 (CH_3CO_2), 1.42 (3H, t, *J* 7.1, OCH_2CH_3); **^{13}C NMR** (75 MHz, $CDCl_3$) δ_C = 169.3 (CH_3CO_2), 166.3 ($ArCO_2Et$), 161.0, 157.9, 145.4 (C-4), 133.2 (C-4a), 124.4 (C-2), 123.4 (C-1), 122.2 (C-8a) 119.1 (C-3), 98.6 (C-5), 91.7 (C-7) 61.0 (OCH_2CH_3), 55.8 (OCH_3), 55.4 (OCH_3), 20.9 (CH_3CO_2), 14.4 (OCH_2CH_3).[4]

6.3.2. Synthesis of Allyl 4-(allyloxy)-6,8-dimethoxy-2-naphthoate 191

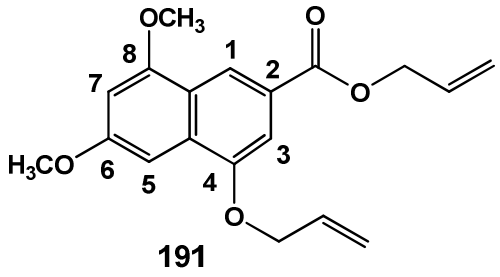

191

Ethyl 4-acetoxy-6,8-dimethoxy-2-naphthoate **189** (10.0 g, 31.4 mmol) was dissolved in MeOH (100 ml) followed by the drop-wise addition of an aqueous KOH solution (8.81 g, 157 mmol, 200 ml H_2O). The dark-orange reaction was stirred for 6 h at rt, before the MeOH was removed *in vacuo*. The aqueous solution was then carefully acidified to pH 4.0 with aqueous HCl (30%), and then extracted with EtOAc (3 × 150 ml). The organic layers were combined, dried over anhydrous $MgSO_4$, filtered and concentrated under reduced pressure. The crude, off-white solid was then dissolved in acetone (150 ml), and allyl bromide (9.41 g, 78.5 mmol) and anhydrous K_2CO_3 (10.8 g, 78.5 mmol) were added to the reaction mixture which was then refluxed for 18 h under a N_2(g) atmosphere. The mixture was then allowed to cool to rt, filtered through a bed of celite, and the solvent was removed *in vacuo*. The light-yellow residue was then purified via column chromatography (10% EtOAc/hexane) to yield allyl 4-(allyloxy)-6,8-dimethoxy-2-naphthoate **191** as a yellow amorphous solid (8.56 g, 83%). $\mathbf{R_f}$ = 0.65 (20 % EtOAc /hexane); **Mp** = 64-65 °C; **IR** $\nu_{max}(cm^{-1})$ = 1647 (C=O), 1600 (C=C), 1429, 1285, 1217, 1146; **^{1}H NMR** (400 MHz, $CDCl_3$) δ_H = 8.53 (1H s, H-1), 7.41 (1H, d, *J* 1.3, H-3), 7.13 (1H, d, *J* 2.0, H-5), 6.51 (1H, d, *J* 2.2, H-7), 6.26–6.01 (2H, m, $COOCH_2CH$=CH_2 and OCH_2CH=CH_2), 5.57–5.39 (2H, m, $COOCH_2CH$=CH_2), 5.38–5.25 (2H, m, OCH_2CH=CH_2), 4.87 (2H, dt, *J* 5.6, 1.3, $COOCH_2CH$=CH_2), 4.75 (2H, d, *J* 5.2, OCH_2CH=CH_2), 3.95 (3H, s, OCH_3), 3.93 (3H, s, OCH_3); **^{13}C NMR** (100 MHz, $CDCl_3$) δ_C = 167.0 (C=O), 160.4, 157.8, 153.3, 133.3 (OCH_2CH=CH_2), 132.8 ($COOCH_2CH$=CH_2), 130.2 (C-2), 124.4 (C-4a), 121.8 (C-8a), 118.4 (C-1) 118.2 (OCH_2CH=CH_2), 117.8 ($COOCH_2CH$=CH_2), 105.9 (C-3), 98.8 (C-4), 92.9 (C-6), 69.4 (OCH_2CH=CH_2) 65.7 ($COOCH_2CH$=CH_2), 55.8 (OCH_3), 55.6 (OCH_3); **HR-TOF-MS**: *m/z* found 329.1389 $[M+H]^+$ (calculated for $C_{19}H_{21}O_5$, 329.1389).

6.3.3. Synthesis of Allyl 3-allyl-4-hydroxy-6,8-dimethoxy-2-naphthoate 192

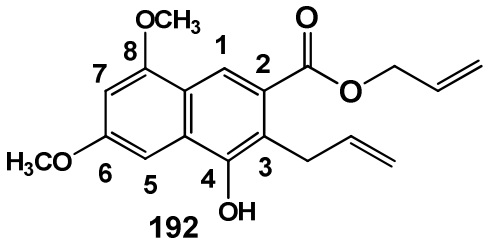

192

Allyl 4-(allyloxy)-6,8-dimethoxy-2-naphthoate **191** (7.20 g, 21.9 mmol) was loaded neat into a round-bottomed flask (100 ml) equipped with a reflux condenser and a magnetic stirrer bar. The reaction vessel was then heated to 180 ^{o}C for 18 h under a N_2(g) atmosphere. The dark viscous residue was allowed to cool to rt and was then purified using column chromatography (20% EtOAc/hexane) to yield allyl 3-allyl-4-hydroxy-6,8-dimethoxy-2-naphthoate **192** as a yellow amorphous solid (6.48 g, 90%). $\mathbf{R_f}$ = 0.60 (20 % EtOAc /hexane); **Mp**. = 90-91 $^{\circ}$C; **IR** ν_{max}(cm^{-1}) = 3539 (OH), 1673 (C=O), 1580 (C=C), 1461, 1291, 1249, 1158; **^{1}H NMR** (300 MHz, $CDCl_3$) δ_H = 8.43 (1H, s, H-1), 7.04 (1H, d, *J* 1.8, H-5), 6.48 (1H, d, *J* 2.2, H-7), 6.20–6.01 (2H, m, $COOCH_2CH$=CH_2 and $ArCH_2CH$=CH_2), 5.82 (1H, s, OH), 5.44 (1H, ddd, *J* 17.2, 3.0, 1.5, one of $COOCH_2CH$=CH_2), 5.37–5.25 (1H, m, one of $COOCH_2CH$=CH_2), 5.18 (2H, ddd, *J* 5.1, 3.9, 1.7, $ArCH_2CH$=CH_2), 4.88–4.80 (2H, m, $COOCH_2CH$=CH_2), 3.97–3.88 (2H, m, $ArCH_2CH$=CH_2, under OCH_3) 3.94 (3H, s, OCH_3), 3.91 (OCH_3); **^{13}C NMR** (75 MHz, $CDCl_3$) δ_C = 167.8 (C=O), 160.1, 157.3, 149.7, 136.5 ($COOCH_2CH$=CH_2), 132.5 ($ArCH_2CH$=CH_2), 128.5 (C-8a), 125.1 (C-4a), 120.3 (C-3), 119.2 (C-2), 118.9 (C-1), 118.3 ($COOCH_2CH$=CH_2), 116.1 ($ArCH_2CH$=CH_2), 98.3 (C-5), 92.1 (C-7), 65.7 ($COOCH_2CH$=CH_2), 55.7 (OCH_3), 55.5 (OCH_3), 31.7 ($ArCH_2CH$=CH_2); **HR-TOF-MS**: *m/z* found 329.1376 $[M+H]^+$ (calculated for $C_{19}H_{21}O_5$, 329.1389).

6.3.4. Synthesis of Allyl 3-allyl-4-(*tert*-butyldimethylsilyloxy)-6,8-dimethoxy-2-naphthoate 193

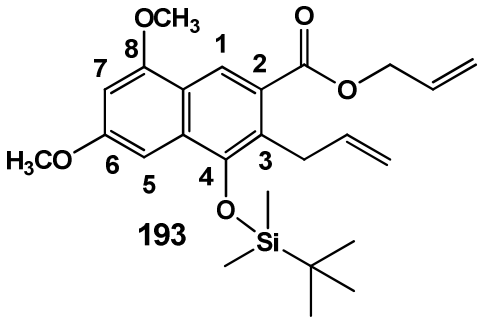

193

Allyl 3-allyl-4-hydroxy-6,8-dimethoxy-2-naphthoate **192** (7.20 g, 21.9 mmol), *tert*-butyldimethylsilyl chloride (4.96 g, 32.9 mmol), imidazole (2.23 g, 32.9 mmol) and dimethylaminopyridine (0.400 g) were dissolved in CH_2Cl_2 (150 ml) and stirred at rt for 24 h under a N_2(g) atmosphere. The mixture was then washed with H_2O (2 × 100 ml), dried over anhydrous $MgSO_4$, filtered, and the filtrate was concentrated *in vacuo*. The residue was purified by column chromatography (10% EtOAc/hexane) to afford allyl 3-allyl-4-(*tert*-butyldimethylsilyloxy)-6,8-dimethoxy-2-naphthoate **193** (9.01 g, 93%) as a clear oil. **R_f** = 0.67 (10 % EtOAc/hexane); **IR** $\nu_{max}(cm^{-1})$ = 1767 (C=O), 1589 (C=C), 1468, 1317, 1251, 1188; **^{1}H NMR** (300 MHz, $CDCl_3$) δ_H = 8.44 (1H, s, H-1), 6.96 (1H, d, *J* 1.9, H-5), 6.47 (1H, d, *J* 2.1, H-7), 6.08 (1H, ddd, *J* 16.1, 10.9, 5.7, $COOCH_2CH$=CH_2), 5.93 (1H, ddt, *J* 16.3, 10.4, 5.9, $ArCH_2CH$=CH_2), 5.43 (1H, dd, *J* 17.2, 1.5, one of $COOCH_2CH$=CH_2), 5.29 (1H, dd, *J* 10.4, 1.2, one of $COOCH_2CH$=CH_2), 4.99–4.86 (2H, m, $ArCH_2CH$=CH_2), 4.82 (2H, d, *J* 5.7, $COOCH_2CH$=CH_2), 3.99–3.93 (2H, m, $ArCH_2CH$=CH_2,under OCH_3), 3.95 (3H, s, OCH_3), 3.92 (3H, s, OCH_3), 1.13 (9H, s, $OSi(CH_3)_2C(CH_3)_3$), 0.23 (6H, s, $OSi(CH_3)_2C(CH_3)_3$); **^{13}C NMR** (75 MHz, $CDCl_3$) δ_C = 168.0 (C=O), 159.6, 157.4, 148.3, 137.5 ($ArCH_2CH$=CH_2), 132.7 ($COOCH_2CH$=CH_2), 131.6, 126.4, 126.2, 120.4, 119.9, 118.1 ($COOCH_2CH$=CH_2), 114.9 ($ArCH_2CH$=CH_2), 97.9 (C-5), 94.2 (C-7), 65.6 ($COOCH_2CH$=CH_2), 55.7 (OCH_3), 55.4 (OCH_3), 31.2 ($ArCH_2CH$=CH_2), 26.2 ($OSi(CH_3)_2C(CH_3)_3$), 18.8 ($OSi(CH_3)_2C(CH_3)_3$), -2.9 ($OSi(CH_3)_2C(CH_3)_3$); **HR-TOF-MS**: *m/z* found 443.2248 $[M+H]^+$ (calculated for $C_{25}H_{35}O_5Si$, 443.2254).

6.3.5. Synthesis of (3-Allyl-4-(*tert*-butyldimethylsilyloxy)-6,8-dimethoxynaphthalen2-yl)methanol 175

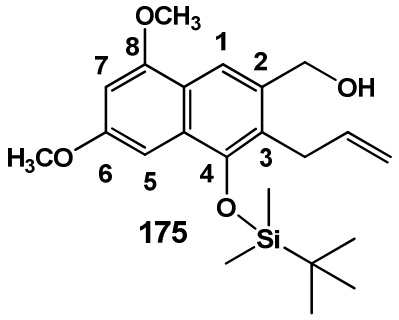

175

Allyl 3-allyl-4-(*tert*-butyldimethylsilyloxy)-6,8-dimethoxy-2-naphthoate **193** (7.90 g, 18.4 mmol) was in dissolved dry THF (100 ml) and cooled to 0 ^{o}C in an ice bath. Lithium aluminium hydride (2.09 g, 55.1 mmol) was added slowly over 15 min. The reaction mixture was then stirred vigorously for 2 h at rt under a N_2 atmosphere. The solution was then cooled to 0 ^{o}C in an ice bath and cold H_2O (1.5 ml) was added drop-wise until the fizzing stopped. Aqueous NaOH (1.5 ml, 15% m/v) and H_2O (4.5 ml) were then added and the resulting mixture was stirred for 3 h at rt. EtOAc (100 ml) was then added and the organic layer was separated, dried over anhydrous $MgSO_4$, filtered and concentrated under reduced pressure. Column chromatography (20% EtOAc/hexane) of the residue afforded (3-allyl-4-(*tert*-butyldimethylsilyloxy)-6,8-dimethoxynaphthalen2-yl)methanol **175** as a clear oil (6.86 g, 96%). $\mathbf{R_f}$ = 0.36 (20 % EtOAc /hexane); **^{1}H NMR** (300 MHz, $CDCl_3$) δ_H = 7.90 (1H, s, H-1), 6.97 (1H, d, J 1.9, H-5), 6.46 (1H, d, J 2.2, H-7), 5.96 (1H, dq, J 10.3, 5.7, $ArCH_2CH{=}CH_2$), 4.98 (1 H, dd, J 10.2, 1.7, one of $ArCH_2CH{=}CH_2$), 4.91 (1 H, dd, J 17.2, 1.7, one of $ArCH_2CH{=}CH_2$), 4.77 (2H, s, $ArCH_2$), 3.91 (3H, s, OCH_3), 3.90 (3H, s, OCH_3), 3.66 (2H, br d, J 5.7, $ArCH_2CH{=}CH_2$), 2.60 (1H, brs, OH), 1.14 (9H, s, $OSi(CH_3)_2C(CH_3)_3$), 0.25 (6H, s, $OSi(CH_3)_2C(CH_3)_3$); **^{13}C** NMR (75 MHz, $CDCl_3$) δ_C = 160.0 (ArC-O), 159.0 (ArC-O), 150.5 (ArC-O), 139.5 ($ArCH_2CH{=}CH_2$), 137.9 (C-1), 131.5 (C-3a), 127.4 (C-2), 123.8 (C-7a), 117.8 (C-8), 117.4 ($ArCH_2CH{=}CH_2$), 99.8 (C-6), 64.4 ($ArCH_2$), 55.7 (OCH_3), 55.5 (OCH_3), 30.9 ($ArCH_2CH{=}CH_2$), 26.3 ($OSi(CH_3)_2C(CH_3)_3$), 19.0 ($OSi(CH_3)_2C(CH_3)_3$), -2.6 ($OSi(CH_3)_2C(CH_3)_3$).[5]

6.3.6. Synthesis of *tert*-butyl(7,9-dimethoxy-3-methyl-1*H*-benzo[*g*]isochromene-5-yloxy)dimethylsilane 174

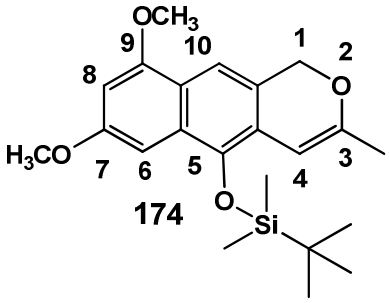

174

Compound **175** (1.27 g, 3.27 mmol) was dissolved in a DMF/H_2O mixture (1:1 v/v, 40 ml). $PdCl_2$ (0.0589 g, 0.327 mmol) and $CuCl_2.2H_2O$ (0.558 g, 3.27 mmol) were added to the solution which was stirred vigorously for 24 h at rt under an O_2(g) atmosphere. The reaction was filtered, and EtOAc (2 × 40 ml) was added. The organic layers were combined, washed with H_2O (3 × 20 ml), separated, dried over anhydrous $MgSO_4$, filtered and concentrated under reduced pressure. Column chromatography (15% EtOAc/hexane) of the residue afforded *tert*-butyl(7,9-dimethoxy-3-methyl-1*H*-benzo[g]isochromene-5-yloxy)dimethylsilane **174** as a clear oil (0.657 g, 52 %). $\mathbf{R_f}$ = 0.71 (10 % EtOAc/hexane); **IR** $\nu_{max}(cm^{-1})$ = 1504, 1450, 1367, 1257, 1154; **^{1}H NMR** (300 MHz, $CDCl_3$) δ_H = 7.50 (1H, s, H-10), 6.95 (1H, d, *J* 2.0, H-6), 6.41 (1H, d, *J* 2.2, H-8), 5.99 (1H, s, H-4), 5.14 (2H, d, *J* 0.8, H-1), 3.92 (3H, s, OCH_3), 3.90 (3H, s, OCH_3), 2.01 (3H, d, *J* 0.5, CH_3), 1.17 (9H, s, $OSi(CH_3)_2C(CH_3)_3$), 0.21 (6H, s, $OSi(CH_3)_2C(CH_3)_3$); **^{13}C NMR** (75 MHz, $CDCl_3$) δ_C = 157.7, 156.6 (C-3), 154.6, 141.8, 129.8 (C-9a), 125.1 (C-10a), 120.9 (C-5a), 119.9 (C-4a), 110.7 (C-10), 97.9 (C-4), 96.9 (C-8), 94.0 (C-6), 69.3 (C-1), 55.6 (OCH_3), 55.3 (OCH_3), 26.2 ($OSi(CH_3)_2C(CH_3)_3$,), 20.1 (CH_3), 18.8 ($OSi(CH_3)_2C(CH_3)_3$,), -3.1 ($OSi(CH_3)_2C(CH_3)_3$); **HR-TOF-MS**: *m/z* found 387.1984 $[M+H]^+$ (calculated for $C_{22}H_{31}O_4Si$, 387.1992).

6.3.7. Synthesis of 7,9-Dimethoxy-3-methyl-1*H*-benzo[*g*]isochromene-5-ol 173

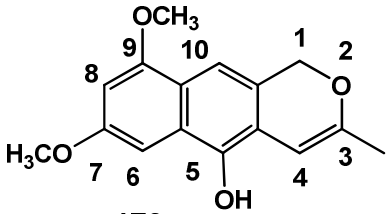

173

Tert-butyl(7,9-dimethoxy-3-methyl-1*H*-benzo[*g*]isochromene-5-yloxy)dimethylsilane **174** (0.456 g, 1.16 mmol) was dissolved in dry THF (3 ml) and was treated with *tetra*-n-butylammonium fluoride (0.609 g, 2.33 mmol) and stirred for 18 h at rt under a N_2(g) atmosphere. H_2O (10 ml) and EtOAc (15 ml) were added and the upper organic layer was separated, dried over anhydrous $MgSO_4$, filtered, and the filtrate was concentrated *in vacuo*. The residue was purified by column chromatography (10% EtOAc/hexane) to afford 7,9-dimethoxy-3-methyl-1*H*-benzo[*g*]isochromene-5-ol **173** (0.256 g, 73%) as a white crystalline solid. $\mathbf{R_f}$ = 0.33 (10 % EtOAc/hexane); **Mp**. = 156-157 °C; **IR** $\nu_{max}(cm^{-1})$ = 3348 (OH), 1508, 1435, 1290, 1204, 1185; **^{1}H NMR** (500 MHz, acetone) δ_H = 7.91 (1H, br s, OH), 7.34 (1H, s, H-10), 7.11 (1H, d, *J* 2.1, H-6), 6.44 (1H, d, *J* 2.1, H-8), 6.15 (1H, s, H-4), 5.07 (2H, d, *J* 0.8, H-1), 3.91 (3H, s, OCH_3), 3.84 (3H, s, OCH_3), 1.91 (3H, d, *J* 0.6, CH_3); **^{13}C NMR** (125 MHz, acetone) δ_C = 158.9, 157.5, 155.3 (C-3), 143.7, 127.8 (C-9a), 125.8 (C-4a), 121.5 (C-5a), 116.1 (C-10a), 109.6 (C-10), 97.7 (C-8), 96.9 (C-4), 93.5 (C-6), 69.7 (C-1), 55.9 (OCH_3), 55.5 (OCH_3),20.0 (CH_3); **HR-TOF-MS**: *m/z* found 273.1118 $[M+H]^+$ (calculated for $C_{16}H_{17}O_4$, 273.1127).

6.3.8. Synthesis of (3-Formyl-4-hydroxy-6,8-dimethoxynaphthalen-2-yl)methyl acetate 201

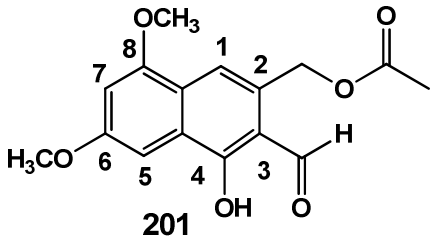

201

7,9-Dimethoxy-3-methyl-1*H*-benzo[*g*]isochromene-5-ol **173** (0.200 g, 0.764 mmol) and salcomine complex *N,N'*-bis(salicylidene)ethylenediaminocobalt(II) hydrate (0.148 g, 0.44 mmol) were dissolved in CH_3CN (30 ml) and stirred for 3 h at rt under an O_2(g) atmosphere. The reaction was then filtered through celite and the solvent was removed *in vacuo*. The resulting residue was purified by column chromatography (30% EtOAc/hexane) to afford (3-formyl-4-hydroxy-6,8-dimethoxynaphthalene-2-yl)methyl acetate **201** (0.070 g , 30%) as an orange solid. **R_f** = 0.25 (20 % EtOAc/hexane); **Mp.** = 118-119 °C; **IR** $\nu_{max}(cm^{-1})$ = 3455 (OH), 1737 (C=O), 1620 (C=O), 1578 (C=C), 1433, 1282, 1208, 1160; **^{1}H NMR** (300 MHz, $CDCl_3$) δ_H = 13.48 (1H, br s, OH), 10.26 (1H, s, CHO), 7.64 (1H, s, H-1), 7.27 (1H, d, *J* 2.1, H-5), 6.67 (1H, d, *J* 2.2, H-7), 5.44 (2H, s, $ArCH_2O$), 3.96 (3H, s, OCH_3), 3.95 (3H, s, OCH_3), 2.10 (3H, s, $OCOCH_3$); **^{13}C NMR** (75 MHz, $CDCl_3$) δ_C = 195.4 (C=O), 170.6 (C=O), 162.6, 159.4, 156.6, 128.5, 127.1, 124.6, 116.0, 113.1, 102.5, 94.6, 64.3 ($ArCH_2O$), 55.9 (OCH_3), 55.8 (OCH_3), 21.1 (CH_3); **HR-TOF-MS**: *m/z* found 305.1027 $[M+H]^+$ (calculated for $C_{16}H_{17}O_6$, 305.1025).

6.3.9. Synthesis of (3R,4R) 3-Hydroxy-7,9-dimethoxy-3-methyl-5,10-dioxo-3,4,5,10-tetrahydro-1*H*-benzo[*g*]isochromen-4-yl nitrate 202

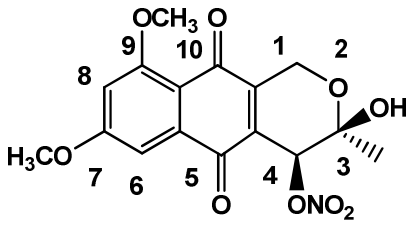

202

7,9-Dimethoxy-3-methyl-1*H*-benzo[*g*]isochromene-5-ol **173** (0.308, 1.01 mmol) was dissolved in CH_3CN/H_2O mixture (2:1 v/v ratio, 75 ml), and CAN (2.41, 4.40 mmol) in H_2O (25 ml) was added drop-wise. The reaction was then stirred for 1 h at rt followed by the addition of H_2O (100 ml) and EtOAc (100 ml). The organic layer was separated, dried over anhydrous $MgSO_4$, filtered, and the filtrate was concentrated *in vacuo*. The residue was purified by column chromatography (30% EtOAc/hexane) to afford (3R,4R) 3-hydroxy-7,9-dimethoxy-3-methyl-5,10-dioxo-3,4,5,10-tetrahydro-1*H*-benzo[*g*]isochromen-4-yl nitrate **202** (0.201 g, 54%) as an orange solid. $\mathbf{R_f}$ = 0.10 (50 % EtOAc/hexane); **Mp**. = 105-106 °C; **IR** $\nu_{max}(cm^{-1})$ = 3427 (OH), 1728 (C=O), 1658 (C=O), 1591, 1457, 1269, 1203; **^{1}H NMR** (300 MHz, acetone-d_6) δ_H = 7.17 (1H, d, *J* 2.4, H-6), 6.93 (1H, d, *J* 2.4, H-8), 5.95 (1H, s, H-4), 4.62–4.56 (2H, m, H-1), 3.97 (3H, s, OCH_3), 3.94 (3H, s, OCH_3), 2.87 (1H, br s, OH), 1.52 (3H, s, CH_3); **^{13}C NMR** (75 MHz, acetone-d_6) δ_C = 183.3 (C=O), 180.6 (C=O), 166.0, 163.4, 149.0 (C-4a), 136.1 (C-5a), 131.6 (C-10a), 114.6 (C-9a), 105.0 (C-6)*, 104.8 (C-8)*, 95.9 (C-3), 73.3 (C-4), 58.6 (C-1), 56.8 (OCH_3), 56.6 (OCH_3), 24.1 (CH_3). *assignments may be interchanged.

6.3.10. Synthesis of Allyl 3-allyl-4-hydroxy-1,6,8-trimethoxy-2-naphthoate 210

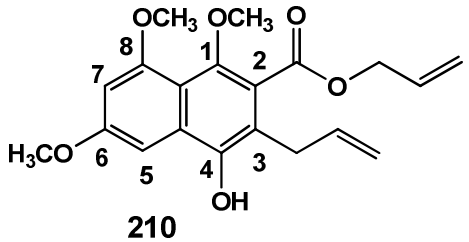

210

Allyl 3-allyl-4-hydroxy-6,8-dimethoxy-2-naphthoate **192** (2.00 g, 6.10 mmol) was dissolved in MeOH (80 ml) in a round-bottom flask (100 ml). PIFA (3.41 g, 7.93 mmol) was added and the reaction was stirred for 15 min at rt. Aqueous $NaHCO_3$ was added until fizzing stopped and the MeOH was removed *in vacuo* to leave only an aqueous medium. The H_2O layer was extracted with EtOAc (2 × 50 ml). The organic layers were combined, dried over anhydrous $MgSO_4$, filtered and concentrated under reduced pressure. The residue was then treated with an ethanolic solution of NaOEt (10.9 ml, 33.5 mmol) with vigorous stirring for 20 min at rt. The reaction was then quenched with the addition of saturated aqueous NH_4Cl (10 ml). EtOAc (30 ml) was added and the resulting upper organic layer was removed, dried over anhydrous $MgSO_4$, filtered and concentrated *in vacuo*. Column chromatography (10% EtOAc/hexane) of the residue afforded allyl 3-allyl-4-hydroxy-1,6,8-trimethoxy-2-naphthoate **210** as a brown oil (1.21 g, 60%). $\mathbf{R_f}$ = 0.54 (20 % EtOAc/hexane); **Mp**. = 58-59 °C; **IR** $\nu_{max}(cm^{-1})$ = 3257 (OH), 1738 (C=O), 1601 (C=C), 1441, 1274, 1229, 1189; **^{1}H NMR** (300 MHz, $CDCl_3$) δ_H = 7.08 (1H, br s, H-5), 6.52 (1H, br s, H-7), 6.10–5.90 (2H, m, $COOCH_2CH$=CH_2 and $ArCH_2CH$=CH_2), 5.57 (1H, s, OH), 5.41 (1H, ddd, *J* 17.2, 2.9, 1.4, one of $COOCH_2CH$=CH_2), 5.33–5.14 (3H, m, one of $COOCH_2CH$=CH_2 and $ArCH_2CH$=CH_2), 4.89–4.79 (2H, m, $COOCH_2CH$=CH_2), 3.94 (3H, s, OCH_3), 3.89 (3H, s, OCH_3), 3.82 (3H, s, OCH_3), 3.43 (2H, br d, *J* 6.1, $ArCH_2CH$=CH_2); **^{13}C NMR** (75 MHz, $CDCl_3$) δ_C = 168.2 (C=O), 158.7, 157.4, 147.6, 145.3, 135.3 ($COOCH_2CH$=CH_2 and C-4a, overlapped), 131.9 ($ArCH_2CH$=CH_2), 129.5 (C-3), 124.3 (C-8a), 118.8 ($COOCH_2CH$=CH_2), 116.8 ($ArCH_2CH$=CH_2), 116.7 (C-2), 114.9, 99.4 (C-7), 92.9 (C-5), 66.0 ($COOCH_2CH$=CH_2), 63.9 (OCH_3), 55.9 (OCH_3), 55.2 (OCH_3), 32.6 ($ArCH_2CH$=CH_2); **HR-TOF-MS-ES**: *m/z* found 381.1314 $[M+Na]^+$ (calculated for $C_{20}H_{22}O_6Na$, 381.1314).

6.3.11. Synthesis of Allyl 3-allyl-1,4,6,8-tetramethoxy-2-naphthoate 212

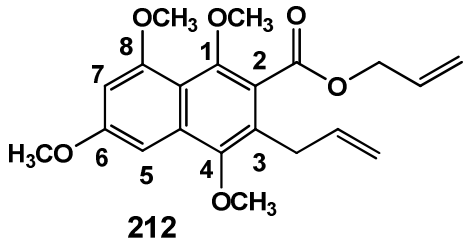

212

Allyl 3-allyl-4-hydroxy-1,6,8-trimethoxy-2-naphthoate **210** (0.513 g, 1.40 mmol), anhydrous K_2CO_3 (0.289 g, 2.10 mmol) and Me_2SO_4 (0.264 g, 2.10 mmol) were dissolved in acetone (30 ml). The mixture was then refluxed for 18 h, cooled to rt, filtered, and the solvent was removed *in vacuo*. The residue was then dissolved in EtOAc (50 ml) and was successively washed with aqueous NH_3 (25%, 50 ml) and H_2O (50 ml). The organic layer was dried over anhydrous $MgSO_4$, filtered and concentrated under reduced pressure. Column chromatography (10% EtOAc/hexane) of the residue afforded allyl 3-allyl-1,4,6,8-tetramethoxy-2-naphthoate **212** as a yellow solid (0.466 g, 89%). $\mathbf{R_f}$ = 0.60 (25 % EtOAc/hexane); **Mp**. = 60-61 °C; **IR** $\nu_{max}(cm^{-1})$ = 1718 (C=O), 1581 (C=C), 1450, 1299, 1214, 1191; **^{1}H NMR** (500 MHz, $CDCl_3$) δ_H = 6.97 (1H, s, H-5), 6.52 (1H, s, H-7), 6.07–5.90 (2H, m, $COOCH_2CH$=CH_2 and $ArCH_2CH$=CH_2), 5.41 (1H, d, *J* 17.2, one of $COOCH_2CH$=CH_2), 5.26 (1H, d, *J* 10.4, one of $COOCH_2CH$=CH_2), 5.04 (2H, t, *J* 14.0, $ArCH_2CH$=CH_2), 4.80 (2H, dd, *J* 6.0, 0.8, $COOCH_2CH$=CH_2), 3.93 (3H, s, OCH_3), 3.90 (3H, s, OCH_3), 3.84 (3H, s, OCH_3) 3.82 (3H, s, OCH_3), 3.55 (2H, d, *J* 6.2, $ArCH_2CH$=CH_2); **^{13}C NMR** (125 MHz, $CDCl_3$) δ_C = 167.7 (C=O), 159.4, 157.9, 150.6, 149.2, 136.2 ($COOCH_2CH$=CH_2), 132.7 (C-4a), 132.1 ($ArCH_2CH$=CH_2), 126.6 (C-3), 124.7 (C-8a), 118.8 ($COOCH_2CH$=CH_2), 115.9 ($ArCH_2CH$=CH_2), 115.3 (C-2), 99.3 (C-5), 93.2 (C-7), 65.9 ($COOCH_2CH$=CH_2), 63.9 (OCH_3), 61.5 (OCH_3), 56.1 (OCH_3), 55.3 (OCH_3), 31.7 ($ArCH_2CH$=CH_2); **HR-TOF-MS-ES**: *m/z* found 395.1466 $[M+Na]^+$ (calculated for $C_{21}H_{24}O_6Na$, 395.1471).

6.3.12. Synthesis of (3-Allyl-1,4,6,8-tetramethoxynaphthalen-2-yl)methanol 213

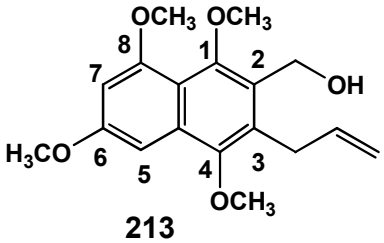

213

Allyl 3-allyl-1,4,6,8-tetramethoxy-2-naphthoate **212** (6.30 g, 16.9 mmol) was dissolved in dry Et_2O (100 ml) and cooled to 0 °C in an ice bath. Lithium aluminium hydride (1.29 g, 33.8 mmol) was added slowly over 5 min. The reaction mixture was then stirred vigorously for 2 h at rt under a N_2(g) atmosphere. The solution was then cooled to 0 °C in an ice bath and cold H_2O was added drop-wise until the fizzing ceased. EtOAc (100 ml) was added and the solution was washed with HCl (aq) (2 M, 30 ml). The organic layer was then dried over anhydrous $MgSO_4$, filtered and concentrated under reduced pressure. Column chromatography (40% EtOAc/hexane) of the residue afforded (3-allyl-1,4,6,8-tetramethoxynaphthalen-2-yl)methanol **213** as a white crystalline solid (4.50 g, 84%). $\mathbf{R_f}$ = 0.22 (40 % EtOAc/hexane); **Mp**. = 122-123 °C; **IR** $\nu_{max}(cm^{-1})$ = 3481 (OH), 1580 (C=C), 1447, 1262, 1204, 1114; **^{1}H NMR** (300 MHz, $CDCl_3$) δ_H = 6.97 (1H, d, *J* 2.3, H-5), 6.52 (1H, d, *J* 2.3, H-7), 6.19–5.98 (1H, m, $ArCH_2CH$=CH_2), 5.05 (1H, dd, *J* 10.2, 1.7, one of $ArCH_2CH$=CH_2), 4.90 (1H, dd, *J* 17.2, 1.8, one of $ArCH_2CH$=CH_2), 4.78 (2H, s, ArCH_2), 3.96 (3H, s, OCH_3), 3.91 (3H, s, OCH_3), 3.84 (3H, s, OCH_3), 3.83 (3H, s, OCH_3), 3.70 (2H, dt, *J* 5.3, 1.7, ArCH_2CH=CH_2), 2.55 (1H, br s, OH); **^{13}C NMR** (75 MHz, $CDCl_3$) δ_C = 158.7, 157.6, 152.2, 149.5, 137.9 ($ArCH_2CH$=CH_2), 131.9 (C-4a), 129.1 (C-3), 128.1 (C-2), 115.6 (C-8a), 115.4 ($ArCH_2CH$=CH_2), 99.0 (C-5), 93.2 (C-7), 63.3 (OCH_3), 61.6 (OCH_3), 57.5 ($ArCH_2$), 56.1 (OCH_3), 55.3 (OCH_3), 30.7 ($ArCH_2CH$=CH_2); **HR-TOF-MS-ES**: *m/z* found 341.1367 $[M+Na]^+$ (calculated for $C_{18}H_{22}O_5Na$, 341.1365).

6.3.13. Synthesis of 5,7,9,10-Tetramethoxy-3-methyl-1*H*-benzo[*g*]isochromene 214

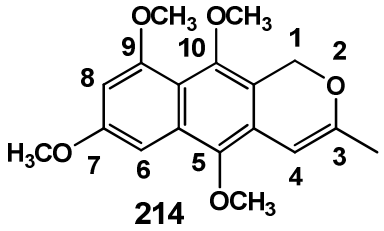

214

(3-Allyl-1,4,6,8-tetramethoxynaphthalen-2-yl)methanol **213** (4.00 g, 12.6 mmol) was dissolved in a DMF/H_2O mixture (1:1 v/v, 100 ml). $PdCl_2$ (0.223 g, 1.26 mmol) and $CuCl_2.2H_2O$ (2.14 g, 12.6 mmol) were added to the solution and O_2(g) was bubbled through the solution which was stirred vigorously for 2 h at rt. The reaction was filtered, and EtOAc (2 × 50 ml) was added. The organic layers were combined, washed with H_2O (3 × 20 ml), separated, dried over anhydrous $MgSO_4$, filtered and concentrated under reduced pressure. Column chromatography (eluant 15 % EtOAc/hexane) of the residue afforded 5,7,9,10-tetramethoxy-3-methyl-1*H*-benzo[*g*]isochromene **214** as a white crystalline solid (2.62 g, 66%). $\mathbf{R_f}$ = 0.63 (20 % EtOAc/hexane); **Mp**. = 134-135 °C; **IR** $\nu_{max}(cm^{-1})$ = 1601 (C=C), 1501, 1444, 1256, 1217, 1155; **^{1}H NMR** (300 MHz, $CDCl_3$) δ_H = 6.96 (1H, d, *J* 2.3, H-6), 6.46 (1H, d, *J* 2.2, H-8), 5.95 (1H, s, H-4), 5.28 (2H, s, H-1), 3.94 (3H, s, OCH_3), 3.91 (3H, s, OCH_3), 3.85 (3H, s, OCH_3), 3.76 (3H, s, OCH_3), 2.02 (3H, s, CH_3); **^{13}C NMR** (125 MHz, $CDCl_3$) δ_C = 158.5, 157.7, 156.1 (C-3), 147.5, 143.0, 131.9 (C-5a), 122.3 (C-4a), 116.9 (C-10a), 114.9 (C-9a), 98.3 (C-6), 95.6 (C-4), 93.1 (C-8), 64.0 (C-1), 62.2 (OCH_3), 61.2 (OCH_3), 56.0 (OCH_3), 55.3 (OCH_3), 20.1 (CH_3); **HR-TOF-MS-ES**: *m/z* found 339.1209 $[M+Na]^+$ (calculated for $C_{18}H_{20}O_5Na$, 339.1208).

6.3.14. Synthesis of 7,9-Dimethoxy-3-methyl-1*H*-benzo[*g*]isochromene-5,10-dione 31

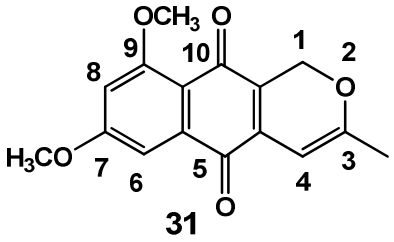

31

5,7,9,10-Tetramethoxy-3-methyl-1*H*-benzo[*g*]isochromene **214** (0.200 g, 0.632 mmol) was dissolved in a CH_3CN/H_2O mixture (1:1 v/v, 8 ml), followed by the addition of PIFA (0.408 g, 0.948 mmol). The reaction was stirred for 2 h at rt, before being quenched by aqueous $NaHCO_3$ (15 ml). EtOAc was added (2 × 30 ml), and the organic layers were separated, combined, dried over anhydrous $MgSO_4$, filtered, and the solvent was removed *in vacuo*. The residue was purified by column chromatography (30% EtOAc/hexane) to afford 7,9-dimethoxy-3-methyl-1*H*-benzo[*g*]isochromene-5,10-dione **31** (0.045 g, 25%) as a dark-red amorphous solid. $\mathbf{R_f}$ = 0.10 (50 % EtOAc/hexane); **^{1}H NMR** (500 MHz, $CDCl_3$) δ_H = 7.21 (1H, d, *J* 2.4, H-6), 6.68 (1H, d, *J* 2.4, H-8), 5.81 (1H, s, H-4), 5.09 (2H, s, H-1), 3.93 (3H, s, OCH_3), 3.92 (3H, s, OCH_3), 1.98 (3H, s, CH_3); **^{13}C NMR** (125 MHz, $CDCl_3$) δ_C 182.4 (C=O), 181.0 (C=O), 164.3, 163.4, 161.6 (C-3), 135.7 (C-4a), 135.5 (C-5a), 124.9 (C-10a), 114.7 (C-9a), 104.4 (C-8) 103.7 (C-6), 93.9 (C-4), 63.5 (C-1), 56.5 (OCH_3), 56.0 (OCH_3), 20.2 (CH_3)[6].

6.3.15. Synthesis of 3,4-Dihydroxy-7,9-dimethoxy-3-methyl-3,4-dihydro-1*H*-benzo[*g*]isochromene-5,10-dione 218

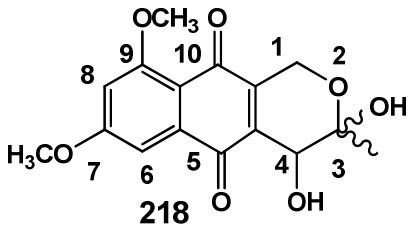

218

5,7,9,10-Tetramethoxy-3-methyl-1*H*-benzo[*g*]isochromene **20** (0.400 g, 1.26 mmol) was dissolved in a CH_3CN/H_2O mixture (1:1 v/v, 20 ml), followed by the addition of PIFA (0.815 g, 1.90 mmol). The reaction was stirred for 2 h at rt, before being quenched by aqueous $NaHCO_3$ (30 ml). EtOAc was added (2 × 30 ml), and the organic layers were separated, combined, dried over anhydrous $MgSO_4$, filtered, and the solvent was removed *in vacuo*. The residue was purified by column chromatography (60% EtOAc/hexane) to afford 3,4-dihydroxy-7,9-dimethoxy-3-methyl-3,4-dihydro-1*H*-benzo[*g*]isochromene-5,10-dione **21** (0.098 g, 24%) as a brown amorphous solid. $\mathbf{R_f}$ = 0.10 (70 % EtOAc/hexane); **IR** $\nu_{max}(cm^{-1})$ = 3415 (OH), 1725 (C=O), 1649 (C=O), 1383, 1321, 1274, 1200; **^{1}H NMR** (300 MHz, acetone-d_6) δ_H = 7.20 (1H, d, *J* 2.3, H-6), 6.91 (1H, d, *J* 2.4, H-8), 4.53 (2H, s, H-1), 4.35 (1H, s, H-4), 3.99 (3H, s, OCH_3), 3.95 (3H, s, OCH_3), 1.56 (3H, s, CH_3); **^{13}C NMR** (75 MHz, DMSO-d_6) δ_C = 182.8 (C=O), 181.1 (C=O), 164.4 (Ar**C**-O), 161.7 (Ar**C**-O), 143.4 (C-4a), 137.5 (C-5a), 135.3 (C-10a), 112.9 (C-9a), 103.8 (*C-8*) 103.7 (C-6), 95.9 (C-3), 61.7 (C-4), 57.5 (C-1), 56.4 (OCH_3), 56.0 (OCH_3), 24.5 (CH_3); **HR-TOF-MS-ES**: *m/z* found 343.0791 [M-Na] (calculated for $C_{16}H_{16}O_7Na$, 343.0794).

6.4. Experimental Work Pertaining to the Synthesis of Anhydrofusarubin

6.4.1. Synthesis of Ethyl 4-acetoxy-5,6,8-trimethoxy-2-naphthoate 162

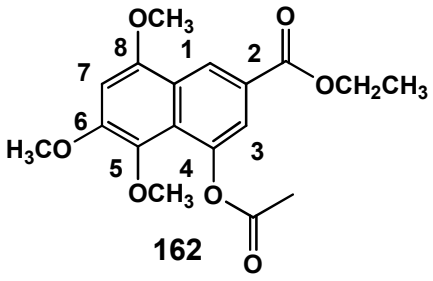

162

To a solution of 2,4,5-trimethoxybenzaldehyde (4.00 g, 24.1 mmol) and diethyl succinate (5.45 g, 31.29 mmol) in dry THF (50 ml), at 0 °C, was added NaOEt (3.28 g, 48.1 mmol). The reaction mixture was refluxed for 2 h, cooled to rt and then acidified to pH 3 with aqueous HCl [33% (v/v)]. The product precipitated and was extracted with EtOAc (2 × 50 ml). The combined organic extracts were dried over $MgSO_4$, filtered, and the filtrate was concentrated *in vacuo*. The residue and anhydrous NaOAc (2.57 g, 31.3 mmol) were dissolved in acetic anhydride (50 ml) and refluxed for 3 h. The solvent was removed *in vacuo* and the resulting residue was dissolved in EtOAc (60 ml). Aqueous $NaHCO_3$ was slowly added to the EtOAc layer until no effervescence was visible and all the traces of acetic acid were eliminated. The organic layer was then separated, dried over $MgSO_4$, filtered, and the filtrate was concentrated *in vacuo*. The residue was purified by column chromatography (30% EtOAc/hexane) to afford ethyl 4-acetoxy-6,8-dimethoxy-2-naphthoate **162** (8.69 g, 82%) as a yellow solid. $\mathbf{R_f}$ = 0.64 (40 % EtOAc/hexane); **^{1}H NMR** (300 MHz, $CDCl_3$) δ_H = 8.83 (1H, d, *J* 1.6, H-1), 7.68 (1H, d, *J* 1.6, H-3), 6.67 (1H, s, H-7), 4.39 (2H, q, *J* 7.1, OCH_2CH_3), 3.98 (6H, s, 2 x OCH_3), 3.82 (3H, s, OCH_3), 2.38 (CH_3CO_2), 1.42 (3H, t, *J* 7.1, OCH_2CH_3)[7].

6.4.2. Synthesis of Allyl 4-(allyloxy-)-5,6,8-trimethoxy-2-naphthoate 220

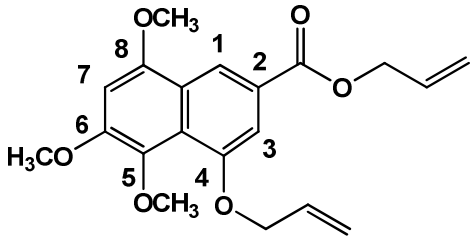

220

Ethyl 4-acetoxy-5,6,8-trimethoxy-2-naphthoate **162** (5.40 g, 15.5 mmol) was dissolved in MeOH (80 ml) followed by the drop-wise addition of aqueous KOH (4.35 g, 77.5 mmol, 150 ml H_2O). The dark-orange reaction was stirred for 6 h at rt, before the MeOH was removed *in vacuo*. The aqueous solution was then carefully acidified to pH 4.0 with aqueous HCl (30%), and then extracted with EtOAc (3 × 100 ml). The organic layers were combined, dried over anhydrous $MgSO_4$, filtered and concentrated under reduced pressure. The crude, off-white solid was then dissolved in Me_2CO (100 ml). Allyl bromide (4.69 g, 38.8 mmol), anhydrous K_2CO_3 (5.36 g, 38.8 mmol) was then added to the solution which was refluxed for 18 h under a N_2(g) atmosphere. The mixture was then allowed to cool to rt, filtered through a bed of celite, and the solvent was removed *in vacuo*. The light-yellow residue was then purified using column chromatography (10% EtOAc/hexane) to yield allyl 4-(allyloxy)-5,6,8-trimethoxy-2-naphthoate **220** as a yellow solid (4.67 g, 84%). $\mathbf{R_f}$ = 0.65 (20 % EtOAc/hexane); **Mp.** = 70-71°C; **IR** $\nu_{max}(cm^{-1})$ = 1712 (C=O), 1505, 1465, 1258, 1201, 1180; **^{1}H NMR** (300 MHz, $CDCl_3$) δ_H = 8.57 (1H, d, *J* 1.2, H-1), 7.41 (1H, d, *J* 1.0, H-3), 6.66 (1H, s, H-7), 6.28–5.97 (2H, m, $COOCH_2CH$=CH_2 and OCH_2CH=CH_2), 5.57 (1H, dd, *J* 17.2, 1.4, one of $COOCH_2CH$=CH_2), 5.41 (1H, dd, *J* 17.2, 1.3, one of $COOCH_2CH$=CH_2), 5.30 (2H, dd, *J* 15.1, 5.7, OCH_2CH=CH_2), 4.84 (2H, d, *J* 5.6, $COOCH_2CH$=CH_2), 4.69 (2H, d, *J* 5.1, OCH_2CH=CH_2), 3.97 (3H, s, OCH_3), 3.96 (3H, s, OCH_3), 3.80 (3H, s, OCH_3); **^{13}C NMR** (75 MHz, $CDCl_3$) δ_C = 166.5 (C=O), 154.6, 153.5, 152.3, 137.7, 133.2 (OCH_2CH=CH_2), 132.6 ($COOCH_2CH$=CH_2), 124.5 (C-2), 124.2 (C-4a), 122.1 (C-8a), 118.8 (C-1), 118.1 (OCH_2CH=CH_2), 117.5 ($COOCH_2CH$=CH_2), 107.7 (C-3), 96.0 (C-7), 70.4 (OCH_2CH=CH_2) 65.6 ($COOCH_2CH$=CH_2), 62.0 (OCH_3), 55.1 (OCH_3), 55.9 (OCH_3); **HR-TOF-MS**: *m/z* found 359.1499 $[M+H]^+$ (calculated for $C_{20}H_{23}O_6$, 359.1495).

6.4.3. Synthesis of Allyl 3-allyl-4-hydroxy-5,6,8-trimethoxy-2-naphthoate 221

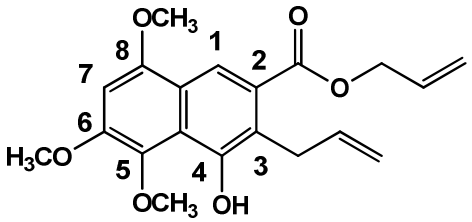

221

Allyl 4-(allyloxy)-5,6,8-trimethoxy-2-naphthoate **220** (3.10 g, 8.65 mmol) was loaded neat into a round-bottom flask (50 ml) equipped with a reflux condenser and a magnetic stirrer bar. The reaction vessel was then heated to 190 °C for 18 h under a N_2(g) atmosphere. The dark viscous residue was allowed to cool to rt and was then purified by column chromatography (20% EtOAc/hexane) to yield allyl 3-allyl-4-hydroxy-5,6,8-trimethoxy-2-naphthoate **221** as a yellow amorphous solid (2.73 g, 88%). $\mathbf{R_f}$ = 0.50 (20 % EtOAc/hexane); **Mp.** = 68-69 °C; **IR** $\nu_{max}(cm^{-1})$ = 3280 (OH), 1738 (C=O), 1604 (C=C), 1365, 1229, 1208, 1182; **^{1}H NMR** (300 MHz, $CDCl_3$) δ_H = 10.07 (1H, br s, OH), 8.25 (1H, s, H-1), 6.55 (1H, s, H-7), 6.15–5.99 (2H, m, $COOCH_2CH$=CH_2 and $ArCH_2CH$=CH_2 overlapped), 5.41 (1H, dd, *J* 17.2, 1.5, one of $COOCH_2CH$=CH_2), 5.27 (1H, dd, *J* 10.4, 1.3, one of $COOCH_2CH$=CH_2), 5.06–4.97 (2H, m, $ArCH_2CH$=CH_2), 4.86–4.77 (2H, m, $COOCH_2CH$=CH_2), 3.98 (3H, s, OCH_3), 3.97 (3H, s, OCH_3), 3.95 (3H, s, OCH_3), 3.88 (2H, br d, *J* 5.9, $ArCH_2CH$=CH_2); (75 MHz, $CDCl_3$) δ_C = 167.7 (C=O), 153.9, 151.1, 149.3, 137.4 ($COOCH_2CH$=CH_2), 135.9, 132.6 ($ArCH_2CH$=CH_2), 127.4 (C-3) 121.1 (C-4a), 120.0 (C-8a), 119.6 (C-2), 118.2 ($COOCH_2CH$=CH_2), 116.7 (C-1), 114.4 ($ArCH_2CH$=CH_2), 94.8 (C-7), 65.6 ($COOCH_2CH$=CH_2), 62.3 (OCH_3), 57.0 (OCH_3), 55.8 (OCH_3), 30.1 ($ArCH_2CH$=CH_2); **HR-TOF-MS-ES**: *m/z* found 381.1307 $[M+Na]^+$ (calculated for $C_{20}H_{22}O_6Na$, 381.1314).

6.4.4. Synthesis of Allyl 3-allyl-4,5,6,8-tetramethoxy-2-naphthoate 222

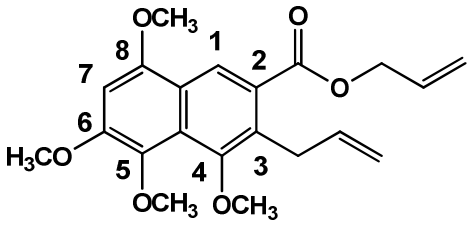

222

Allyl 3-allyl-4-hydroxy-5,6,8-trimethoxy-2-naphthoate **221** (2.60 g, 7.25 mmol), anhydrous K_2CO_3 (1.50 g, 10.9 mmol) and Me_2SO_4 (1.37 g, 10.9 mmol) were dissolved in acetone (50 ml) in a round-bottom flask (100 ml). The solution was refluxed for 12 h under a N_2(g) atmosphere. The mixture was then allowed to cool to rt, filtered through a bed of celite, and the solvent was removed *in vacuo*. The residue was then dissolved in EtOAc (50 ml) and was successively washed with aqueous NH_3 (25%, 3 × 20 ml), HCl (0.5 M, 2 × 20 ml) and H_2O (50 ml). The EtOAc layer was dried over anhydrous $MgSO_4$, filtered and concentrated under reduced pressure. Column chromatography (10% EtOAc/hexane) of the residue afforded allyl 3-allyl-4,5,6,8-tetramethoxy-2-naphthoate **222** (2.43 g, 90%) as an off-white solid. $\mathbf{R_f}$ = 0.60 (25 % EtOAc/hexane); **Mp**. = 66-67 °C; **IR** ν_{max}(cm^{-1}) = 1740 (C=O), 1602 (C=C), 1358, 1442, 1225, 1137; **^{1}H NMR** (300 MHz, $CDCl_3$) δ_H = 8.52 (1H, s, H-1), 6.65 (1H, s, H-7), 6.13–5.95 (2H, m, $COOCH_2CH$=CH_2 and $ArCH_2CH$=CH_2 overlapped), 5.39 (1H, ddd, *J* 17.2, 3.0, 1.5, one of $COOCH_2CH$=CH_2), 5.26 (1H, dd, *J* 10.4, 1.3, one of $COOCH_2CH$=CH_2), 4.98–4.91 (2H, m, $ArCH_2CH$=CH_2), 4.79 (2H, dt, *J* 5.6, 1.3, $COOCH_2CH$=CH_2), 3.98 (3H, s, OCH_3), 3.96 (5H, br s, OCH_3 and $ArCH_2CH$=CH_2 overlapped), 3.79 (3H, s, OCH_3), 3.79 (3H, s, OCH_3); **^{13}C NMR** (75 MHz, $CDCl_3$) δ_C = 167.4 (C=O), 156.6, 153.1, 152.2, 138.2 ($COOCH_2CH$=CH_2), 135.8, 132.4 ($ArCH_2CH$=CH_2), 130.4 (C-3) 126.3 (C-4a), 125.4 (C-8a), 122.2 (C-1), 120.7 (C-2) 118.2 ($COOCH_2CH$=CH_2), 114.7 ($ArCH_2CH$=CH_2), 94.8 (C-7), 65.5 ($COOCH_2CH$=CH_2), 62.7 (OCH_3), 62.0 (OCH_3), 56.9 (OCH_3), 55.8 (OCH_3), 30.1 ($ArCH_2CH$=CH_2); **HR-TOF-MS-ES:** *m/z* found 395.1465 $[M+Na]^+$ (calculated for $C_{21}H_{24}O_6Na$, 395.1471).

6.4.5. Synthesis of (3-Allyl-4,5,6,8-tetramethoxynaphthalen-2-yl)methanol 223

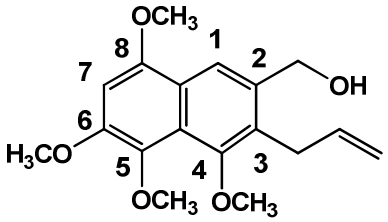

223

Allyl 3-allyl-4,5,6,8-tetramethoxy-2-naphthoate **222** (1.80 g, 4.83 mmol) was dissolved dry Et_2O (50 ml) and cooled to 0 °C in an ice bath. Lithium aluminium hydride (0.367 g, 9.67 mmol) was added slowly over 5 min. The reaction mixture was then stirred vigorously for 2 h at rt under a nitrogen atmosphere. The solution was then cooled to 0 °C in an ice bath and cold H_2O was added drop-wise until the fizzing stopped. EtOAc (50 ml) was added and the solution was washed with aqueous HCl (2 M, 10 ml). The organic layer was then dried over anhydrous $MgSO_4$, filtered and concentrated under reduced pressure. Column chromatography (40% EtOAc/hexane) of the residue afforded (3-allyl-4,5,6,8-tetramethoxynaphthalen-2-yl)methanol **233** as a white crystalline solid (1.32 g, 86%). $\mathbf{R_f}$ = 0.24 (40 % EtOAc/hexane); **^{1}H NMR** (300 MHz, $CDCl_3$) δ_H = 8.02 (1H, s, H-1), 6.64 (1H, s, H-7), 6.07 (1H, tdd, *J* 15.7, 10.5, 5.5, $ArCH_2CH$=CH_2), 5.05–4.94 (1H, m, one of $ArCH_2CH$=CH_2), 4.94–4.81 (1H, m, one of $ArCH_2CH$=CH_2), 4.76 (2H, s, $ArCH_2OH$), 3.98 (3H, s, OCH_3), 3.94 (3H, s, OCH_3), 3.82 (3H, s, OCH_3), 3.81 (3H, s, OCH_3), 3.71–3.61 (2H, m, $ArCH_2CH$=CH_2), 2.33 (1H, br s, OH); **^{13}C NMR** (75 MHz, $CDCl_3$) δ_C = 152.9, 152.6, 150.0, 138.0 ($ArCH_2CH$=CH_2), 136.2 (C-4a), 135.8, 129.3 (C-3), 123.2 (C-2), 122.0 (C-8a), 117.5 (C-1), 115.1 ($ArCH_2CH$=CH_2), 95.0 (C-7), 63.6 ($ArCH_2OH$), 62.8 (OCH_3), 62.0 (OCH_3), 57.1 (OCH_3), 55.8 (OCH_3), 29.8 ($ArCH_2CH$=CH_2).[7]

6.4.6. Synthesis of 5,6,7,9-Tetramethoxy-3-methyl-1*H*-benzo[*g*]isochromene 169

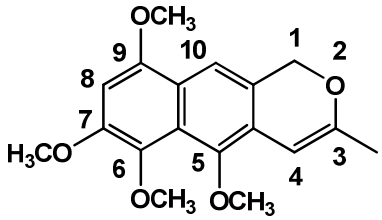

169

(3-Allyl-4,5,6,8-tetramethoxynaphthalen-2-yl)methanol **223** (1.40 g, 4.40 mmol) was dissolved in a DMF/H_2O mixture (1:1 v/v, 20 ml). $PdCl_2$ (0.0780 g, 0.440 mmol) and $CuCl_2.2H_2O$ (0.750 g, 4.40 mmol) were added to the solution and O_2(g) was bubbled through the solution which was stirred vigorously for 2 h at rt. The reaction was filtered, and EtOAc (2 × 30 ml) was added. The organic layers were combined, washed with H_2O (3 × 20 ml), separated, dried over anhydrous $MgSO_4$, filtered and concentrated under reduced pressure. Column chromatography (15% EtOAc/hexane) of the residue afforded 5,6,7,9-tetramethoxy-3-methyl-1*H*-benzo[*g*]isochromene **169** as a white crystalline solid (0.890 g, 64%). $\mathbf{R_f}$ = 0.65 (20 % EtOAc/hexane); **Mp.** = 101-102 °C; **^{1}H NMR** (300 MHz, $CDCl_3$) δ_H = 7.61 (1H, s, H-10), 6.57 (1H, s, H-8), 6.18–6.03 (1H, m, H-4), 5.12 (2H, s, H-1), 3.97 (3H, s, OCH_3), 3.93 (3H, s, OCH_3), 3.84 (3H, s, OCH_3), 3.84 (3H, s, OCH_3), 2.00 (3H, s, CH_3); **^{13}C NMR** (75 MHz, $CDCl_3$) δ_C = 156.1 (C-3), 152.6, 149.9, 146.1, 136.6, 125.5 (C-4a), 123.9 (C-10a), 123.4 (C-9a), 121.4 (C-5a), 113.0 (C-10), 96.0 (C-4), 94.3 (C-8), 68.7 (C-1), 62.3 (OCH_3), 62.0 (OCH_3), 55.8 (OCH_3), 55.7 (OCH_3), 20.1 (CH_3); **HR-TOF-MS-ES:** *m/z* found 339.1207 $[M+Na]^+$ (calculated for $C_{18}H_{20}O_5Na$, 339.1209).

6.4.7. Synthesis of Allyl 3-allyl-4-hydroxy-1,5,6,8-tetramethoxy-2-naphthoate 225

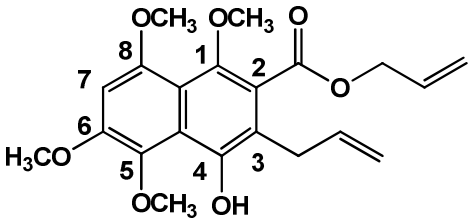

225

Allyl 3-allyl-4-hydroxy-5,6,8-trimethoxy-2-naphthoate **221** (8.00 g, 22.3 mmol) was dissolved in MeOH (120 ml) in a round-bottom flask (250 ml). PIFA (12.5 g, 29.0 mmol) was added and the reaction was stirred for 10 min at rt. Aqueous $NaHCO_3$ was added until fizzing stopped and the MeOH was removed *in vacuo* to leave only an aqueous medium. The H_2O layer was extracted with EtOAc (2 × 100 ml). The organic layers were combined, dried over anhydrous $MgSO_4$, filtered and concentrated under reduced pressure. The residue was then treated with an ethanolic solution of NaOEt (36.1 ml, 111.5 mmol) with vigorous stirring for 20 min at rt. The reaction was quenched with the addition of saturated aqueous NH_4Cl (50 ml). EtOAc (100 ml) was added and the resulting upper organic layer was removed, dried over anhydrous $MgSO_4$, filtered and concentrated *in vacuo*. Column chromatography (15% EtOAc/hexane) of the residue afforded allyl 3-allyl-4-hydroxy-1,5,6,8-tetramethoxy-2-naphthoate **225** as an orange amorphous solid (4.70 g, 54%). $\mathbf{R_f}$ = 0.54 (20 % EtOAc/hexane); **IR** $\nu_{max}(cm^{-1})$ = 3215 (OH), 1724 (C=O), 1609 (C=C), 1580 (C=C), 1287, 1260, 1152; **^{1}H NMR** (300 MHz, $CDCl_3$) δ_H = 10.18 (1H, br s, OH), 6.59 (1H, s, H-7), 6.07–5.89 (2H, m, $COOCH_2CH$=CH_2 and $ArCH_2CH$=CH_2), 5.44–5.33 (1H, m, one of $COOCH_2CH$=CH_2), 5.24 (1H, dd, *J* 10.4, 1.3, one of $COOCH_2CH$=CH_2), 5.08–4.93 (2H, m, $ArCH_2CH$=CH_2), 4.83–4.77 (2H, m, $COOCH_2CH$=CH_2), 3.92 (3H, s, OCH_3), 3.91 (3H, s, OCH_3), 3.91 (3H, s, OCH_3), 3.74 (3H, s, OCH_3), 3.42 (2H, br d, *J* 6.3 $ArCH_2CH$=CH_2); **^{13}C NMR** (75 MHz, $CDCl_3$) δ_C = 167.8 (C=O), 154.0, 148.3, 147.1, 145.7, 136.5 (C-4a), 135.9 ($ArCH_2CH$=CH_2), 132.1 ($COOCH_2CH$=CH_2), 126.3 (C-3), 120.2 (C-8a), 118.8 ($COOCH_2CH$=CH_2), 118.0 (C-2), 115.23 ($ArCH_2CH$=CH_2), 115.19, 96.8 (C-7), 65.9 ($COOCH_2CH$=CH_2), 63.9 (OCH_3), 62.3 (OCH_3), 56.8 (OCH_3), 56.7 (OCH_3), 31.5 ($ArCH_2CH$=CH_2); **HR-**

TOF-MS-ES: *m/z* found 411.1417 $[M+Na]^+$ (calculated for $C_{21}H_{24}O_7Na$, 411.1420).

6.4.8. Synthesis of Allyl 3-allyl-1,4,5,6,8-pentamethoxy-2-naphthoate 226

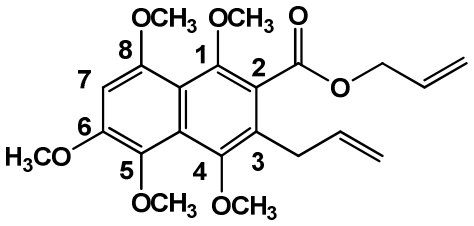

226

Allyl 3-allyl-4-hydroxy-1,5,6,8-tetramethoxy-2-naphthoate **225** (3.80 g, 10.09 mmol), anhydrous K_2CO_3 (2.09 g, 15.1 mmol) and Me_2SO_4 (1.91 g, 15.1 mmol) were dissolved in acetone (60 ml). The mixture was then refluxed for 18 h, cooled to rt, filtered, and the solvent was removed *in vacuo*. The residue was then dissolved in EtOAc (80 ml) and was successively washed with aqueous NH_3 (25%, 80 ml) and H_2O (80 ml). The organic layer was dried over anhydrous $MgSO_4$, filtered and concentrated under reduced pressure. Column chromatography (15% EtOAc/hexane) of the residue afforded allyl 3-allyl-1,4,5,6,8-pentamethoxy-2-naphthoate **226** as a yellow oil (3.30 g, 81%). $\mathbf{R_f}$ = 0.59 (20 % EtOAc/hexane); **IR** $\nu_{max}(cm^{-1})$ = 1738 (C=O), 1603 (C=C), 1438, 1364, 1216, 1045; **^{1}H NMR** (300 MHz, $CDCl_3$) δ_H = 6.69 (1H, s, H-7), 6.07–5.86 (2H, m, $COOCH_2CH$=CH_2 and $ArCH_2CH$=CH_2), 5.38 (1H, dd, *J* 17.2, 1.5, one of $COOCH_2CH$=CH_2), 5.23 (1H, dd, *J* 10.4, 1.2, one of $COOCH_2CH$=CH_2), 5.07–4.93 (2H, m, $ArCH_2CH$=CH_2), 4.82–4.73 (2H, m, $COOCH_2CH$=CH_2), 3.95 (3H, s, OCH_3), 3.93 (3H, s, OCH_3), 3.77 (3H, s, OCH_3), 3.75 (3H, s, OCH_3), 3.73 (3H, s, OCH_3), 3.53 (2H, br d, *J* 6.2, $ArCH_2CH$=CH_2); ^{13}C NMR (75 MHz, $CDCl_3$) δ_C = 167.7 (C=O), 153.8, 151.1, 150.2, 149.2, 136.7 (C-4a), 136.6 ($ArCH_2CH$=CH_2), 132.1 ($COOCH_2CH$=CH_2), 127.7 (C-8a), 126.5 (C-2)*, 125.3 (C-3)*, 119.0 ($COOCH_2CH$=CH_2), 116.0 ($ArCH_2CH$=CH_2), 115.9, 97.1 (C-7), 66.1 ($COOCH_2CH$=CH_2), 63.9 (OCH_3), 62.8 (OCH_3), 62.1 (OCH_3), 56.9 (OCH_3), 56.8 (OCH_3), 31.6 ($ArCH_2CH$=CH_2); *assignments may be interchanged; **HR-TOF-MS-ES**: *m/z* found 425.1573 $[M+Na]^+$ (calculated for $C_{22}H_{26}O_7Na$, 425.1576).

6.4.9. Synthesis of 5,6,7,9,10-Pentamethoxy-3-methyl-1*H*-benzo[*g*]isochromene 228

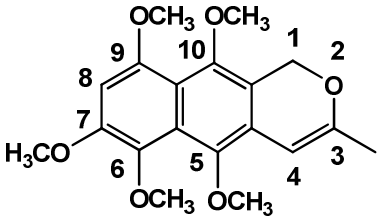

228

Allyl 3-allyl-1,4,5,6,8-pentamethoxy-2-naphthoate **226** (3.30 g, 8.20 mmol) was dissolved in dry Et_2O (100 ml) and cooled to 0 °C in an ice bath. Lithium aluminium hydride (0.622 g, 16.4 mmol) was added slowly over 5 min. The reaction mixture was stirred vigorously for 2 h at 40 °C under a N_2(g) atmosphere. The solution was then cooled to 0 °C in an ice bath and cold H_2O was added drop-wise until the fizzing stopped. EtOAc (100 ml) was added and the solution was washed with aqueous HCl (2M, 20 ml). The organic layer was then dried over anhydrous $MgSO_4$, filtered through a short pad of silica, and concentrated under reduced pressure to yield a yellow residue of what was presumed to be (3-allyl-1,4,5,6,8-pentamethoxy-2-naphthalen-2-yl)methanol **227**. This residue was dissolved in a DMF/H_2O mixture (1:1 v/v, 70 ml). $PdCl_2$ (0.145 g, 0.820 mmol) and $CuCl_2.2H_2O$ (1.40 g, 8.20 mmol) were added to the solution and O_2(g) was bubbled through the solution which was stirred vigorously for 2 h at rt. The reaction was filtered, and EtOAc (2 × 50 ml) was added. The organic layers were combined, washed with H_2O (3 × 50 ml), separated, dried over anhydrous $MgSO_4$, filtered and concentrated under reduced pressure. Column chromatography (10% EtOAc/hexane) of the residue afforded 5,6,7,9,10-pentamethoxy-3-methyl-1*H*-benzo[*g*]isochromene **228** as a white crystalline solid (1.40 g, 49% over two steps). $\mathbf{R_f}$ = 0.64 (20 % EtOAc/hexane); **Mp.** = 122-123 °C; **IR** $\nu_{max}(cm^{-1})$ = 1654 (C=C), 1597 (C=C), 1339, 1178, 1134; (500 MHz, $CDCl_3$) δ_H = 6.64 (1H, s, H-8), 6.03 (1H, s, H-4), 5.26 (2H, s, H-1), 3.99 (3H, s, OCH_3), 3.97 (3H, s, OCH_3), 3.80 (3H, s, OCH_3), 3.79 (3H, s, OCH_3), 3.74 (3H, s, OCH_3), 2.00 (3H, s, CH_3); **^{13}C NMR** (125 MHz, $CDCl_3$) δ_C = 156.9 (C-3), 153.3, 150.0, 147.3, 142.6, 136.8, 125.8 (C-5a), 122.6 (C-10a), 117.6 (C-4a), 115.7 (C-9a), 96.1 (C-8), 95.6 (C-4), 63.8 (C-1), 62.3 (OCH_3), 62.2 (OCH_3), 62.0 (OCH_3), 56.9 (OCH_3), 56.5 (OCH_3),

20.1 (CH_3); **HR-TOF-MS-ES**: *m/z* found 369.1312 $[M+Na]^+$ (calculated for $C_{19}H_{22}O_6Na$, 369.1314).

6.4.10. Synthesis of 5,7,10-Trimethoxy-3-methyl-1*H*-benzo[*g*]isochromene-6,9-dione 229 and 5,9,10-trimethoxy-3-methyl-1*H*-benzo[*g*]isochromene-6,7-dione 230

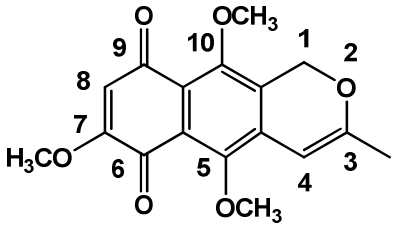

229

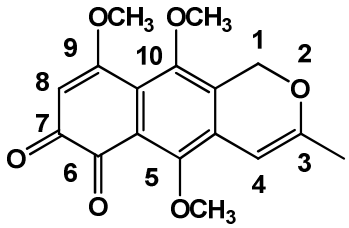

230

5,6,7,9,10-Pentamethoxy-3-methyl-1*H*-benzo[*g*]isochromene **228** (0.400 g, 1.15 mmol) was dissolved in 1,4-dioxane (30 ml) at RT. AgO (5.77 mmol, 0.715 g) was then added to the stirred solution, followed by the dropwise addition of HNO_3 (6 M, 6.4 ml) to the solution which was the stirred for a further 5 min. CH_2Cl_2 (50 ml) and H_2O (50 ml) were added and the lower organic layer was separated, dried over anhydrous $MgSO_4$, filtered and concentrated under reduced pressure. Column chromatography (20% EtOAc/hexane) of the residue afforded 5,7,10-trimethoxy-3-methyl-1*H*-benzo[*g*]isochromene-6,9-dione **229** as an orange amorphous solid (0.230 g, 63%). $\mathbf{R_f}$ = 0.62 (40 % EtOAc/hexane); **Mp**. = 205-206 °C. **IR** $\nu_{max}(cm^{-1})$ = 1782 (C=O), 1755 (C=O), 1705 (C=C), 1440, 1407; **^{1}H NMR** (500 MHz, $CDCl_3$) δ_H = 5.98 (1H, s, H-8), 5.96 (1H, s, H-4), 5.22 (2H, s, H-1), 3.84 (3H, s, OCH_3), 3.82 (6H, s, 2 × OCH_3), 2.00 (3H, s, CH_3); **^{13}C NMR** (125 MHz, $CDCl_3$) δ_C = 183.7 (C=O), 179.3 (C=O), 159.8 (C-3), 159.0, 151.8, 149.8, 134.6 (C-10a), 128.2 (C-4a), 124.3 (C-5a), 122.0 (C-9a), 110.2 (C-8), 95.2 (C-4), 63.5 (C-1), 61.8 (OCH_3), 61.6 (OCH_3), 56.3 (OCH_3), 20.0 (CH_3); **HR-TOF-MS-ES**: *m/z* found 317.1022 $[M+H]^+$ (calculated for $C_{17}H_{17}O_6$, 317.1025).

Further elution (50% EtOAc/hexane) led to the isolation of 5,9,10-trimethoxy-3-methyl-1*H*-benzo[*g*]isochromene-6,7-dione **230** as a dark red solid (0.100 g, 27%). $\mathbf{R_f}$ = 0.27 (40 % EtOAc/hexane); **Mp**. = 205-206 °C; **IR** ν_{max} (cm^{-1}) = 1794 (C= O),

1758 (C= O), 1698 (C=C), 1465, 1401; **^{1}H NMR** (500 MHz, $CDCl_3$) δ_H = 5.91 (1H, s, H-4), 5.88 (1H, s, H-8), 5.17 (2H, s, H-1), 3.99 (3H, s, OCH_3), 3.81 (3H, s, OCH_3), 3.73 (3H, s, OCH_3), 2.00 (3H, s, CH_3); **^{13}C NMR** (125 MHz, $CDCl_3$) δ_C = 179.8 (C=O), 179.4 (C=O), 170.7, 159.4 (C-3), 152.6, 150.4, 132.8 (C-10a), 129.0 (C-4a), 123.6 (C-5a), 121.2 (C-9a), 101.9 (C-8), 95.0 (C-4), 63.5 (C-1), 62.4 (OCH_3), 61.8 (OCH_3), 57.0 (OCH_3), 20.0 (CH_3); **HR-TOF-MS-ES**: *m/z* found 317.1027 $[M+H]^+$ (calculated for $C_{17}H_{17}O_6$, 317.1025).

6.4.11. Synthesis of 5,10-dihydroxy-7-methoxy-3-methyl-1*H*-benzo[*g*]isochromene-6,9-dione (anhydrofusarubin) 26

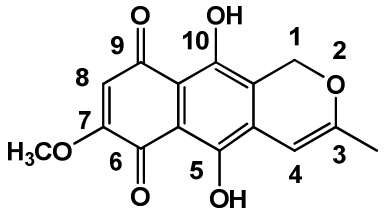

26

5,7,10-Trimethoxy-3-methyl-1*H*-benzo[*g*]isochromene-6,9-dione **229** (0.200 g, 1.15 mmol) was dissolved in dry CH_2Cl_2 (50 ml) and cooled to – 78 ℃ under a N_2(g) atmosphere. BCl_3 (1.58 ml, 1.58 mmol) was added dropwise to the solution which was stirred for a further 40 min at – 78 ℃, and then allowed to warm to rt. The reaction was then carefully quenched with a few drops of cold H_2O and then CH_2Cl_2 (50 ml) and H_2O (100 ml) were added. The lower organic layer was separated, dried over anhydrous $MgSO_4$, filtered and concentrated under reduced pressure. Column chromatography (20% EtOAc/hexane) of the residue afforded 5,10-dihydroxy-7-methoxy-3-methyl-1*H*-benzo[*g*]isochromene-6,9-dione **26** as a crystalline purple solid (0.130 g, 65%). $\mathbf{R_f}$ = 0.60 (30 % EtOAc/hexane); **Mp**. = 195-196 ˚C (199-202 ˚C)[18]; **^{1}H NMR** (500 MHz, $CDCl_3$) δ_H = 13.04 (1H, s, OH), 12.65 (1H, s, OH), 6.17 (1H, s, H-8), 5.99 (1H, s, H-4), 5.22 (2H, s, H-1), 3.92 (3H, s, OCH_3), 2.02 (3H, s, CH_3); **^{13}C NMR** (125 MHz, $CDCl_3$) δ_C = 183.0 (C=O), 177.9 (C=O), 161.7 (C-3), 160.1, 158.1, 158.0, 133.2 (C-4a), 122.9 (C-10a), 111.1 (C-5a), 110.1 (C-8), 108.1 (C-9a), 94.9 (C-4), 63.1 (C-1), 56.8 (OCH_3), 20.2 (CH_3); **HR-TOF-MS-ES**: *m/z* found 288.0633 $[M]^+$ (calculated for $C_{15}H_{12}O_6$, 288.0634)[8].

6.5. Experimental Work Pertaining to the Syntheisis of Bicyclic Acetal Compounds

6.5.1. Synthesis of 1-(5-Allyloxy-2-hydroxyphenyl)ethanone 243

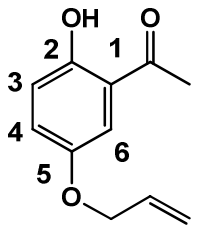

243

2,5-Dihydroxyacetophenone (8.00 g, 52.6 mmol) was dissolved in Me_2CO (300 ml) in a round-bottom flask (500 ml) equipped with a reflux condenser and a magnetic stirrer bar. Allyl bromide (8.28 g, 68.4mmol) and anhydrous K_2CO_3 (9.45 g, 68.4 mmol) were added to the solution, which was then refluxed for 18h under a N_2(g) atmosphere. The mixture was then allowed to cool to rt, filtered through a bed of celite, and the solvent was removed *in vacuo*. The residue was purified by column chromatography (20% EtOAc/hexane) to afford 1-(5-allyloxy-2-hydroxyphenyl)ethenone **234** (8.69 g, 86%) as a yellow crystalline solid. $\mathbf{R_f}$ = 0.79 (20 % EtOAc/hexane); **^{1}H NMR** (300 MHz, $CDCl_3$) δ_H = 11.84 (1H, s, OH), 7.16 (1H, d, *J* 3.0, H-6), 7.08 (1H, dd, *J* 9.0, 3.0, H-4), 6.86 (1H, d, *J* 9.0, H-3), 6.02 (1H, ddt, *J* 17.2, 10.5, 5.3, OCH_2CH=CH_2), 5.38 (1H, dt, *J* 17.2, 3.6, one of OCH_2CH=CH_2), 5.28 (1H, dd, *J* 10.5, 1.3, one of OCH_2CH=CH_2), 4.47 (2H, dt, *J* 5.3, 1.3, OCH_2CH=CH_2), 2.56 (3H, s, $COCH_3$; **^{13}C NMR** (75 MHz, $CDCl_3$) δ_C = 204.0 (C=O), 156.8 (ArC-O), 150.6 (ArC-O), 133.1 (OCH_2CH=CH_2), 124.9 (C-3), 119.2 (ArC), 119.1 (C-6), 117.8 (OCH_2CH=CH_2) 114.9 (C-4′), 69.8 (OCH_2CH=CH_2), 26.6 ($COCH_3$).[10]

6.5.2. Synthesis of 1-(2-Allyl-3,6-dimethoxyphenyl)ethanone 182

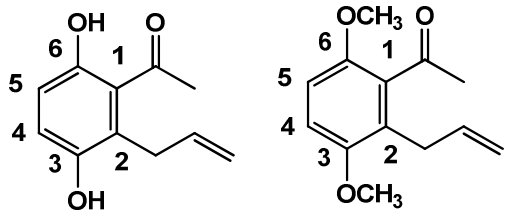

244 **182**

1-[5-(Allyloxy)-2-hydroxyphenyl]ethanone **243** (5.82 g, 30.3 mmol) was loaded neat into in a round-bottom flask (50 ml) equipped with a reflux condenser and a magnetic stirrer bar. The reaction vessel was then heated to 140 °C for 18 h under a N_2(g) atmosphere. The dark viscous residue was allowed to cool to rt and was then purified via column chromatography (15% EtOAc/hexane) to yield 1-(2-allyl-3,6-dihydroxyphenyl)ethanone **244** as a yellow oil (4.26 g, 73%). $\mathbf{R_f}$ = 0.24 (30 % EtOAc/hexane); **^{1}H NMR** (300 MHz, acetone) δ_H = 8.39 (1H, br s, OH), 7.93 (1H, br s, OH), 6.79 (1H, d, *J* 8.7, H-4′*), 6.66 (1H, d, *J* 8.7, H-5′*), 5.92 (1H, ddt, *J* 16.5, 10.2, 6.3, $ArCH_2CH$=CH_2), 5.00–4.88 (2H, m, $ArCH_2CH$=CH_2), 3.36 (2H, d, *J* 6.3, $ArCH_2CH$=CH_2), 2.48 (3H, s, $COCH_3$); **^{13}C NMR** (75 MHz, acetone) δ_C = 205.4 (C=O), 149.0 (ArC-O), 148.2 (ArC-O), 137.8 ($ArCH_2CH$=CH_2), 131.3 (ArC), 124.3 (ArC), 117.8 (C-5), 115.3 (C-4), 115.3 ($ArCH_2CH$=CH_2), 32.6 ($COCH_3$), 31.4 ($ArCH_2CH$=CH_2)[10]. The intermediate, 1-(2-allyl-3,6-dihydroxyphenyl)ethanone **244** (3.68 g, 19.1 mmol), anhydrous K_2CO_3 (7.94 g, 57.4 mmol) and Me_2SO_4 (9.66 g, 75.6 mmol) were dissolved in Me_2CO (200 ml). The solution was refluxed for 24 h under a N_2(g) atmosphere. The mixture was then allowed to cool to rt, filtered through a bed of celite, and the solvent was removed *in vacuo*. The residue was then dissolved in EtOAc (100 ml) and was successively washed with aqueous NH_3 (25%, 3 × 50 ml), HCl (0.5 M, 2 × 50 ml) and H_2O (100 ml). The EtOAc layer was dried over anhydrous $MgSO_4$, filtered and concentrated under reduced pressure. Column chromatography (10% EtOAc/hexane) of the residue afforded 1-(2-allyl-3,6-dimethoxyphenyl)ethanone **182** as a yellow oil (3.20 g, 76%). $\mathbf{R_f}$ = 0.57 (20 % ethyl acetate/hexane); **^{1}H NMR** (300 MHz, $CDCl_3$) δ_H = 6.77 (1H, d, *J* 9.0, H-4), 6.69 (1H, d, *J* 9.0, H-5), 5.86 (1H, ddt, *J* 18.0, 9.3, 6.2, $ArCH_2CH$=CH_2), 4.96–4.86 (2H, m, $ArCH_2CH$=CH_2), 3.72 (3H, s, OCH_3), 3.70 (3H, s, OCH_3), 3.28 (2H, br d, *J* 6.3,

ArC*H*$_2$CH=CH$_2$), 2.42 (3H, s, COCH$_3$); **^{13}C NMR** (75 MHz, CDCl$_3$) δ_C = 205.1 (C=O), 151.8 (ArC-O), 149.8 (ArC-O), 136.5 (ArCH$_2$*C*H=CH$_2$), 132.8 (ArC), 125.5 (ArC), 115.1 (ArCH$_2$CH=*C*H$_2$), 111.6 (C-4), 109.4 (C-5), 55.9 (2 × OCH$_3$), 32.3 (COCH$_3$), 30.7 (Ar*C*H$_2$CH=CH$_2$).[10]

6.5.3. Synthesis of (Z)-Ethyl 4-(2-allyl-3,6-dimethoxyphenyl)-2-hydroxy-4-oxobut-2-enoate 181a

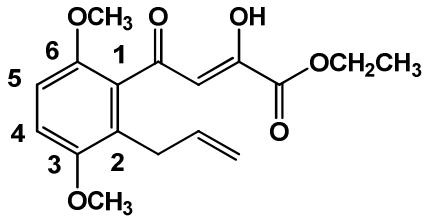

181a

To a stirred solution of 1-(2-allyl-3,6-dihydroxyphenyl)ethanone **182** (3.00 g, 13.6 mmol) and diethyl oxalate (3.98 g, 27.2 mmol) in dry THF (50 ml) at 0 °C, NaOEt (1.85 g, 27.2 mmol) was slowly added. The reaction mixture was then stirred vigorously for 3 h at rt before being acidified with aqueous HCl (100 ml, 2.0 M). EtOAc (100 ml) was then added to the mixture. The organic layer was separated, dried over anhydrous MgSO$_4$, filtered and concentrated under reduced pressure. Column chromatography (10% EtOAc/hexane) of the residue afforded (*Z*)-ethyl 4-(2-allyl-3,6-dimethoxyphenyl)-2-hydroxy-4-oxobut-2-enoate **181a** as a yellow solid (3.92 g, 90%). **R_f** = 0.55 (20 % EtOAc/hexane); Mp. = 65-66 °C; **IR** ν_{max} (cm^{-1})= 3007 (OH), 1738 (C=O), 1730 (C=O), 1625 (C=C), 1597 (C=C), 1228, 1216; **^{1}H NMR** (300 MHz, CDCl$_3$) δ_H = 14.30 (1H, br s, OH), 6.89 (1H, d, *J* 9.0, H-4), 6.77 (1H, d, *J* 9.0, H-5), 6.57 (1H, s, COC*H*=C(OH)CO$_2$Et), 5.87 (1H, ddt, *J* 16.6, 10.3, 6.2, ArCH$_2$C*H*=CH$_2$), 4.97–4.84 (2 H, m, ArCH$_2$CH=C*H*$_2$), 4.34 (3H, q, *J* 7.1, CO$_2$C*H*$_2$CH$_3$), 3.78 (3H, s, OCH$_3$), 3.75 (3H, s, OCH$_3$), 3.35 (2H, d, *J* 6.2, ArC*H*$_2$CH=CH$_2$), 1.35 (3H, t, *J* 7.1, CO$_2$CH$_2$C*H*$_3$); **^{13}C NMR** (75 MHz, CDCl$_3$) δ_C = 197.6 (C=O), 164.5 (COCH=*C*(OH)CO$_2$Et), 162.3 (CO*C*H=C(OH)CO$_2$Et), 151.8 (ArC-O), 150.5 (ArC-O), 136.1 (ArCH$_2$*C*H=CH$_2$), 128.8 (ArC), 127.5 (ArC), 115.3 (ArCH$_2$CH=*C*H$_2$), 113.15 (C-4), 109.7 (C-5), 105.92 (CO*C*H=C(OH)CO$_2$Et), 62.8 (CO$_2$*C*H$_2$CH$_3$), 56.2 (2 × OCH$_3$),

30.9 (Ar*C*H_2CH=CH_2), 13.9 (CO_2CH_2*C*H_3); **HR-TOF-MS:** *m/z* found 321.1338 $[M-H]^+$ (calculated for $C_{17}H_{21}O_6$, 321.1342).

6.5.4. Synthesis of Ethyl 4-(2-allyl-3,6-dimethoxyphenyl)-2-hydroxy-4-oxobutanoate 248

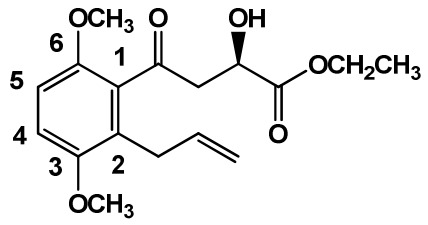

rac-**248**

(*Z*)-Ethyl 4-(2-allyl-3,6-dimethoxyphenyl)-2-hydroxy-4-oxobut-2-enoate **181a** (3.00 g, 9.37 mmol) was dissolved in dry THF (50 ml) and cooled to 0 °C in an ice bath. Sodium borohydride (0.711 g, 18.7 mmol) was added to the stirred reaction solution over 15 min. The reaction mixture was then stirred vigorously for 2 h at rt, before being acidified with a dilute aqueous solution of HCl (100 ml, 0.5 M). Once the fizzing stopped, the mixture was extracted with EtOAc (100 ml). The organic layer was then separated, dried over anhydrous $MgSO_4$, filtered and concentrated under reduced pressure. Column chromatography (20% EtOAc/hexane) of the residue afforded ethyl 4-(2-allyl-3,6-dimethoxyphenyl)-2-hydroxy-4-oxobutanoate **248** as a yellow liquid (1.20 g, 40%). $\mathbf{R_f}$ = 0.15 (30 % EtOAc/hexane); **IR** ν_{max} (cm^{-1}) = 3015 (OH), 1738 (C=O), 1588 (C=C), 1228, 1216; **^{1}H NMR** (300 MHz, $CDCl_3$) δ_H = 6.82 (1H, d, *J* 9.0, H-4), 6.72 (1H, d, *J* 9.0, H-5), 5.97–5.81 (1H, m, $ArCH_2CH$=CH_2), 5.01–4.90 (2H, m, $ArCH_2CH$=CH_2), 4.56 (1H, br s, $COCH_2CH(OH)CO_2Et$), 4.25 (2H, q, *J* 7.1, $CO_2CH_2CH_3$), 3.76 (3H, s, OCH_3), 3.74 (3H, s, OCH_3), 3.34 (1H, dd, *J* 18.3, 3.7, one of $COCH_2CH(OH)CO_2Et$), 3.32 (1H, br s, OH), 3.26 (2H, d, *J* 6.3, $ArCH_2CH$=CH_2), 3.23 (1H, dd, *J* 18.3, 6.3, one of $COCH_2CH(OH)CO_2Et$), 1.28 (3H, t, *J* 7.1, $CO_2CH_2CH_3$); **^{13}C NMR** (75 MHz, $CDCl_3$) δ_C = 204.4 (C=O), 173.8 (CO_2Et), 151.9 (ArC-O), 149.9 (ArC-O), 136.4 ($ArCH_2CH$=CH_2), 131.1 (ArC), 126.4 (ArC), 115.3 ($ArCH_2CH$=CH_2), 112.2 (C-4′)*, 109.4 (C-5′)*, 66.9 ($COCH_2CH(OH)CO_2Et$), 61.6 ($CO_2CH_2CH_3$), 56.1 (2 × OCH_3), 48.3 ($COCH_2CH(OH)CO_2Et$), 30.9 ($ArCH_2CH$=CH_2),

14.1 ($CO_2CH_2CH_3$); **HR-TOF-MS**: *m/z* found 323.1495, $[M-H]^+$ (calculated for $C_{17}H_{23}O_6$, 323.1484).

6.5.5. Synthesis of Ethyl 4-[3,6-dimethoxy-2-(2-oxopropyl)phenyl]-2-hydroxy-4-oxobutanoate 249

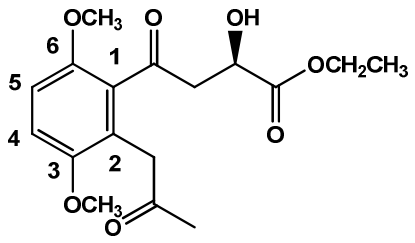

rac- **249**

Ethyl 4-(2-allyl-3,6-dimethoxyphenyl)-2-hydroxy-4-oxobutanoate **248** (1.10 g, 3.41 mmol) was dissolved in a DMF/H_2O mixture (1:1 v/v, 20 ml). $PdCl_2$ (0.0605 g, 0.341 mmol) and $CuCl_2.2H_2O$ (0.582 g, 3.41 mmol) were added to the solution. Oxygen gas was bubbled through the solution which was stirred vigorously for 2 h at 70 °C. The reaction was filtered, and EtOAc (30 ml) was added. The organic layer was washed with H_2O (3 × 30 ml), separated, dried over anhydrous $MgSO_4$, filtered and concentrated under reduced pressure. Column chromatography (30% EtOAc/hexane) of the residue afforded ethyl 4-[3,6-dimethoxy-2-(2-oxopropyl)phenyl]-2-hydroxy-4-oxobutanoate **249** as a yellow liquid (0.773 g, 67%). $\mathbf{R_f}$ = 0.15 (40 % EtOAc/hexane); **IR** ν_{max} (cm^{-1}) = 3015 (OH), 1738 (C=O), 1257, 1216; **^{1}H NMR** (300 MHz, $CDCl_3$) δ_H = 6.86 (1H, d, *J* 9.0, H-4), 6.79 (1H, d, *J* 9.0, H-5), 4.54 (1H, ddd, *J* 6.8, 5.6, 3.6, $COCH_2CH(OH)CO_2Et$), 4.24 (2H, q, *J* 7.1, $CO_2CH_2CH_3$), 3.77 (3H, s, OCH_3), 3.73 (3H, s, OCH_3), 3.68 (2H, s, $ArCH_2COCH_3$), 3.39 (1H, dd, *J* 17.6, 3.6, one of $COCH_2CH(OH)CO_2Et$), 3.25 (1H, d, *J* 5.6, OH), 3.23 (2H, dd, *J* 17.6, 6.8, one of $COCH_2CH(OH)CO_2Et$), 2.16 (3H, s, $ArCH_2COCH_3$), 1.28 (3H, t, *J* 7.1, $CO_2CH_2CH_3$); **^{13}C NMR** (75 MHz, $CDCl_3$) δ_C = 206.3 ($ArCH_2COCH_3$), 204.3 ($COCH_2CH(OH)CO_2Et$), 173.6 ($COCH_2CH(OH)CO_2Et$), 151.9 (ArC-O), 150.4 (ArC-O), 122.6 (ArC), 112.5 (ArC), 110.3 (C-4), 77.1 (C-5), 67.4 ($COCH_2CH(OH)CO_2Et$), 61.7 ($CO_2CH_2CH_3$), 56.1 (2 × OCH_3), 48.0 ($COCH_2CH(OH)CO_2Et$), 41.1 ($ArCH_2COCH_3$), 29.6 ($ArCH_2COCH_3$), 14.1

($CO_2CH_2CH_3$); **HR-TOF-MS**: *m/z* found 339.1444, $[M-H]^+$ (calculated for $C_{17}H_{23}O_7$, 339.1437).

6.5.6. Synthesis of 1-(2-Allyl-3,6-dimethoxyphenyl)-3,4-dihydroxybutan-1-one 255

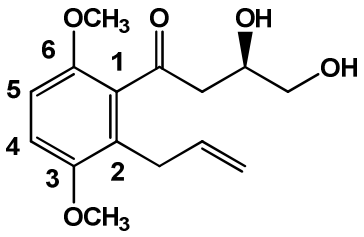

rac-**255**

(*Z*)-Ethyl 4-(2-allyl-3,6-dimethoxyphenyl)-2-hydroxy-4-oxobut-2-enoate **181a** (1.00 g, 3.12 mmol) was dissolved in dry THF (20 ml). The solution was cooled to -10 °C in a Me_2CO-ice bath and lithium aluminium hydride (0.237 g, 6.24 mmol) was added slowly over 5 min. The reaction mixture was then stirred vigorously for 2 h at rt under a N_2(g) atmosphere. The solution was then cooled to 0 °C in an ice bath and cold H_2O was added drop-wise until the fizzing stopped. EtOAc (20 ml) was added and the solution was washed with aqueous HCl (2 M, 20 ml). The organic layer was then dried over anhydrous $MgSO_4$, filtered and concentrated under reduced pressure. Column chromatography (eluant 40% EtOAc/hexane) of the residue afforded 1-(2-allyl-3,6-dimethoxyphenyl)-3,4-dihydroxybutan-1-one **255** as a yellow liquid (0.30 g, 34%). $\mathbf{R_f}$ = 0.26 (50 % EtOAc/hexane); **IR** ν_{max} (cm^{-1}) = 3015 (OH), 1738 (C=O), 1595 (C=C), 1255, 1228; **^{1}H NMR** (300 MHz, $CDCl_3$) δ_H = 6.78 (1H, d, *J* 9.0, H-4), 6.69 (1H, d, *J* 9.0, H-5), 5.92–5.76 (1H, m, $ArCH_2CH$=CH_2), 4.95–4.85 (2H, m, $ArCH_2CH$=CH_2), 4.31–4.21 (1H, m, $COCH_2CH(OH)CH_2OH$), 3.72 (3H, s, OCH_3), 3.70 (3H, s, OCH_3), 3.63 (2H, dd, *J* 11.7, 2.8, one of $COCH_2CH(OH)CH_2OH$ and OH), 3.48 (1H, dd, *J* 11.3, 6.6, one of $COCH_2CH(OH)CH_2OH$), 3.25 (2H, d, *J* 5.0, $ArCH_2CH$=CH_2), 2.92 (2H, d, *J* 6.1, $COCH_2CH(OH)CH_2OH$); **^{13}C NMR** (75 MHz, $CDCl_3$) δ_C = 207.3 (C=O), 151.8 (ArC-O), 149.7 (ArC-O), 136.4 ($ArCH_2CH$=CH_2), 131.6 (ArC), 126.3 (ArC), 115.3 ($ArCH_2CH$=CH_2), 112.1 (C-4), 109.5 (C-5), 68.6 ($COCH_2CH(OH)CH_2OH$), 65.8 ($COCH_2CH(OH)CH_2OH$), 55.8 (2 × OCH_3), 47.7

(CO*C*H_2CH(OH)CH_2OH), 30.1 (Ar*C*H_2CH=CH_2); **HR-TOF-MS**: *m/z* found 281.1389, $[M-H]^+$ (calculated for $C_{15}H_{21}O_5$, 281.1382).

6.5.7. Synthesis of 1-(2-Allyl-3,6-dimethoxyphenyl)butane-1,4-diol 256

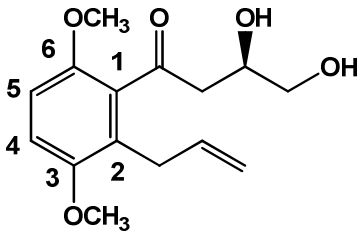

rac-**255**

1-(2-Allyl-3,6-dimethoxyphenyl)-3,4-dihydroxybutan-1-one **255** (2.20 g, 7.85 mmol) was dissolved in dry THF (50 ml). The solution was cooled to -10 °C in a Me_2CO-ice bath and lithium aluminium hydride (0.447 g, 11.8 mmol) was added slowly over 5 min. The reaction mixture was heated for 3 h at reflux under a N_2(g) atmosphere. The solution was then cooled to 0 °C in an ice bath and cold H_2O was added drop-wise until the fizzing stopped. EtOAc (50 ml) was added and the solution was washed with aqueous HCl (2 M, 50 ml). The organic layer was then dried over anhydrous $MgSO_4$, filtered and concentrated under reduced pressure. Column chromatography (40% EtOAc/hexane) of the residue afforded 1-(2-allyl-3,6-dimethoxyphenyl)butane-1,4-diol **256** as a clear liquid (1.30 g, 62%). $\mathbf{R_f}$ = 0.25 (50 % EtOAc/hexane); **IR** ν_{max} (cm^{-1}) = 3373 (OH), 1596 (C=C), 1228, 1217, 1051; **^{1}H NMR** (300 MHz, $CDCl_3$) δ_H = 6.74 (1H, d, *J* 9.0, H-4′)*, 6.70 (1H, d, *J* 9.0, H-5′)*, 5.88 (1H, ddt, *J* 16.3, 10.2, 5.8, $ArCH_2CH$=CH_2), 5.02–4.87 (2H, m, $ArCH_2CH$=CH_2), 4.83 (1H, dd, *J* 9.6, 3.2, C*H*(OH)$CH_2CH_2CH_2OH$), 3.80 (3H, s, OCH_3), 3.73 (3H, s, OCH_3), 3.68–3.58 (2H, m, CH(OH)$CH_2CH_2CH_2$OH), 3.54–3.32 (2H, m, $ArCH_2CH$=CH_2), 2.09–1.55 (4H, m, CH(OH)$CH_2CH_2CH_2OH$); **^{13}C NMR** (75 MHz, $CDCl_3$) δ_C 151.8 (ArC-O), 151.7 (ArC-O), 136.5 ($ArCH_2CH$=CH_2), 131.6 (ArC), 126.4 (ArC), 114.9 ($ArCH_2CH$=CH_2), 109.6 (C-4), 109.5 (C-5), 71.3 (*C*H(OH)$CH_2CH_2CH_2OH$), 62.7 (CH(OH)$CH_2CH_2CH_2OH$), 55.8 (2 × OCH_3), 34.4 (CH(OH)$CH_2CH_2CH_2OH$), 30.2 (CH(OH)$CH_2CH_2CH_2OH$), 29.9 ($ArCH_2CH$=CH_2).

6.5.8. Synthesis of 3,6-Dimethoxy-9-methyl-10,14-dioxatricyclo[7.3.1.0^{2,7}]tetradeca-2,4,6-triene 259

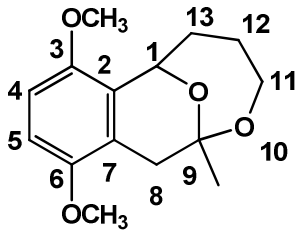

259

1-(2-Allyl-3,6-dimethoxyphenyl)butane-1,4-diol **256** (1.20 g, 4.51 mmol) was dissolved in a DMF/H_2O mixture (1:1 v/v, 50 ml). $PdCl_2$ (0.0800 g, 0.451 mmol) and $CuCl_2.2H_2O$ (0.768 g, 4.51 mmol) were added to the solution. Oxygen gas was bubbled through the solution which was stirred vigorously for 2 h at 70 °C. The reaction was filtered, and EtOAc (20 ml) was added. The organic layer was washed with H_2O (3 × 20 ml), separated, dried over anhydrous $MgSO_4$, filtered and concentrated under reduced pressure. Column chromatography (30% EtOAc/hexane) of the residue afforded **259** as a clear liquid (0.858 g, 72 %). $\mathbf{R_f}$ = 0.54 (40 % EtOAc/hexane); **IR** ν_{max} (cm^{-1}) = 1254, 1228, 1065; **^{1}H NMR** (300 MHz, $CDCl_3$) δ_H = 6.67 (1H, d, *J* 9.0, H-4), 6.63 (1H, d, *J* 9.0, H-5), 5.17 (1H, br d, *J* 4.8, H-1), 3.80 (1H, dd, *J* 11.8, 1.5, H-11a), 3.76 (3H, s, OCH_3), 3.75 (3H, s, OCH_3), 3.56 (1H, ddd, *J* 11.8, 3.3, 2.0, H-11b), 3.05 (1H, d, *J* 16.8, H-8a), 2.65–2.54 (1H, m, H-13a), 2.50 (1H, d, *J* 16.8, H-8b), 1.90–1.76 (1H, m, H-13b), 1.64–1.54 (1 H, m, H-12a), 1.49 (3H, s, CH_3), 1.47–1.32 (1H, m, H-12b); **^{13}C NMR** (75 MHz, $CDCl_3$) δ_C = 151.1 (ArC-O), 149.4 (ArC-O), 125.1 (C-2), 123.0 (C-7), 107.8 (C-5), 107.4 (C-4), 97.4 (C-9), 72.2 (C-1), 61.8 (C-11), 55.4 (2 × OCH_3), 33.6 (C-8), 32.3 (C-13), 27.6 (C-12), 25.0 (CH_3); **HR-TOF-MS**: *m/z* found 265.1440, $[M-H]^+$ (calculated for $C_{15}H_{21}O_4$, 265.1429).

6.5.9. Synthesis of 1-(2-Allyl-3,6-dimethoxyphenyl)-4-(*tert*butyldimethylsilyloxy)-3-hydroxybutan-1-one 260

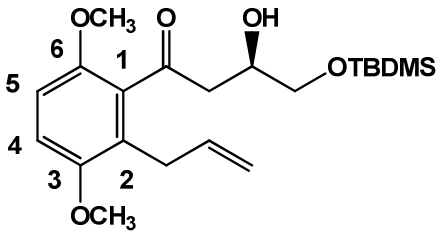

rac-**260**

1-(2-Allyl-3,6-dimethoxyphenyl)-3,4-dihydroxybutan-1-one **255** (2.44 g, 8.74 mmol) was dissolved in dry CH_3CN at 0 °C under a N_2(g) atmosphere. Imidazole (0.595 g, 8.74 mmol) and *tert*-butyldimethylsilyl chloride (1.32 g, 8.74 mmol) were added in three portions to the reaction mixture, every 15 min for a 45 min period. Once addition of the reactants was complete, the mixture was stirred for 1 h at rt. The solution was then filtered and the solvent was removed in *vacuo*. The residue was then dissolved in EtOAc (50 ml), and was sequentially washed with aqueous $NaHCO_3$ (50 ml) followed by aqueous NaCl (50 ml). The organic layer was then dried over anhydrous $MgSO_4$, filtered and concentrated under reduced pressure. Column chromatography (10% EtOAc/hexane) of the residue afforded 1-(2-allyl-3,6-dimethoxyphenyl)-4-(*tert*-butyldimethylsilyloxy)-3-hydroxybutan-1-one **260** as a clear liquid (2.20 g, 64%). $\mathbf{R_f}$ = 0.37 (20 % EtOAc/hexane); **IR** ν_{max} (cm^{-1}) = 3015 (OH), 1738 (C=O), 1255, 1228; **^{1}H NMR** (300 MHz, $CDCl_3$) δ_H = 6.83 (1H, d, *J* 9.0, H-4), 6.74 (1H, d, *J* 9.0, H-5), 5.90 (1H, ddt, *J* 16.6, 10.4, 6.2, $ArCH_2CH{=}CH_2$), 5.01–4.90 (2H, m, $ArCH_2CH{=}CH_2$), 4.31–4.19 (1H, m, $COCH_2CH(OH)CH_2OTBDMS$), 3.78 (3H, s, OCH_3), 3.75 (3H, s, OCH_3), 3.69–3.56 (2H, m, $COCH_2CH(OH)CH_2OTBDMS$), 3.30 (2H, dd, *J* 6.2, 1.4, $ArCH_2CH{=}CH_2$), 3.04 (1H, dd, *J* 17.9, 4.4, one of $COCH_2CH(OH)CH_2OTBDMS$), 2.98 (1H, d, *J* 3.6, OH), 2.91 (1H, dd, *J* 17.9, 7.8, one of $COCH_2CH(OH)CH_2OTBDMS$), 0.89 (9H, s, 3 × CH_3), 0.07 (6H, s, 2 × CH_3); **^{13}C NMR** (75 MHz, $CDCl_3$) δ_C = 207.0 (C=O), 151.9 (Ar**C**-O), 149.8 (Ar**C**-O), 136.4 (Ar**C**), 131.5 (Ar**C**), 126.1 ($ArCH_2CH{=}CH_2$), 115.3 ($ArCH_2CH{=}CH_2$), 111.9 (C-4), 109.4 C-5), 68.3 ($COCH_2CH(OH)CH_2OTBDMS$), 66.4 ($COCH_2CH(OH)CH_2OTBDMS$) 56.1 (2 × OCH_3), 48.1 ($COCH_2CH(OH)CH_2OTBDMS$), 30.9 ($ArCH_2CH{=}CH_2$), 25.9 ($OSi(CH_3)_2C(CH_3)_3$),

18.*3* *(OSi(CH$_3$)$_2$C(CH$_3$)$_3$),* *-5.4* *(OSi(CH$_3$)$_2$C(*CH$_3$)$_3$); **HR-TOF-MS**: *m/z* found 395.2254, $[M-H]^+$ (calculated for $C_{21}H_{35}O_5Si$, 395.2245).

6.5.10. Synthesis of (3,6-Dimethoxy-9-methyl-10,13-dioxatricyclo[7.3.1.0^{2,7}]trideca-2,4,6-trien-11-yl)methanol 254

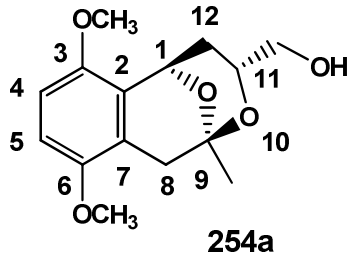

254a

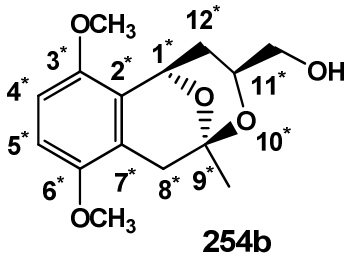

254b

1-(2-Allyl-3,6-dimethoxyphenyl)-4-(*tert*-butyldimethylsilyloxy)-3-hydroxybutan-1-one **260** (2.10 g, 5.34 mmol) was dissolved in dry THF (80 ml). The solution was cooled to -10 °C in a Me_2CO-ice bath and lithium aluminium hydride (0.303 g, 8.00 mmol) was added slowly over 5 min. The reaction mixture was then heated for 2 h at reflux under a N_2(g) atmosphere. The solution was then cooled to 0 °C in an ice bath and cold water was added drop-wise until the fizzing stopped. EtOAc (60 ml) was added and the solution was washed with aqueous HCl (2 M, 60 ml). The organic layer was then dried over anhydrous $MgSO_4$, filtered and concentrated under reduced pressure to afford a clear crystalline compound (0.700 g) of presumably **253**. A ^{1}H NMR spectrum of the crude mixture confirmed that no starting material was present. The crystalline material (0.423 g, 2.48 mmol) was dissolved in a mixture of DMF/H_2O (1:1 v/v, 40 ml). Oxygen gas was bubbled through the solution which was stirred vigorously for 2 h at 70 °C. The reaction was filtered, and EtOAc (50 ml) was added. The organic layer was washed with H_2O (3 × 30 ml), separated, dried over anhydrous $MgSO_4$, filtered and concentrated under reduced pressure. Column chromatography (50% EtOAc/hexane) of the residue afforded of mixture of diastereoisomers of **254** as a white solid (0.601 g, 86%) in a ratio of 1:0.43 as determined by ^{1}H NMR spectroscopy. $\mathbf{R_f}$ = 0.58 (50 % EtOAc/hexane); **Mp**. = 142-143 °C; **IR** ν_{max} (cm^{-1}) = 1229, 1215, 1172; **^{1}H NMR** (500 MHz, $CDCl_3$) δ_H Major diastereomer **254a** = 6.67 (1H, d, *J* 8.8, H-4), 6.64 (1H, d, *J* 8.8, H-5), 5.40 (1H, brd,

J 3.9, H-1), 3.91–3.83 (1H, m, H-11), 3.79 (3H, s, OCH_3), 3.76 (3H, s, OCH_3), 3.48 (2H, br s, C*H*$_2$OH), 2.98 (1H, d, *J* 18.8, H-8a), 2.85 (1H, d, *J* 18.8, H-8b), 2.20 (1H, br t, *J* 5.8, OH), 2.09–2.02 (1H, m, H-12a), 1.53 (3H, s, CH_3), 1.40 (1H, dt, *J* 12.9, 2.0, H-12b); Minor diastereomer **254b** = 6.67 (1H, d, *J* 8.8, H-4)*, 6.63 (1H, d, *J* 8.8, H-5)*, 5.25 (1H, brd, *J* 9.1, H-1)*, 4.09–4.03 (1H, m, H-11)*, 3.77 (3H, s, OCH_3), 3.76 (3H, s, OCH_3), 3.60–3.54 (1H, m, one of C*H*$_2$OH), 3.41–3.35 (1H, m, one of C*H*$_2$OH), 2.83 (1H, d, *J* 17.3, H-8a)*, 2.59 (1H, d, *J* 17.3, H-8b)*, 2.30 (1H, ddd, *J* 13.0, 10.1, 5.3, H-12a)*, 2.08 (1H, br s, OH), 1.57 (1H, ddd, *J* 13.0, 11.1, 1.55, H-12b)*, 1.52 (3H, s, CH_3); **^{13}C NMR** (125 MHz, $CDCl_3$) Major diastereomer **254a** δ_C = 149.9 (Ar**C**-O), 148.7 (Ar**C**-O), 126.0 (C-7), 124.1 (C-2), 107.8 (C-5), 107.3 (C-4), 96.0 (C-9), 68.3 (C-11), 65.9 (*C*H_2OH), 65.7 (C-1), 55.9 (OCH_3), 55.3 (OCH_3), 32.8 (C-8), 30.4 (C-12), 29.5 (CH_3); Minor diastereomer **254b** δ_C = 151.2 (Ar**C**-O), 148.6 (Ar**C**-O), 128.9 (C-2*), 121.5 (C-7*), 107.9 (C-5*), 107.0 (C-4*), 97.4 (C-9*), 66.7 (C-11*), 65.0 (C-1*), 64.9 (*C*H_2OH), 55.5 (OCH_3), 55.4 (OCH_3), 33.2 (C-8*), 32.8 (C-12*), 24.6 (CH_3); **HR-TOF-MS**: *m/z* found 281.1389, $[M-H]^+$ (calculated for $C_{15}H_{21}O_5$, 281.1382).

6.5.11. Attempted Dess-Martin Periodinane 270 oxidation of (3,6-Dimethoxy-9-methyl-10,13-dioxatricyclo[7.3.1.0^{2,7}]trideca-2,4,6-trien-11-yl)methanol 254

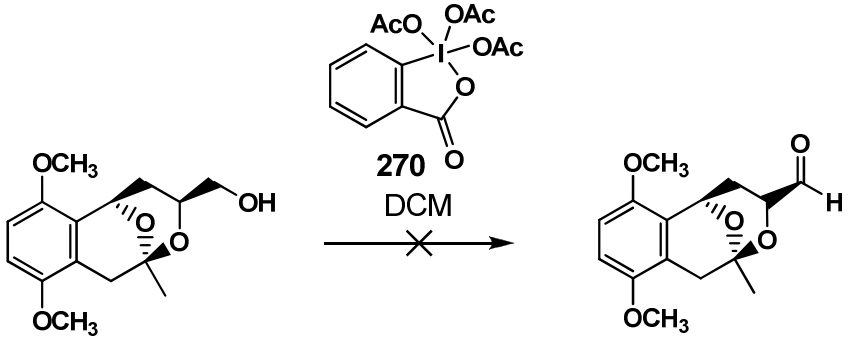

Acetal **254** (0.120 g, 0.431 mmol) was dissolved in DCM (10 ml) and the Dess-Martin Periodinane reagent **270** was added slowly over 5 min to the stirred reaction mixture. The solution was stirred vigorously for 24 h at rt. H_2O (20 ml) was then added and the lower organic layer was separated, dried over anhydrous $MgSO_4$, filtered and

concentrated under reduced pressure. The column chromatography of the resultant residue yielded no characterizable product(s) or recovered starting material.

6.5.12. Synthesis of 11-(Hydroxymethyl)-9-methyl-10,13-dioxatricyclo[7.3.1.$0^{2,7}$]trideca-2(7),4-diene-3,6-dione 271

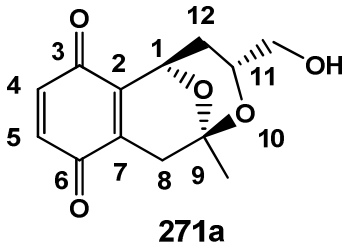

271a

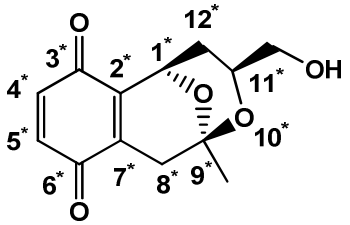

271b

Compound **254** (0.400 g, 1.44 mmol) was dissolved in a mixture of CH_3CN and H_2O (40 ml, 50:50 v/v ratio). CAN (2.36 g, 4.31 mmol) was added to the reaction mixture which was stirred vigorously for 30 min at rt. EtOAc (40 ml) and aqueous NaCl were then added and the upper organic layer was separated, dried over anhydrous $MgSO_4$, filtered and concentrated under reduced pressure. Column chromatography (30% EtOAc/hexane) of the residue afforded **271** as an amorphous red solid (0.320 g, 89%). $\mathbf{R_f}$ = 0.36 (50 % EtOAc/hexane); **IR** ν_{max} (cm^{-1}) = 3015 (OH), 1754 (C=O), 1111; **^{1}H NMR** (300 MHz, $CDCl_3$) δ_H Major diastereomer **271a** = 6.79 (1H, d, *J* 10.2, H-4), 6.74 (1H, d, *J* 10.2, H-5), 5.15 (1H, d, *J* 5.3, H-1), 3.90–3.80 (1H, m, H-11), 3.55 (2H, brs, C*H*$_2$OH), 2.82 (1H, d, *J* 20.9, H-8a), 2.82 (1H, d, *J* 20.9, H-8b), 2.17–2.06 (1H, m, H-12a), 1.52 (3H, s, CH_3), 1.40–1.33 (1H, m, H-12b); Minor diastereomer **271b** = 6.77 (1H, d, *J* 10.1, H-4)*, 6.74 (1H, d, *J* 10.2, H-5)*, 5.03 (1H, brd, *J* 10.7, H-1)*, 4.06–3.95 (1H, m, H-11)*, 3.58–3.69 (1H, m, one of C*H*$_2$OH), 3.50–3.37 (1H, m, one of C*H*$_2$OH), 2.64 (1H, d, *J* 19.1, H-8a)*, 2.82 (1H, d, *J* 19.1, H-8b)*, 2.36–2.23 (1H, m, H-12a)*, 1.58–1.52 (1H, m, H-12b)*, 1.52 (3H, s, CH_3); **^{13}C NMR** (75 MHz, $CDCl_3$) δ_C Major diastereomer **271a** = 185.3 (C=O), 184.7 (C=O), 141.3 (C-2), 141.1 (C-7), 136.1 (C-4), 136.0 (C-5), 96.0 (C-9), 68.2 (C-11), 65.6 (CH_2OH), 64.4 (C-1), 32.3 (C-8), 28.8 (C-12), 29.4 (CH_3); Minor diastereomer **271b** = 186.4 (C=O), 185.3 (C=O), 143.6 (C-2*), 137.7 (C-7*), 136.1 (C-4)*, 136.0 (C-5)*,

97.5 (C-9*), 66.1 (C-11*), 64.6 (CH_2OH), 63.7 (C-1*), 33.6 (C-8*), 29.7 (C-12*), 24.1 (CH_3).

6.6. References

1. Bruker (2005a). APEX2. Version 2.0-1. Bruker AXS Inc., Madison, Wisconsin, USA
2. Bruker (2005b). SAINT+. Version 6.0. (includes XPREP and SADABS) Bruker AXS Inc., Madison, Wisconsin, USA.
3. Bruker (1999). SHELXTL. Version 5.1. (includes XS, XL, XP, XSHELL) AXS Inc., Madison, Wisconsin, USA.
4. Mmutlane, E. M., Michael, J.P., Green, I.R., de Koning, C.B., *Organic and Biomolecular Chemistry*, 2004, **2**, 2461-2470.
5. Kraus, G.A., Ogutu, H., *Tetrahedron*, 2002, **58**, 7391-7395.
6. Kesteleyn, B., De Kimpe, N., *Journal of Organic Chemistry*, 2000, 65, 640-644.
7. de Koning, C..B., Manzini, S.S., Michael, J.P., Mmutlane, E.M., Tshabidi, T.R., van Otterlo, W.A.L., *Tetrahedron*, 2005, **61**, 555-564.
8. Kurobane, I., Vining, L.C., McInnes, A.G., Walter, J.A., *Canadian Journal of Chemistry*, 1980, **58**, 1380-1385.
9. Pelly, S., *Novel Methods for the Synthesis of Naturally Occurring Oxygen and Nitrogen Heterocycles*, 2009, PhD Thesis, University of the Witwatersrand.
10. Green, I.R., Hugo, V.I., Oosthuisen, F.J., van Eeden, N., Giles, R.G.F., South African Journal of Chemistry, 1995, **48**, 15-22.
11. Spek, A.L., *Journal of Applied Crystallography*, 2003, **36**, 7-13.
12. L. Farrugia, J., *Journal of Applied Crystallography,* 1997, **30**, 565.

Appendices

A1 X-ray crystallographic data

The intensity data were collected on a Bruker APEX II CCD area detector diffractometer with graphite monochromated Mo *K*α radiation (50kV, 30mA) using the APEX 2 data collection software[1]. The data collection process involved ω-scans of width 0.5° and 512×512 bit data frames. Data reduction was carried out using the program *SAINT+* and face indexed absorption corrections were made using *XPREP*[2]. Crystal structures were solved by direct methods using *SHELXTL*[3]. Non-hydrogen atoms were first refined isotropically followed by anisotropic refinement by full matrix least-*squares* calculations based on F^2 using *SHELXTL*. Hydrogen atoms were first located in the difference map and then positioned geometrically and allowed to ride on their respective parent atoms. Figures and publication material were generated using SHELXTL, PLATON[11] and ORTEP-3[12].

A1.1 X-Ray crystallographic data for (3-Formyl-4-hydroxy-6,8-dimethoxynaphthalene-2-yl)methyl acetate 201

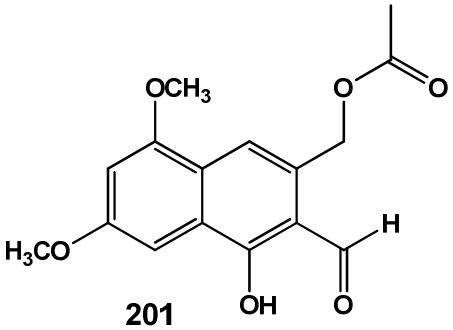

201

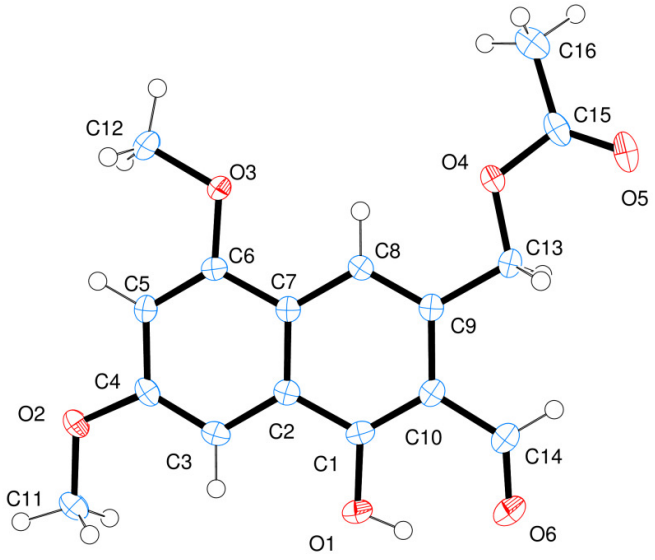

Table A1.1.1 Crystal data and structure refinement for 201

Empirical formula	$C_{16}H_{16}O_6$	
Formula weight	304.29	
Temperature	173(2) K	
Wavelength	0.71073 Å	
Crystal system	Monoclinic	
Space group	C2/m	
Unit cell dimensions	a = 19.2003(6) Å	α = 90°.
	b = 6.7203(2) Å	β = 99.379(2)°.
	c = 11.0340(4) Å	γ = 90°.
Volume	1404.70(8) $Å^3$	
Z	4	
Density (calculated)	1.439 Mg/m^3	
Absorption coefficient	0.111 mm^{-1}	
F(000)	640	
Crystal size	0.42 x 0.25 x 0.22 mm^3	
Theta range for data collection	1.87 to 27.99°.	
Index ranges	-25<=h<=23, -8<=k<=8, -12<=l<=14	
Reflections collected	8613	
Independent reflections	1842 [R(int) = 0.0473]	
Completeness to theta = 27.99°	100.0 %	
Absorption correction	None	
Max. and min. transmission	0.9760 and 0.9550	
Refinement method	Full-matrix least-squares on F^2	
Data / restraints / parameters	1842 / 0 / 140	
Goodness-of-fit on F^2	1.069	
Final R indices [I>2sigma(I)]	R1 = 0.0439, wR2 = 0.1176	
R indices (all data)	R1 = 0.0561, wR2 = 0.1261	
Largest diff. peak and hole	0.247 and -0.363 e.$Å^{-3}$	

Table A1.1.2 Atomic coordinates (x 10^4) and equivalent isotropic displacement parameters ($Å^2$x 10^3) for 201. U(eq) is defined as one third of the trace of the orthogonalized U^{ij} tensor.

	x	y	z	U(eq)
C(1)	3554(1)	0	4961(2)	21(1)
C(2)	3191(1)	0	3731(1)	20(1)
C(3)	3564(1)	0	2724(1)	23(1)
C(4)	3191(1)	0	1559(2)	24(1)
C(5)	2442(1)	0	1344(1)	24(1)
C(6)	2083(1)	0	2321(1)	21(1)
C(7)	2448(1)	0	3557(1)	19(1)
C(8)	2081(1)	0	4576(1)	19(1)
C(9)	2435(1)	0	5747(1)	19(1)
C(10)	3193(1)	0	5963(1)	21(1)
C(11)	4232(1)	0	657(2)	34(1)
C(12)	982(1)	0	988(2)	44(1)
C(13)	2046(1)	0	6832(1)	22(1)
C(14)	3595(1)	0	7188(2)	28(1)
C(15)	876(1)	287(12)	7218(2)	26(2)
C(16)	125(1)	557(4)	6628(2)	45(1)
O(1)	4261(1)	0	5103(1)	32(1)
O(2)	3480(1)	0	506(1)	32(1)
O(3)	1367(1)	0	2213(1)	29(1)
O(4)	1307(1)	0	6368(1)	32(1)
O(5)	1081(1)	0	8294(1)	43(1)
O(6)	4245(1)	0	7431(1)	38(1)

Table A1.1.3. Bond lengths [Å] and angles [°] for 201.

C(1)-O(1)	1.3410(17)
C(1)-C(10)	1.397(2)
C(1)-C(2)	1.421(2)
C(2)-C(7)	1.4090(19)
C(2)-C(3)	1.416(2)
C(3)-C(4)	1.367(2)
C(3)-H(3)	0.9500
C(4)-O(2)	1.3670(18)
C(4)-C(5)	1.417(2)
C(5)-C(6)	1.371(2)
C(5)-H(5)	0.9500
C(6)-O(3)	1.3601(16)
C(6)-C(7)	1.428(2)
C(7)-C(8)	1.421(2)
C(8)-C(9)	1.359(2)
C(8)-H(8)	0.9500
C(9)-C(10)	1.4353(19)
C(9)-C(13)	1.511(2)
C(10)-C(14)	1.444(2)
C(11)-O(2)	1.4269(18)
C(11)-H(11A)	0.9800
C(11)-H(11B)	0.9800
C(11)-H(11C)	0.9800
C(12)-O(3)	1.4320(18)
C(12)-H(12A)	0.9800
C(12)-H(12B)	0.9800
C(12)-H(12C)	0.9800
C(13)-O(4)	1.4285(17)
C(13)-H(13A)	0.9900
C(13)-H(13B)	0.9900
C(14)-O(6)	1.2333(19)

C(14)-H(14)	0.9500
C(15)-O(5)	1.204(3)
C(15)-O(4)	1.361(2)
C(15)-C(16)	1.494(3)
C(16)-H(16A)	0.9800
C(16)-H(16B)	0.9800
C(16)-H(16C)	0.9800
O(1)-H(1)	0.8400
O(4)-C(15)#1	1.361(2)
O(5)-C(15)#1	1.204(3)
O(1)-C(1)-C(10)	122.15(14)
O(1)-C(1)-C(2)	116.13(13)
C(10)-C(1)-C(2)	121.72(14)
C(7)-C(2)-C(3)	121.56(14)
C(7)-C(2)-C(1)	117.27(14)
C(3)-C(2)-C(1)	121.16(14)
C(4)-C(3)-C(2)	118.89(13)
C(4)-C(3)-H(3)	120.6
C(2)-C(3)-H(3)	120.6
C(3)-C(4)-O(2)	125.15(14)
C(3)-C(4)-C(5)	121.33(14)
O(2)-C(4)-C(5)	113.52(14)
C(6)-C(5)-C(4)	119.61(14)
C(6)-C(5)-H(5)	120.2
C(4)-C(5)-H(5)	120.2
O(3)-C(6)-C(5)	124.17(14)
O(3)-C(6)-C(7)	114.52(13)
C(5)-C(6)-C(7)	121.31(13)
C(2)-C(7)-C(8)	120.98(13)
C(2)-C(7)-C(6)	117.29(13)
C(8)-C(7)-C(6)	121.73(13)
C(9)-C(8)-C(7)	121.04(13)
C(9)-C(8)-H(8)	119.5

C(7)-C(8)-H(8)	119.5
C(8)-C(9)-C(10)	119.68(14)
C(8)-C(9)-C(13)	121.18(13)
C(10)-C(9)-C(13)	119.15(13)
C(1)-C(10)-C(9)	119.30(14)
C(1)-C(10)-C(14)	118.78(14)
C(9)-C(10)-C(14)	121.91(14)
O(2)-C(11)-H(11A)	109.5
O(2)-C(11)-H(11B)	109.5
H(11A)-C(11)-H(11B)	109.5
O(2)-C(11)-H(11C)	109.5
H(11A)-C(11)-H(11C)	109.5
H(11B)-C(11)-H(11C)	109.5
O(3)-C(12)-H(12A)	109.5
O(3)-C(12)-H(12B)	109.5
H(12A)-C(12)-H(12B)	109.5
O(3)-C(12)-H(12C)	109.5
H(12A)-C(12)-H(12C)	109.5
H(12B)-C(12)-H(12C)	109.5
O(4)-C(13)-C(9)	107.87(12)
O(4)-C(13)-H(13A)	110.1
C(9)-C(13)-H(13A)	110.1
O(4)-C(13)-H(13B)	110.1
C(9)-C(13)-H(13B)	110.1
H(13A)-C(13)-H(13B)	108.4
O(6)-C(14)-C(10)	124.87(16)
O(6)-C(14)-H(14)	117.6
C(10)-C(14)-H(14)	117.6
O(5)-C(15)-O(4)	121.3(3)
O(5)-C(15)-C(16)	125.95(19)
O(4)-C(15)-C(16)	111.60(18)
C(1)-O(1)-H(1)	109.5
C(4)-O(2)-C(11)	116.43(13)

C(6)-O(3)-C(12)	116.26(12)
C(15)#1-O(4)-C(13)	115.63(14)
C(15)-O(4)-C(13)	115.63(14)

Symmetry transformations used to generate equivalent atoms

Table A1.1.4. Anisotropic displacement parameters ($Å^2$x 10^3) for 201. The anisotropic displacement factor exponent takes the form: $-2\pi^2[h^2a^{*2}U^{11} + ... + 2 h k a^* b^* U^{12}]$.

	U^{11}	U^{22}	U^{33}	U^{23}	U^{13}	U^{12}
C(1)	17(1)	22(1)	24(1)	0	0(1)	0
C(2)	20(1)	19(1)	21(1)	0	4(1)	0
C(3)	17(1)	27(1)	26(1)	0	6(1)	0
C(4)	24(1)	29(1)	21(1)	0	10(1)	0
C(5)	23(1)	33(1)	15(1)	0	3(1)	0
C(6)	16(1)	26(1)	20(1)	0	2(1)	0
C(7)	20(1)	18(1)	18(1)	0	3(1)	0
C(8)	18(1)	20(1)	20(1)	0	4(1)	0
C(9)	22(1)	17(1)	18(1)	0	3(1)	0
C(10)	22(1)	20(1)	19(1)	0	1(1)	0
C(11)	23(1)	54(1)	28(1)	0	13(1)	0
C(12)	25(1)	86(2)	18(1)	0	-2(1)	0
C(13)	24(1)	25(1)	15(1)	0	2(1)	0
C(14)	26(1)	35(1)	22(1)	0	-1(1)	0
C(15)	33(1)	24(5)	25(1)	1(1)	15(1)	-2(1)
C(16)	30(1)	70(3)	37(1)	0(1)	13(1)	2(1)
O(1)	16(1)	52(1)	26(1)	0	0(1)	0
O(2)	23(1)	55(1)	21(1)	0	11(1)	0
O(3)	17(1)	54(1)	15(1)	0	1(1)	0
O(4)	21(1)	59(1)	18(1)	0	7(1)	0
O(5)	46(1)	65(1)	21(1)	0	14(1)	0
O(6)	26(1)	59(1)	28(1)	0	-5(1)	0

Table A1.1.5. Hydrogen coordinates (x 10^4) and isotropic displacement parameters ($Å^2$x 10^3) for 201.

	x	y	z	U(eq)
H(3)	4066	0	2857	28
H(5)	2191	0	527	28
H(8)	1579	0	4436	23
H(11A)	4381	0	-152	51
H(11B)	4416	-1191	1113	51
H(11C)	4416	1191	1113	51
H(12A)	475	102	1015	65
H(12B)	1076	-1239	574	65
H(12C)	1130	1136	534	65
H(13A)	2174	-1195	7345	26
H(13B)	2174	1195	7345	26
H(14)	3340	0	7857	34
H(16A)	-87	-745	6405	67
H(16B)	107	1373	5887	67
H(16C)	-137	1222	7204	67
H(1)	4429	0	5855	48

Table A1.1.6. Torsion angles [°] for 201.

O(1)-C(1)-C(2)-C(7)	180.0
C(10)-C(1)-C(2)-C(7)	0.0
O(1)-C(1)-C(2)-C(3)	0.0
C(10)-C(1)-C(2)-C(3)	180.0
C(7)-C(2)-C(3)-C(4)	0.0
C(1)-C(2)-C(3)-C(4)	180.0
C(2)-C(3)-C(4)-O(2)	180.0
C(2)-C(3)-C(4)-C(5)	0.0
C(3)-C(4)-C(5)-C(6)	0.0
O(2)-C(4)-C(5)-C(6)	180.0

C(4)-C(5)-C(6)-O(3)	180.0
C(4)-C(5)-C(6)-C(7)	0.0
C(3)-C(2)-C(7)-C(8)	180.0
C(1)-C(2)-C(7)-C(8)	0.0
C(3)-C(2)-C(7)-C(6)	0.0
C(1)-C(2)-C(7)-C(6)	180.0
O(3)-C(6)-C(7)-C(2)	180.0
C(5)-C(6)-C(7)-C(2)	0.0
O(3)-C(6)-C(7)-C(8)	0.0
C(5)-C(6)-C(7)-C(8)	180.0
C(2)-C(7)-C(8)-C(9)	0.0
C(6)-C(7)-C(8)-C(9)	180.0
C(7)-C(8)-C(9)-C(10)	0.0
C(7)-C(8)-C(9)-C(13)	180.0
O(1)-C(1)-C(10)-C(9)	180.0
C(2)-C(1)-C(10)-C(9)	0.0
O(1)-C(1)-C(10)-C(14)	0.0
C(2)-C(1)-C(10)-C(14)	180.0
C(8)-C(9)-C(10)-C(1)	0.0
C(13)-C(9)-C(10)-C(1)	180.0
C(8)-C(9)-C(10)-C(14)	180.0
C(13)-C(9)-C(10)-C(14)	0.0
C(8)-C(9)-C(13)-O(4)	0.0
C(10)-C(9)-C(13)-O(4)	180.0
C(1)-C(10)-C(14)-O(6)	0.0
C(9)-C(10)-C(14)-O(6)	180.0
C(3)-C(4)-O(2)-C(11)	0.0
C(5)-C(4)-O(2)-C(11)	180.0
C(5)-C(6)-O(3)-C(12)	0.0
C(7)-C(6)-O(3)-C(12)	180.0
O(5)-C(15)-O(4)-C(15)#1	74.0(6)
C(16)-C(15)-O(4)-C(15)#1	-94.3(5)
O(5)-C(15)-O(4)-C(13)	-20.0(8)

C(16)-C(15)-O(4)-C(13)	171.7(3)
C(9)-C(13)-O(4)-C(15)#1	171.0(4)
C(9)-C(13)-O(4)-C(15)	-171.0(4)
O(4)-C(15)-O(5)-C(15)#1	-74.5(6)
C(16)-C(15)-O(5)-C(15)#1	92.0(7)

Symmetry transformations used to generate equivalent atoms

A1.2 X-Ray crystallographic data for (3R,4R) 3-Hydroxy-7,9-dimethoxy-3-methyl-5,10-dioxo-3,4,5,10-tetrahydro-1*H*-benzo[g]isochromen-4-yl nitrate 202

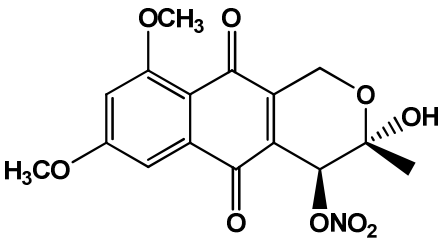

202

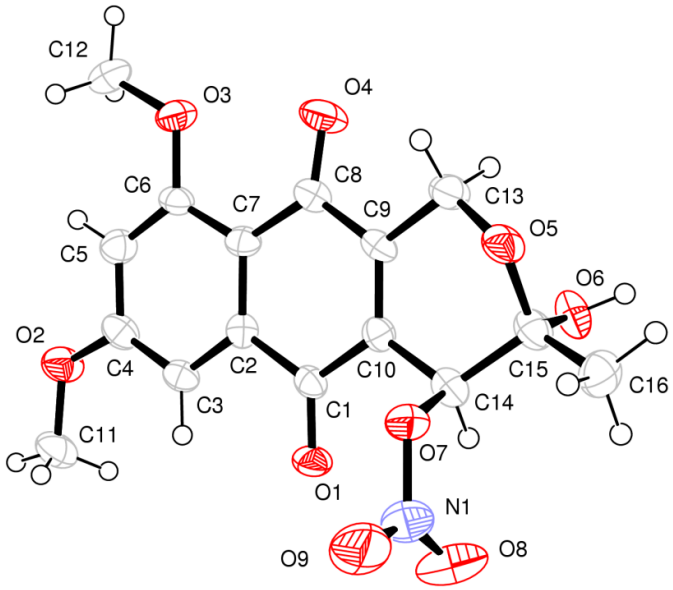

Table A1.2.1 Crystal data and structure refinement for 202

Empirical formula	$C_{16}H_{15}NO_9$	
Formula weight	365.29	
Temperature	173(2) K	
Wavelength	0.71073 Å	
Crystal system	Monoclinic	
Space group	P2(1)/c	
Unit cell dimensions	a = 13.913(4) Å	α = 90°.
	b = 13.475(4) Å	β = 94.246(9)°.

	c = 8.404(3) Å γ = 90°.
Volume	1571.2(9) $Å^3$
Z	4
Density (calculated)	1.544 Mg/m^3
Absorption coefficient	0.129 mm^{-1}
F(000)	760
Crystal size	0.32 x 0.06 x 0.03 mm^3
Theta range for data collection	1.47 to 25.00°.
Index ranges	-16<=h<=16, -14<=k<=16, -9<=l<=9
Reflections collected	7954
Independent reflections	2722 [R(int) = 0.1022]
Completeness to theta = 25.00°	98.9 %
Absorption correction	None
Refinement method	Full-matrix least-squares on F^2
Data / restraints / parameters	2722 / 0 / 239
Goodness-of-fit on F^2	0.874
Final R indices [I>2sigma(I)]	R1 = 0.0497, wR2 = 0.0821
R indices (all data)	R1 = 0.1857, wR2 = 0.1160
Largest diff. peak and hole	0.184 and -0.196 $e.Å^{-3}$

Table A1.2.2 Atomic coordinates (x 10^4) and equivalent isotropic displacement parameters (Å^{2}x 10^3) for 202. U(eq) is defined as one third of the trace of the orthogonalized U^{ij} tensor.

	x	y	z	U(eq)
C(1)	7945(3)	1080(3)	4411(5)	28(1)
C(2)	7955(3)	2193(3)	4379(5)	27(1)
C(3)	8691(3)	2662(3)	5322(5)	31(1)
C(4)	8726(3)	3694(4)	5297(5)	35(1)
C(5)	8058(3)	4232(3)	4356(5)	36(1)
C(6)	7334(3)	3772(3)	3420(5)	29(1)
C(7)	7251(3)	2724(3)	3442(5)	29(1)
C(8)	6490(3)	2185(3)	2524(5)	32(1)
C(9)	6534(3)	1081(3)	2477(5)	28(1)
C(10)	7196(3)	571(3)	3377(5)	28(1)
C(11)	10123(3)	3787(3)	7148(5)	47(1)
C(12)	6764(3)	5339(3)	2411(5)	42(1)
C(13)	5786(3)	576(3)	1393(5)	36(1)
C(14)	7220(3)	-544(3)	3320(5)	32(1)
C(15)	6283(3)	-989(4)	2535(5)	36(1)
C(16)	6377(3)	-2054(3)	2016(5)	44(1)
N(1)	8732(3)	-1393(3)	3048(6)	55(1)
O(1)	8538(2)	597(2)	5232(3)	36(1)
O(2)	9372(2)	4262(2)	6185(4)	44(1)
O(3)	6672(2)	4274(2)	2468(3)	38(1)
O(4)	5792(2)	2579(2)	1775(3)	47(1)
O(5)	6003(2)	-441(2)	1120(3)	37(1)
O(6)	5612(2)	-862(2)	3695(3)	43(1)
O(7)	7998(2)	-789(2)	2317(3)	39(1)
O(8)	8618(3)	-1766(3)	4321(5)	75(1)
O(9)	9389(2)	-1480(3)	2182(4)	76(1)

Table A1.2.3. Bond lengths [Å] and angles [°] for 202.

C(1)-O(1)	1.223(4)
C(1)-C(10)	1.475(5)
C(1)-C(2)	1.501(5)
C(2)-C(3)	1.398(5)
C(2)-C(7)	1.406(5)
C(3)-C(4)	1.392(6)
C(3)-H(3)	0.9500
C(4)-O(2)	1.361(5)
C(4)-C(5)	1.380(5)
C(5)-C(6)	1.379(5)
C(5)-H(5)	0.9500
C(6)-O(3)	1.354(4)
C(6)-C(7)	1.417(5)
C(7)-C(8)	1.457(5)
C(8)-O(4)	1.237(5)
C(8)-C(9)	1.490(6)
C(9)-C(10)	1.338(5)
C(9)-C(13)	1.495(5)
C(10)-C(14)	1.504(5)
C(11)-O(2)	1.425(4)
C(11)-H(11A)	0.9800
C(11)-H(11B)	0.9800
C(11)-H(11C)	0.9800
C(12)-O(3)	1.442(4)
C(12)-H(12A)	0.9800
C(12)-H(12B)	0.9800
C(12)-H(12C)	0.9800
C(13)-O(5)	1.425(4)
C(13)-H(13A)	0.9900
C(13)-H(13B)	0.9900
C(14)-O(7)	1.458(4)

C(14)-C(15)	1.539(5)
C(14)-H(14)	1.0000
C(15)-O(6)	1.409(4)
C(15)-O(5)	1.430(5)
C(15)-C(16)	1.510(5)
C(16)-H(16A)	0.9800
C(16)-H(16B)	0.9800
C(16)-H(16C)	0.9800
N(1)-O(8)	1.203(5)
N(1)-O(9)	1.216(4)
N(1)-O(7)	1.411(4)
O(6)-H(6)	0.8400
O(1)-C(1)-C(10)	120.2(4)
O(1)-C(1)-C(2)	122.3(4)
C(10)-C(1)-C(2)	117.4(4)
C(3)-C(2)-C(7)	122.5(4)
C(3)-C(2)-C(1)	116.7(4)
C(7)-C(2)-C(1)	120.8(4)
C(4)-C(3)-C(2)	117.9(4)
C(4)-C(3)-H(3)	121.1
C(2)-C(3)-H(3)	121.1
O(2)-C(4)-C(5)	114.1(4)
O(2)-C(4)-C(3)	125.2(4)
C(5)-C(4)-C(3)	120.7(4)
C(6)-C(5)-C(4)	121.6(4)
C(6)-C(5)-H(5)	119.2
C(4)-C(5)-H(5)	119.2
O(3)-C(6)-C(5)	123.3(4)
O(3)-C(6)-C(7)	116.9(4)
C(5)-C(6)-C(7)	119.8(4)
C(2)-C(7)-C(6)	117.4(4)
C(2)-C(7)-C(8)	119.5(4)
C(6)-C(7)-C(8)	123.1(4)

O(4)-C(8)-C(7)	124.6(4)
O(4)-C(8)-C(9)	116.6(4)
C(7)-C(8)-C(9)	118.8(4)
C(10)-C(9)-C(8)	121.7(4)
C(10)-C(9)-C(13)	122.0(4)
C(8)-C(9)-C(13)	116.3(4)
C(9)-C(10)-C(1)	121.4(4)
C(9)-C(10)-C(14)	120.7(4)
C(1)-C(10)-C(14)	117.8(4)
O(2)-C(11)-H(11A)	109.5
O(2)-C(11)-H(11B)	109.5
H(11A)-C(11)-H(11B)	109.5
O(2)-C(11)-H(11C)	109.5
H(11A)-C(11)-H(11C)	109.5
H(11B)-C(11)-H(11C)	109.5
O(3)-C(12)-H(12A)	109.5
O(3)-C(12)-H(12B)	109.5
H(12A)-C(12)-H(12B)	109.5
O(3)-C(12)-H(12C)	109.5
H(12A)-C(12)-H(12C)	109.5
H(12B)-C(12)-H(12C)	109.5
O(5)-C(13)-C(9)	113.0(3)
O(5)-C(13)-H(13A)	109.0
C(9)-C(13)-H(13A)	109.0
O(5)-C(13)-H(13B)	109.0
C(9)-C(13)-H(13B)	109.0
H(13A)-C(13)-H(13B)	107.8
O(7)-C(14)-C(10)	105.3(3)
O(7)-C(14)-C(15)	107.8(3)
C(10)-C(14)-C(15)	112.5(4)
O(7)-C(14)-H(14)	110.3
C(10)-C(14)-H(14)	110.3
C(15)-C(14)-H(14)	110.3

O(6)-C(15)-O(5)	111.0(4)
O(6)-C(15)-C(16)	113.0(4)
O(5)-C(15)-C(16)	106.0(3)
O(6)-C(15)-C(14)	103.9(3)
O(5)-C(15)-C(14)	109.0(4)
C(16)-C(15)-C(14)	113.9(4)
C(15)-C(16)-H(16A)	109.5
C(15)-C(16)-H(16B)	109.5
H(16A)-C(16)-H(16B)	109.5
C(15)-C(16)-H(16C)	109.5
H(16A)-C(16)-H(16C)	109.5
H(16B)-C(16)-H(16C)	109.5
O(8)-N(1)-O(9)	130.3(5)
O(8)-N(1)-O(7)	119.3(4)
O(9)-N(1)-O(7)	110.3(4)
C(4)-O(2)-C(11)	119.0(4)
C(6)-O(3)-C(12)	117.3(3)
C(13)-O(5)-C(15)	114.2(3)
C(15)-O(6)-H(6)	109.5
N(1)-O(7)-C(14)	115.0(3)

Symmetry transformations used to generate equivalent atoms

Table A1.2.4. Anisotropic displacement parameters ($Å^2 x\ 10^3$) for 202. The anisotropic displacement factor exponent takes the form: $-2\pi^2[\ h^2 a^{*2} U^{11} + ... + 2\ h\ k\ a^*\ b^*\ U^{12}\ ]$.

	U^{11}	U^{22}	U^{33}	U^{23}	U^{13}	U^{12}
C(1)	22(2)	35(3)	27(3)	0(2)	3(2)	-1(2)
C(2)	30(3)	28(3)	23(3)	-3(2)	3(2)	-3(2)
C(3)	25(3)	36(3)	32(3)	-2(2)	3(2)	5(2)
C(4)	30(3)	41(4)	32(3)	-9(2)	-1(2)	0(2)
C(5)	37(3)	33(3)	38(3)	0(3)	2(2)	3(3)
C(6)	26(3)	38(3)	23(3)	4(2)	-1(2)	3(2)
C(7)	30(3)	34(3)	22(3)	1(2)	-1(2)	2(2)
C(8)	26(3)	36(3)	33(3)	-3(2)	-1(2)	3(2)
C(9)	21(2)	38(3)	24(3)	-4(2)	-2(2)	0(2)
C(10)	27(2)	28(3)	28(3)	-3(2)	2(2)	-2(2)
C(11)	35(3)	54(4)	50(3)	-6(3)	-12(2)	-1(2)
C(12)	52(3)	35(3)	41(3)	10(2)	5(3)	12(3)
C(13)	32(3)	35(3)	38(3)	-2(2)	-7(2)	3(2)
C(14)	28(2)	44(3)	25(3)	-3(2)	3(2)	-4(2)
C(15)	32(3)	44(3)	31(3)	-3(2)	-2(2)	-6(2)
C(16)	55(3)	35(3)	41(3)	-5(3)	-4(3)	-6(3)
N(1)	48(3)	40(3)	77(4)	2(3)	3(3)	15(3)
O(1)	34(2)	35(2)	37(2)	1(2)	-14(2)	1(2)
O(2)	44(2)	35(2)	52(2)	-8(2)	-14(2)	1(2)
O(3)	43(2)	33(2)	36(2)	5(2)	-5(2)	7(2)
O(4)	38(2)	43(2)	56(2)	-7(2)	-18(2)	11(2)
O(5)	37(2)	43(2)	30(2)	-5(2)	-9(1)	-3(2)
O(6)	35(2)	52(2)	42(2)	-7(2)	3(2)	-16(2)
O(7)	35(2)	37(2)	44(2)	5(2)	0(2)	7(2)
O(8)	95(3)	69(3)	61(3)	17(2)	-4(2)	36(2)
O(9)	57(3)	57(3)	117(4)	12(2)	24(2)	25(2)

Table A1.2.5. Hydrogen coordinates (x 10^4) and isotropic displacement parameters (Å^{2}x 10^3) for 202.

	x	y	z	U(eq)
H(3)	9152	2288	5961	37
H(5)	8099	4935	4353	44
H(11A)	9841	3330	7891	70
H(11B)	10507	4289	7752	70
H(11C)	10537	3417	6464	70
H(12A)	6677	5617	3468	64
H(12B)	6272	5609	1635	64
H(12C)	7405	5514	2090	64
H(13A)	5157	620	1864	43
H(13B)	5728	929	357	43
H(14)	7358	-822	4416	39
H(16A)	6593	-2463	2939	66
H(16B)	6848	-2097	1208	66
H(16C)	5750	-2295	1563	66
H(6)	5116	-1199	3442	64

Table A1.2.6. Torsion angles [°] for 202.

O(1)-C(1)-C(2)-C(3)	1.0(6)
C(10)-C(1)-C(2)-C(3)	-177.8(4)
O(1)-C(1)-C(2)-C(7)	-178.8(4)
C(10)-C(1)-C(2)-C(7)	2.4(6)
C(7)-C(2)-C(3)-C(4)	-1.2(6)
C(1)-C(2)-C(3)-C(4)	179.0(4)
C(2)-C(3)-C(4)-O(2)	177.6(4)
C(2)-C(3)-C(4)-C(5)	-0.5(6)
O(2)-C(4)-C(5)-C(6)	-177.9(4)
C(3)-C(4)-C(5)-C(6)	0.4(7)
C(4)-C(5)-C(6)-O(3)	-179.2(4)

C(4)-C(5)-C(6)-C(7)	1.5(7)
C(3)-C(2)-C(7)-C(6)	3.0(6)
C(1)-C(2)-C(7)-C(6)	-177.3(4)
C(3)-C(2)-C(7)-C(8)	-178.2(4)
C(1)-C(2)-C(7)-C(8)	1.5(6)
O(3)-C(6)-C(7)-C(2)	177.6(4)
C(5)-C(6)-C(7)-C(2)	-3.1(6)
O(3)-C(6)-C(7)-C(8)	-1.1(6)
C(5)-C(6)-C(7)-C(8)	178.2(4)
C(2)-C(7)-C(8)-O(4)	173.5(4)
C(6)-C(7)-C(8)-O(4)	-7.8(7)
C(2)-C(7)-C(8)-C(9)	-6.0(6)
C(6)-C(7)-C(8)-C(9)	172.7(4)
O(4)-C(8)-C(9)-C(10)	-172.7(4)
C(7)-C(8)-C(9)-C(10)	6.8(6)
O(4)-C(8)-C(9)-C(13)	6.1(6)
C(7)-C(8)-C(9)-C(13)	-174.4(4)
C(8)-C(9)-C(10)-C(1)	-2.8(6)
C(13)-C(9)-C(10)-C(1)	178.4(4)
C(8)-C(9)-C(10)-C(14)	179.4(4)
C(13)-C(9)-C(10)-C(14)	0.6(6)
O(1)-C(1)-C(10)-C(9)	179.5(4)
C(2)-C(1)-C(10)-C(9)	-1.8(6)
O(1)-C(1)-C(10)-C(14)	-2.7(6)
C(2)-C(1)-C(10)-C(14)	176.1(3)
C(10)-C(9)-C(13)-O(5)	-15.0(6)
C(8)-C(9)-C(13)-O(5)	166.1(3)
C(9)-C(10)-C(14)-O(7)	101.4(4)
C(1)-C(10)-C(14)-O(7)	-76.5(4)
C(9)-C(10)-C(14)-C(15)	-15.8(5)
C(1)-C(10)-C(14)-C(15)	166.4(3)
O(7)-C(14)-C(15)-O(6)	170.7(3)
C(10)-C(14)-C(15)-O(6)	-73.6(4)

O(7)-C(14)-C(15)-O(5)	-70.9(4)
C(10)-C(14)-C(15)-O(5)	44.8(5)
O(7)-C(14)-C(15)-C(16)	47.2(5)
C(10)-C(14)-C(15)-C(16)	162.9(4)
C(5)-C(4)-O(2)-C(11)	-177.2(4)
C(3)-C(4)-O(2)-C(11)	4.6(6)
C(5)-C(6)-O(3)-C(12)	2.1(6)
C(7)-C(6)-O(3)-C(12)	-178.7(3)
C(9)-C(13)-O(5)-C(15)	47.5(5)
O(6)-C(15)-O(5)-C(13)	51.1(4)
C(16)-C(15)-O(5)-C(13)	174.3(3)
C(14)-C(15)-O(5)-C(13)	-62.7(4)
O(8)-N(1)-O(7)-C(14)	9.6(6)
O(9)-N(1)-O(7)-C(14)	-173.5(4)
C(10)-C(14)-O(7)-N(1)	122.3(3)
C(15)-C(14)-O(7)-N(1)	-117.3(4)

Symmetry transformations used to generate equivalent atoms

Table A1.2.7. Hydrogen bonds for 202.

D-H...A	d(D-H)	d(H...A)	d(D...A)	<(DHA)
O(6)-H(6)...O(4)#1	0.84	2.08	2.876(4)	159.2

Symmetry transformations used to generate equivalent atoms

A1.3 X-Ray crystallographic data for 5,7,10-Trimethoxy-3-methyl-1*H*-benzo[*g*]isochromene-6,9-dione 229

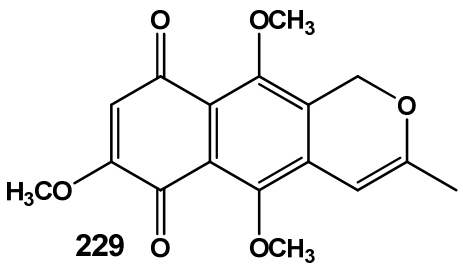

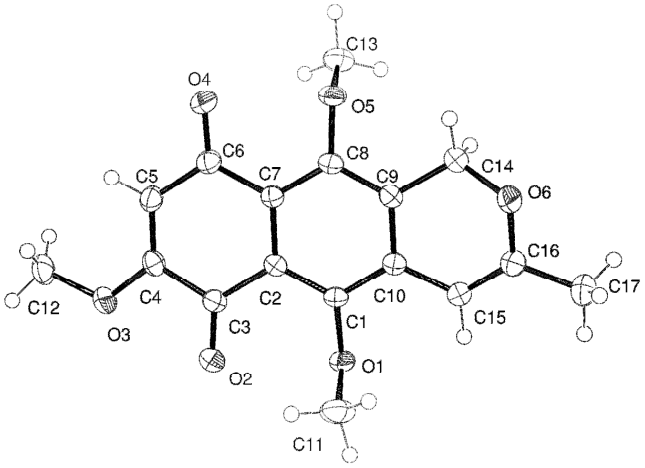

Table A1.3.1 Crystal data and structure refinement for 229.

Empirical formula	$C_{17}H_{16}O_6$	
Formula weight	316.30	
Temperature	173(2) K	
Wavelength	0.71073 Å	
Crystal system	Triclinic	
Space group	P-1	
Unit cell dimensions	a = 8.4652(2) Å	α = 111.5360(10)°.
	b = 9.6050(2) Å	β = 90.649(2)°.
	c = 9.6340(2) Å	γ = 98.224(2)°.
Volume	719.41(3) $Å^3$	
Z	2	
Density (calculated)	1.460 Mg/m^3	
Absorption coefficient	0.111 mm^{-1}	
F(000)	332	
Crystal size	0.41 x 0.40 x 0.06 mm^3	
Theta range for data collection	2.28 to 28.00°.	
Index ranges	-11<=h<=11, -12<=k<=12, -12<=l<=12	
Reflections collected	17177	

Independent reflections	3470 [R(int) = 0.0442]
Completeness to theta = 28.00°	100.0 %
Absorption correction	None
Refinement method	Full-matrix least-squares on F^2
Data / restraints / parameters	3470 / 0 / 212
Goodness-of-fit on F^2	1.017
Final R indices [I>2sigma(I)]	R1 = 0.0421, wR2 = 0.1150
R indices (all data)	R1 = 0.0665, wR2 = 0.1269
Largest diff. peak and hole	0.346 and -0.222 e.$Å^{-3}$

Table A1.3.2 Atomic coordinates (x 10^4) and equivalent isotropic displacement parameters ($Å^2$x 10^3) for 229. U(eq) is defined as one third of the trace of the orthogonalized U^{ij} tensor.

	x	y	z	U(eq)
C(1)	8145(2)	10799(1)	4342(2)	21(1)
C(2)	8556(2)	11047(2)	5838(2)	22(1)
C(3)	9696(2)	12417(2)	6782(2)	26(1)
C(4)	10179(2)	12539(2)	8322(2)	26(1)
C(5)	9570(2)	11512(2)	8882(2)	29(1)
C(6)	8411(2)	10186(2)	8018(2)	27(1)
C(7)	7885(2)	9988(2)	6463(2)	22(1)
C(8)	6756(2)	8747(2)	5582(2)	23(1)
C(9)	6338(2)	8544(2)	4117(2)	24(1)
C(10)	7024(2)	9540(2)	3473(2)	23(1)
C(11)	8143(2)	12946(2)	3688(2)	41(1)
C(12)	11724(2)	14075(2)	10558(2)	38(1)
C(13)	6881(2)	6482(2)	5961(2)	39(1)
C(14)	5227(2)	7148(2)	3121(2)	32(1)
C(15)	6547(2)	9218(2)	1916(2)	26(1)
C(16)	5255(2)	8193(2)	1244(2)	28(1)
C(17)	4544(2)	7821(2)	-294(2)	35(1)
O(1)	8903(1)	11684(1)	3630(1)	27(1)

O(2)	10215(2)	13438(1)	6378(1)	47(1)
O(3)	11257(1)	13790(1)	9025(1)	33(1)
O(4)	7923(1)	9276(1)	8587(1)	39(1)
O(5)	6009(1)	7698(1)	6117(1)	29(1)
O(6)	4369(1)	7398(1)	1966(1)	33(1)

Table A1.3.3. Bond lengths [Å] and angles [°] for 229.

C(1)-O(1)	1.3734(15)
C(1)-C(2)	1.4027(19)
C(1)-C(10)	1.4051(18)
C(2)-C(7)	1.4181(19)
C(2)-C(3)	1.4926(18)
C(3)-O(2)	1.2105(17)
C(3)-C(4)	1.492(2)
C(4)-C(5)	1.335(2)
C(4)-O(3)	1.3456(16)
C(5)-C(6)	1.4569(19)
C(5)-H(5)	0.9500
C(6)-O(4)	1.2209(17)
C(6)-C(7)	1.4932(19)
C(7)-C(8)	1.4025(18)
C(8)-O(5)	1.3742(16)
C(8)-C(9)	1.3863(19)
C(9)-C(10)	1.3874(19)
C(9)-C(14)	1.5088(18)
C(10)-C(15)	1.4553(18)
C(11)-O(1)	1.4360(19)
C(11)-H(11A)	0.9800
C(11)-H(11B)	0.9800
C(11)-H(11C)	0.9800
C(12)-O(3)	1.4392(18)
C(12)-H(12A)	0.9800

C(12)-H(12B)	0.9800
C(12)-H(12C)	0.9800
C(13)-O(5)	1.4318(18)
C(13)-H(13A)	0.9800
C(13)-H(13B)	0.9800
C(13)-H(13C)	0.9800
C(14)-O(6)	1.4322(18)
C(14)-H(14A)	0.9900
C(14)-H(14B)	0.9900
C(15)-C(16)	1.3391(19)
C(15)-H(15)	0.9500
C(16)-O(6)	1.3667(17)
C(16)-C(17)	1.488(2)
C(17)-H(17A)	0.9800
C(17)-H(17B)	0.9800
C(17)-H(17C)	0.9800
O(1)-C(1)-C(2)	122.15(11)
O(1)-C(1)-C(10)	117.14(12)
C(2)-C(1)-C(10)	120.49(12)
C(1)-C(2)-C(7)	119.87(12)
C(1)-C(2)-C(3)	120.59(12)
C(7)-C(2)-C(3)	119.54(12)
O(2)-C(3)-C(4)	118.76(12)
O(2)-C(3)-C(2)	123.71(13)
C(4)-C(3)-C(2)	117.51(12)
C(5)-C(4)-O(3)	126.44(13)
C(5)-C(4)-C(3)	122.16(12)
O(3)-C(4)-C(3)	111.39(12)
C(4)-C(5)-C(6)	122.05(13)
C(4)-C(5)-H(5)	119.0
C(6)-C(5)-H(5)	119.0
O(4)-C(6)-C(5)	118.76(13)
O(4)-C(6)-C(7)	122.70(12)

C(5)-C(6)-C(7)	118.54(12)
C(8)-C(7)-C(2)	118.73(12)
C(8)-C(7)-C(6)	121.23(12)
C(2)-C(7)-C(6)	120.02(12)
O(5)-C(8)-C(9)	117.13(11)
O(5)-C(8)-C(7)	122.45(12)
C(9)-C(8)-C(7)	120.41(12)
C(8)-C(9)-C(10)	121.55(12)
C(8)-C(9)-C(14)	120.85(12)
C(10)-C(9)-C(14)	117.38(12)
C(9)-C(10)-C(1)	118.87(12)
C(9)-C(10)-C(15)	117.89(12)
C(1)-C(10)-C(15)	123.24(12)
O(1)-C(11)-H(11A)	109.5
O(1)-C(11)-H(11B)	109.5
H(11A)-C(11)-H(11B)	109.5
O(1)-C(11)-H(11C)	109.5
H(11A)-C(11)-H(11C)	109.5
H(11B)-C(11)-H(11C)	109.5
O(3)-C(12)-H(12A)	109.5
O(3)-C(12)-H(12B)	109.5
H(12A)-C(12)-H(12B)	109.5
O(3)-C(12)-H(12C)	109.5
H(12A)-C(12)-H(12C)	109.5
H(12B)-C(12)-H(12C)	109.5
O(5)-C(13)-H(13A)	109.5
O(5)-C(13)-H(13B)	109.5
H(13A)-C(13)-H(13B)	109.5
O(5)-C(13)-H(13C)	109.5
H(13A)-C(13)-H(13C)	109.5
H(13B)-C(13)-H(13C)	109.5
O(6)-C(14)-C(9)	112.87(12)
O(6)-C(14)-H(14A)	109.0

C(9)-C(14)-H(14A)	109.0
O(6)-C(14)-H(14B)	109.0
C(9)-C(14)-H(14B)	109.0
H(14A)-C(14)-H(14B)	107.8
C(16)-C(15)-C(10)	120.03(13)
C(16)-C(15)-H(15)	120.0
C(10)-C(15)-H(15)	120.0
C(15)-C(16)-O(6)	122.01(13)
C(15)-C(16)-C(17)	126.53(14)
O(6)-C(16)-C(17)	111.38(12)
C(16)-C(17)-H(17A)	109.5
C(16)-C(17)-H(17B)	109.5
H(17A)-C(17)-H(17B)	109.5
C(16)-C(17)-H(17C)	109.5
H(17A)-C(17)-H(17C)	109.5
H(17B)-C(17)-H(17C)	109.5
C(1)-O(1)-C(11)	114.85(11)
C(4)-O(3)-C(12)	116.00(12)
C(8)-O(5)-C(13)	113.75(11)
C(16)-O(6)-C(14)	115.51(11)

Symmetry transformations used to generate equivalent atoms

Table A1.3.4. Anisotropic displacement parameters ($Å^2 x\ 10^3$) for 229. The anisotropic displacement factor exponent takes the form: $-2\pi^2[\ h^2 a^{*2} U^{11} + ... + 2\ h\ k\ a^*\ b^*\ U^{12}\ ]$.

	U^{11}	U^{22}	U^{33}	U^{23}	U^{13}	U^{12}
C(1)	21(1)	21(1)	25(1)	11(1)	5(1)	4(1)
C(2)	21(1)	20(1)	24(1)	8(1)	2(1)	3(1)
C(3)	28(1)	23(1)	27(1)	10(1)	2(1)	2(1)
C(4)	21(1)	24(1)	28(1)	6(1)	-2(1)	3(1)
C(5)	29(1)	32(1)	23(1)	9(1)	-2(1)	2(1)
C(6)	26(1)	29(1)	25(1)	11(1)	4(1)	3(1)
C(7)	22(1)	22(1)	23(1)	9(1)	2(1)	5(1)
C(8)	22(1)	22(1)	27(1)	11(1)	5(1)	2(1)
C(9)	23(1)	21(1)	26(1)	8(1)	1(1)	3(1)
C(10)	22(1)	22(1)	24(1)	9(1)	3(1)	5(1)
C(11)	39(1)	37(1)	58(1)	31(1)	-3(1)	4(1)
C(12)	41(1)	34(1)	32(1)	5(1)	-13(1)	-2(1)
C(13)	50(1)	28(1)	43(1)	19(1)	3(1)	4(1)
C(14)	36(1)	28(1)	29(1)	11(1)	-4(1)	-5(1)
C(15)	28(1)	26(1)	24(1)	11(1)	2(1)	3(1)
C(16)	27(1)	29(1)	27(1)	10(1)	2(1)	5(1)
C(17)	32(1)	41(1)	30(1)	10(1)	-3(1)	3(1)
O(1)	28(1)	27(1)	28(1)	15(1)	3(1)	0(1)
O(2)	65(1)	33(1)	36(1)	17(1)	-12(1)	-19(1)
O(3)	35(1)	28(1)	31(1)	9(1)	-8(1)	-5(1)
O(4)	48(1)	42(1)	29(1)	20(1)	-3(1)	-10(1)
O(5)	29(1)	28(1)	33(1)	17(1)	2(1)	-2(1)
O(6)	31(1)	35(1)	30(1)	13(1)	-5(1)	-6(1)

Table A1.3.5. Hydrogen coordinates (x 10^4) and isotropic displacement parameters (Å^{2}x 10^3) for 229.

	x	y	z	U(eq)
H(5)	9903	11649	9875	34
H(11A)	7006	12592	3366	62
H(11B)	8652	13414	3023	62
H(11C)	8251	13694	4715	62
H(12A)	10780	14188	11146	58
H(12B)	12506	15007	10964	58
H(12C)	12204	13223	10608	58
H(13A)	6933	5880	4897	58
H(13B)	6339	5836	6453	58
H(13C)	7967	6899	6426	58
H(14A)	5858	6323	2657	38
H(14B)	4451	6814	3741	38
H(15)	7153	9735	1377	31
H(17A)	5238	8360	-803	53
H(17B)	3485	8131	-236	53
H(17C)	4439	6726	-854	53

Table A1.3.6. Torsion angles [°] for 229.

O(1)-C(1)-C(2)-C(7)	-171.86(11)
C(10)-C(1)-C(2)-C(7)	2.6(2)
O(1)-C(1)-C(2)-C(3)	8.1(2)
C(10)-C(1)-C(2)-C(3)	-177.50(12)
C(1)-C(2)-C(3)-O(2)	6.6(2)
C(7)-C(2)-C(3)-O(2)	-173.48(14)
C(1)-C(2)-C(3)-C(4)	-175.07(12)
C(7)-C(2)-C(3)-C(4)	4.85(19)
O(2)-C(3)-C(4)-C(5)	175.25(14)
C(2)-C(3)-C(4)-C(5)	-3.2(2)

O(2)-C(3)-C(4)-O(3)	-4.20(19)
C(2)-C(3)-C(4)-O(3)	177.38(11)
O(3)-C(4)-C(5)-C(6)	-179.57(13)
C(3)-C(4)-C(5)-C(6)	1.1(2)
C(4)-C(5)-C(6)-O(4)	178.71(14)
C(4)-C(5)-C(6)-C(7)	-0.5(2)
C(1)-C(2)-C(7)-C(8)	-3.19(19)
C(3)-C(2)-C(7)-C(8)	176.89(12)
C(1)-C(2)-C(7)-C(6)	175.42(12)
C(3)-C(2)-C(7)-C(6)	-4.50(19)
O(4)-C(6)-C(7)-C(8)	1.7(2)
C(5)-C(6)-C(7)-C(8)	-179.10(12)
O(4)-C(6)-C(7)-C(2)	-176.89(13)
C(5)-C(6)-C(7)-C(2)	2.32(19)
C(2)-C(7)-C(8)-O(5)	-177.72(11)
C(6)-C(7)-C(8)-O(5)	3.7(2)
C(2)-C(7)-C(8)-C(9)	1.6(2)
C(6)-C(7)-C(8)-C(9)	-176.97(12)
O(5)-C(8)-C(9)-C(10)	179.99(11)
C(7)-C(8)-C(9)-C(10)	0.6(2)
O(5)-C(8)-C(9)-C(14)	-5.57(19)
C(7)-C(8)-C(9)-C(14)	175.05(12)
C(8)-C(9)-C(10)-C(1)	-1.3(2)
C(14)-C(9)-C(10)-C(1)	-175.89(12)
C(8)-C(9)-C(10)-C(15)	178.38(12)
C(14)-C(9)-C(10)-C(15)	3.76(19)
O(1)-C(1)-C(10)-C(9)	174.37(11)
C(2)-C(1)-C(10)-C(9)	-0.3(2)
O(1)-C(1)-C(10)-C(15)	-5.26(19)
C(2)-C(1)-C(10)-C(15)	-179.97(12)
C(8)-C(9)-C(14)-O(6)	153.50(13)
C(10)-C(9)-C(14)-O(6)	-31.84(18)
C(9)-C(10)-C(15)-C(16)	13.9(2)

C(1)-C(10)-C(15)-C(16)	-166.46(13)
C(10)-C(15)-C(16)-O(6)	-1.4(2)
C(10)-C(15)-C(16)-C(17)	175.08(13)
C(2)-C(1)-O(1)-C(11)	-92.92(15)
C(10)-C(1)-O(1)-C(11)	92.46(15)
C(5)-C(4)-O(3)-C(12)	-3.5(2)
C(3)-C(4)-O(3)-C(12)	175.90(12)
C(9)-C(8)-O(5)-C(13)	93.52(15)
C(7)-C(8)-O(5)-C(13)	-87.12(16)
C(15)-C(16)-O(6)-C(14)	-28.69(19)
C(17)-C(16)-O(6)-C(14)	154.31(13)
C(9)-C(14)-O(6)-C(16)	44.03(17)

Symmetry transformations used to generate equivalent atoms

A1.4 X-Ray crystallographic data for (3,6-Dimethoxy-9-methyl-10,13-dioxatricyclo[7.3.1.$0^{2,7}$]trideca-2,4,6-trien-11-yl)methanol 254

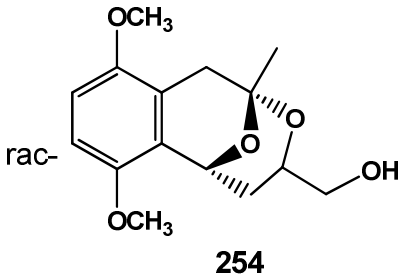

254

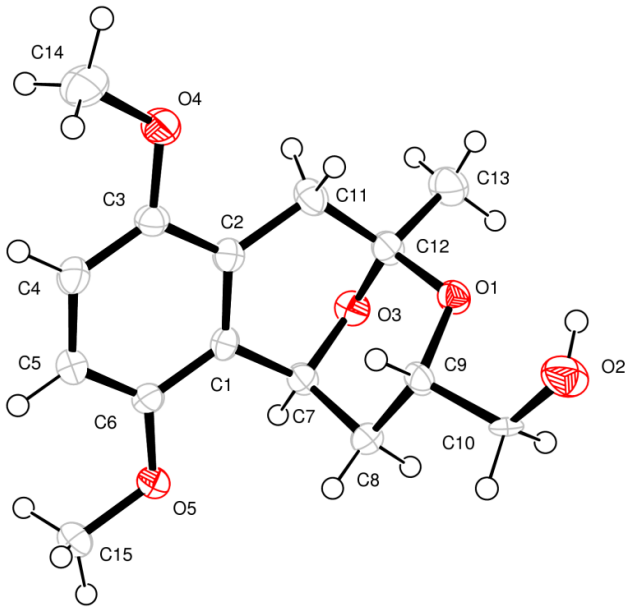

Table A1.4.1 Crystal data and structure refinement for 254.

Empirical formula	$C_{15}H_{20}O_5$
Formula weight	280.31

Temperature	173(2) K	
Wavelength	0.71073 Å	
Crystal system	Monoclinic	
Space group	P2(1)/c	
Unit cell dimensions	a = 9.8703(4) Å	α = 90°.
	b = 20.4560(7) Å	β = 93.068(2)°.
	c = 6.8483(3) Å	γ = 90°.
Volume	1380.74(9) $Å^3$	
Z	4	
Density (calculated)	1.348 Mg/m^3	
Absorption coefficient	0.101 mm^{-1}	
F(000)	600	
Crystal size	0.48 x 0.15 x 0.05 mm^3	
Theta range for data collection	1.99 to 26.00°.	
Index ranges	-12<=h<=8, -25<=k<=25, -8<=l<=8	
Reflections collected	15409	
Independent reflections	2722 [R(int) = 0.0789]	
Completeness to theta = 26.00°	100.0 %	
Absorption correction	None	
Refinement method	Full-matrix least-squares on F^2	
Data / restraints / parameters	2722 / 0 / 224	
Goodness-of-fit on F^2	0.827	
Final R indices [I>2sigma(I)]	R1 = 0.0400, wR2 = 0.0723	
R indices (all data)	R1 = 0.0873, wR2 = 0.0831	
Largest diff. peak and hole	0.167 and -0.185 e.$Å^{-3}$	

Table A1.4.2 Atomic coordinates (x 10^4) and equivalent isotropic displacement parameters ($Å^2$x 10^3) for 254. U(eq) is defined as one third of the trace of the orthogonalized U^{ij} tensor.

	x	y	z	U(eq)
C(1)	2376(2)	3662(1)	7657(3)	22(1)
C(2)	3713(2)	3708(1)	8381(3)	23(1)
C(3)	4721(2)	3369(1)	7428(3)	24(1)
C(4)	4394(2)	3000(1)	5788(3)	28(1)
C(5)	3055(2)	2959(1)	5056(3)	29(1)
C(6)	2054(2)	3288(1)	5985(3)	25(1)
C(7)	1280(2)	4033(1)	8642(3)	25(1)
C(8)	948(2)	4682(1)	7615(3)	27(1)
C(9)	2172(7)	5138(3)	7920(9)	24(1)
C(10)	1831(5)	5833(4)	7439(12)	22(2)
O(1)	2635(5)	5148(2)	9972(7)	24(1)
O(2)	2872(8)	6289(5)	7642(12)	39(1)
C(9A)	1745(12)	5246(5)	8580(20)	33(2)
C(10A)	1838(18)	5793(9)	7180(30)	67(6)
O(1A)	3023(9)	5027(4)	9301(15)	29(2)
O(2A)	2446(17)	6368(9)	8120(30)	52(3)
C(11)	4058(2)	4109(1)	10182(3)	29(1)
C(12)	2895(2)	4524(1)	10854(3)	26(1)
C(13)	3116(2)	4725(1)	12964(3)	41(1)
C(14)	7096(2)	3152(1)	7249(3)	44(1)
C(15)	319(2)	2887(1)	3721(3)	38(1)
O(3)	1665(1)	4162(1)	10667(2)	28(1)
O(4)	6013(1)	3433(1)	8280(2)	34(1)
O(5)	693(1)	3283(1)	5389(2)	32(1)

Table A1.4.3. Bond lengths [Å] and angles [°] for 254.

C(1)-C(2)	1.388(2)
C(1)-C(6)	1.399(2)
C(1)-C(7)	1.509(2)
C(2)-C(3)	1.402(2)
C(2)-C(11)	1.505(2)
C(3)-C(4)	1.377(2)
C(3)-O(4)	1.380(2)
C(4)-C(5)	1.391(2)
C(4)-H(4)	0.9500
C(5)-C(6)	1.379(2)
C(5)-H(5)	0.9500
C(6)-O(5)	1.383(2)
C(7)-O(3)	1.4427(19)
C(7)-C(8)	1.530(2)
C(7)-H(7)	1.0000
C(8)-C(9A)	1.527(11)
C(8)-C(9)	1.531(6)
C(8)-H(8A)	0.9900
C(8)-H(8B)	0.9900
C(8)-H(8C)	0.9900
C(8)-H(8D)	0.9900
C(9)-O(1)	1.454(8)
C(9)-C(10)	1.494(10)
C(9)-H(9)	1.0000
C(10)-O(2)	1.390(12)
C(10)-H(10A)	0.9900
C(10)-H(10B)	0.9900
O(1)-C(12)	1.429(4)
O(2)-H(2)	0.8400
C(9A)-O(1A)	1.402(16)
C(9A)-C(10A)	1.48(2)

C(9A)-H(9A)	1.0000
C(10A)-O(2A)	1.46(3)
C(10A)-H(10C)	0.9900
C(10A)-H(10D)	0.9900
O(1A)-C(12)	1.491(8)
O(2A)-H(2A)	0.8400
C(11)-C(12)	1.518(2)
C(11)-H(11A)	0.9900
C(11)-H(11B)	0.9900
C(12)-O(3)	1.421(2)
C(12)-C(13)	1.508(2)
C(13)-H(13A)	0.9800
C(13)-H(13B)	0.9800
C(13)-H(13C)	0.9800
C(14)-O(4)	1.432(2)
C(14)-H(14A)	0.9800
C(14)-H(14B)	0.9800
C(14)-H(14C)	0.9800
C(15)-O(5)	1.4333(19)
C(15)-H(15A)	0.9800
C(15)-H(15B)	0.9800
C(15)-H(15C)	0.9800
C(2)-C(1)-C(6)	119.91(17)
C(2)-C(1)-C(7)	119.80(16)
C(6)-C(1)-C(7)	120.26(16)
C(1)-C(2)-C(3)	119.02(17)
C(1)-C(2)-C(11)	119.91(16)
C(3)-C(2)-C(11)	121.06(15)
C(4)-C(3)-O(4)	124.58(17)
C(4)-C(3)-C(2)	120.63(17)
O(4)-C(3)-C(2)	114.78(16)
C(3)-C(4)-C(5)	120.27(17)
C(3)-C(4)-H(4)	119.9

C(5)-C(4)-H(4)	119.9
C(6)-C(5)-C(4)	119.59(17)
C(6)-C(5)-H(5)	120.2
C(4)-C(5)-H(5)	120.2
C(5)-C(6)-O(5)	124.65(16)
C(5)-C(6)-C(1)	120.57(17)
O(5)-C(6)-C(1)	114.79(16)
O(3)-C(7)-C(1)	111.30(14)
O(3)-C(7)-C(8)	108.75(14)
C(1)-C(7)-C(8)	111.82(15)
O(3)-C(7)-H(7)	108.3
C(1)-C(7)-H(7)	108.3
C(8)-C(7)-H(7)	108.3
C(9A)-C(8)-C(7)	111.3(4)
C(7)-C(8)-C(9)	108.5(2)
C(9A)-C(8)-H(8A)	85.9
C(7)-C(8)-H(8A)	110.0
C(9)-C(8)-H(8A)	110.0
C(9A)-C(8)-H(8B)	127.7
C(7)-C(8)-H(8B)	110.0
C(9)-C(8)-H(8B)	110.0
H(8A)-C(8)-H(8B)	108.4
C(9A)-C(8)-H(8C)	109.4
C(7)-C(8)-H(8C)	109.4
C(9)-C(8)-H(8C)	87.6
H(8A)-C(8)-H(8C)	128.2
C(9A)-C(8)-H(8D)	109.5
C(7)-C(8)-H(8D)	109.3
C(9)-C(8)-H(8D)	130.8
H(8B)-C(8)-H(8D)	85.1
H(8C)-C(8)-H(8D)	108.0
O(1)-C(9)-C(10)	104.8(6)
O(1)-C(9)-C(8)	110.2(5)

C(10)-C(9)-C(8)	112.5(5)
O(1)-C(9)-H(9)	109.7
C(10)-C(9)-H(9)	109.7
C(8)-C(9)-H(9)	109.7
O(2)-C(10)-C(9)	117.4(6)
O(2)-C(10)-H(10A)	107.9
C(9)-C(10)-H(10A)	107.9
O(2)-C(10)-H(10B)	107.9
C(9)-C(10)-H(10B)	107.9
H(10A)-C(10)-H(10B)	107.2
C(12)-O(1)-C(9)	115.8(4)
O(1A)-C(9A)-C(10A)	112.5(12)
O(1A)-C(9A)-C(8)	110.2(10)
C(10A)-C(9A)-C(8)	109.7(12)
O(1A)-C(9A)-H(9A)	108.1
C(10A)-C(9A)-H(9A)	108.1
C(8)-C(9A)-H(9A)	108.1
O(2A)-C(10A)-C(9A)	111.2(17)
O(2A)-C(10A)-H(10C)	109.4
C(9A)-C(10A)-H(10C)	109.4
O(2A)-C(10A)-H(10D)	109.4
C(9A)-C(10A)-H(10D)	109.4
H(10C)-C(10A)-H(10D)	108.0
C(9A)-O(1A)-C(12)	111.2(10)
C(10A)-O(2A)-H(2A)	109.5
C(2)-C(11)-C(12)	114.29(15)
C(2)-C(11)-H(11A)	108.7
C(12)-C(11)-H(11A)	108.7
C(2)-C(11)-H(11B)	108.7
C(12)-C(11)-H(11B)	108.7
H(11A)-C(11)-H(11B)	107.6
O(3)-C(12)-O(1)	107.1(2)
O(3)-C(12)-O(1A)	113.6(3)

O(3)-C(12)-C(13)	107.94(15)
O(1)-C(12)-C(13)	100.1(2)
O(1A)-C(12)-C(13)	118.8(4)
O(3)-C(12)-C(11)	109.76(14)
O(1)-C(12)-C(11)	119.4(3)
O(1A)-C(12)-C(11)	94.3(5)
C(13)-C(12)-C(11)	111.72(15)
C(12)-C(13)-H(13A)	109.5
C(12)-C(13)-H(13B)	109.5
H(13A)-C(13)-H(13B)	109.5
C(12)-C(13)-H(13C)	109.5
H(13A)-C(13)-H(13C)	109.5
H(13B)-C(13)-H(13C)	109.5
O(4)-C(14)-H(14A)	109.5
O(4)-C(14)-H(14B)	109.5
H(14A)-C(14)-H(14B)	109.5
O(4)-C(14)-H(14C)	109.5
H(14A)-C(14)-H(14C)	109.5
H(14B)-C(14)-H(14C)	109.5
O(5)-C(15)-H(15A)	109.5
O(5)-C(15)-H(15B)	109.5
H(15A)-C(15)-H(15B)	109.5
O(5)-C(15)-H(15C)	109.5
H(15A)-C(15)-H(15C)	109.5
H(15B)-C(15)-H(15C)	109.5
C(12)-O(3)-C(7)	111.23(13)
C(3)-O(4)-C(14)	116.79(15)
C(6)-O(5)-C(15)	116.37(14)

Symmetry transformations used to generate equivalent atoms

Table A1.4.4. Anisotropic displacement parameters ($Å^2 x\ 10^3$) for 254. The anisotropic displacement factor exponent takes the form: $-2\pi^2[\ h^2 a^{*2} U^{11} + ... + 2\ h\ k\ a^*\ b^*\ U^{12}\ ]$.

	U^{11}	U^{22}	U^{33}	U^{23}	U^{13}	U^{12}
C(1)	25(1)	16(1)	25(1)	1(1)	3(1)	1(1)
C(2)	24(1)	20(1)	25(1)	1(1)	3(1)	-2(1)
C(3)	21(1)	25(1)	26(1)	0(1)	-1(1)	-1(1)
C(4)	28(1)	28(1)	28(1)	-4(1)	5(1)	5(1)
C(5)	32(1)	26(1)	28(1)	-6(1)	-2(1)	2(1)
C(6)	25(1)	21(1)	29(1)	0(1)	-4(1)	2(1)
C(7)	25(1)	25(1)	25(1)	-3(1)	0(1)	-1(1)
C(8)	24(1)	28(1)	28(1)	-4(1)	-2(1)	5(1)
C(9)	32(3)	23(2)	16(3)	-4(2)	-1(2)	1(2)
C(10)	15(3)	26(4)	24(3)	-1(2)	-11(2)	5(2)
O(1)	30(2)	24(2)	19(2)	0(1)	0(2)	-1(1)
O(2)	42(3)	35(3)	39(3)	7(2)	-8(2)	-11(2)
C(9A)	35(6)	31(5)	35(6)	-3(4)	3(5)	10(4)
C(10A)	139(14)	25(9)	39(8)	-2(6)	16(8)	-23(8)
O(1A)	33(4)	24(3)	28(5)	1(3)	1(3)	-6(3)
O(2A)	72(9)	29(5)	53(8)	9(5)	-26(6)	-12(6)
C(11)	25(1)	31(1)	30(1)	-7(1)	4(1)	-5(1)
C(12)	33(1)	22(1)	23(1)	2(1)	-1(1)	-3(1)
C(13)	39(1)	52(1)	32(1)	-14(1)	0(1)	7(1)
C(14)	24(1)	60(2)	48(1)	-7(1)	5(1)	6(1)
C(15)	40(1)	30(1)	42(1)	-10(1)	-14(1)	1(1)
O(3)	27(1)	31(1)	25(1)	0(1)	5(1)	-1(1)
O(4)	22(1)	44(1)	35(1)	-11(1)	2(1)	2(1)
O(5)	28(1)	31(1)	37(1)	-10(1)	-9(1)	3(1)

Table A1.4.5. Hydrogen coordinates (x 10^4) and isotropic displacement parameters (Å^{2}x 10^3) for 254.

	x	y	z	U(eq)
H(4)	5086	2773	5153	34
H(5)	2831	2704	3923	34
H(7)	440	3759	8588	30
H(8A)	140	4883	8167	32
H(8B)	749	4607	6201	32
H(8C)	1169	4650	6226	32
H(8D)	-36	4770	7660	32
H(9)	2923	4986	7107	28
H(10A)	1458	5849	6069	27
H(10B)	1098	5972	8281	27
H(2)	3261	6254	8758	59
H(9A)	1236	5403	9714	40
H(10C)	2391	5655	6084	81
H(10D)	918	5903	6626	81
H(2A)	2900	6255	9132	78
H(11A)	4828	4400	9918	34
H(11B)	4360	3811	11258	34
H(13A)	2360	5001	13336	61
H(13B)	3967	4971	13134	61
H(13C)	3165	4335	13794	61
H(14A)	7008	2675	7244	66
H(14B)	7968	3275	7898	66
H(14C)	7053	3313	5900	66
H(15A)	779	3048	2582	56
H(15B)	-666	2909	3454	56
H(15C)	587	2433	3986	56

Table A1.4.6. Torsion angles [°] for 254.

C(6)-C(1)-C(2)-C(3)	-0.8(3)
C(7)-C(1)-C(2)-C(3)	-178.94(16)
C(6)-C(1)-C(2)-C(11)	-179.87(16)
C(7)-C(1)-C(2)-C(11)	2.0(3)
C(1)-C(2)-C(3)-C(4)	0.6(3)
C(11)-C(2)-C(3)-C(4)	179.61(17)
C(1)-C(2)-C(3)-O(4)	-178.65(15)
C(11)-C(2)-C(3)-O(4)	0.4(2)
O(4)-C(3)-C(4)-C(5)	179.02(17)
C(2)-C(3)-C(4)-C(5)	-0.1(3)
C(3)-C(4)-C(5)-C(6)	-0.1(3)
C(4)-C(5)-C(6)-O(5)	179.87(16)
C(4)-C(5)-C(6)-C(1)	-0.1(3)
C(2)-C(1)-C(6)-C(5)	0.6(3)
C(7)-C(1)-C(6)-C(5)	178.73(16)
C(2)-C(1)-C(6)-O(5)	-179.41(15)
C(7)-C(1)-C(6)-O(5)	-1.3(2)
C(2)-C(1)-C(7)-O(3)	-25.0(2)
C(6)-C(1)-C(7)-O(3)	156.91(15)
C(2)-C(1)-C(7)-C(8)	96.89(19)
C(6)-C(1)-C(7)-C(8)	-81.2(2)
O(3)-C(7)-C(8)-C(9A)	28.5(7)
C(1)-C(7)-C(8)-C(9A)	-94.8(7)
O(3)-C(7)-C(8)-C(9)	55.4(3)
C(1)-C(7)-C(8)-C(9)	-67.9(3)
C(9A)-C(8)-C(9)-O(1)	52.4(11)
C(7)-C(8)-C(9)-O(1)	-48.5(7)
C(9A)-C(8)-C(9)-C(10)	-64.2(13)
C(7)-C(8)-C(9)-C(10)	-165.0(5)
O(1)-C(9)-C(10)-O(2)	61.0(11)
C(8)-C(9)-C(10)-O(2)	-179.3(5)

C(10)-C(9)-O(1)-C(12)	173.7(3)
C(8)-C(9)-O(1)-C(12)	52.5(9)
C(7)-C(8)-C(9A)-O(1A)	33.5(15)
C(9)-C(8)-C(9A)-O(1A)	-55.0(13)
C(7)-C(8)-C(9A)-C(10A)	157.8(10)
C(9)-C(8)-C(9A)-C(10A)	69.3(16)
O(1A)-C(9A)-C(10A)-O(2A)	-64(2)
C(8)-C(9A)-C(10A)-O(2A)	173.1(9)
C(10A)-C(9A)-O(1A)-C(12)	174.4(10)
C(8)-C(9A)-O(1A)-C(12)	-62.9(17)
C(1)-C(2)-C(11)-C(12)	-9.6(2)
C(3)-C(2)-C(11)-C(12)	171.35(16)
C(9)-O(1)-C(12)-O(3)	-58.8(7)
C(9)-O(1)-C(12)-O(1A)	50.1(9)
C(9)-O(1)-C(12)-C(13)	-171.3(6)
C(9)-O(1)-C(12)-C(11)	66.6(6)
C(9A)-O(1A)-C(12)-O(3)	27.5(13)
C(9A)-O(1A)-C(12)-O(1)	-53.1(12)
C(9A)-O(1A)-C(12)-C(13)	-101.1(10)
C(9A)-O(1A)-C(12)-C(11)	141.2(11)
C(2)-C(11)-C(12)-O(3)	40.6(2)
C(2)-C(11)-C(12)-O(1)	-83.5(3)
C(2)-C(11)-C(12)-O(1A)	-76.3(3)
C(2)-C(11)-C(12)-C(13)	160.30(16)
O(1)-C(12)-O(3)-C(7)	64.7(3)
O(1A)-C(12)-O(3)-C(7)	37.7(5)
C(13)-C(12)-O(3)-C(7)	171.64(14)
C(11)-C(12)-O(3)-C(7)	-66.37(17)
C(1)-C(7)-O(3)-C(12)	58.11(18)
C(8)-C(7)-O(3)-C(12)	-65.51(17)
C(4)-C(3)-O(4)-C(14)	7.1(3)
C(2)-C(3)-O(4)-C(14)	-173.78(16)
C(5)-C(6)-O(5)-C(15)	2.1(3)

C(1)-C(6)-O(5)-C(15) -177.89(15)

Symmetry transformations used to generate equivalent atoms

B1 Selected NMR Spectra of Important End Products

B1.1. (3-Formyl-4-hydroxy-6,8-dimethoxynaphthalene-2-yl)methyl acetate 201

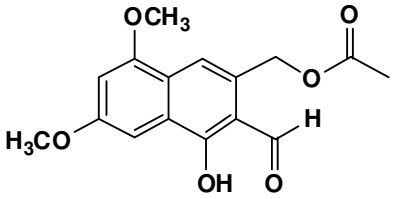

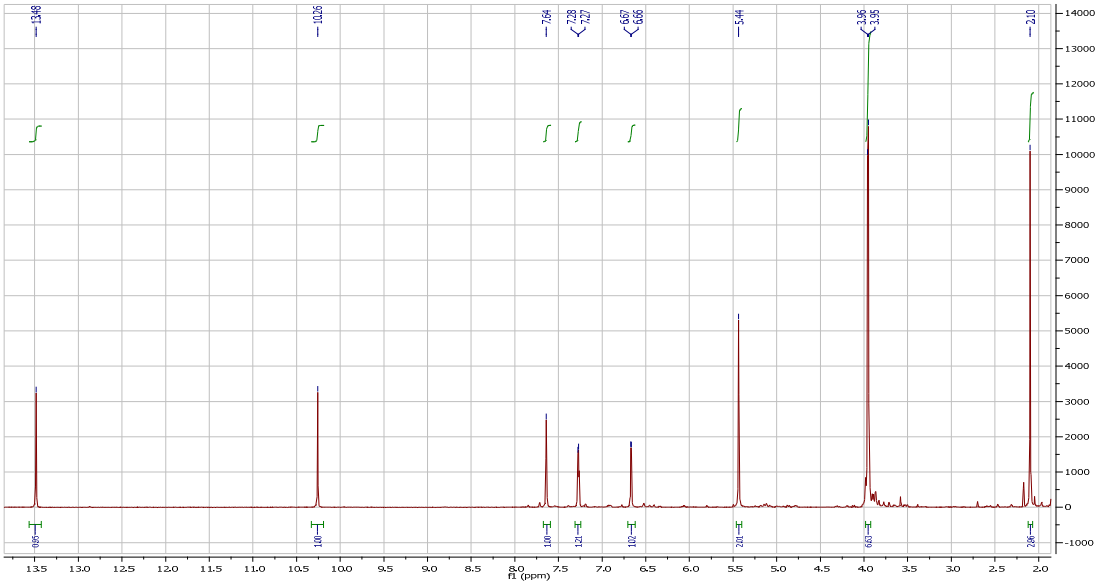

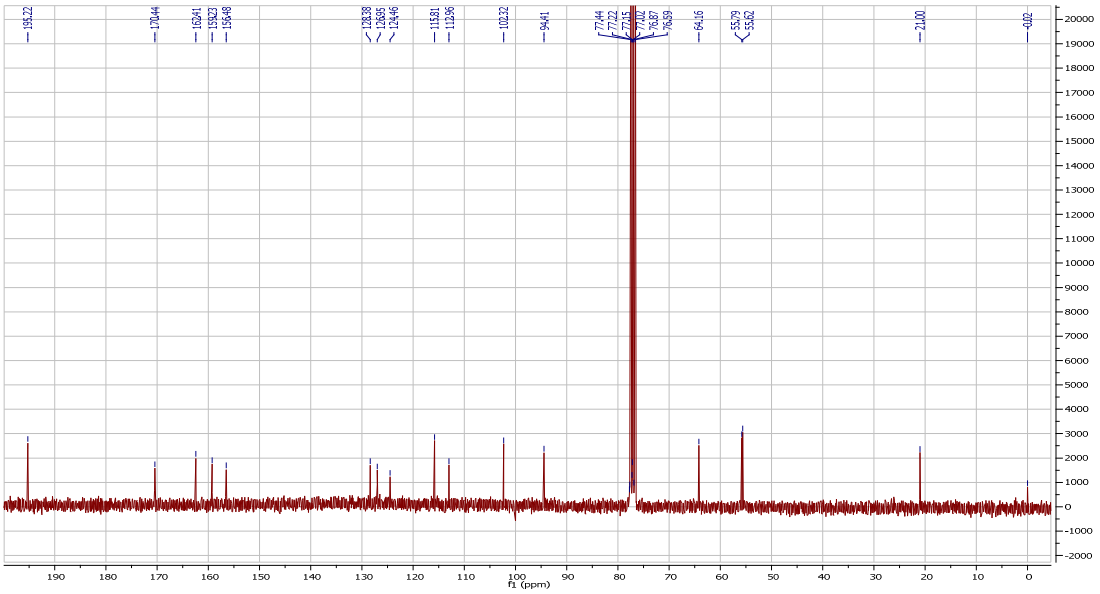

B1.2. (3R,4R) 3-Hydroxy-7,9-dimethoxy-3-methyl-5,10-dioxo-3,4,5,10-tetrahydro-1*H*-benzo[*g*]isochromen-4-yl nitrate 202

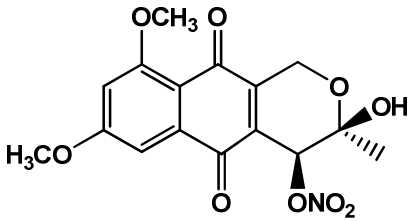

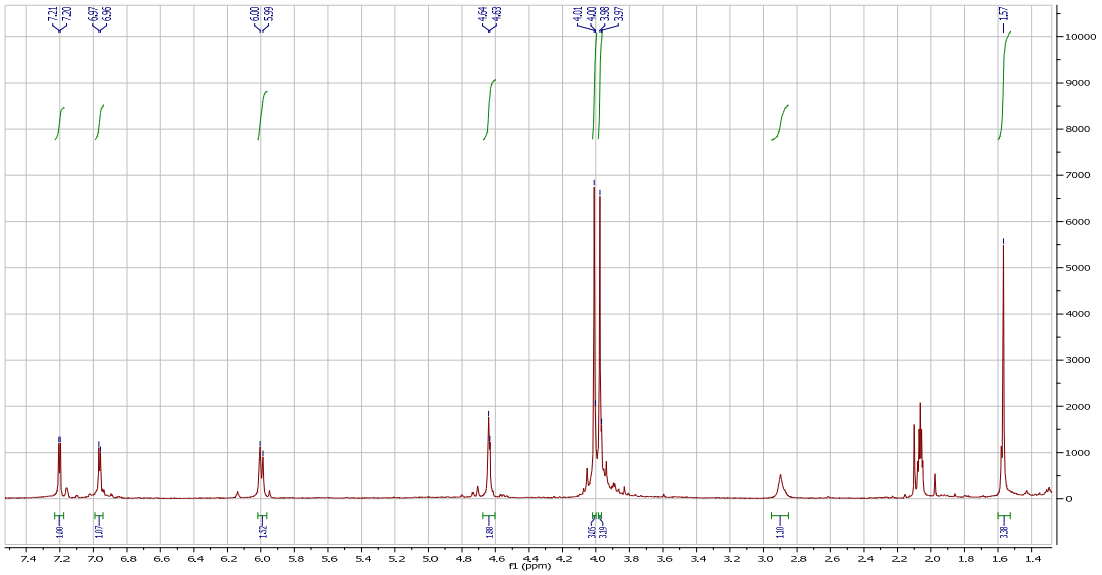

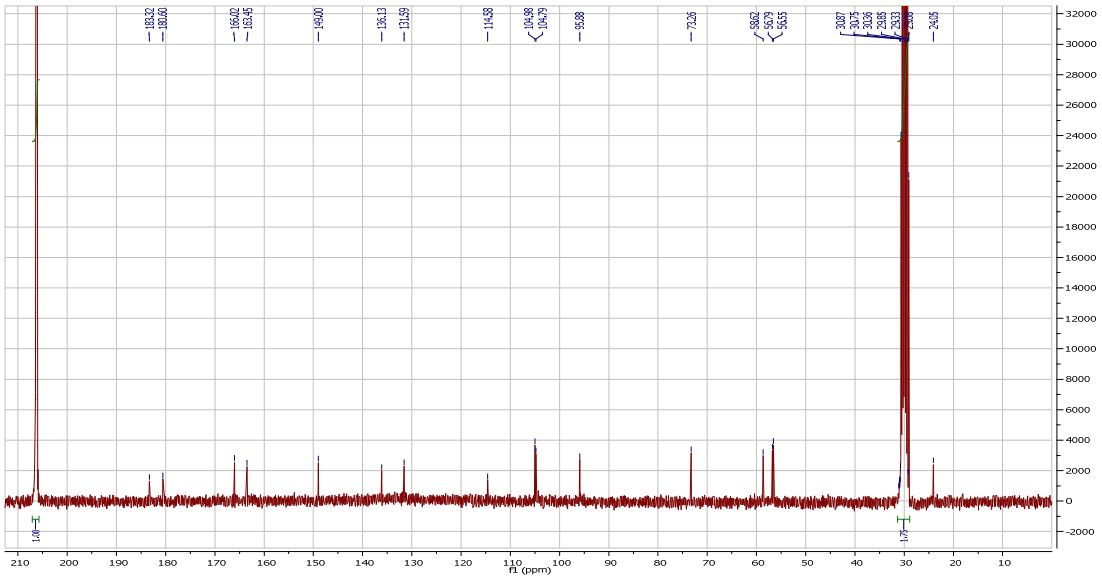

B1.3. 7,9-Dimethoxy-3-methyl-1*H*-benzo[*g*]isochromene-5,10-dione 31

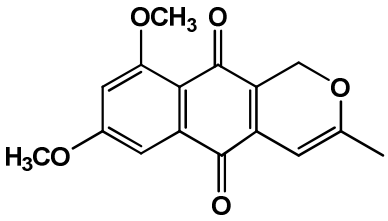

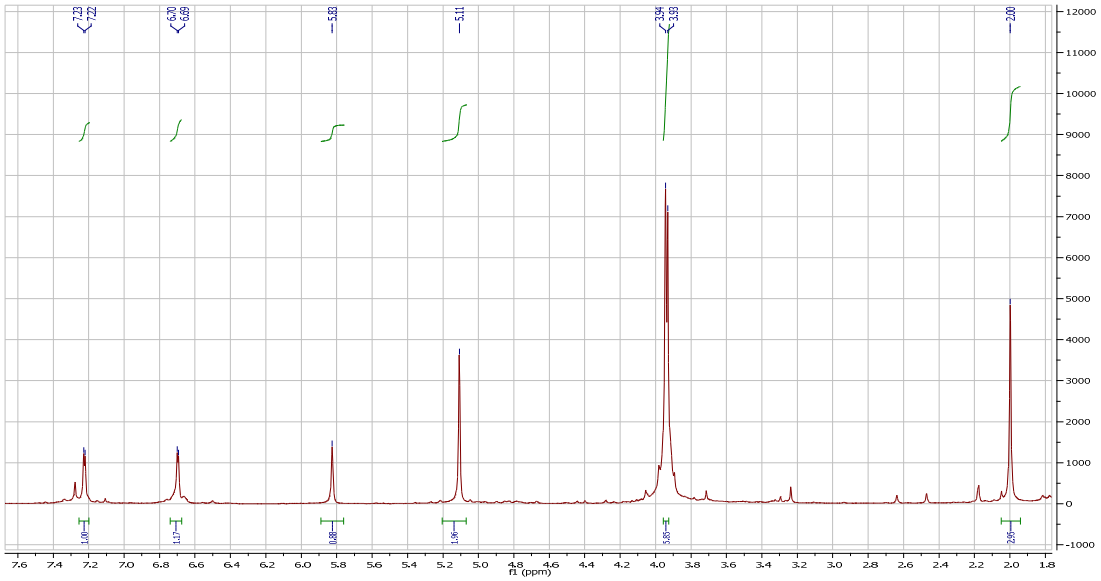

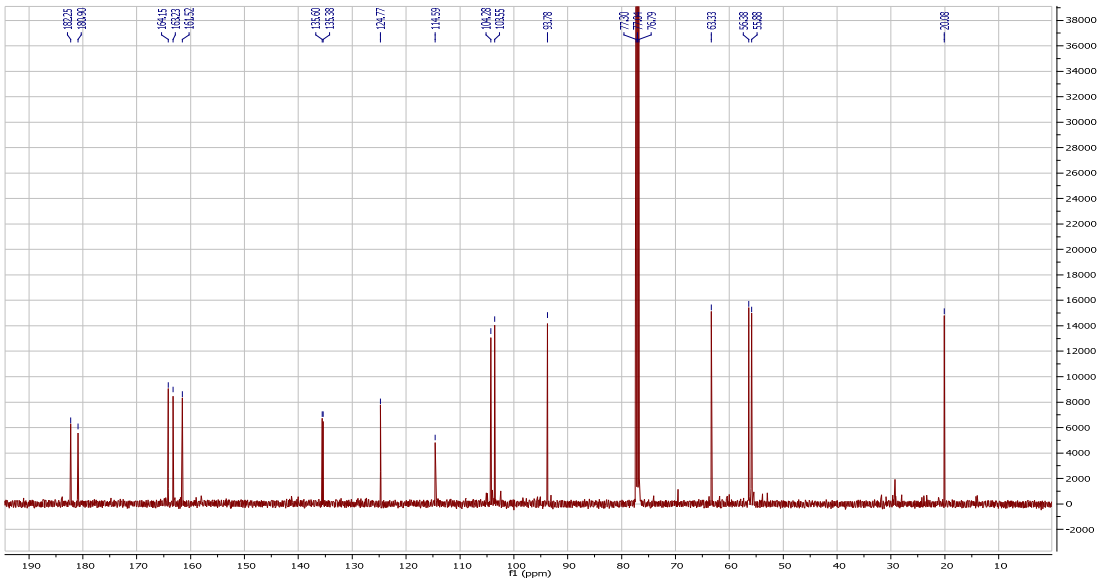

B1.4. 5,7,10-Trimethoxy-3-methyl-1*H*-benzo[*g*]isochromene-6,9-dione 229

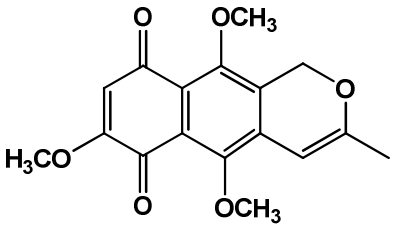

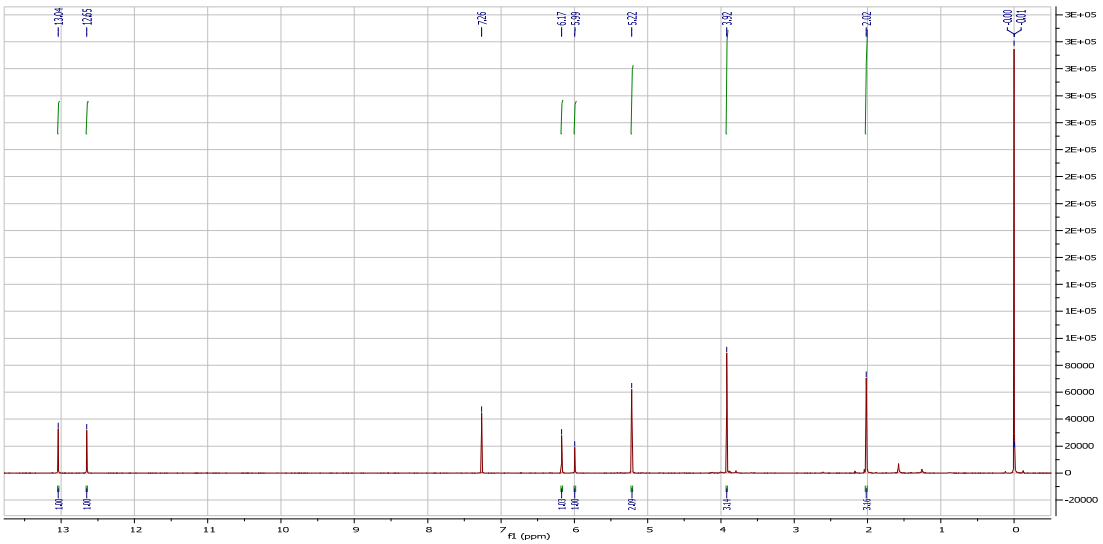

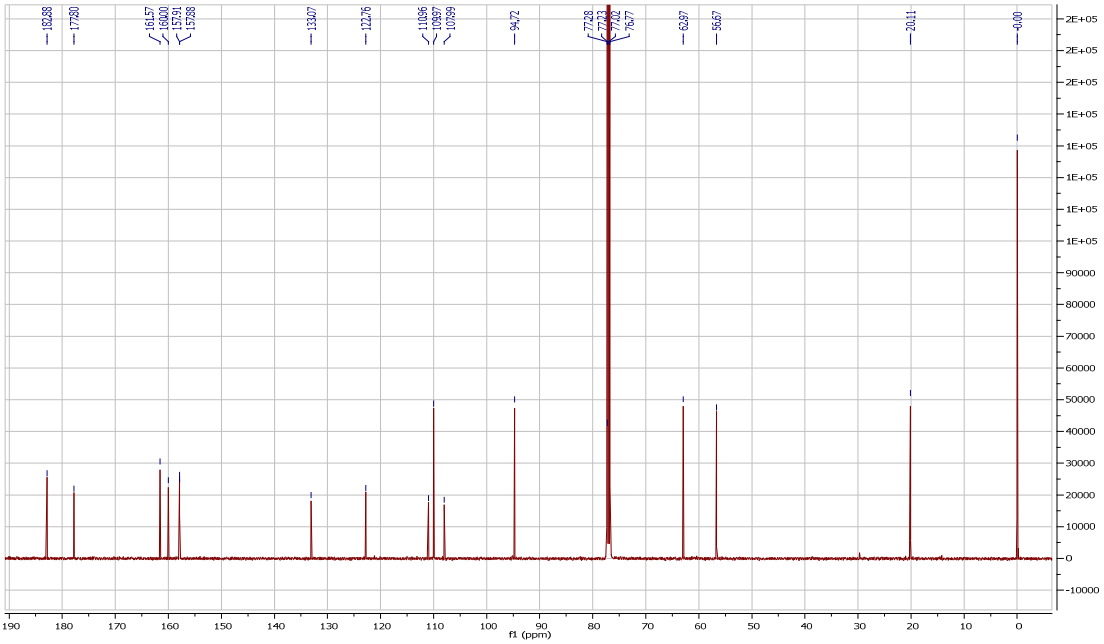

B1.5. 5,9,10-trimethoxy-3-methyl-1*H*-benzo[*g*]isochromene-6,7-dione 230

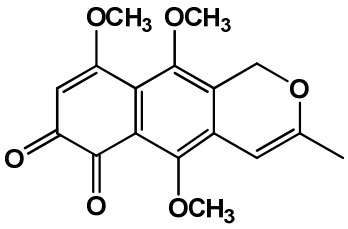

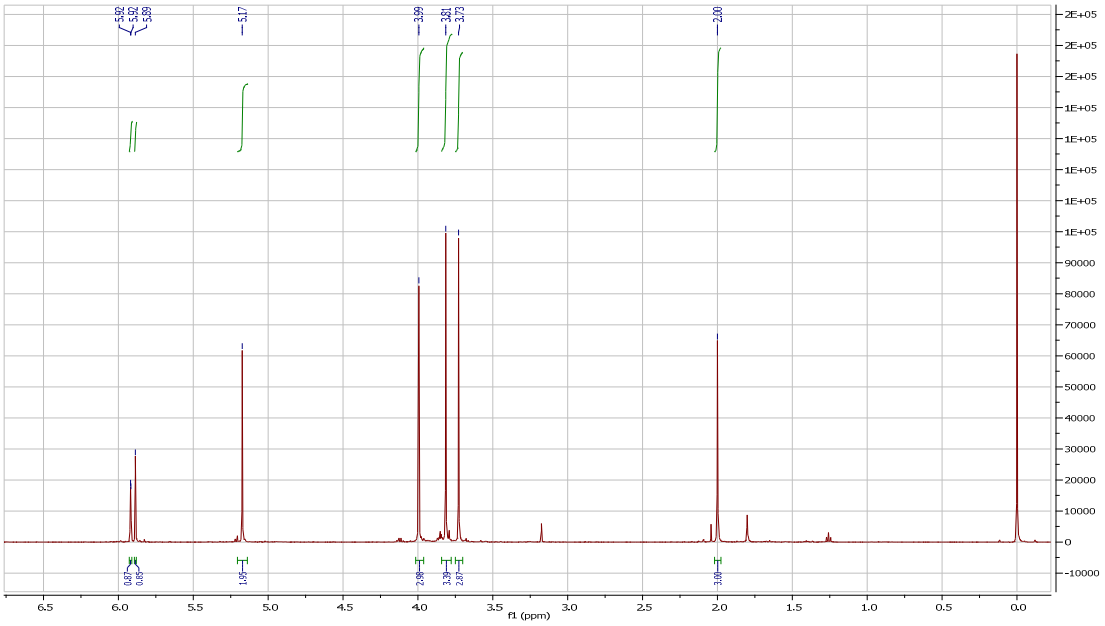

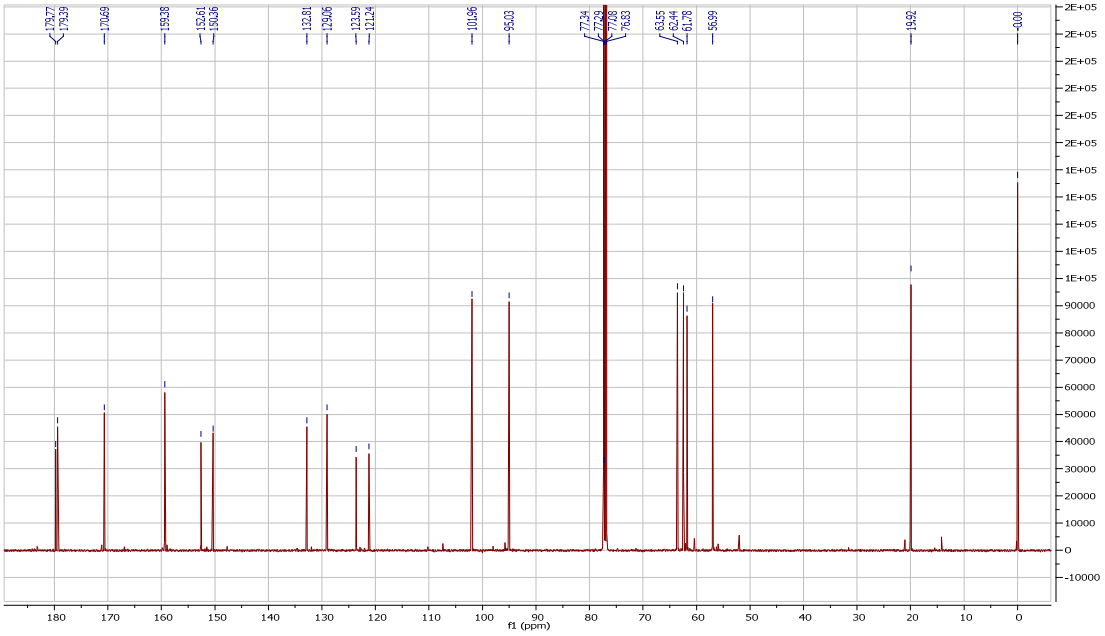

B1.6. 5,1-dihydroxy-7-methoxy-3-methyl-1*H*-benzo[*g*]isochromene-6,9-dione (anhydrofusarubin) 26

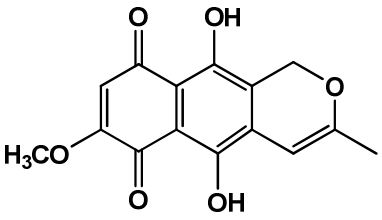

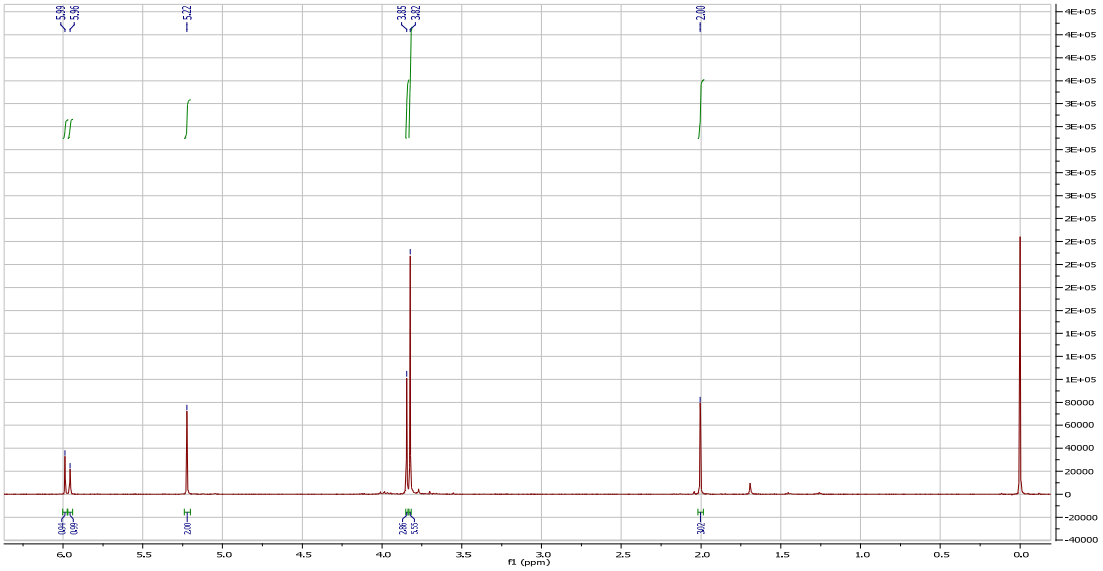

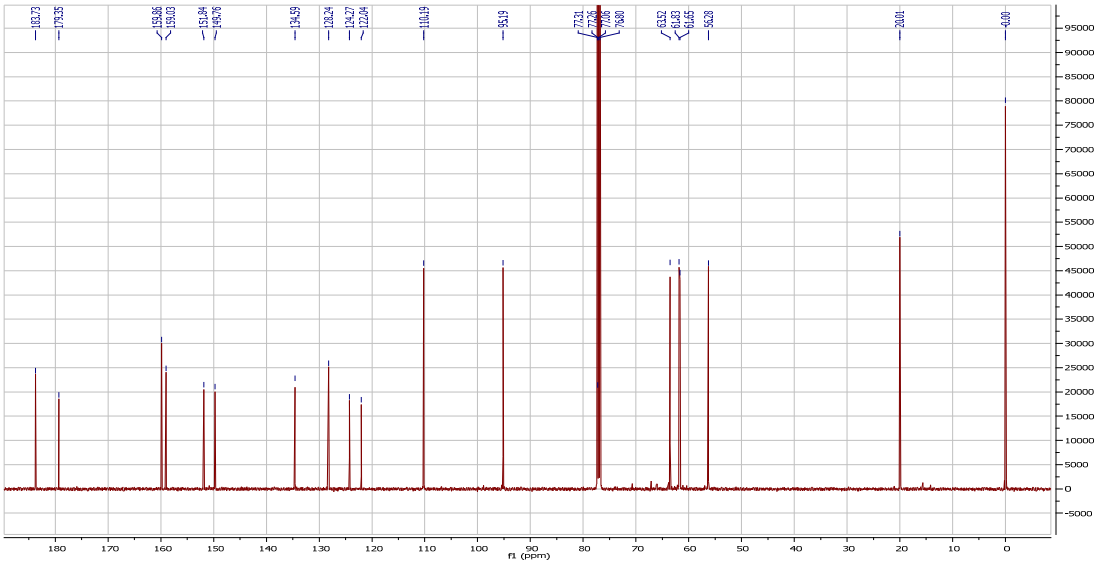

B1.7. 3,6-Dimethoxy-9-methyl-10,14-dioxatricyclo[7.3.1.$0^{2,7}$]tetradeca-2,4,6-triene 259

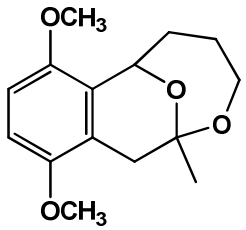

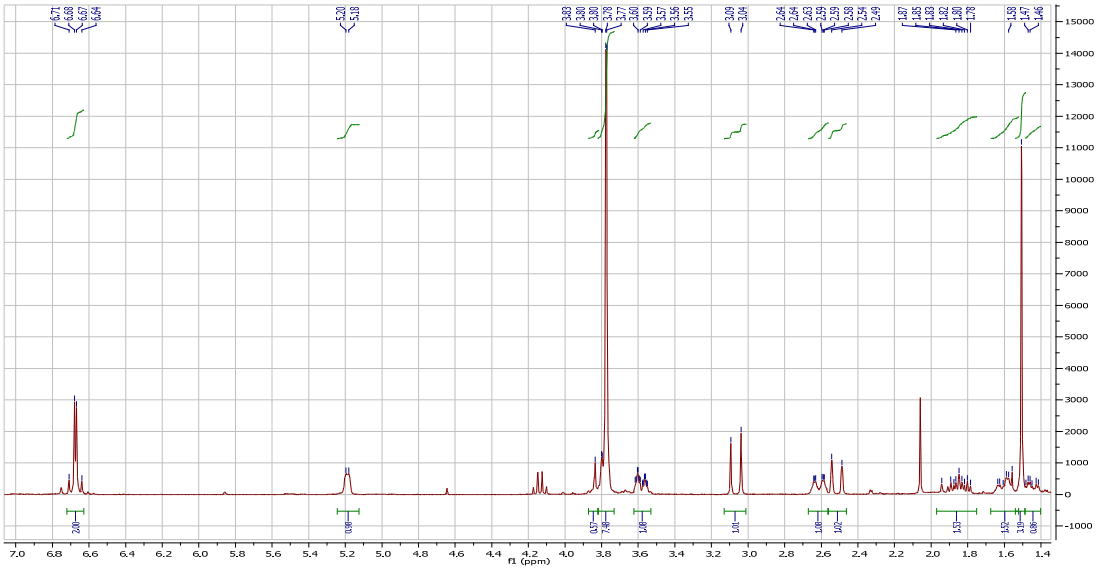

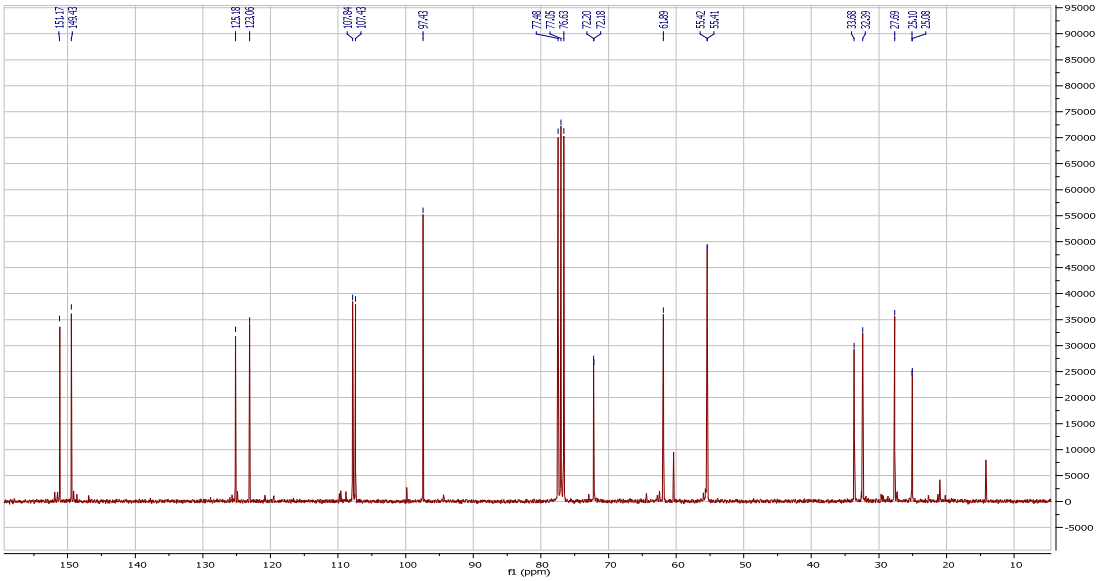

B1.8. (3,6-Dimethoxy-9-methyl-10,13-dioxatricyclo[7.3.1.0^{2,7}]trideca-2,4,6-trien-11-yl)methanol 254

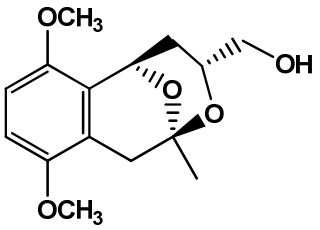

major

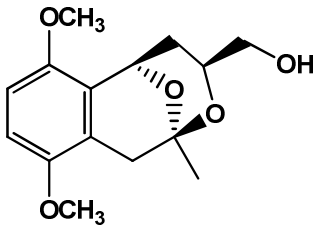

minor

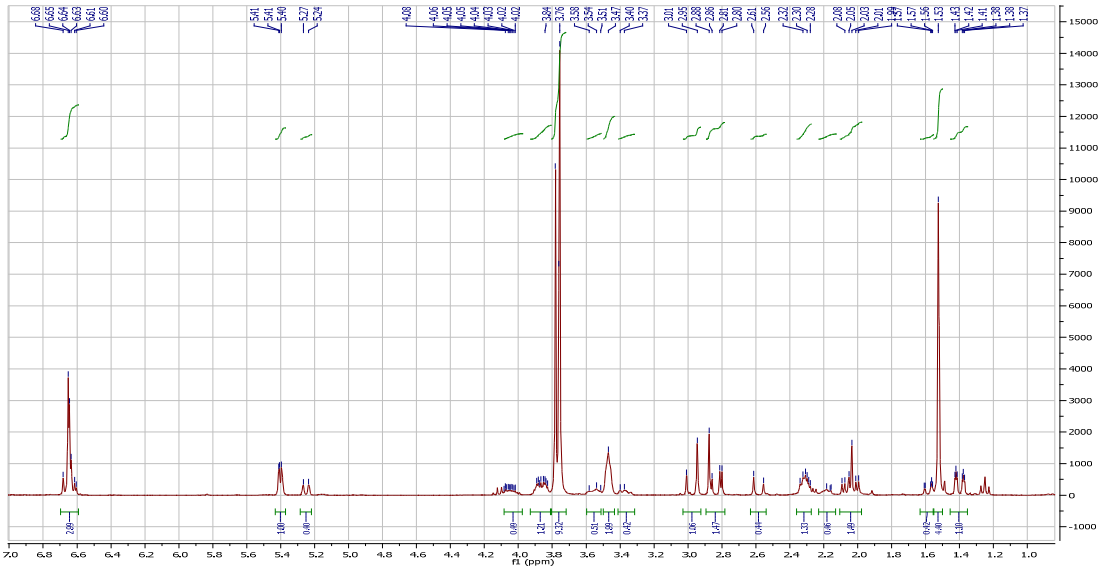

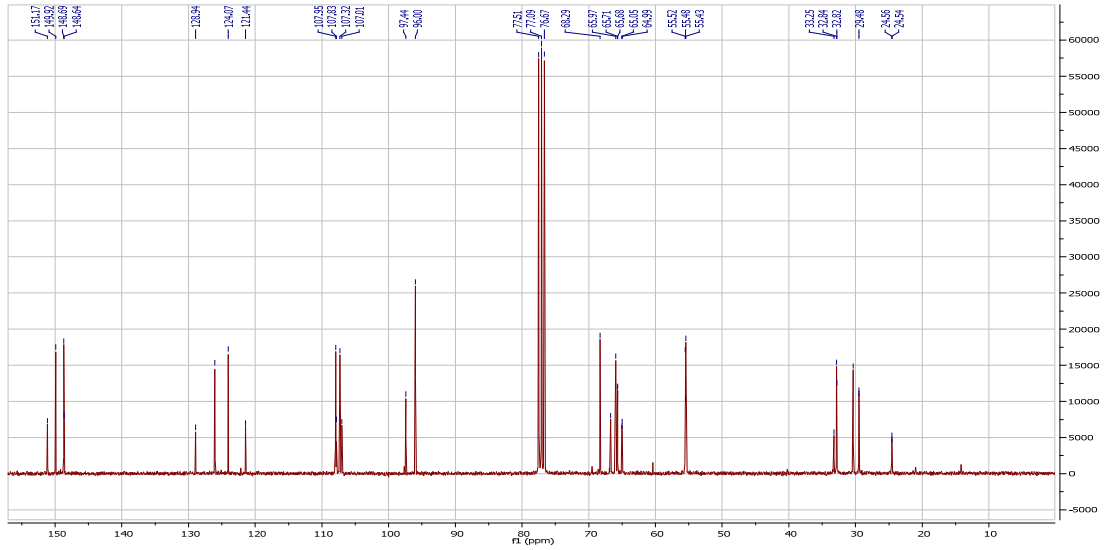

C1 Literature Published during PhD

1. Pillay, A., de Koning, C.B., Rousseau, A.L., Fernandes, M.A., *Tetrahedron*, 2012, **68**, 7116-7121.

2. Pillay, A., de Koning, C.B., Rousseau, A.L., Fernandes, M.A., *Organic and Biomolecular Chemistry*, 2012, **10**, 7809-7819.